THE DEVELOPMENT OF ASPHALT MIX CREEP PARAMETERS AND FINITE ELEMENT MODELING OF ASPHALT RUTTING

By:

Ludomir Uzarowski

A thesis
presented to the University of Waterloo
in fulfillment of the
thesis requirement for the degree of
Doctor of Philosophy
in
Civil Engineering

Waterloo, Ontario, Canada, 2006

AUTHOR'S DECLARATION

I hereby declare that I am the sole author of this thesis. This is a true copy of the thesis, including any required final revisions, as accepted by my examiners.

I understand that my thesis may be made electronically available to the public.

ABSTRACT

Asphalt pavement rutting is one of the most commonly observed pavement distresses and is a major safety concern to transportation agencies. Millions of dollars are reportedly spent annually to repair rutted asphalt pavements. Research into improvements of hot-mix asphalt materials, mix designs and methods of pavement evaluation and design, including laboratory and field testing, can provide extended pavement life and significant cost savings in pavement maintenance and rehabilitation.

This research describes a method of predicting the behaviour of various asphalt mixes and linking these behaviours to an accelerated performance testing tool and pavement in-situ performance. The elastic, plastic, viscoelastic and viscoplastic components of asphalt mix deformation are also examined for their relevance to asphalt rutting prediction. The finite element method (FEM) allows for analysis of nonlinear viscoplastic behaviour of asphalt mixes.

This research determines the critical characteristics of asphalt mixes which control rutting potential and investigates the methods of laboratory testing which can be used to determine these characteristics. The Hamburg Wheel Rut Tester (HWRT) is used in this research for asphalt laboratory accelerated rutting resistance testing and for calibration of material parameters developed in triaxial repeated load creep and creep recovery testing. The rutting resistance criteria used in the HWRT are developed for various traffic loading levels.

The results and mix ranking associated with the laboratory testing are compared with the results and mix ranking associated with FEM modeling and new mechanistic-empirical method of pavement design analyses. A good relationship is observed between laboratory measured and analytically predicted performance of asphalt mixes.

The result of this research is a practical framework for developing material parameters in laboratory testing which can be used in FEM modeling of accelerated performance testing and pavement in-situ performance.

ACKNOWLEDGEMENTS

I would like to thank those individuals who were instrumental in the completion of this research. Specially, I would like to thank my supervisor, Professor Susan Tighe, for willingly sharing her knowledge, for her guidance, encouragement and patience. Your support and enthusiasm are greatly appreciated. I look forward to future endeavors.

I would also like to thank my co-supervisor, Professor Leo Rothenburg for sharing his experience and for his advice and excellent comments. A special thank you goes to Professor Ralph Haas for his help and advice. Thank you to the reminder of my examining committee members, Professor Gerhard Kennepohl, Professor Mark Knight and Professor Mike Worswick.

My special thank you goes to Golder Associates Ltd. staff for their support and help in conducting this research and their patience and understanding. I would like to express my appreciation to Dr. Michael Maher, Mr. Andrew Balasundaram, Mr. David Noonan, Mr. Steve Keenan, Mrs. Hana Prilesky, Mr. Jery Prilesky and Mrs. Donna Walsh. Also, I would like to acknowledge help I received from the laboratory staff in the Golder Whitby Office.

I also thank Mr. Alan Schoubel and Dr. Ota Vacin for their help in laboratory testing.

I would like to give my deepest thanks to my wife, Ela, and my son, Bart, for their understanding and unlimited patience. Without your support this work would not have been possible.

TABLE OF CONTENTS

LIST OF FIGURES

LIST OF TABLES

CHAPTER ONE
INTRODUCTION

1.1 BACKGROUND

Pavements represent the largest component of public investment in transport. In Canada, the pavement portion of highways and streets have a current asset value of more than $ 150 billion [Tighe 2003]. About 95 percent of all pavements in Canada are asphalt pavements. These pavements deteriorate with time due to traffic loading and environmental exposure. Asphalt pavement rutting is one of the most commonly observed pavement distresses and is a major safety concern to transportation agencies. Millions of dollars are reportedly spent annually to repair rutted asphalt pavements. As traffic loading increases significantly and Canada experiences more frequent periods of hot weather due to global warming, the problem of pavement rutting is anticipated to escalate. Research into improvements of hot-mix asphalt materials, mix designs and methods of pavement evaluation and design including laboratory and field testing is considered necessary to provide extended pavement life and significant cost savings in pavement maintenance and rehabilitation.

There are currently several test methods available to evaluate hot-mix asphalt materials in the laboratory and in the field. Some of these methods, such as the Marshall method, have been used for many years, while others, such as dynamic modulus, the Superpave method and uniaxial and triaxial creep testing, are relatively new. Some of these newer methods are currently used primarily as research tools. Ideally, laboratory tests should closely simulate the field conditions and correlate well with observed field performance. However, in practice this is not always the case.

A typical asphalt pavement consists of layers of asphalt concrete, and layers of granular base and/or subbase resting on a prepared subgrade soil as shown in Figure 1.1. The asphalt concrete layers are the major contributors to the structural capacity of the pavement. Although the condition of the granular layers and subgrade may have a significant impact on the structural condition of the pavement and contribute to pavement permanent deformation (rutting), a number of research studies have indicated that pavement rutting occurs mainly in the asphalt layers. This research is focused on the performance of asphalt mixes only.

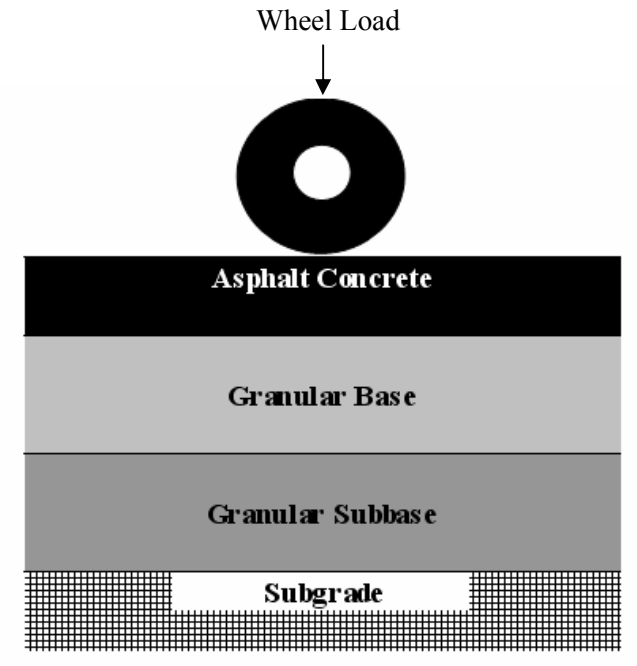

Figure 1.1 Typical asphalt pavement structure.

Hot-mix asphalt laboratory testing typically includes preselection of materials, mix design, sample preparation, sample conditioning and then applying static, dynamic or cyclic loading and measuring the response of the material. The measured properties vary from purely empirical, such as Marshall stability and flow, to fundamental mechanistic properties such as resilient modulus, static and dynamic creep, resistance to permanent deformation and fatigue endurance.

Asphalt is a visco-elasto-plastic material with behaviour depending on temperature and rate of loading. However, in numerous pavement analysis programs, hot-mix asphalt is assumed to be linearly elastic. This assumption is considered to be oversimplified for more detailed analysis. Currently available finite element programs have the ability to consider linear and nonlinear elastic, viscoelastic and viscoplastic behaviour of materials and analyze asphalt concrete permanent deformation, fracturing, thermal cracking, reflection cracking, hardening and healing.

The finite element method (FEM) has been used in recent years for asphalt materials and pavement performance analysis. In a typical FEM asphalt pavement simulation, the required material parameters are determined using backcalculated values to match the results of the FEM analysis [White 2002]. However, each asphalt mix (i.e. dense graded, open graded, stone mastic asphalt, etc.) has its own unique set of elastic and nonelastic parameters that should be supported by results of laboratory testing. Also, it is imperative that the backcalculated values are calibrated against the laboratory determined values.

1.2 SUMMARY OF RESEARCH APPROACH

This research describes a method of predicting the behaviour of various asphalt mixes and linking this behaviour to an accelerated performance testing tool and pavement in-situ performance. Within this research methodology, various laboratory test methods of determining asphalt mix characteristics are examined in terms of their use in performance prediction. The elastic, plastic, viscoelastic and viscoplastic components of the mix deformation are also examined for their relevance to asphalt rutting prediction. Detailed analysis completed in this research indicates that asphalt rutting occurs mainly due to its nonlinear viscoplastic nature. A finite element method (FEM) was selected for use in this research as it allows for the evaluation of nonlinear viscoplastic behaviour of asphalt mixes. Once the material parameters are determined, their use in the FEM analysis is investigated. It is considered critical that the predicted performance in FEM analysis is calibrated against laboratory measured performance and the material parameters are adjusted accordingly.

An analytical solution supplemented by the acquisition of material specific data from extensive laboratory testing is utilized in this research. The result is a framework for developing material parameters in laboratory testing that can be used in FEM modeling of accelerated performance testing and pavement in-situ performance. Asphalt mixes used in this research represent typical mixes used on paving projects in Ontario. One of the practical outcomes of this research is the development of rutting resistance criteria in the accelerated performance testing for various levels of traffic loading.

1.3 RESEARCH SCOPE

This research study is focused on identifying the critical parameters that contribute to asphalt permanent deformation (rutting). A detailed literature review revealed that, although there were a number of publications on asphalt rutting and simulation using finite element method, the asphalt mix viscoplastic parameters that control the rate of rutting have not been fully investigated and linked to observed laboratory and field performance. Defining the behaviour of asphalt material, asphalt mix critical parameters and the method of their determination should help in addressing the pavement rutting problem and defining effective remediation and/or prevention methods.

The analyses used in this research are different from those typically used in conventional pavement mechanistic-empirical analyses. Some of the unique characteristics in these analyses are as follows:

- Determining critical characteristics of asphalt mixes which control the rate of rutting. Asphalt is a visco-elasto-plastic material and it is important to determine what parameters control the potential for rutting and how to define them;

- Utilizing two-dimensional (2D) finite element simulation in ABAQUS program to describe observed performance of asphalt mixes in the Hamburg Wheel Rut Tester (HWRT). Material parameters calibrated against the measured test results are also incorporated in this analysis. As well, static loading applied for the total time of the applied loading passes is incorporated to represent the HWRT loading conditions; and

- Utilizing 2D finite element simulation to predict pavement in-situ performance. As the focus of this research is on rutting of the asphalt layer only, the assumed pavement structure consists of a single layer of asphalt concrete placed over a Portland cement concrete base. This reflects the conditions in the HWRT testing. The impact of granular base and subgrade is not considered in this research.

Some important assumptions in this analysis include:

- The creep power law model in the ABAQUS library is utilized to reflect the nonlinear character of asphalt concrete mix;

- Plane strain conditions are assumed for 2D analyses and stress-strain response. Axisymmetric analyses in two-dimensional space and three-dimensional slice analyses are also completed and the results are compared with the plane strain analyses;

- Application of a dual wheel loading system for a standard axle load of 80 kN is used in the study. The stress configuration applied by a radial tire is used in the pavement performance simulation;

- The New Mechanistic-Empirical Pavement Design Guide (MEPDG) is used to predict asphalt pavement rutting for the purpose of comparison with the ABAQUS pavement performance simulation; and

- The accelerated rutting performance testing in the HWRT was carried out only at a temperature of 50ºC; therefore, the temperature in the triaxial creep testing and in the rutting analyses is also fixed at 50ºC.

1.4 RESEARCH PROBLEM

This research problem focuses on asphalt mix rutting prediction. Asphalt mix rutting prediction is based on material characteristics, wheel loading, and environmental conditions, including temperature. Material characteristics are critical but are also difficult to accurately measure. However, once they are known, the extent of pavement rutting can be predicted using various models.

Asphalt pavement rutting is one of the most common and destructive pavement distresses observed on Canadian roads, particularly at intersections in the urban environment. Rutting repairs can be very costly and disruptive to traffic operations. Asphalt rutting is a major safety concern because it affects the handling of vehicles. Pavement designers attempt to mitigate rutting through proper pavement and asphalt mix design. Rutting can be caused by insufficient pavement structural support allowing excessive stress to be transferred to the subgrade (structural rutting). However, the most common type of rutting is asphalt 'instability' rutting caused by the plastic movement of the asphalt mix under heavy, often slow moving loading.

The prediction of asphalt rutting is considered to be one of the more complex issues in pavement engineering. The sensitivity of asphalt mixes to rutting should be determined at the mix design stage. The conventional methods, such as Marshall, Hveem and even Superpave methods, only partially and indirectly address the problem [Coree 1998, Anderson 2003, Shah 2004, Faheem 2006]. The laboratory asphalt accelerated performance testing can be of assistance, provided that it represents the in-situ conditions and that the appropriate performance criteria are used. If asphalt mixes are rut resistant for the design traffic level, this can reduce the long-term pavement maintenance requirements, reduce traffic interruptions and cost of operation, and improve safety.

The nature of the asphalt mix in terms of its rutting potential must be known. Laboratory testing should determine the necessary characteristics so that the proper materials are selected for use in road construction. The reliable material parameters determined during laboratory testing should then be used in asphalt pavement in-situ performance prediction so that the designer knows if the selected materials and design mixes will provide the anticipated service life of the pavement.

1.5 RESEARCH OBJECTIVES

The main objectives of this research study are as follows:

- To determine the critical characteristics of asphalt mixes that control rutting potential;

- To investigate the method of laboratory testing that can be used to determine these necessary characteristics;

- To investigate and identify the method of developing material parameters to be used in asphalt mixes performance prediction;

- To evaluate the use of asphalt laboratory accelerated performance via the use of a loaded wheel tester in rutting potential evaluation and to develop rutting resistance criteria for various traffic loading levels. Before any inferences can be made about the use of the rut testing equipment, it is necessary to develop a theory about the relationship between the pavement in-situ performance and the testing in the loaded wheel tester; and

- To compare the results and mix ranking associated with the laboratory testing with the results and mix ranking associated with an analytical solution, finite element modeling and the new mechanistic-empirical method of pavement design analysis.

1.6 ORGANIZATION OF THESIS

This thesis contains nine chapters as follows:

Chapter One: Introduction - includes a brief background of the research subject and describes the approach to solving the problem.

Chapter Two: Literature Review - describes currently available approaches to rutting prediction, asphalt material parameters, finite element modeling and asphalt laboratory accelerated performance testing.

Chapter Three: Research Methodology - presents the research framework and the source of data. It also describes the analytical approach used in the study.

Chapter Four: Asphalt Mixes - describes the types of asphalt mixes used in the research and some of their characteristics such as gradations and volumetrics.

Chapter Five: Material Characterization - describes and provides results for laboratory testing including the accelerated performance testing in the HWRT, dynamic modulus testing and triaxial repeated load creep and creep recovery testing in the Interlaken Universal Test Machine/Simple Performance Tester, and performance graded asphalt cement testing.

Chapter Six: Asphalt Mixes Viscoplastic Behaviour - describes the elastic, plastic, viscoelastic and viscoplastic components of asphalt mix deformation. It presents the analysis of the laboratory triaxial repeated load creep testing results and the development of the asphalt mix creep parameters.

Chapter Seven: Finite Element Modeling - presents the ABAQUS finite element program used in the study and describes the FEM simulation of asphalt mix behaviour in the HWRT testing and the simulation of pavement in-situ performance.

Chapter Eight: Asphalt Pavement and Mix Performance - describes the pavement performance prediction analysis using the New Mechanistic-Empirical Pavement Design Guide (MEPDG). It emphasizes the importance of rutting resistance testing at the design stage, and provides the recommended criteria for the laboratory accelerated performance testing in the HWRT. It also compares the ranking of asphalt mixes in HWRT testing, ABAQUS simulation and MEPDG analyses.

Chapter Nine: Conclusions and Recommendations - summarizes the findings and recommendations of the thesis.

CHAPTER TWO
LITERATURE REVIEW

The purpose of this chapter is to review the basic concepts of hot-mix asphalt rutting related to rutting mechanism, asphalt mix behaviour, material creep and plasticity, laboratory testing and rutting analysis using finite element method and the new mechanistic-empirical method of pavement design.

2.1 ASPHALT PAVEMENT RUTTING

Asphalt pavement rutting is one of the most common asphalt pavement distresses. Rutting is typically considered to be a surface depression in the wheel path. However, in most cases, it is a combination of densification and shear-related deformation [White 2002]. It may occur in any layer of pavement structure, including subgrade, untreated base, or in the asphalt mix itself [Kandhal 1998]. Shear deformation, rather than densification, is considered to be the primary rutting mechanism in hot-mix asphalt (HMA) surface mixes when reasonably stiff supporting layers are present [White 2002].

An extensive rutting study in the United States [Brown 1992] looked into the impact of asphalt mix characteristics and construction on the severity of rutting. The impact of asphalt layer properties on pavement rutting in Canada was summarized by [Emery 1990]

Four primary types of rutting, each related to different causes, have been identified [Walker 1999]:

1. Consolidation – occurs due to insufficient compaction during pavement construction. An asphalt mix with insufficient density is prone to further compaction under traffic;

2. Surface wear – occurs due to surface abrasion by chains and studded tires;

3. Plastic flow – occurs when there is insufficient stability in the hot-mix asphalt. The reasons for plastic flow include excessive amount of asphalt cement, asphalt cement being too soft, too low air voids, high content of rounded aggregate, or too high minus 75 μm material. Plastic flow typically occurs within the surface course but may also occur in lower lifts. Plastic flow rutting is also called instability rutting; and

4. Mechanical deformation – results from insufficient structural capacity of the pavement when the strength and thickness of the pavement layers are insufficient to support the existing traffic on the given subgrade.

Hot-mix asphalt rutting is categorized in two types in the New Mechanistic-Empirical Pavement Design Guide [NCHRP 2004b]:

1. One-dimensional densification or vertical compression. A rut depth caused by materials densification is a depression near the centre of the wheel path without an accompanying hump on either side of the depression. Densification of material is generally caused by excessive air voids or inadequate compaction for any of the bound or unbound layers; and

2. Lateral flow of plastic movement. A rut depth caused by the lateral flow (downward and upward) of material is a depression near the centre of the wheel path with shear upheavals on both sides of the depression. This type of rut depth usually results in moderate to high severity rutting. This type of rutting is considered to be the most difficult to predict and measure in the laboratory.

The depth of rutting is determined by measuring the difference in elevation (perpendicular to the wire) between the wire and pavement surface. Shear failure (lateral movement) of the HMA courses generally occurs in the top 100 mm of the pavement surface. Rutting at WesTrack, for instance, was confined entirely to the top 50-75 mm of the 150 mm HMA surface [White 2002]. It was observed that when failure occurs in the supporting granular layers, there are depressions in the wheel paths, but upheaval along the sides of the wheel paths is minimal [White 2002].

2.2 CLASSIC APPROACH

Classic pavement rutting analysis is focused on protecting the subgrade, leaving the issue of sufficient rut resistance of asphalt layers to mix designers. The conventional procedures of pavement analysis are based on limiting the vertical stress or strain at the top of the subgrade to control rutting of the entire pavement structure and the tensile stress or strain at the bottom of the lowest hot-mix asphalt layer to control fatigue cracking [NCHRP 2004b]. A typical classic rutting prediction model used in pavement design is given in [TRAC 1990]:

$$N_f = 1.077 \times 10^{18} (10^{-6}/\varepsilon_v)^{4.4843} \quad (2.1)$$

where:

N_f = load applications

ε_v = vertical compressive strain at the top of subgrade

More recently, extensive studies have been conducted using a number of test methods such as laboratory wheel-track tests, dynamic modulus tests, creep and triaxial tests, and Superpave shear tests, supported by a number of extensive pavement field rutting investigations [NCHRP 2004b]. It was observed that rutting was not only due to subgrade or granular base problems but also the result of an asphalt mix problem (instability rutting). It has become obvious that in proper pavement design, the cumulative permanent deformation in all layers of the pavement structure must be considered.

In conventional pavement analysis methods, hot-mix asphalt is assumed to be elastic [Brown 1990]. Elastic material deforms instantaneously when loaded and the deformation is immediately and fully recovered when the load is removed. Elastic material behaviour can be defined by the use of modulus of elasticity and Poisson's ratio. Modulus of elasticity (Young's modulus) is defined by Hooke's law [Brown 1990]:

$$E = \sigma/\varepsilon \tag{2.2}$$

where:

E = modulus of elasticity

σ = applied stress

ε = strain

For some practical analysis, hot-mix asphalt can be assumed to be linear elastic when it is solid and non-viscous. However, in reality, hot-mix asphalt materials are viscous at elevated temperatures, elastic at low temperatures and exhibit viscoelastic behaviour under intermediate conditions [Brown 1990].

There are a number of structural analysis programs available for pavement designs and behaviour analyses. For example, BISAR developed by Shell and ELSYM 5 developed for the Federal Highway Administration (FHWA) use the elastic layer theory while VESYS, also developed for FHWA, uses the viscoelastic layer analysis [Haas 1994, Yandel 1997].

Another one of these programs is CAMA [AI 1992], developed by the Asphalt Institute to assist pavement engineers in asphalt mix designs. In this program, the characteristics of the actual materials from construction are used in the mix design analysis. The program allows the prediction of pavement performance in terms of rutting and cracking under designed traffic loading. The prediction of rutting in asphalt concrete layers is based on the analysis of the in-situ stresses. They are calculated from the elastic

response under the wheel load and from the calculated stiffness of the mix. The following formula is used in CAMA to predict rutting [AI 1992]:

$$\log \varepsilon_p = -14.97 + 0.408 \log (N) + 6.85 \log (T) + 1.107 \log (\sigma_d) - 0.117 \log (Vis) + 1.908 \log (P_{eff}) + 0.971 \log (V_v) \quad (2.3)$$

where:

ε_p = permanent strain

P_{eff} = percent by volume of effective asphalt cement

V_v = percent volume of air voids

σ_d = deviator stress (psi) determined at the mid-depth of the layer

N = number of load applications

Vis = viscosity at 70°F (21°C) in poises x 10^6

T = pavement temperature (ºF)

2.3 ASPHALT MIX VISCO-ELASTO-PLASTIC BEHAVIOUR

Continuum mechanics describes the behaviour of solids and fluids based on large scale observations. It assumes that materials are uniformly distributed and ignores that, in fact, the materials are discontinuous[Spencer 1988]. The assumption of material continuity allows the determination of such properties as densities, displacements, and other. Rothenburg used a distinct element method to analyze discontinuous character of granular material [Rothenburg 1992]. Collop used the distinct element method for modeling the behaviour of an idealised asphalt mix [Collop 2003]. Sadd investigated the heterogeneous nature of asphalt material and considered micromechanical behaviour between aggregate and binder [Sadd 2002].

Constitutive equations are required to analyze the mechanical behaviour of materials. These equations are specific to particular materials. The mechanical constitutive equation of a material describes the dependence of the stress in a body on variables such as strain or the rate of deformation [Spencer 1988]. The constitutive equation or stress-strain equation plays a significant role in providing solutions to engineering problems.

An important step in pavement performance analysis is the selection of a suitable constitutive equation to model the behaviour of an asphalt mix under an external load [Von Quintus 1994]. A linear elastic model cannot always properly model the behaviour of pavement materials. There are nonlinear models that have

been developed recently that are suitable for pavement analysis. For the majority of pavement materials, the unloading material response follows an alternative path in the loading phase in the nonelastic zone. When the loading is removed, the strains are not fully recovered and some permanent deformation remains [Von Quintus 1994].

At elevated temperatures and constant stress or load, asphalt mix will continue to deform at a slow rate. This behaviour is called creep [Spencer 1988]. At a constant stress and temperature, the rate of creep is approximately constant for a long period of time. After this period of time and after a certain amount of deformation, the rate of creep increases, and fracture may occur. Figure 2.1 shows the relationship between the elongation e and time t. The initial force F_0 is rapidly applied to a viscoelastic body at time t = 0, and then held constant. This is shown in Figure 2.1a. The initial elongation e_0 is followed by an increasing elongation under the maintained load as shown in Figure 2.1b. This is the creep phenomenon.

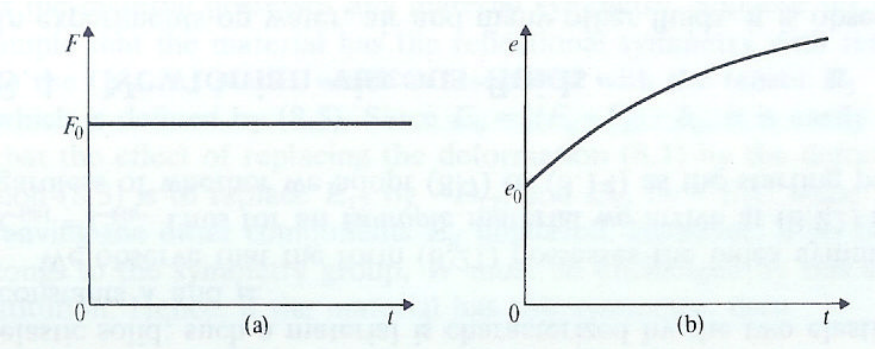

Figure 2.1 Creep Curve [Spencer 1988].

If the stress does not exceed certain limits the behaviour of many materials is linear elastic [Spencer 1988]. However, if the stress is beyond these limits, they exhibit a permanent deformation, which does not disappear when the stress is removed. This behaviour is inelastic. It is not a viscoelastic behaviour, because the viscoelastic stress depends on the rate of deformation. Although the stress in these materials depends on the previous deformation, it is independent of the rate of deformation. This material behaviour is called plasticity [Spencer 1988].

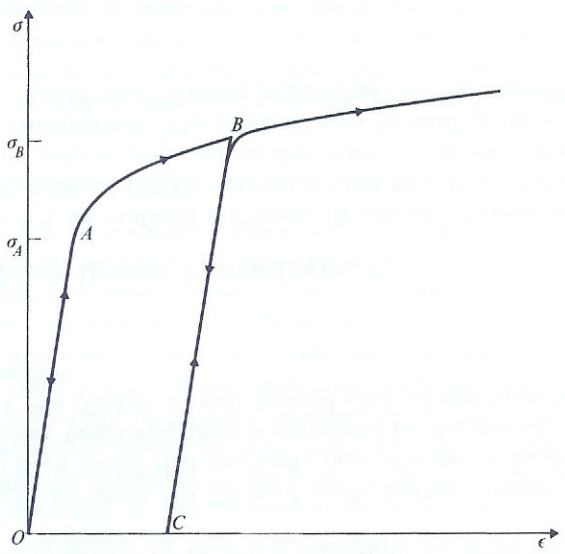

Figure 2.2 Typical Stress-Strain Curve for a Plastic Material [Spencer 1988].

For Section OA of the deformation curve in Figure 2.2, the relationship between stress σ and strain ε can be considered as linear. If the stress is removed before σ reaches the value σ_A, the strain returns to zero. In this range, the behaviour is considered to be linear elastic. σ_A is the initial yield stress. If the stress is increased to $\sigma_B > \sigma_A$, and then reduced to zero, the BC unloading curve is followed. BC is considered to be parallel to OA. The remaining residual strain OC is the plastic deformation. On reloading, the CB path will be followed and eventually continue the curve to OAB. The theory of elasticity does not apply in this case as there is no unique relation between the stress and the strain. There are two phenomena involved in this case: elasticity, where deformation disappears upon unloading; and plasticity, where a permanent deformation occurs [Spencer 1988].

An asphalt mix's response to an applied load is assumed to be visco-elasto-plastic and can be divided into four basic deformation components as follows [Von Quintus 1994]:

1) Elastic deformation which is recoverable and time independent;
2) Plastic deformation which is nonrecoverable and time independent;
3) Viscoelastic deformation which is recoverable and time dependent; and
4) Viscoplastic deformation which is nonrecoverable and time dependent.

The creep/recovery test can be used for characterizing these four components of asphalt mix deformation. By applying a step load function for a loading period of time and unloading that stepped function for an

unloading period of time, all four components of the mix responses can be identified. These responses are [Von Quintus 1994]:

1. The elastic component of deformation (ε_e) – represents the instantaneous response of asphalt mix measured during unloading phase;
2. The instantaneous response measured during the loading phase which includes the elastic (ε_e) and plastic (ε_p) components of deformation. The plastic component of deformation (ε_p) can be determined by subtracting the elastic component (ε_e) from the total instantaneous loading phase deformation; and
3. The viscoelastic and viscoplastic components are more difficult to determine. The delayed response measured during the unloading phase represents the viscoelastic response (ε_{ve}) only. The delayed response in the loading phase consists of both the viscoelastic and viscoplastic responses ($\varepsilon_{ve} + \varepsilon_{vp}$). The viscoplastic component of asphalt mix deformation can be determined by subtracting the delayed response during the unloading phase from the delayed response during the loading phase.

Asphalt mix responses can be assumed to have two major parts: the recoverable and non-recoverable components [Von Quintus 1994]. At low temperatures, asphalt mix can be considered to behave like a linear viscoelastic material, but the higher the temperature, the more important and significant are the response components which describe the viscoelastic and viscoplastic components. The plasticity theory is used to describe the nonlinear and inelastic behaviour of materials. As the behaviour of various pavement materials is basically inelastic, unloading follows an entirely different path from that followed by the loading phase.

When analyzing asphalt mix permanent deformation, all non-recoverable components must be included, particularly viscous deformation. The plastic strain can normally be divided into three phases [NCHRP 2004c]:

1. In the primary stage the strain rate decreases. The additional permanent deformation caused by applied load is decreasing with the number of load applications. It is mainly associated with volumetric change;
2. In the second stage the strain rate is constant. It is also associated with volumetric change; however, shear deformation increases at an increasing rate; and
3. In the third stage the strain rate is increasing until failure occurs. It is associated with plastic (shear) deformation under no volume change. The three stages are shown in Figure 2.3.

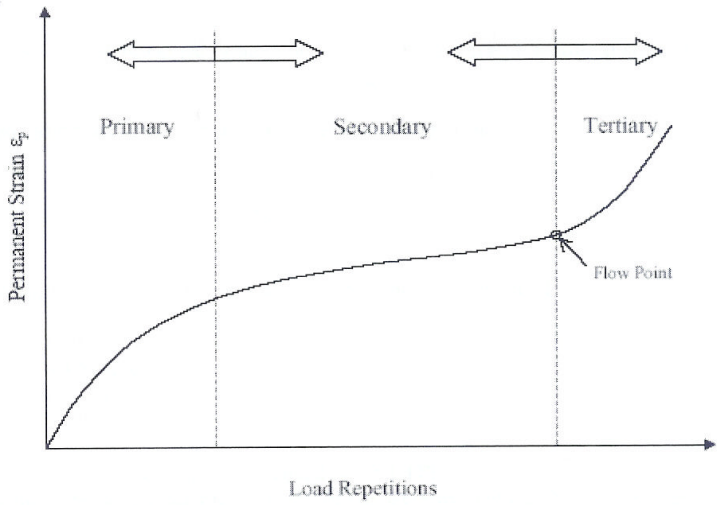

Figure 2.3 Three Stages of Plastic Strain in Repeated Load Creep Testing [NCHRP 2004c].

Because asphalt mix plays a major role in pavement behaviour, a constitutive law must be used to characterize the effects occurring in in-situ behaviour. The constitutive law can be expressed as [Perl 1983]:

$$\varepsilon_{ij} = \varepsilon_{ij} (\sigma_{ij}, t, N, T) \quad (2.4)$$

where :

ε_{ij} and σ_{ij} = strain and stress tensor components, respectively

t = time

N = number of loading cycles

T = temperature

Perl considered the elastic, plastic, viscoelastic and viscoplastic strain components of asphalt mix behaviour in his research on asphalt mixes permanent deformation [Perl 1983]. The total creep was expressed as:

$$\varepsilon_{total}(\sigma, t, N) = \varepsilon_e(\sigma) + \varepsilon_p(\sigma, N) + \varepsilon_{ve}(\sigma, t) + \varepsilon_{vp}(\sigma, t, N) \quad (2.5)$$

where:

ε_{total} = total strain

ε_e = elastic strain

ε_p = plastic strain

ε_{ve} = viscoelastic strain

ε_{vp} = viscoplastic strain

σ = stress

t = time

N = number of load repetitions

Perl used in his research a single very fine sand-asphalt mix that contained 8.5 percent asphalt cement. His experiments were carried out at a constant temperature of 25ºC.

Lai conducted uniaxial compressive creep tests of an asphalt mix under constant loading, multiple–step loading, and repeated loading [Lai 1973]. He used a fine mix with 95 percent passing No. 4 sieve size and 9.0 percent asphalt cement. The total plastic creep strain was defined as:

$$\varepsilon_p(t) = (b_1\sigma + b_2\sigma^2)\, t^{n_p} \qquad (2.6)$$

and the rate of the irrecoverable strain as:

$$\dot{\varepsilon}_p(t) = n_p(b_1\sigma + b_2\sigma^2)\, t^{n_p-1} \qquad (2.7)$$

where:

ε_p = total irrecoverable strain

$\dot{\varepsilon}_p$ = total irrecoverable strain rate

σ = loading stress

t = time

n_p = slope of the creep compliance curve

b_1 and b_2 = parameters of the stress-strain curve

2.4 ASPHALT FINITE ELEMENT MODELING

A number of theoretical models have been developed to predict asphalt pavement rutting in the United States, Canada and Europe. Kandhal listed the developers of these models in [Kandhal 1998]. In Canada, Haas and Meyer developed the model based on the cyclic creep test in the mid 1970s [Haas 1975].

The mechanistic approach to pavement analysis allows for geometry, nonhomogeneities, anisotropy and nonlinear material properties of all layers in a unified manner [Desai 2000a]. As a result, the distresses are evaluated as a part of the finite element procedure, without the need for empirical formulas. It is a superior method because it can consider actual properties of the materials, almost infinite pavement structure alternatives, and various environmental and traffic loadings [Desai 2002].

No analytical solution currently exist for non-linear stress-strain relationships, but with the finite element method it is possible to treat non-linear elastic materials through an iterative process [Ullidtz 1998]. First, the stress condition in each element is calculated with an estimated modulus. The modulus of each element is then modified according to the stress condition, and new stresses are calculated, until the changes between two iterations converge. With the FEM method, it is possible to consider the non-linear relationships between stress and elastic, as well as plastic strain, and to include viscous and viscoelastic strains.

The techniques available for deformations in flexible pavements include analytical methods, multilayer elastic theory (MLET), finite difference methods (FLAC), finite element methods (FEM), boundary element methods (BEASY), and hybrid methods [NCHRP 2004c]. The finite element method is considered to be the most versatile of the analysis techniques, providing capabilities for nonlinear material characterization, large strains/deformations, dynamic analysis and other sophisticated features [NCHRP 2004c]. The finite element method is a technique in which the body to be analyzed is divided into finite elements connected at their nodal points [Roberts 2003]. The continuous variation of stresses and strains in the body is represented by an assumed displacement function over each finite element. The element stiffness matrix can be established for a given element geometry and constitutive equation describing material behaviour. The global structural stiffness can then be formulated by integrating the individual element stiffness matrices. The result is a set of simultaneous equations that reflect the unknown displacement of nodes and the loading force. Solving these equations gives all nodal displacements. With the calculated nodal displacements, strains and stresses within each element can be calculated [Roberts 2003]. Generally, pavement analysis and wheel loading would require a three-dimensional analysis, particularly to predict microcracking and fracture response. However, a two-dimensional procedure can provide satisfactory solutions for certain applications [Desai 2002].

FEM allows the pavement designer to consider the non-linear relationships between stress and elastic, plastic, viscous and viscoelastic strains. FEM has been successfully used for pavement analysis but still on an experimental basis [Desai 2000b, Desai 2002]. Desai used the disturbed state constitutive model in

the DSC-SST2D two-dimensional code [DSC 2002] for static, dynamic, creep and thermal analysis. The code can be used for analysis of asphalt pavement permanent deformation. A two-dimensional analysis in DSC-SST2D can provide satisfactory solutions for symmetrical test configurations [Desai 2000]. Other FEM programs used for asphalt pavement analysis include ABAQUS, LS-DYNA, ILLI-PAVE and MICH-PAVE, for instance (NCHRP 2004c]. A 3D finite element code CAPA-3D has been developed in the Netherlands for investigation of dynamic, non-linear response of asphalt pavements [Scarpas 1997, Erkens 2002].

Uddin used LS-DYNA and ABAQUS finite element programs in pavement analysis [Uddin 2000a, Uddin 200b and Uddin 2002]. He also described a successful use of advanced finite element analysis procedures for correct simulation of pavements subjected to dynamic loads produced by nondestructive evaluation equipment and dynamic wheel loads [Uddin 2002].

ABAQUS is a general purpose finite element program that can solve problems ranging from relatively simple linear analyses to the most challenging nonlinear simulations. Simulations in ABAQUS were used for theoretical analysis to develop relationships between transverse profile characteristics and contribution of individual layers to rutting of HMA pavements in a study described by [White 2002]. Limited full-scale accelerated pavement test (APT) data were used to evaluate the correctness of the relationships. An approximate approach was used to simulate the APT loading conditions.

The analyses in [White 2002] were two-dimensional simulations using four-node quadrilateral plane strain elements. Based on the asphalt mix performance in the APT, material constants in the creep model were back-calculated. Regression analyses were conducted to correlate these material constants with mix physical properties. The single tire pressure used in the design criteria in the analysis was 517-552 kPa (75-80 psi). Loading time to achieve the desired rut depths was established by trial and error.

Flexible pavement deformation, which occurs as a result of repeated loading, depend on the total cumulative traffic loading time [White 2002]. Loading time relates to vehicle speed and the length of loaded area. In reality, the loaded area is oval and shows distinct treads. Therefore, variable length rectangular segments were used to represent the loaded contact area. Resulting variable loading time was accounted for in the loading model. The loading cycle consisted of using one single-step function to approximate the wheel loading. The total cumulative loading time of this single step was calculated using the speed and number of load repetitions. In this study, the effect of temperature was fixed.

Stress and time dependency in the analysis of pavement rutting was accounted for using a creep model from the ABAQUS material library [White 2002]. Rutting failure limits were 0.25 in. (6.25 mm) for hot-mix asphalt layers and 0.50 in. (12.5 mm) for the total pavement rutting. In the analysis, parameters n and m were fixed, while parameter A was varied. Parameter A is the value of the y-axis intercept in the log plot of rutting versus time relationship. Rutting increases linearly with the value of A. By varying the value of A in the creep model, the amount of rutting is controlled. If the first attempt with the finite element program did not produce the desired amount of rutting, the analyses were repeated with the appropriate parameters changed. The following material parameters were assigned to layers allowed to rut: E (modulus of elasticity); μ (Poisson's ratio); A; n; and m. The following were the final values used in the analysis: E = 3,100 MPa; $\mu = 0.3$; $A = 0.8 \times 10^{-4}$; $n = 1.2$; and $m = -0.5$.

In equation form, the creep rate can be represented as [White 2002]:

$$\dot{\varepsilon} = A\sigma^n t^m \qquad (2.8)$$

where

$\dot{\varepsilon}$ = creep strain rate

σ = uniaxial equivalent deviatoric stress

t = total loading time

A, n, m = parameters related to material properties.

Hua modeled flexible pavement rutting as a plane strain two-dimensional (2D) problem rather that a three-dimensional (3D) problem [Hua 2000]. With a 2D analysis, the total computation time is significantly decreased without significant loss in accuracy. Hua selected the four-mode, quadrilateral plane strain CPE4 element from the ABAQUS two-dimensional, solid-element library for the use in the analysis. The effects of elastic modulus and Poisson's ratio on distortion parameters were negligible. The material parameters used by Hua in the creep model (A, n and m) were based on the research completed by [Perl 1983]. Based on an assumption suggested by [Huang 1995], Hua fixed the n parameter, which is associated with the contact pressure, as 0.8 and adjusted the A and m parameters to match the measured deformation. Hua concluded that if a creep model is used to describe the time dependent material behaviour, repeated loading and continuous loading will have the same effect on the predicted creep strain as long as the total loading times are the same.

Extensive finite element pavement analyses were carried out during the MEPDG development [NCHRP 2004c]. In its current version (Summer 2006), the MEPDG uses linear material model for asphalt mixes and stress-dependent material model (nonlinear resilient modulus with tension cutoff) for unbound materials. A single wheel load was modeled as a uniform pressure of 550 kPa over a circular area of 150 mm radius. The element models used in the Guide consist of regular meshes, simple material models with at most only relatively gentle nonlinearities, and straightforward monotonic quasi-static loadings. Computation time for a three-dimensional analysis was up to two to three orders of magnitude longer than for a corresponding two-dimensional calculation.

One pavement test lane from the Louisiana Accelerated Loading Facility (ALF) was used to calibrate the numerical simulation in a research study described by [Huang 2001]. The ABAQUS program was selected for the numerical simulation. A step load was applied on the pavement surface over the equivalent amount of time to the number of passes of ALF loads. Viscoplastic models were successfully used in ABAQUS to simulate the dynamic response and predict permanent deformation of flexible pavements. The rate dependent parameters for the asphalt concrete were obtained from uniaxial compressive tests at different strain rates conducted by Seibi in 1993.

Sukumaran explored the use of symmetry in the ABAQUS finite element three-dimensional modeling of a pavement system under moving aircraft loads [Sukumaran 2004]. He also analyzed the impact of single and multiple loads. He modeled asphalt mixes as elastic materials specifying the modulus of elasticity and Poisson's ratio, and granular base and subbase using the Mohr-Coulomb elasto-plastic model. Sukumaran concluded that stress-strain response could be better captured if stress versus strain data from unconfined compression tests, triaxial tests or direct simple shear tests are input to obtain the plasticity model parameters. The development of an anisotropic viscoplastic continuum damage model to determine asphalt pavement permanent deformation based on Perzyna's formulation with Dracke-Prager yield function is described by [Tashman 2004].

The creep power law model can be used in its "time hardening" form or in the corresponding "strain hardening" form [ABAQUS 2004a]. Huang used the time hardening model for pavement rutting ABAQUS simulation [Huang 1995] while Hua compared the rutting in both models [Hua 2000]. Time hardening formulation is as follows [ABAQUS 2004a]:

$$\dot{\varepsilon}_c = d\varepsilon_c/dt = A\tilde{q}^n t^m \qquad (2.9)$$

where:

$\dot{\varepsilon}_c$ = the uniaxial creep strain rate

$\tilde{q}$ = the uniaxial deviatoric Mises stress for isotropic creep behaviour

t = the total time

A, n and m = material parameters

The equation shows that creep strain rate depends on stress, time and, through the constants A, n and m, on temperature.

Von Mises stress is used as a criterion in determining the onset of failure in ductile materials [Chandrupatla 2002]. The failure criterion states that the Mises stress σ_{VM} should be less than the yield stress σ_Y of the material. In the inequality form, the criterion is [Chandrupatla 2002]:

$$\sigma_{VM} \leq \sigma_Y \tag{2.10}$$

The von Mises stress is given by:

$$\sigma_{VM} = \sqrt{I_1^2 - 3I_2} \tag{2.11}$$

where

I_1 and I_2 are the first two invariants of the stress tensor.

$I_1 = \sigma_x + \sigma_y + \sigma_z$

$I_2 = \sigma_x\sigma_y + \sigma_y\sigma_z + \sigma_z\sigma_x - \tau_{yz}^2 - \tau_{xz}^2 - \tau_{xy}^2$

In terms of principal stresses

$I_1 = \sigma_1 + \sigma_2 + \sigma_3$

$I_2 = \sigma_1\sigma_2 + \sigma_2\sigma_3 + \sigma_3\sigma_1$

Many computational problems can be solved using plane theory in a two-dimensional finite element analysis. In the case of plane strain, the stress in a direction perpendicular to the x-y plane is not zero. However, by definition, the strain in that direction is zero, and therefore no contribution to internal work is made by this stress [Zienkiewicz 1968].

A state of plane strain exists if the only non-zero strains are ε_{xx}, ε_{yy} and γ_{xy} and if nothing depends on the z-coordinate. This is equivalent to the following displacements [Ottosen 1992]:

$$ux = ux(x,y); \quad uy = uy(x,y); \quad uz = 0 \tag{2.11}$$

Plane strain occurs in practice when a long body is loaded by forces which are perpendicular to the longitudinal axis and which do not vary along this axis [Ottosen 1992]. It can be assumed that all cross-sections are in the same state and if, moreover, the body is restricted from moving in the length direction. The plane strain is applicable to long bodies while the plane stress is applicable to thin bodies [Ottosen 1992].

The effect of wheel path distribution on pavement rutting can be very significant. One of the objectives of the National Pooled Fund Study (PFS) pavement testing conducted by the Indiana Department of Transportation/Purdue University at the Accelerated Pavement Test Facility was to investigate wheel wander [White 2002]. The effect of wander can substantially reduce (i.e. compress) uplift between the wheels and cause uplift or upheaval outside the tires to migrate away from the wheel paths. In PFS tests, rutting for the single-wheel-path loading (i.e. no wander) was 1.4 to 1.7 times that of rutting with 250 mm (10 in.) wander. In a study completed by Kasahara and described by [White 2002], this ratio was higher than 3.0.

2.5 ACCELERATED RUTTING PERFORMANCE TESTING

The link between laboratory testing and potential field performance of asphalt mixes is very important to improve asphalt pavement life-cycle performance. There are relatively few full scale pavement testing facilities such as the Accelerated Pavement Testing Device (APT) in Indiana [Huang 1995, Hua 2000, White 2003, Sivasubramaniam 2004] and Acceleratd Loading Facility (ALF) [LTRC 2004] in the United States or Canterbury Accelerated Pavement Testing Indoor Facility (CAPTIF) [Saleh 2002] in New Zeland and LINTRACK in the Netherlands [Van Dommelen 2002], for instance. Using these types of facilities for mix evaluation would be impractical and expensive. The test tracks, such as the Centre for Pavement and Transportation Technology (CPATT) Test Track in Ontario [Tighe 2003], or WesTrack [Williams 1999, Epps 2002], MnROAD [Timm 2003] and the Pavement Oval Track [Brown 2002] in the United States, are used mainly for research purposes. The Heavy Vehicle Simulator (HVS) is used to test in-service pavements or specially developed test sections [Monismith 1998, Novak 2004].

There have been numerous attempts to form the missing link between laboratory testing and field performance by developing small-scale laboratory equipment and procedures for accelerated, simulative asphalt concrete mix performance testing. It has been recognized that the most fundamental tests are very complex while simulative tests are generally easy to perform [Zhang 2002].

A standardized accelerated laboratory test to predict HMA rutting potential that is relatively inexpensive and useful for quality control/quality assurance (QC/QA) testing would be of great benefit. Currently, the most commonly type of standardized laboratory test of this nature is a loaded wheel tester (LWT) [Kandhal 2002a, Kandhal 2003].

There are three loaded wheel rut testers that are in some use for asphalt mix testing in Canada: the Asphalt Pavement Analyzer (APA); the Hamburg Wheel Rut Tester (HWRT); and the French Laboratory Rutting Tester (FLRT) [Uzarowski 2004]. APA, HWRT and FLRT testers are used by a number of researchers and road agencies in the United States [Hall 1999, Cross 2001, Kandhal 2001, Yildrim 2001, Kandhal 2002a, Harman 2002, Zhang 2002, FHWA 2002]. Other rut testers used in the United States include the Purdue University Laboratory Wheel Tracking Device (PURWheel), One-Third Scale Model Mobile Lab Simulator (MMLS3) [Kandhal 2002a], NCSU Wheel Tracking Device (NCSU WTD) [Sadasivam 2004] and rotary wheel rut testers [Powell 2003, Buchanan 2005].

Hot-mix asphalt rut resistance testing using the French Rutting Tester is required by the Quebec Ministere des Transports on high volume roads. Other provinces in Canada currently do not routinely require rut resistance testing, even for roads with very heavy traffic loading [Uzarowski 2004]. The criteria currently used in the wheel rut testing are pass/fail with no clear link to mix type or traffic level.

Although the resistance to permanent deformation in rut testers is considered to simulate road conditions, it is an empirical test. Research from loaded wheel testing encompass the empirical approach, while results from shear and creep testing facilitate mechanistic analysis [Powell 2002].

The evaluation of loaded wheel testers in the United States reported by [Cooley 2000] compared GLWT, APA, HWRT, LCPC, PURWheel, and MMLS3 testers. It was concluded that the results obtained from the wheel tracking devices seem to correlate reasonably well to actual field performance when the in-service loading and environmental conditions of that location are considered. Wheel tracking devices, when properly correlated to a specific site's traffic and environmental conditions, have the potential to allow the user agency the option of a pass/fail or "go/no go" criteria. The wheel tracking devices seem to

reasonably differentiate between performance grades of binders. However, the ability of the wheel tracking devices to adequately predict the magnitude of the rutting for a particular pavement has not been determined.

A comparative study of two fundamental tests, repeated shear at constant height (RSCH) and repeated load confined creep test (RLCC), and one simulative test, APA rut test, was reported by [Zhang 2002]. The tests had good correlation with each other. The rut depth correlated well with the initial deformation and mixes that had higher deformation corresponded to a higher rut depth.

Although the wheel testers have gained acceptance and are used in the asphalt concrete rutting resistance evaluation, their link to the asphalt pavement field performance is rarely addressed. An empirical formula for the wheel tracking test specified by [BS 2003] is described by [O'Flaherty 2002]. The test involves subjecting a 50 mm thick slab of hot-mix asphalt material to a rolling standard wheel which transversed the specimen at a constant temperature of 45°C. The sample may be either manufactured in the laboratory or a 200 mm diameter core can be sampled from a surface course. The test measures rutting under the wheel over a period of time. A formula was developed from the field test site results that suggest the number of commercial vehicles traveling at 100 km/hr that are required to form a 10 mm deep rut at the end of a 20-year design life [O'Flaherty 2002]:

$$\text{Maximum WTR} = 14{,}000/(C_v + 100) \qquad (2.12)$$

where:

WTR = wheel tracking rate (mm/h); and

C_v = number of commercial vehicles per lane per day.

The Hamburg Wheel Rut Tester (HWRT), was developed by Helmut-Wind Incorporated in Hamburg, Germany in the 1970s [Cooley 2000]. It is used as a specification requirement for some of the most traveled roadways in Germany to evaluate rutting and stripping. HWRT is currently used by a number of researchers and road agencies in the United States. NCAT recommends the APA as the most appropriate for the accelerated rutting resistance testing followed by the HWRT [Brown 2001a, Brown 2001b].

The HWRT measures the combined effects of rutting and moisture damage by rolling a steel wheel across the surface of an asphalt concrete specimen that is immersed in hot water [Cooley 2000, Yildrim 2001]. The tests are performed underwater at typically 50ºC, even though the temperature can vary between 25ºC and 70ºC. Each sample is typically loaded for 20,000 passes or until 20 mm deformation occurs.

Approximately 6.5 hours are required for a test. The creep slope is used to measure rutting susceptibility. Based on the examination of many slabs and pavement cores, the tertiary regions of the curves produced by the HWRT appeared to be primarily related to moisture damage rather than to other mechanisms that cause permanent deformation [Yildrim 2001].

Texas Department of Transportation specifies the Hamburg Wheel-Tracking Test in the Bituminous Test Procedures Manual [Texas DOT 2004]. The rut resistance testing criteria in the HWRT in their pavement construction specification are given in Table 2.1 [Texas DOT 2003].

Table 2.1 Texas DOT Asphalt Mix Performance Criteria.

High Temperature Binder grade	Minimum Number of Passes @ 12.5 mm (0.5 in.) Rut Depth – Tested @ 50ºC (122ºF)
PG 64 or lower	10,000
PG 70	15,000
PG 76 of higher	20,000

2.6 MATERIAL CHARACTERIZATION

There are four main groups of laboratory fundamental tests to characterize permanent deformation [Harvey 2001, Witczak 2002a, Witczak 2002b]:

1. Dynamic modulus tests – uniaxial, triaxial, SST at constant height;
2. Strength tests – triaxial shear test and unconfined compressive strength test;
3. Creep tests – uniaxial unconfined and confined, indirect tensile; and
4. Repeated load creep test – uniaxial unconfined, triaxial confined, and SST at constant height.

The dynamic modulus test is recommended as the primary simple performance test for rutting for the MEPDG [Witczak 2005]; the flow number, determined from the repeated load procurement deformation test, is recommended as an optional, complimentary procedure for evaluating the resistance of asphalt mix to testing flows. Very extensive research on the dynamic modulus, flow time and flow member tests, including the development and evaluation of the testing procedures, is described in the NCHRP Report

513 [Bonaquist 2003]. More information on the dynamic modulus test is given in Section 2.7, New Mechanistic Empirical Pavement Design Method.

The repeated load creep test, which is also called repetitive creep test or repeated load permanent deformation test, is probably the most frequently used test to determine asphalt concrete permanent deformation parameters. The use of the repeated load triaxial test to estimate rutting in asphalt concrete pavements is described by [Haas 1975] and [Meyer 1977]. Recently, the use of this test was investigated under the development of Simple Performance Test (SPT) for the MEPDG [Witczak 2001, Witczak 2000a, Witczak 2000b, Witczak 2005, Kaloush 2001, Tashman 2004]. Some researchers use the static creep test specified by Texas DOT (the recent version is covered by [Texas DOT 2005]) for asphalt mix rutting resistance evaluation [Maupin 1999, Uddin 2002b]. Monismith investigated the use of both triaxial creep and repeated load permanent deformation tests to define permanent deformation response characteristics [Monismith 2000].

Applying a confining pressure in a triaxial test allows better duplication of in-place pressure and temperature without prematurely failing the test sample. The triaxial repeated load test better expresses traffic conditions [Brown 2001a, Brown 2001b]. However, it has been recognized that the confined repeated load deformation test is more difficult to conduct and requires relatively complex and expensive equipment.

In the NCHRP 2003 Research Results Digest [NCHRP 2003], the triaxial creep and triaxial repeated load permanent deformation tests are considered as important tests for predicting rut depth of HMA mixes and estimating the life of HMA pavements and overlays using different mechanistic-empirical distress prediction models. It is recommended that the triaxial repeated load permanent deformation test be performed at a test temperature of 40 or 50ºC. Powell conducted the triaxial creep test at the NCAT test track at a temperature of 64°C [Powell 2003].

The creep tests at the MnRoad track were conducted at temperatures of 37.8 ºC and 54.4 ºC [Witczak 2002b]. ALF tests were performed at a temperature of 54.4ºC which was similar to the field test temperature of 58ºC. The flow number, slope and permanent strain in confined and unconfined repeated load tests had the best correlation with the rutting observed in the field on MnROAD, ALF and WesTrack studies [Witczak 2002b].

Examination of conventional Superpave Gyratory Compactor (SGC) compaction data from Superpave asphalt mixes presented in [Anderson 2003] indicated that compaction slope in SGC was not related to

asphalt mix stiffness or rutting resistance because compaction slope was insensitive to changes in asphalt binder content.

2.7 NEW MECHANISTIC-EMPIRICAL PAVEMENT DESIGN METHOD

The methods of pavement design being used in Canada are mainly empirical [Haas 1997]. However, there is growing interest in mechanistic-empirical methodology and the coming challenge for road agencies is to get ready for its application for pavement design [Hein 2004].

The development of better, more realistic theoretical modeling and the availability of higher quality data from modern testing facilities and in the field is one of the major achievements in pavement engineering [Brown 1997, Monismith 1999]. The New Mechanistic-Empirical Pavement Design Guide (MEPDG) includes a procedure for predicting asphalt pavement rutting [NCHRP 2004b]. The mechanistic-empirical (M-E) approach is based on the limited use of principles of mechanics such as elasticity and viscoelasticity. The stresses and strains caused by application of the wheel load are computed and then used in empirical formulas for calculation of rutting, damage and cracking under load cycles.

The primary material property of interest in the MEPDG for asphalt stabilized layers is their dynamic modulus, E*. MEPDG Level 1 design requires the following steps [NCHRP 2004b]:

1. Conduct dynamic modulus (E*) laboratory test at loading frequencies and temperatures of interest for the given mix;
2. Conduct binder test complex shear modulus (G*) and phase angle (δ) testing on the proposed asphalt binder at $\omega = 1.59$ Hz (10 rad) over a range of temperatures;
3. From binder test estimate Ai-VTS (regression intercept and regression slope of viscosity temperature susceptibility) for mix-compaction temperature; and
4. Develop master curve for the asphalt mix that accurately defines the time and temperature dependence including aging.

The requirements for Levels 2 and 3 are different:

1. No E* laboratory testing required;
2. Use E* predictive equation;

3. Use typical Ai-VTS values provided in the Design Guide software based on PG, viscosity, or penetration grade of the binder; and
4. Develop master curve for asphalt mix that accurately defines the time temperature including aging.

Other inputs to the flexible pavement response model include [NCHRP 2004b].

1. Pavement geometry
    a. Layer thickness
2. Environment
    a. Temperature vs. depth for each season
    b. Moisture vs. depth for each season
3. Material properties (adjusted for environmental and other effects, as necessary)
    a. Elastic properties
    b. Nonlinear properties (where appropriate)
4. Traffic
    a. Load spectrum – i.e. frequencies of vehicle types and loads within each vehicle type
    b. Tire contact pressure and areas

Dynamic modulus is determined as [NCHRP 2004b, Yoder 1975]:

$$|E^*| = \sigma_o/\varepsilon_o \quad (2.13)$$

where:

$|E^*|$ = dynamic modulus

σ_o = maximum (peak) dynamic stress

ε_o = peak recoverable axial strain

The phase angle, ϕ, is the angle by which ε_o lags behind σ_o. It is an indicator of the viscous properties of the tested material. Mathematically, this is expressed as:

$$E^* = |E^*| \cos\phi + |E^*| \sin\phi \quad (2.14)$$

$$\phi = (t_i/t_p) \times (360) \quad (2.15)$$

where:

t_i = time lag between a cycle of stress and strain (s)

t_p = time for a stress cycle (s)

i = imaginary number

For pure elastic material $\phi = 0$ and the complex modulus (E*) is equal to the absolute value, or dynamic modulus. For pure viscous material $\phi = 90^o$.

The Witczak model is used in Levels 2 and 3 to predict the dynamic modulus of asphalt mixes over a range of temperatures, rates of loading and aging conditions, from material specification and volumetric design of the mix [NCHRP 2004a]:

$$\text{Log } E^* = 3.750063 + 0.02932\rho_{200} - 0.001767(\rho_{200})2 - 0.002841\rho_4 - 0.058097V_a - 0.802208\,(V_{beff}/(V_{beff} + V_a)) + (3.871977 - 0.0021\rho_4 + 0.003958\rho_{38} - 0.000017(\rho_{38})2 + 0.005470\rho_{34}) / (1+e^{(-0.603313 - 0.313351\log(f) - 0.393532\log(\eta))}) \quad (2.14)$$

where:

E* = the dynamic modulus (psi)

η = the bitumen viscosity (10^6 Poise)

f = loading frequency (Hz)

Va = air voids content (%)

V_{beff} = effective bitumen content (% by volume)

ρ_{34} = cumulative % retained on the 3/4 in sieve

ρ_{38} = cumulative % retained on the 3/8 in sieve

ρ_4 = cumulative % retained on the No. 4 sieve

ρ_{200} = % passing the No. 200 sieve

The dynamic modulus master curves can be developed either by shifting laboratory test data or by using the dynamic modulus equation.

The output from the pavement response model used in the MEPDG are the stresses, strains and displacements within the pavement layers. Compressive vertical stresses/strains within the HMA layer are used for rutting prediction in HMA layers. Rutting is calculated from the following formula [NCHRP 2004b]:

$$RD = \sum_{i=1}^{Nsublayers} \varepsilon_{pi} h_i \quad (2.16)$$

where:

RD = pavement permanent deformation

Nsublayers = number of sublayers

ε_p' = total plastic strain in sublayer i

h' = thickness of sublayer i

The constitutive relationship used in the MEPDG to predict rutting in asphalt mixes is based upon a field calibrated statistical analysis of laboratory repeated load permanent deformation tests. This laboratory model form selected is [NCHRP 2004b]:

$$\varepsilon_p/\varepsilon_r = a_1 T^{a_2} N^{a_3} \quad (2.17)$$

where:

ε_p = accumulated plastic strain at N repetitions of load (in/in)

ε_r = resilient strain of the asphalt material as a function of mix properties, temperature and time rate of loading (in/in)

N = number of load repetitions

T = temperature (ºF)

a_i = non-linear regression coefficients

The national field calibrated model used in the MEPDG was determined by numerical optimization and other models comparison. The resulted model is [NCHRP 2004b]:

$$\varepsilon_p/\varepsilon_r = k_1 * 10^{-3.4488} T^{1.5606} N^{0.479244} \quad (2.18)$$

where :

k_1 = function of total asphalt layers thickness (h_{ac}, in) and depth (depth, in) to computational point, to correct for the confining pressure at different depth.

k_1 = $(C_1 + C_2 * depth) * 0.328196^{depth}$

C_1 = $-0.1039 * h_{ac}^2 + 2.4868 * h_{ac} - 17.342$

C_2 = $0.0172 * h_{ac}^2 - 1.7331 * h_{ac} + 27.428$

Several studies have been conducted to verify the relationship between the dynamic modulus and observed pavement rutting and to evaluate the Witczak dynamic modulus prediction model. Schwartz observed that overall the Witczak model can provide sufficiently accurate and robust estimates of dynamic modulus [Schwartz 2005]. Very good correlation between the predictive equation and measured dynamic modulus values was reported by [Tran 2004].

The dynamic modulus correlated well with observed pavement rutting on 20 SPS-1 sections in Texas and could be used to differentiate between good and poor performance [Zhou 2001]. Powell did not find a good correlation between dynamic modulus and permanent deformation on the NCAT track test; however, significant rutting was not observed on the track [Powell 2003]. Shah reported that, in general, mixes designed for warmer climates and higher traffic level had higher dynamic moduli [Shah 2004]. Chehab reported that calibration of the rutting model led to a better match of predicted rutting with measured rutting as compared to predictions using the un-calibrated model [Chehab 2005].

In the MEPDG approach, the direct factor that can be controlled to improve rutting resistance is to increase the HMA mix stiffness (modulus) by increasing the mix master curve location. This can be accomplished by using a stiffer grade of binder, using less asphalt and insuring that field compaction specifications are fully complied with. In addition, all of the known, historic factors that tend to enhance the stability of an HMA mix must also be considered in the design phase (i.e. crushed particles, nominal aggregate particle size, etc.) [NCHRP 2004b].

2.8 SUMMARY

There have been a number of research studies conducted on asphalt mix rutting that included extensive laboratory testing. Various methods of pavement rutting mechanistic analysis have been used with more attention placed recently on nonlinear pavement behaviour analysis using finite element method. However, an extensive literature review reveals that the link between the laboratory testing and the finite element analysis has not been well explored. Typically, the material parameters are back-calculated to match the final output of the finite element analyses without comparison with laboratory measured parameters. There is also a need for analyzing the link between a small-scale accelerated laboratory rutting performance testing of asphalt mixes using loaded wheel testers and predicted pavement in-situ performance. Calibration of the rutting model leads to a better match of predicted rutting with measured rutting as compared to prediction using un-calibrated model.

CHAPTER THREE
RESEARCH METHODOLOGY

The purpose of this chapter is to outline the analytical approach used in this research, present the research framework, identify the data sources used for the analysis and describe the method of parameter calibration and results verification used. In addition, the importance of recognizing the mechanism controlling the behaviour of the asphalt mix is also described.

3.1 ANALYTICAL APPROACH

An analytical approach is used in this research to investigate critical factors in asphalt mix permanent deformation. The basic objective was to determine the method of developing mechanistic parameters, based on laboratory testing of the mix, that can be used in asphalt rutting simulation and a suitable method of analysis that takes into account its nonlinear viscoplastic nature. The finite element method that includes models based on constitutive stress-strain relations in an analyzed structure is used in this analysis. It is considered critical that the laboratory developed parameters to be used in pavement in-situ rutting performance prediction be calibrated against laboratory measured rutting in accelerated rutting performance testing. The practical way of doing this was to initially model the accelerated laboratory testing using the parameters developed from the results of the laboratory triaxial repeated load creep testing and compare the predicted rutting with the measured rutting. Then, the necessary material parameters are adjusted accordingly so that the predicted rutting matches the laboratory measured rutting. These calibrated parameters can be used in pavement in-situ performance simulation. Another step selected in the validation process was to compare the pavement in-situ performance from the finite element simulation with the rutting predicted using the new, state-of-the-art, MEPDG methodology.

The framework for this research is shown in Figure 3.1. The research has three major parts: accelerated performance testing using the HWRT; finite element modeling using the ABAQUS program; and MEPDG pavement performance analysis.

In the accelerated performance testing portion of the research, asphalt mix samples are subjected to a predetermined number of loaded wheel passes and the permanent deformation is monitored and recorded. The objective is not only to determine the final accumulated depth of rutting but also to define the shape

of the deformation curve. Both these factors are used for the material parameters calibration and mix performance analysis.

In the finite element modeling, the asphalt mixes are tested in the laboratory to determine the material characteristics that are necessary for the development of creep parameters. An investigation into the visco-elasto-plastic behaviour of asphalt mixes is necessary for the parameters development. This part includes the finite element modeling using the commercially available ABAQUS program and the calibration of the initially developed parameters against the measured rutting in the HWRT testing.

In the MEPDG pavement performance analyses, the dynamic modulus and phase angle of the asphalt mixes are determined in the laboratory. The shear modulus and phase angle of the asphalt cement are also determined. MEPDG rutting modeling is conducted using Level 1 or Level 3 analysis. The predicted rutting in the pavement in-situ performance analysis using MEPDG methodology is compared with the rutting predicted in the ABAQUS simulation.

The ranking of asphalt mixes in the HWRT testing, ABAQUS modeling and MEPDG analyses is also compared. The results of all three parts of the research form the basis for the development of the rutting criteria for the accelerated rutting performance in the HWRT testing for low, medium and high traffic loading levels.

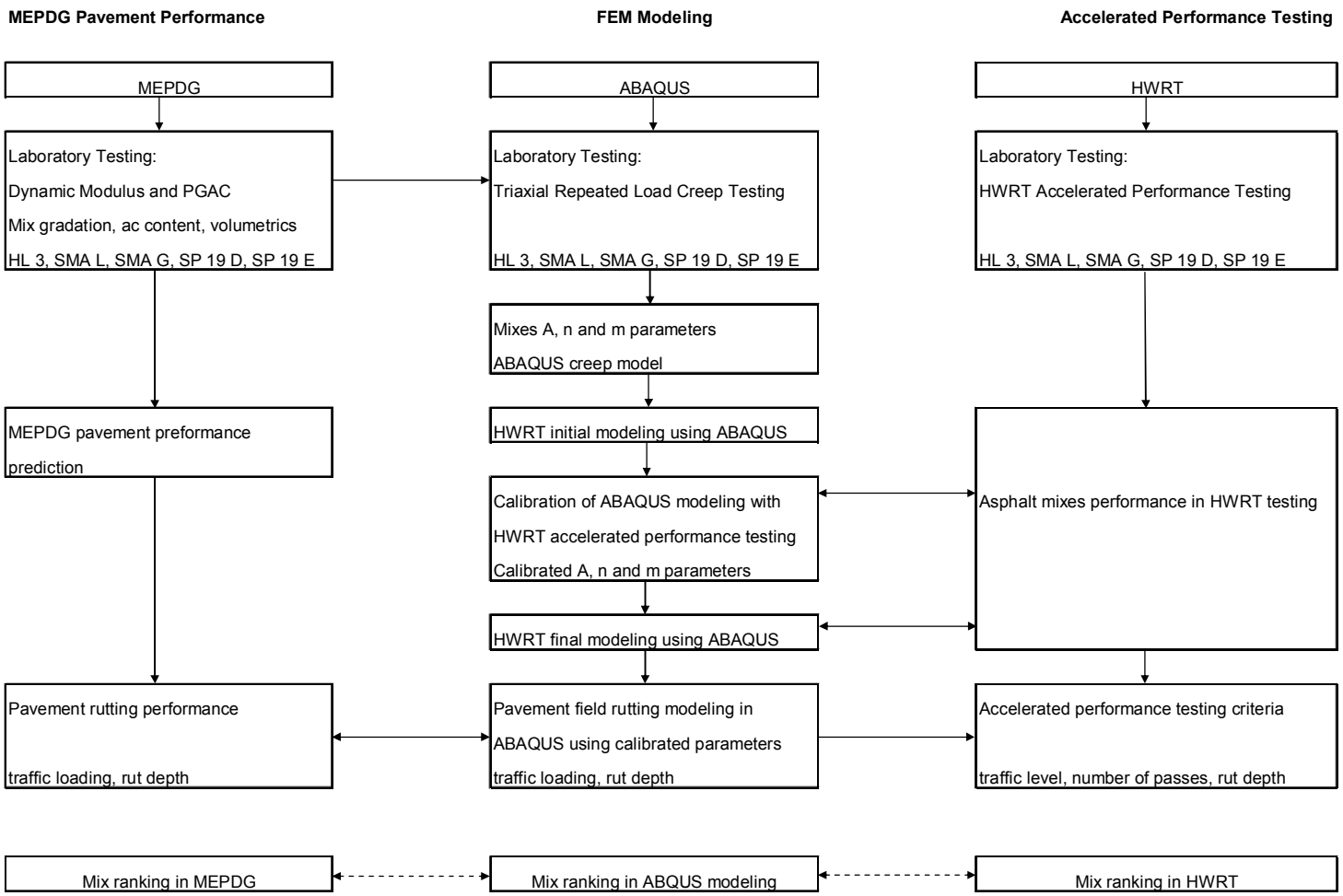

Figure 3.1 Research Framework.

3.2 INTEGRATED MODEL

As the three parts of the research are very closely interrelated and overlap in some areas, it was not practical to consider them separately. An integrated model has been developed, calibrated and validated. It consists of four major tasks as outlined below. Each task is covered by a separate chapter in this thesis. The tasks are as follows:

Task One	Material Characterization (Chapter Five)
Task Two	Qantify Fundamental Asphalt Properties (Chapter Six)
Task Three	Develop Finite Element Model (Chapter Seven)
Task Four	Calibrate and Validate Pavement Performance (Chapter Eight)

The integrated model is presented in Figure 3.2.

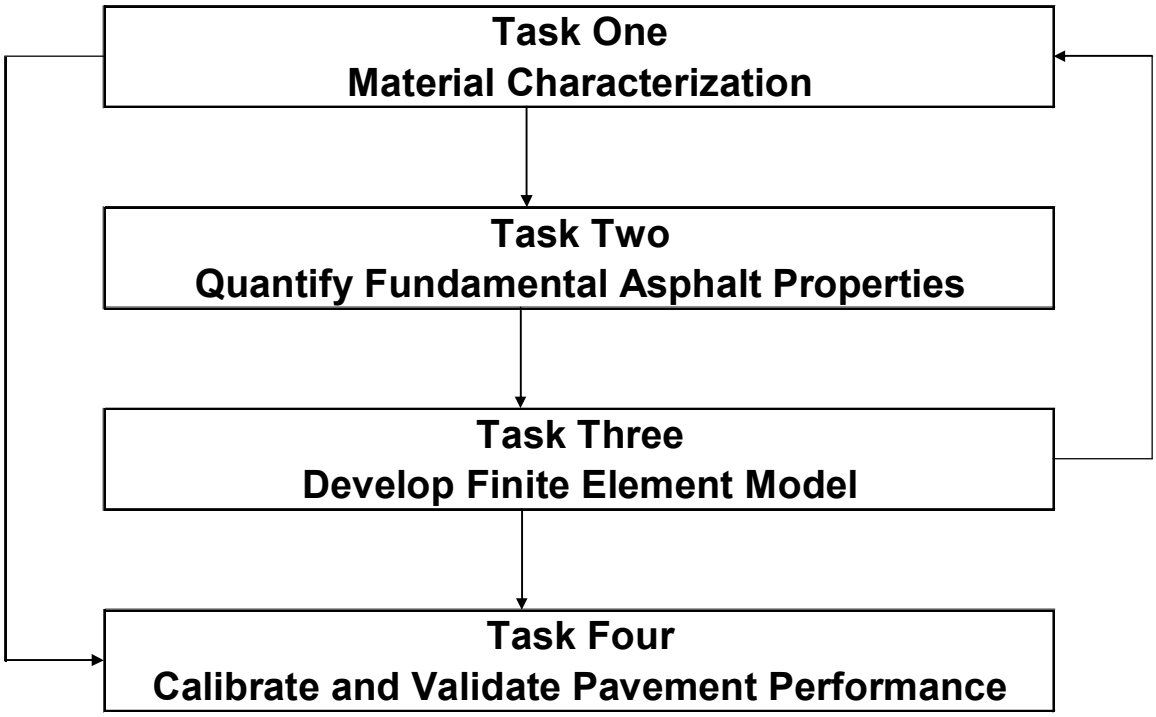

Figure 3.2 Integrated Research Model.

Before the project tasks are discussed, it is important to describe the data sources utilized in this research.

3.3 DATA SOURCE

It is common practice to evaluate an asphalt mix in the laboratory and then backcalculate all or some of the material parameters required for the finite element analyses. The results are then validated with field data [White 2002]. If the creep model is used, the A, n and m parameters are required. Typically, the researchers fix the n parameter only and adjust A and m to match the measured deformation [Huang 1995, Hua 2000].

A number of pavement researchers use the asphalt mix parameters developed by Perl and Lai [Perl 1983, Lai 1973] in pavement performance analyses. However, they typically use mixes that are significantly different from what Perl and Lai used. Perl used a very fine sand asphalt mix (all of the aggregates passed the 2.0 mm sieve) with 8.5 percent asphalt cement. Lai also used a fine mix with 95 percent passing the 4.75 mm sieve and 9.0 percent asphalt cement. Each asphalt mix has a unique set of parameters that determines the potential to rutting. Using the parameters developed for totally different mixes as the base may give misleading results. In addition, both Perl and Lai have conducted their testing at a temperature of 25ºC while the majority of the current rutting tests are typically conducted at a temperature of 50ºC or higher.

Although some adjustment of the mix parameters is necessary at the calibration stage, the initial parameters in this research are based on the results of the laboratory testing of the asphalt mixes obtained for this research. In short, this research examines typical mixes used in Ontario for small to large paving projects. Therefore, their parameters and performance are what can typically be anticipated in the province.

3.4 RESEARCH TASKS

The research tasks are summarized below.

Task One: Material Characterization

- Conduct laboratory accelerated rutting performance testing using the Hamburg Wheel Rut Tester (HWRT) recording the depth of rutting after 10,000 passes and 20,000 passes and the shape of the deformation curve;
- Measure dynamic modulus E* and phase angle δ of asphalt mixes and develop the master curves;
- Measure shear modulus G* and phase angle ϕ of asphalt cement used in each mix; and

- Conduct triaxial repeated load creep and creep recovery testing at two deviatoric stress levels, two different loading scenarios and recovery times and two different load repetitions.

Task Two: Quantify Fundamental Asphalt Properties

- Analyze the visco-elasto-plastic behaviour of asphalt mixes;
- Determine elastic, plastic, viscoelastic and viscoplastic strain components; evaluate their contribution to rutting; and
- Develop creep parameters for each asphalt mix.

Task Three: Develop Finite Element Model

- Model the accelerated rutting performance testing in the HWRT using the ABAQUS finite element program and the materials parameters developed from the laboratory testing results analysis;
- Calibrate the predicted rutting against the laboratory measured rutting; adjust the material parameters accordingly;
- Develop the pavement in-situ performance model – model the pavement structure to simulate the HWRT testing conditions. Develop wheel tire model and continuous loading time model;
- Model pavement in-situ performance using the adjusted material parameters. Predict pavement rutting for all mixes for traffic loading of 4 million, 10 million, 20 million and 30 million ESAL's;
- Analyze the impact of wheel wander; and
- Compare asphalt mixes rankings in the HWRT laboratory testing and ABAQUS pavement in-situ performance modeling.

Task Four: Calibrate and Validate Pavement Performance

- Conduct MEPDG pavement design analysis for the same type of pavement structure as used in the ABAQUS simulation – calculate the depth of asphalt layer rutting for the traffic loading of 20 and 30 million ESAL's. Use the material characteristics from the laboratory testing for Level 1 analysis or Witczak model for Level 3 analysis;
- Compare the predicted rutting in the ABAQUS simulation with the results of the MEPDG analysis;
- Compare asphalt mixes ranking in the MEPDG analysis, ABAQUS simulation and HWRT testing; and
- Develop rutting resistance criteria in the HWRT testing correlated to site's traffic loading conditions.

CHAPTER FOUR
ASPHALT MIXES

This chapter describes the mix types used in the research and provides information about their designs including mix ingredients, gradations and volumetrics.

4.1 MIX TYPES

Five asphalt mixes were used in the study. These mixes were selected to represent a wide range of applications, from high traffic freeways to low to medium volume municipal roads. The mixes are typical Ontario mixes from two major groups: dense graded mixes; and gap graded SMA mixes. Specifically, the mixes were: conventional HL 3 dense graded Marshall surface course mix, two Stone Mastic Asphalt 12.5 mm surface course mixes (marked as SMA L and SMA G), and two Superpave 19.0 mm dense graded binder course mixes (marked as SP 19 D and SP 19 E). The HL 3 mix was anticipated to have fair resistance to rutting and the SMA mixes were anticipated to have very good to excellent resistance to rutting. Of the two Superpave 19 mixes, the SP 19 D mix was anticipated to have good resistance to rutting while the SP 19 E mix was anticipated to be slightly better with very good resistance to rutting. The mixes incorporate different performance graded asphalt cements ranging from PG 58-28 to PG 70-28.

All five mixes were obtained from paving projects in Ontario and delivered to the Golder Associates Ltd. (Golder) Laboratory in Whitby, Ontario for sample preparation and mix volumetrics testing. In total, about one ton of asphalt mixes was used in the research. After determining the specific gradations, asphalt cement contents, and maximum relative densities, the asphalt materials were used to prepare specimens for the dynamic modulus and creep testing in the Interlaken Universal Test Machine/Simple Performance Tester (Interlaken) at the Centre for Pavement and Transportation Technology (CPATT) at the University of Waterloo. Another group of specimens was prepared for the rut resistance testing in the Hamburg Wheel Rut Tester (HWRT) in the Golder Laboratory in Burnaby, British Columbia.

4.2 MIX DESIGNS

Mix designs for all five mixes were provided by the contractors who supplied the mixes. There was a general request by the mix suppliers that the name of the contractor and the mix designer, source of materials and the location of the mix placement should remain confidential.

Both SMA mixes and SP 19 D and SP 19 E mixes were designed using the Superpave methodology [AI 2003b] and were required to meet the Ontario Provincial Standard Specifications (OPSS) 1151 requirements [MTO 2004]. Conversely, the HL 3 mix was designed using the Marshall methodology to meet the requirements of OPSS 1150 [MTO 2002].

The mixes incorporated the aggregate types and asphalt cements listed in Table 4.1. Table 4.2 summarizes the gradations, asphalt cement contents and the maximum theoretical specific gravities of all five mixes from their mix designs. Individual gradation plots for each mix with the specified gradation envelope for the HL 3 mix and control points and maximum density line for the mixes designed using the Superpave methodology are shown in Figures 4.1 to 4.3.

Table 4.1 Asphalt Mix Ingredients.

Mix	Aggregate		Additives	Asphalt Cement Grade
	Coarse	Fine		
HL 3	Crushed gravel (40%)	Asphalt sand (45%) and screenings (15 %)	-	PG 58-28
SMA L	Traprock (79%)	Traprock (13%) and mineral filler (8%)	Cellulose fibre (0.3%)	PG 70-28 PM*
SMA G	Traprock	Traprock and mineral filler	Cellulose fibre (0.3%)	PG 70-28 PM*
SP 19 D	Crushed rock (39%)	Screenings (10%) and manufactured sand (51%)	-	PG 64-28
SP 19 E	Crushed rock (63%)	High stability sand (37%)	-	PG 70-28

* Both PG 70-28 PM asphalt cements were polymer modified.

Table 4.2 Mix Gradations and Asphalt Cement Contents

Property	Mix Type				
	HL 3	SMA L	SMA G	SP 19 D	SP 19 E
Gradation					
Sieve Sizes	Percent Passing				
25.0 mm	-	-	-	100.0	100.0
19.0 mm	100.0	100.0	100.0	97.2	97.0
12.5 mm	96.0	98.8	90.0	77.9	80.2
9.5 mm	86.0	71.1	65.7	68.2	63.2
4.75 mm	60.0	25.4	25.0	60.2	38.0
2.36 mm	50.7	21.3	18.3	44.6	33.4
1.18 mm	40.9	17.5	14.3	29.7	22.5
600 µm	28.8	14.8	13.0	18.8	14.4
300 µm	13.3	13.0	10.6	9.9	8.7
150 µm	5.7	10.8	9.0	5.3	5.2
75 µm	3.7	9.1	8.0	4.2	3.8
Asphalt Cement Content (%)	5.30	5.70	5.70	4.35	4.60
Maximum Relative Density	2.496	2.599	2.684	2.582	2.570

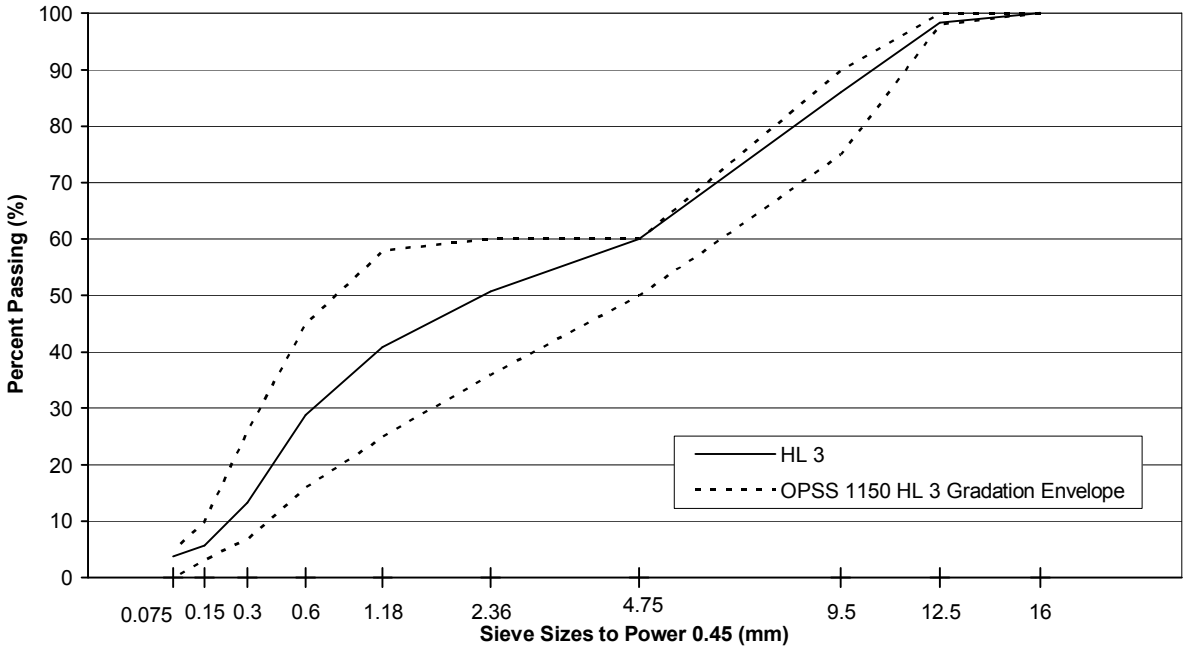

Figure 4.1 Gradation of the HL 3 Mix.

Error! Objects cannot be created from editing field codes.

Figure 4.2 Gradations of the SMA L and SMA G Mixes.

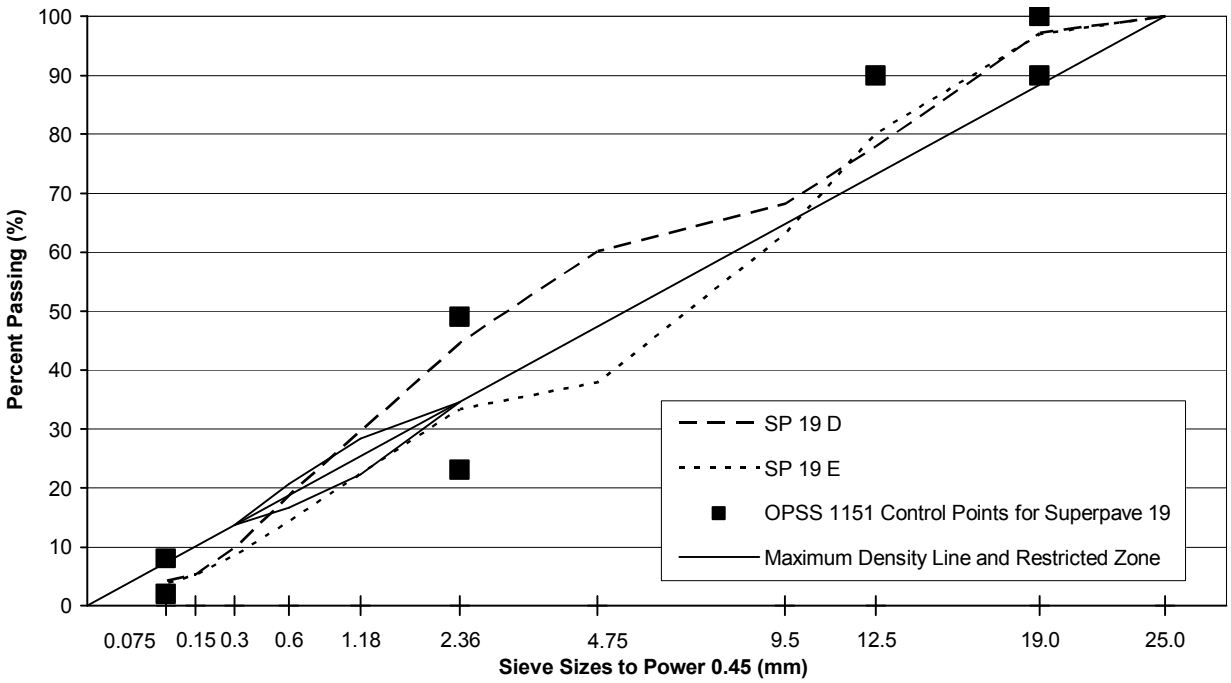

Figure 4.3 Gradations of the SP 19 D and SP 19 E Mixes.

Figure 4.4 compares the gradations of all five mixes. Mix volumetrics and other properties from mix designs are summarized in Table 4.3.

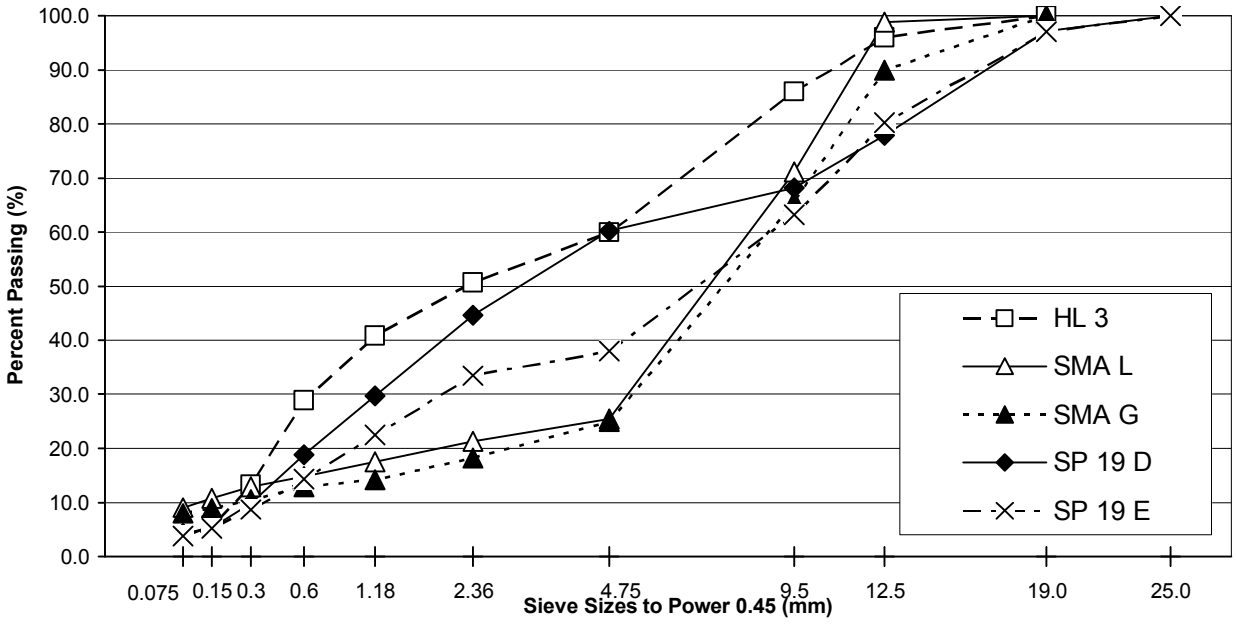

Figure 4.4 Gradations of the HL 3, SMA L, SMA G, SP 19 D and SP 19 E Mixes.

Table 4.3 Summary of Mix Properties

Property	Mix				
	HL 3	SMA L	SMA G	SP 19 D	SP 19 E
Air Voids, %	4.0	4.0	4.0	4.0	4.0
VMA, %	15.5	18.2	17.5	13.3	13.0
VFA, %	74.2	78.0	77.1	69.9	69.4
% G_{mm} @ N_{ini}	NA	-	-	88.5	86.8
% G_{mm} @ N_{max}	NA	-	-	96.9	97.2
Dust Proportion	NA	1.5	-	0.9	1.02
Marshall Stability, N	9,600	NA	NA	NA	NA
Flow, 0.25 mm	8.7	NA	NA	NA	NA

Notes: NA - Not Applicable

The HL 3 mix is a typical dense graded Marshall surface course mix with a maximum aggregate size of 16.0 mm used in Ontario on low to medium volume roads. It is a relatively low cost mix which may typically contain some natural aggregate. The OPSS 1150 standard requires that there must be not less than 5.0 percent asphalt cement in the mix. The HL 3 mix used in this research has met the specified gradation, volumetric, stability and flow requirements.

The SMA is a gap graded premium surface course mix with enhanced rutting resistance. It is used in Ontario on high volume roads, mainly freeways and very busy major arterial city roads for traffic category D (10 to 30 million ESAL's) and E (more than 30 million ESAL's). Only 100 percent crushed and quarried coarse and fine aggregates can be used in SMA mixes. Currently, SMA mixes are designed in Ontario using the Superpave methodology [MTO 2004]. Both, the SMA L and SMA G mixes have been designed for category E roads and both met the specified gradation and volumetric requirements. The gradations of both mixes are very close and asphalt cement contents are the same.

The initial intention was to use only one, SMA G, mix. However, early in the research, the laboratory testing indicated that the asphalt cement in this mix was too soft and did not meet the $G^*/\sin\delta$ requirements when checked on the RTFO residue (as described in Chapter Five, Material Characterization). Another mix, SMA L, was obtained for the research. However, including the SMA G mix in this research provides a unique opportunity to investigate the importance of the stone-on-stone contact for the mix's rutting resistance when the asphalt cement is much softer than specified.

The Superpave 19 mix is typically used as a binder course in Ontario and can be designed for traffic category A, B, C, D and E, i.e. from less than 0.3 million ESAL's to more than 30 million ESAL's. The SP 19 D mix was designed for category D (10 to 30 million ESAL's) and the SP 19 E mix for category E (more than 30 million ESAL's) traffic loading. Both mixes have met the Superpave gyratory compaction requirements at the $N_{initial}$ and N_{max} number of gyrations. Both mixes have also met the gradation and volumetric requirements. The SP 19 E mix is much coarser than the SP 19 D mix. Although the restricted zone is no longer a requirement in Ontario, it is considered to be a good indicator of the coarseness of the mix. The gradation curve of the SP 19 E mix is below the restricted zone while the gradation curve of the SP 19 D mix is on the fine side of the zone, slightly crossing it in the vicinity of the 600 μm sieve. The SP 19 E mix has significantly higher asphalt cement content than the SP 19 D, 4.60 percent and 4.35 percent, respectively. Visually, the SP 19 D mix looked much leaner than the SP 19 E mix.

4.3 SUMMARY

Five asphalt mixes are used in the study, three dense graded mixes and two gap graded SMA mixes. These are typical mixes used for paving projects in Ontario on low to very high volume roads. They include a conventional HL 3 Marshall mix that is anticipated to have only fair resistance to rutting, two SMA mixes with anticipated very good to excellent resistance to rutting, and two Superpave 19 mm mixes with anticipated good to very good resistance to rutting. The mixes incorporate different performance graded asphalt cements ranging from PG58-28 to PG70-28.

All mixes met the Ontario asphalt paving specifications requirements. The SP 19 E mix is much coarser and has significantly higher asphalt cement than the SP 19 D mix.

CHAPTER FIVE
TASK ONE: MATERIAL CHARACTERIZATION

After defining what material characteristics are required for the analysis of the asphalt mix permanent deformation, comprehensive laboratory testing was carried out. This chapter describes the laboratory testing and summarizes the results.

5.1 ACCELERATED LABORATORY PERFORMANCE TESTING

5.1.1 Hamburg Wheel Rut Tester

The Hamburg Wheel Tracking Device (HWTD) is better known in Canada as the Hamburg Wheel Rut Tester (HWRT) and this name is used herein. The HWRT (Figure 5.1) is used for asphalt mix accelerated performance testing in terms of its rutting resistance. In addition, the moisture susceptibility of asphalt mixes can also be evaluated [Cooley 2000, Yildrim 2001]. In a conventional HWRT test, a sample of hot-mix asphalt is submerged in hot water and a steel wheel is rolled across its surface. Two samples can be tested simultaneously in one HWRT run. The wheels can be either steel (47 mm wide) or solid rubber (50 mm wide), and the load applied to the wheels is 710 ± 1 N. The test can also be conducted in dry conditions. The testing is carried out in a temperature controlled cabinet. The customary temperature for the HWRT test in Canada and the United States is 50ºC; this temperature is also typically used in Europe for a climate close to a Superpave high temperature PG of 58. The test path is 230 ± 10 mm long and the average speed of each wheel is approximately 1.1 km/h (53 ± 2 wheel passes per minute). Samples can be either 260 mm x 300 mm and typically 40 mm, 80 mm, or 120 mm thick slabs or three cores or laboratory prepared Superpave Gyratory Compactor (SGC) briquettes of 150 mm diameter. Figure 5.2 shows the configuration of the accelerated rutting performance testing in the HWRT. The number of wheel passes being used in the United States (Texas, Washington, and Colorado), is typically 20,000 although up to 100,000 passes can be applied. Susceptibility to rutting (and moisture susceptibility) is mainly based on pass/fail criteria. The Colorado Department of Transportation, for instance, recommends a maximum allowable rut depth of 4.0 mm at 10,000 wheel passes [FHWA 2002] and 10.0 mm at 20,000 wheel passes while the Texas Department of Transportation specification requires that the rut depth be less than 12.0 mm at 20,000 passes (in a wet test using a steel wheel) [Texas DOT 2003]. The analysis of HWRT testing results can include post-compaction consolidation, creep slope, stripping inflection point,

and stripping slope [FHWA 2002]. In Europe, standard prEN 12697-22 [CEN 2004] is used, although some countries have developed their own standards (United Kingdom – BS EN 12697 -22:2003 [BS 2003], for instance). Some researchers use the rut tester with a solid rubber wheel [Cooley 2000]. The author of this thesis observed significant aggregate damage caused by the steel wheel in a study completed in 2004 [Uzarowski 2004].

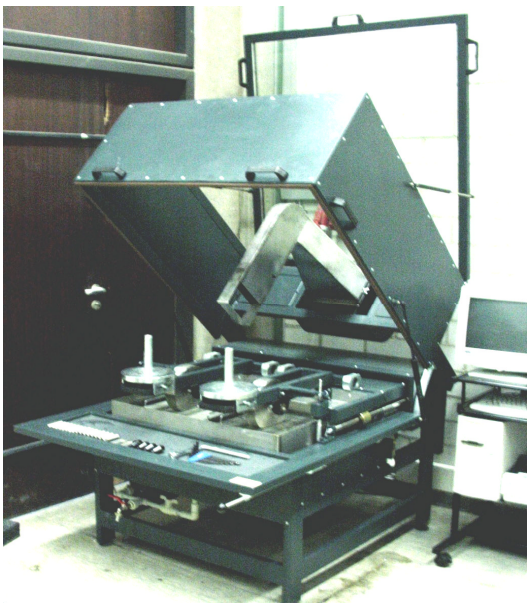

Figure 5.1 General View of the Hamburg Wheel Rut Tester

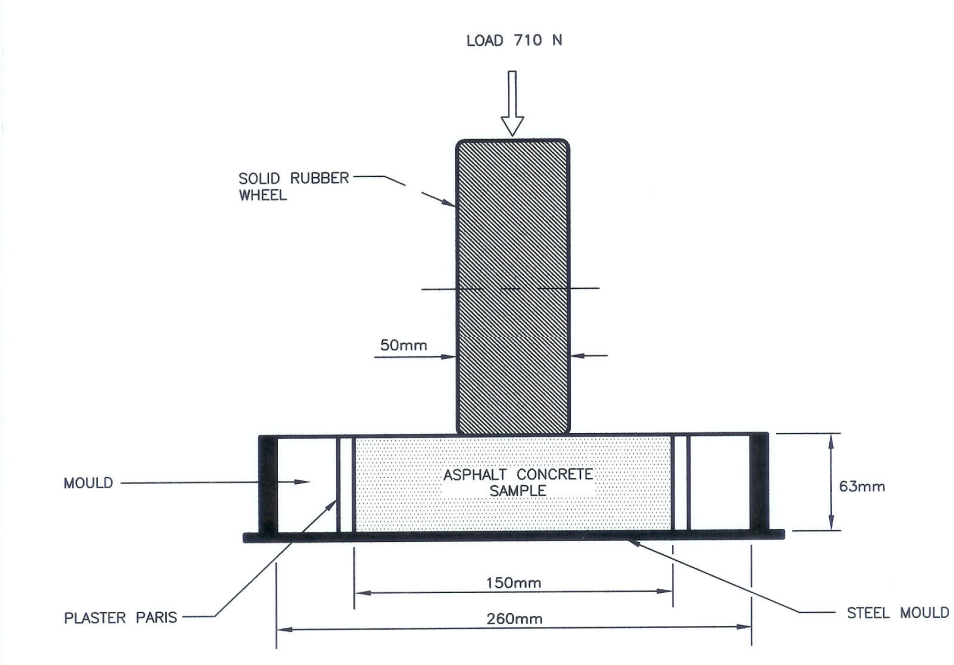

Figure 5.2 Diagram of the Rutting Resistance Testing in the HWRT

The objective of the HWRT testing in this research was to evaluate the asphalt mix resistance to rutting only, without analysing the impact of moisture stripping. Therefore, only the dry test was used in this research. Also, in order to avoid any additional damage to the aggregates in the mixes, only the solid rubber wheel was used. All the HWRT testing was carried out at a temperature of 50ºC. During the test, the permanent deformation was computer monitored and stored every 10 passes. The deformation at 10,000 passes, deformation increase from 10,000 to 15,000 passes and from 10,000 to 20,000 passes, and the final deformation at 20,000 passes are reported in HWRT by default.

5.1.2 Sample Preparation

Each HWRT sample consisted of three cylindrical specimens, trimmed to fit into the mould, as shown in Figure 5.3. In order to avoid any movement of the samples during the testing, plaster of Paris was used to fix the specimens in the moulds. The height of the specimens was 63 mm (2.5 inch).

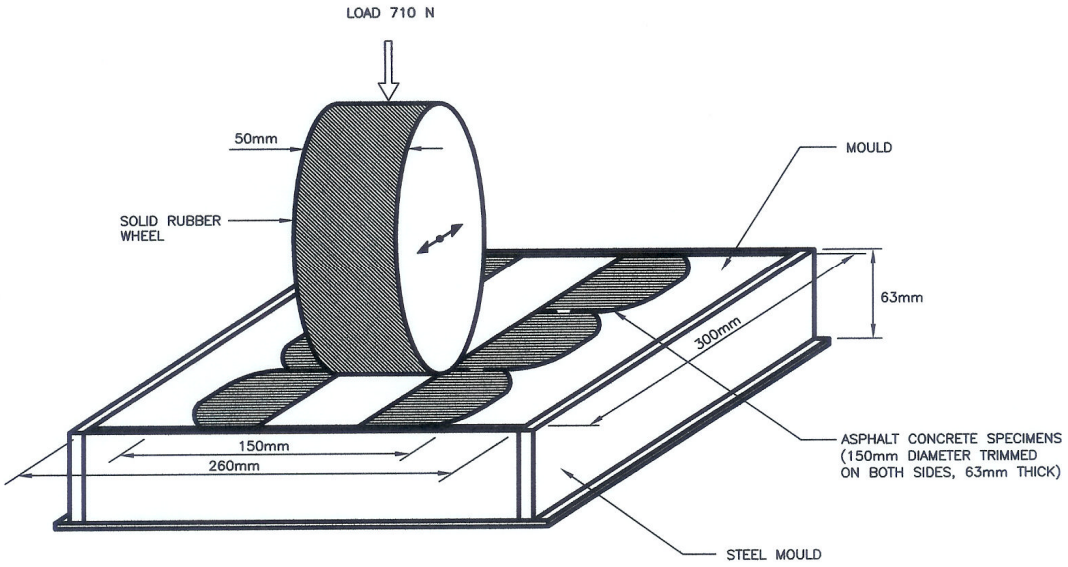

Figure 5.3 Sample setup in the HWRT.

All of the cylindrical specimens were prepared in the Superpave Gyratory Compactor (SGC). The target air voids in the specimens were the same as for the dynamic modulus and creep testing, i.e. 6.0 ± 1.0 percent. Table 5.1 shows a summary of the air voids results in the HWRT specimens. Detailed data is provided in Appendix A.

Table 5.1 Summary of Air Voids in HWRT Specimens.

Mix	Air Voids (%)	
	Mean	Standard Deviation
HL 3	6.5	0.3
SMA L	6.8	0.2
SMA G	6.2	0.2
SP 19 D	6.5	0.2
SP 19 E	6.7	0.3

5.1.3 HWRT Testing Results

The results of the testing in the HWRT are summarized in Table 5.2. Table 5.3 shows the ranking of the mixes. The ranking after 10,000 and 20,000 passes is the same, with SP 19 D being the best and exhibiting the smallest rutting, SMA L being the second, SP 19 E being the third, SMA G being the fourth and HL 3 being the last and exhibiting the largest rutting. However, the ranking for the zone from 10,000 to 15,000 passes and from 10,000 to 20,000 passes is different. SMA L is the best one with the smallest rutting increase, SP 19 D is the second, SMA G is the third, SP 19 E is the fourth and HL 3 is the last one. Generally, the rutting in this HWRT in this research using the dry test and a solid rubber wheel is much lower than the maximum allowable rut depth in the HWRT in a wet test using a steel wheel.

Table 5.2 Summary of HWRT Testing Results.

Mix Type	Set	Temperature (ºC)	Rut Depth (mm)			Total Rut Depth after 20,000 Passes
			Number of Passes			
			10,000	10,000 to 15,000	10,000 to 20,000	
HL 3	1	50	1.52	0.18	0.32	1.84
	2		1.80	0.20	0.36	2.16
	3		2.06	0.36	0.68	2.74
	4		2.00	0.36	0.70	2.70
	Average		1.85	0.28	0.52	2.36
SMA L	1	50	1.28	0.08	0.14	1.42
	2		1.34	0.10	0.16	1.50
	3		1.34	0.10	0.18	1.52
	Average		1.32	0.09	0.16	1.48
SMA G	1	50	1.52	0.14	0.24	1.76
	2		1.82	0.14	0.24	2.06
	3		1.44	0.14	0.22	1.66
	Average		1.59	0.14	0.23	1.83
SP 19 D	1	50	0.86	0.12	0.18	1.04
	2		0.96	0.08	0.16	1.12
	Average		0.91	0.10	0.17	1.08
SP 19 E	1	50	1.72	0.20	0.32	2.04
	2		1.22	0.16	0.28	1.50
	3		1.04	0.10	0.16	1.20
	Average		1.33	0.15	0.25	1.58

Table 5.3 Mix Ranking in HWRT Testing.

Mix Type	Mix Ranking			
	Number of Passes			
	10,000	10,000 to 15,000	10,000 to 20,000	20,000
HL 3	5	5	5	5
SMA L	2	1	1	2
SMA G	4	3	3	4
SP 19 D	1	2	2	1
SP 19 E	3	4	4	3

Figures 5.4 to 5.13 show the permanent deformation in the HWRT versus the number of cycles and the time of loading of all five mixes. The time of loading for one pass is 0.21 sec; therefore, the total loading time for the entire test of 20,000 passes is 4,200 sec or 70 minutes. Figures 5.14 and 5.15 compare the rutting of all five mixes.

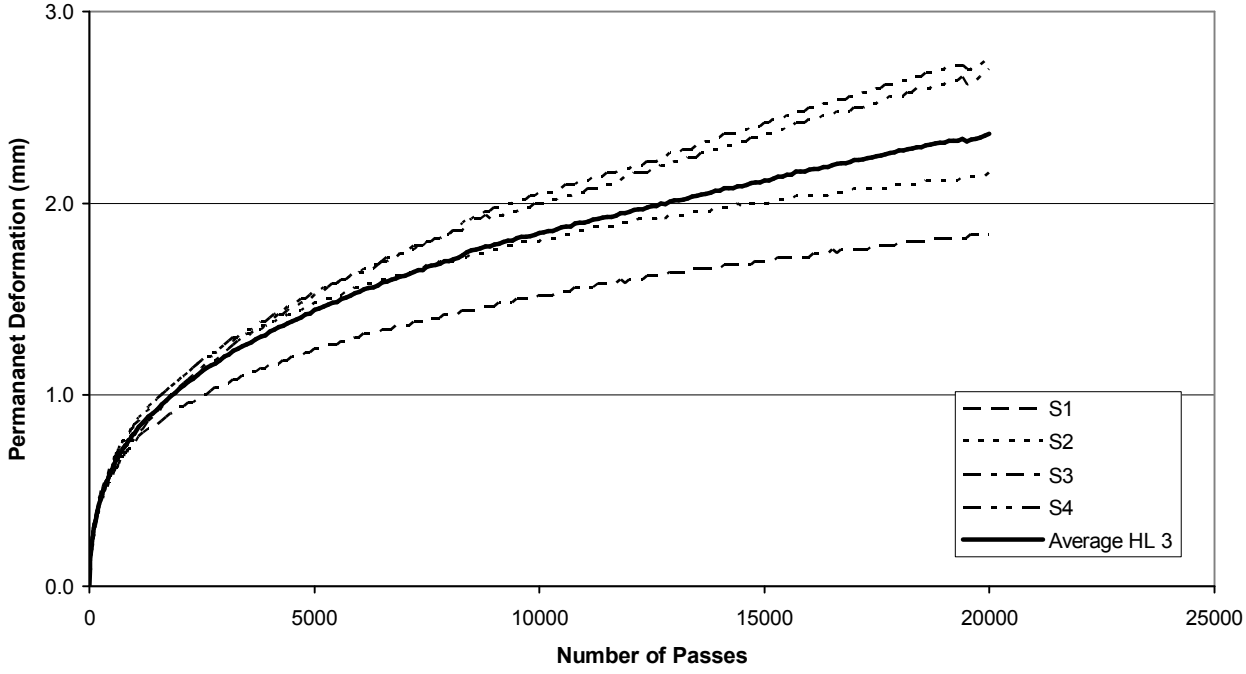

Figure 5.4 Permanent Deformation versus Number of Passes in HWRT Testing of the HL 3 Mix.

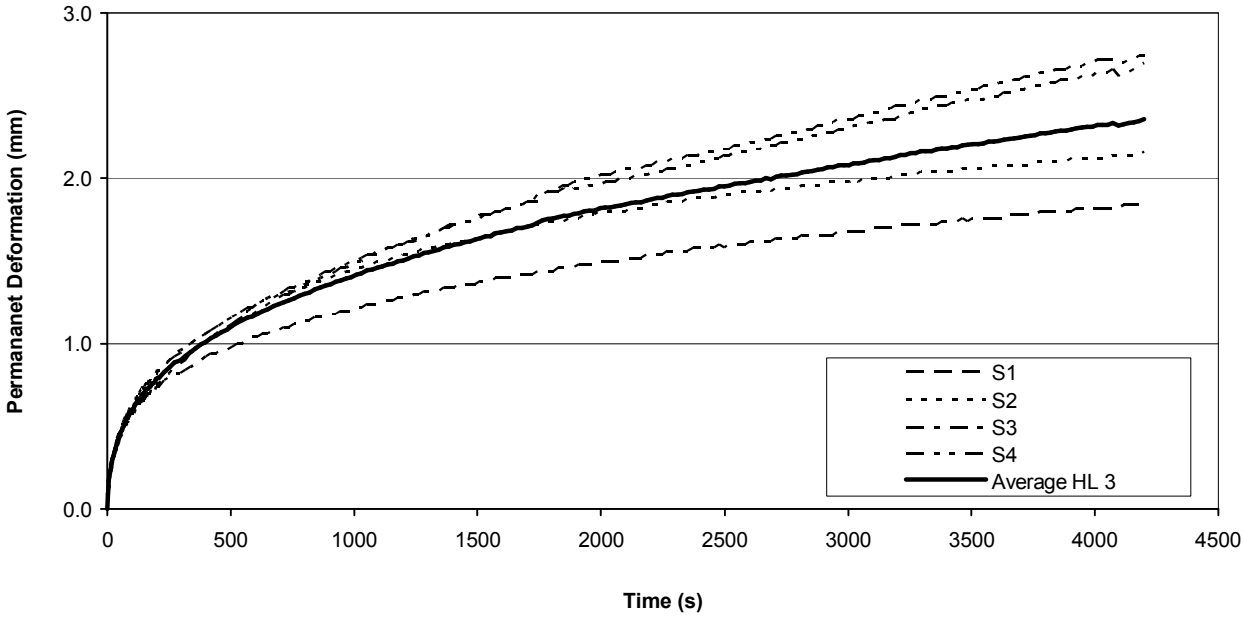

Figure 5.5 Permanent Deformation versus Time of Loading in HWRT Testing of the HL 3 Mix.

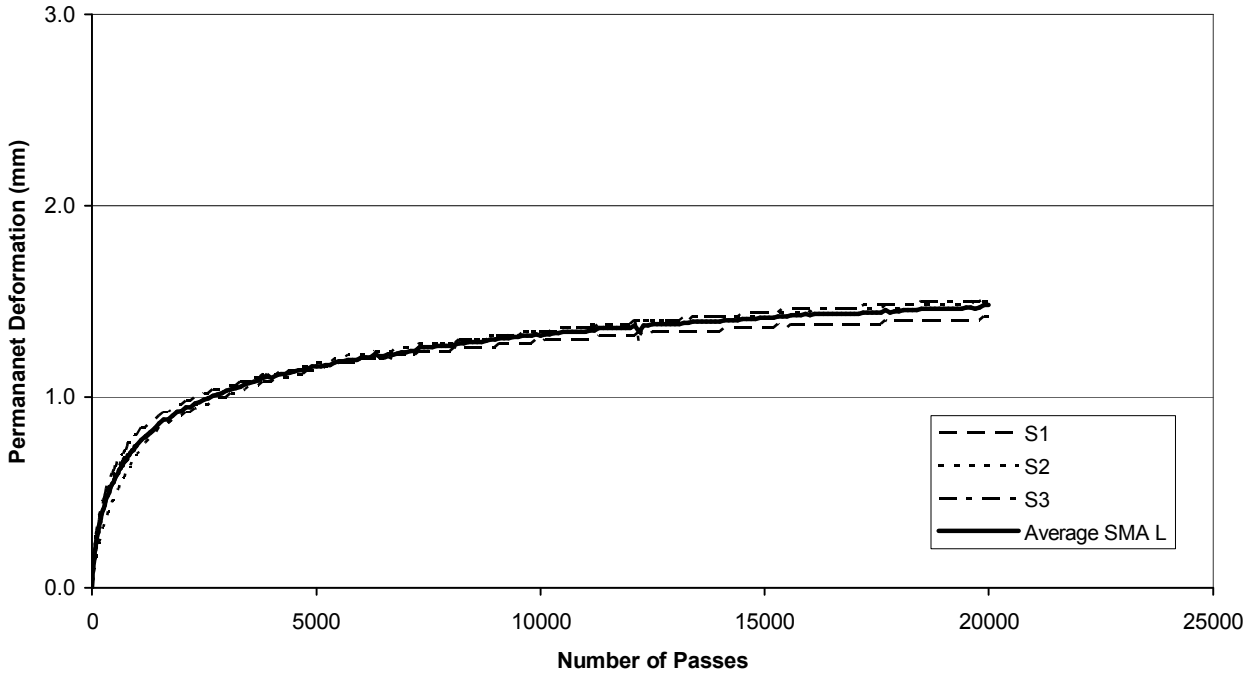

Figure 5.6 Permanent Deformation versus Number of Passes in HWRT Testing of the SMA L Mix.

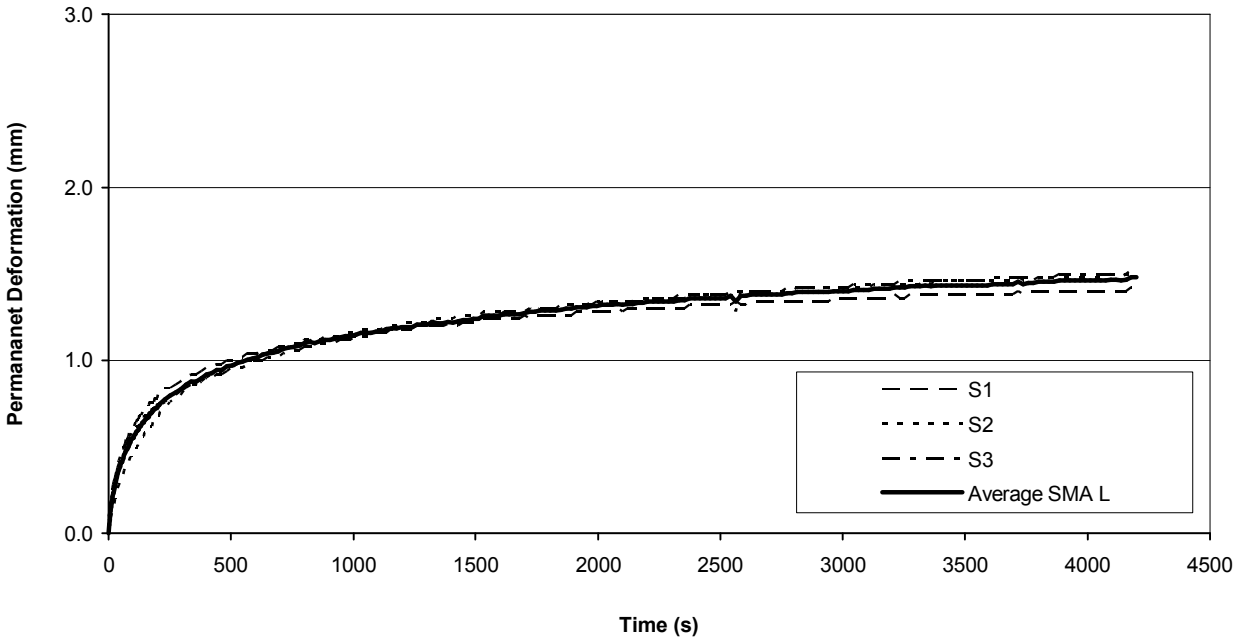

Figure 5.7 Permanent Deformation versus Time of Loading in HWRT Testing of the SMA L Mix.

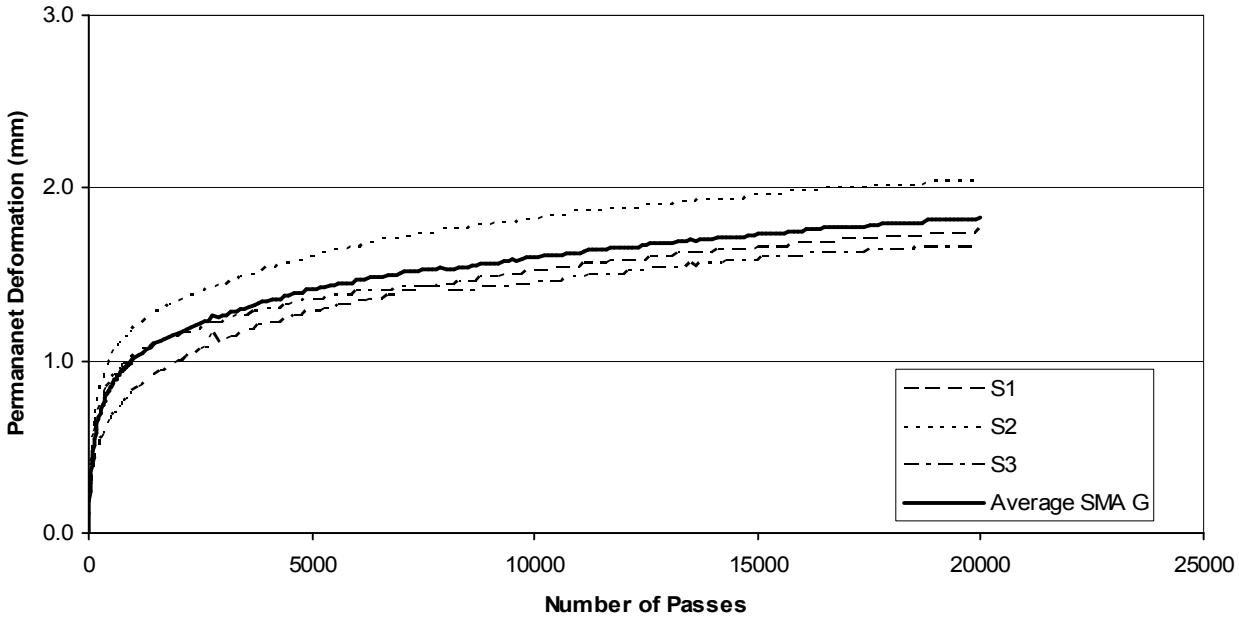

Figure 5.8 Permanent Deformation Versus Number of Passes in HWRT Testing of the SMA G Mix.

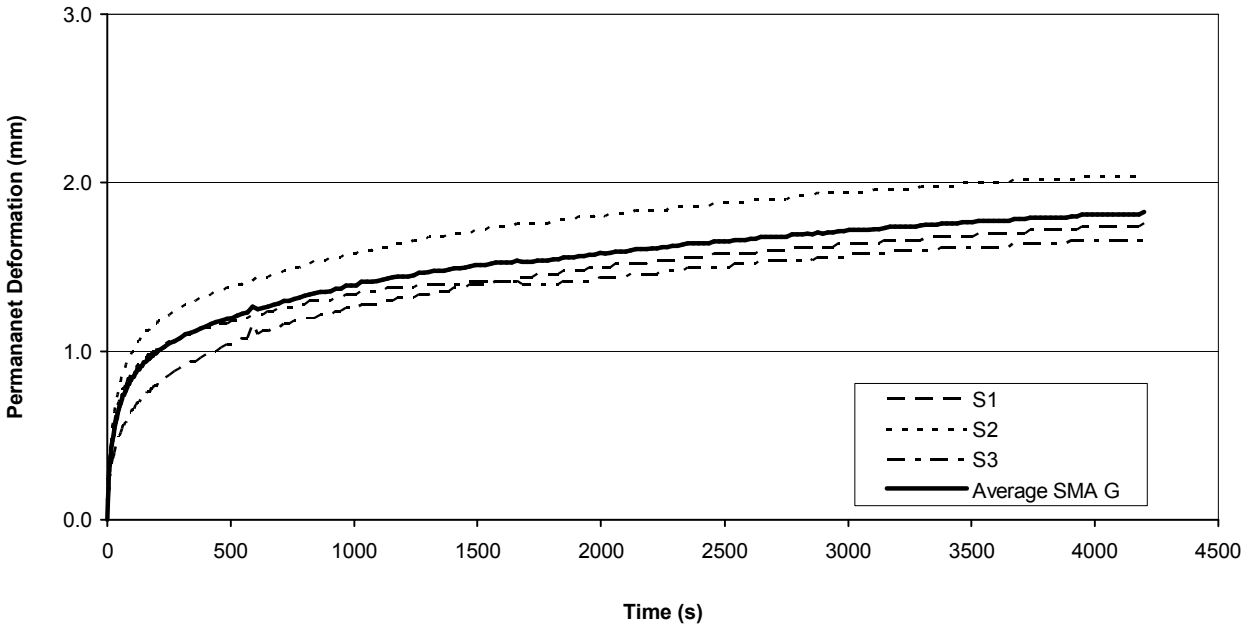

Figure 5.9 Permanent Deformation versus Time of Loading in the HWRT Testing of the SMA G mix.

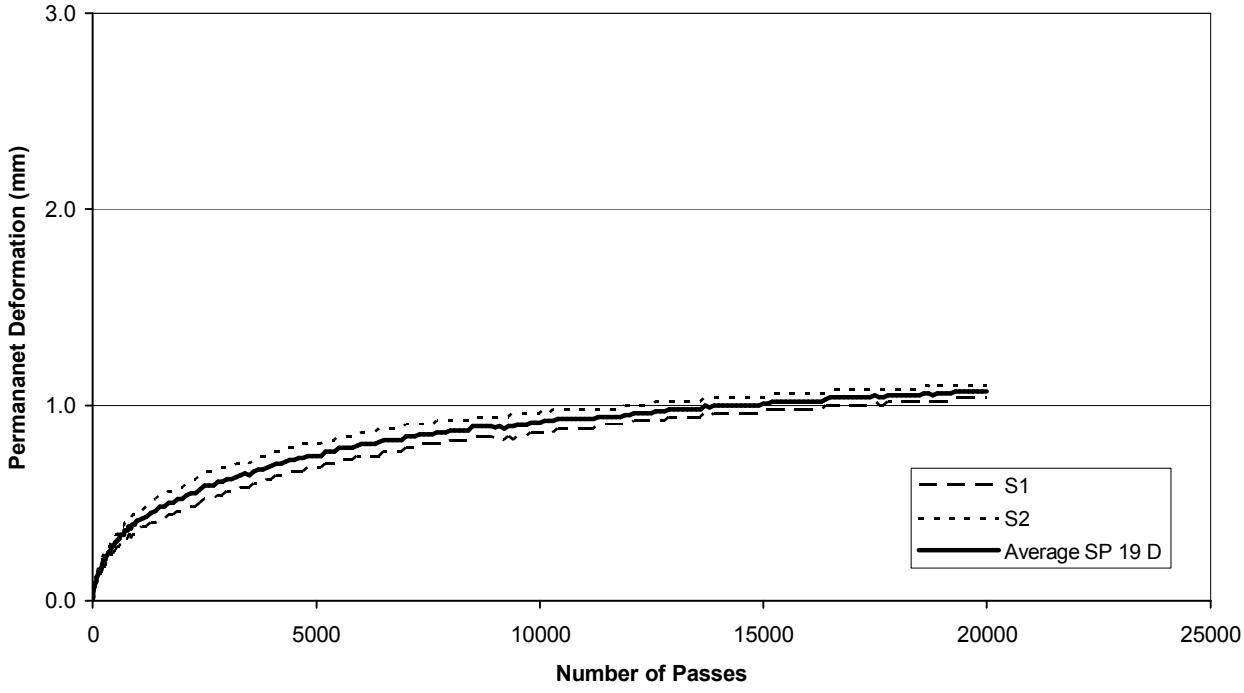

Figure 5.10 Permanent Deformation versus Number of Passes in HWRT Testing of the SP 19 D Mix.

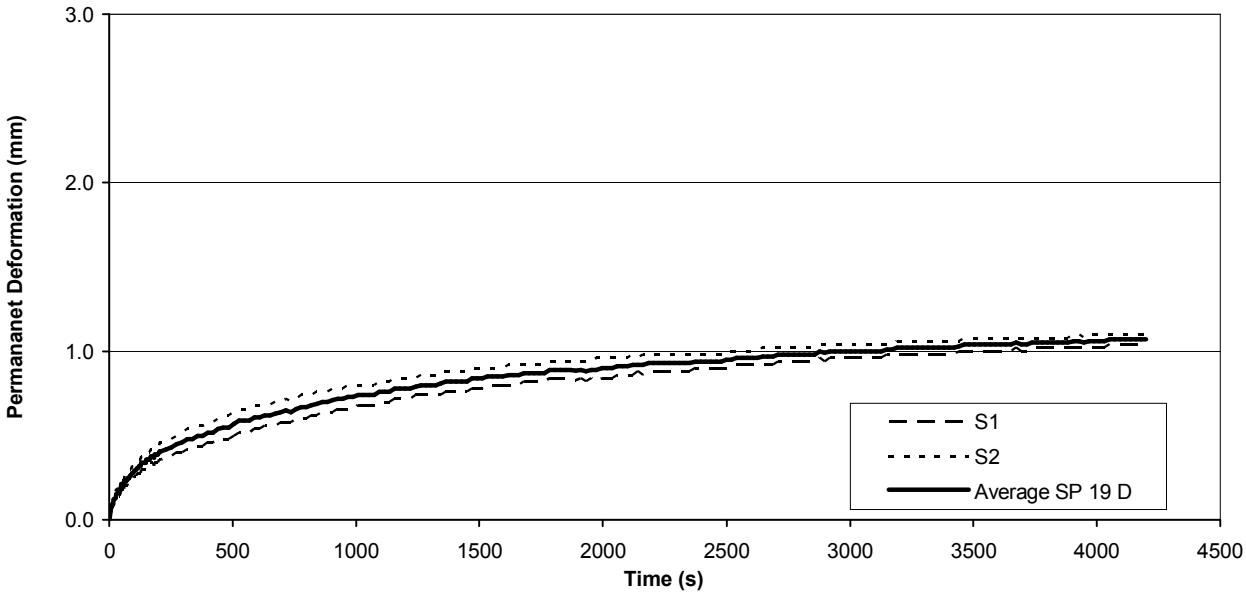

Figure 5.11 Permanent Deformation versus Time of Loading in HWRT Testing of the SP 19 D Mix.

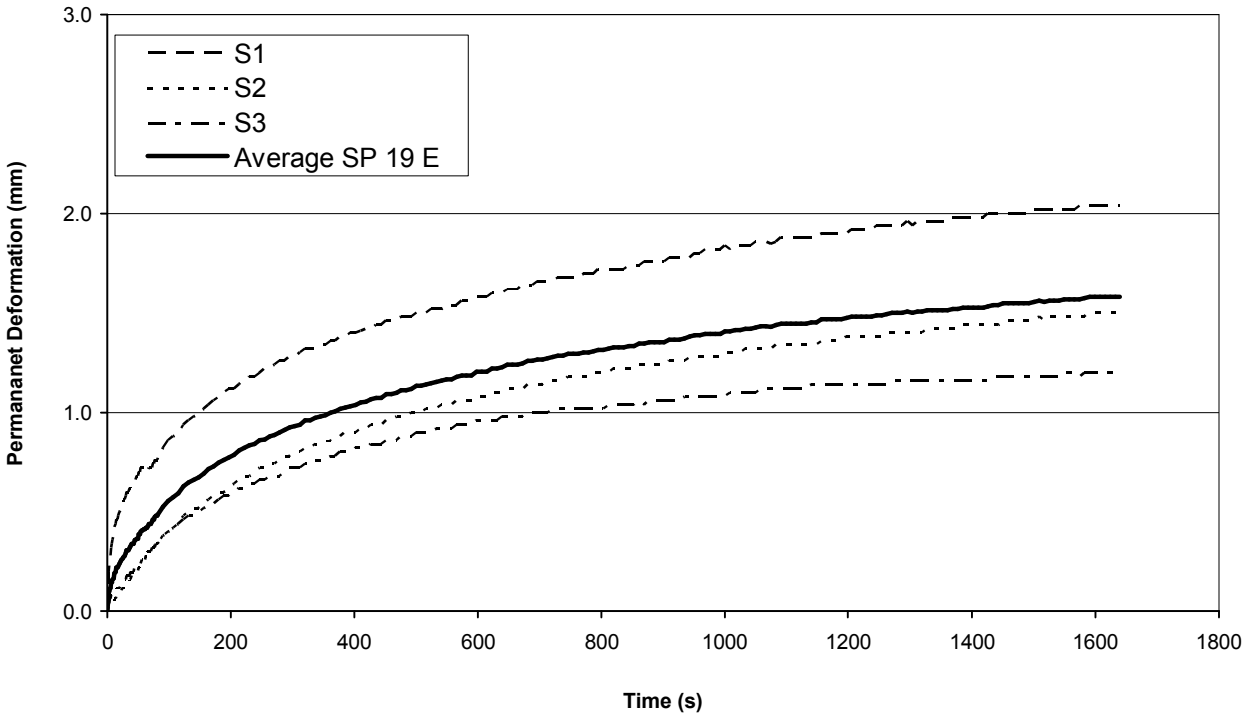

Figure 5.12 Permanent Deformation versus Number of Passes in HWRT Testing of the SP 19 E Mix.

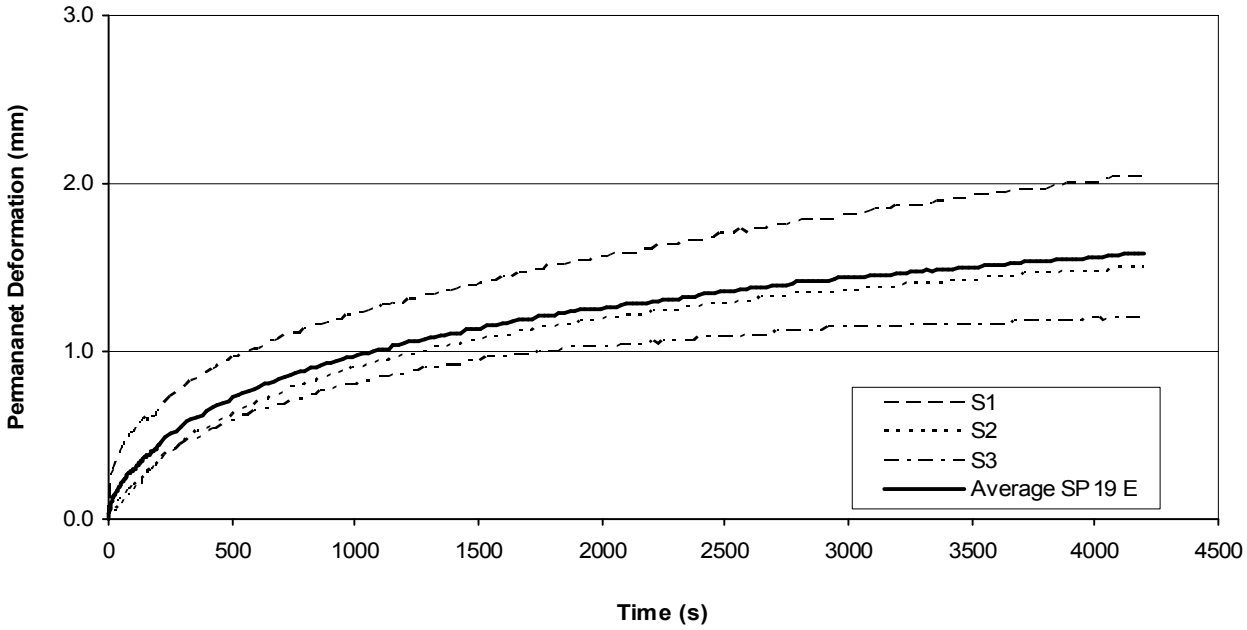

Figure 5.13 Permanent Deformation versus Time of Loading in HWRT Testing of the SP 19 E Mix.

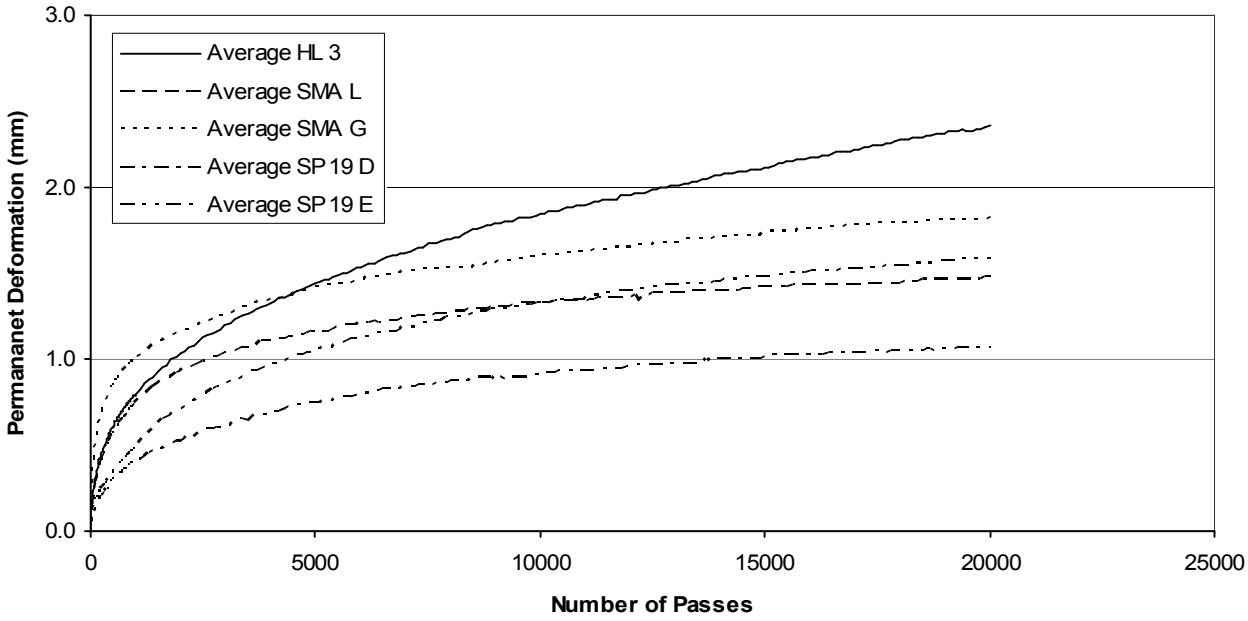

Figure 5.14 Comparison of Permanent Deformations versus Number of Passes Relationships in HWRT Testing of all Five Mixes.

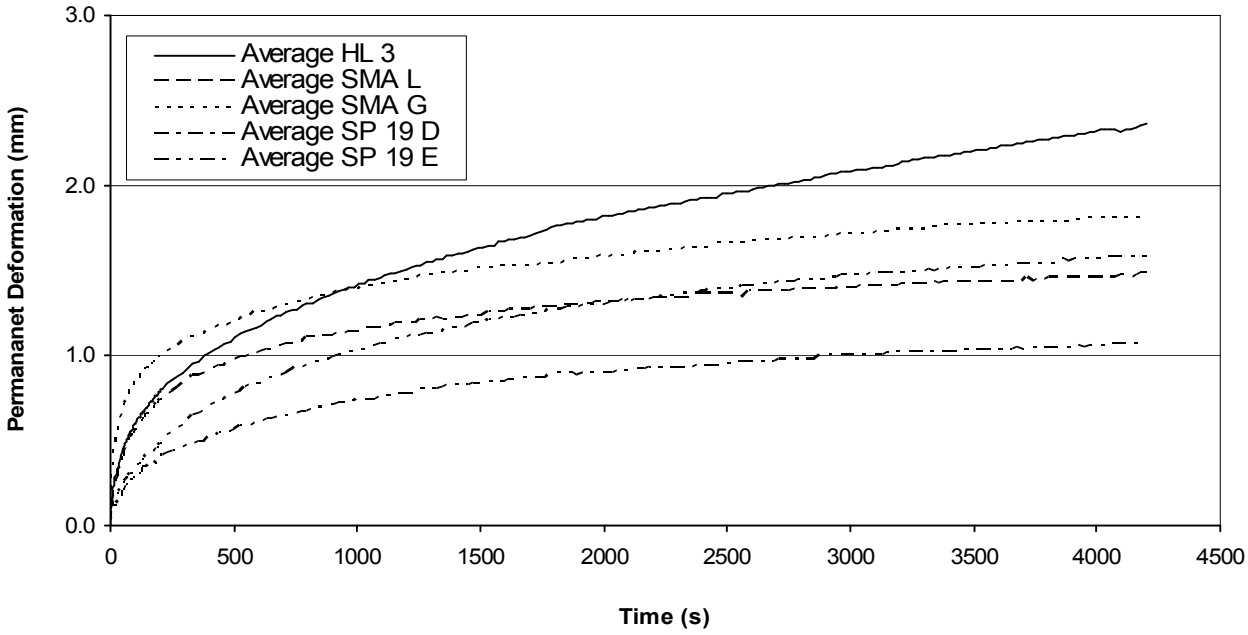

Figure 5.15 Comparison of Permanent Deformations versus Time of Loading Relationships in HWRT Testing of all Five Mixes.

There is a significant difference between the shape of the permanent deformation curves of the gap graded SMA L and SMA G mixes and the dense graded HL 3, SP 19 D and SP 19 E mixes. The densification of the SMA mixes is high at the beginning of the test (Phase 1) and then the deformation curve flattens to reach the constant slope (Phase 2) after about 6,000 passes. The densification of the dense graded mixes is gradual, proportionally small at the beginning of the test (Phase 1) and then after about 8,000 passes the deformation reaches Phase 2 and a constant slope. The slope of the dense graded mixes in Phase 2 is generally steeper than that of the SMA mixes.

Table 5.4 shows the parameters, slope and intercept, of the rutting curves in Phase 2 in the HWRT testing and the mix ranking in the 10,000 to 20,000 passes zone. The ranking is based on the slope, i.e. the better the ranking the flatter the slope in Phase 2. Generally, the SMA mixes performed better in this zone than the dense graded mixes.

Table 5.4 Rutting Curve Parameters in HWRT Testing.

Mix	Slope	Intercept	Ranking in 10,000 to 20,000 Passes Zone
HL 3	0.00065	1.3	5
SMA L	0.00019	1.2	1
SMA G	0.00030	1.4	3
SP 19 D	0.00021	0.7	2
SP 19 E	0.00034	1.1	4

Better performance of SMA mixes in Phase 2 is considered to be due to different mechanisms that control the behaviour of both groups of mixes. In the dense graded mixes, the resistance to permanent deformation relies mainly on the asphalt cement – aggregate matrix, i.e. the mixture of the asphalt cement and fine aggregates, with coarse particles "suspended" in the mix and not playing the major role. In the gap-graded SMA mixes, the resistance to permanent deformation is mainly provided by stone-on-stone contact. The SMA mixes are rich in asphalt cement and the film of the asphalt cement is thicker than that in the dense graded mixes. Therefore, the initial densification is relatively high until the stone-on-stone contact is triggered. Then, the rate of permanent deformation slows down, eventually becoming slower than that of the dense graded mixes. For a long loading time, this typically results in total SMA rutting lower than the rutting of the dense graded mixes.

5.2 DYNAMIC MODULUS TESTING

The new MEPDG Level 1 requires that a time-temperature dependent dynamic modulus (E*) and Poisson's ratio be determined for hot-mix asphalt materials [NCHRP 2004a]. The procedure for the dynamic modulus testing is covered by the AASHTO TP62-03 standard [AASHTO 2003].

5.2.1 Interlaken Asphalt Testing System

The Interlaken Universal Test Machine/Simple Performance Tester (Interlaken) consists of an integrated load frame which contains its own hydraulic power supply, a triaxial cell, an environmental chamber and a control console. The Interlaken was used for the dynamic modulus testing and the triaxial repeated load creep and creep recovery testing. The Interlaken can also be used for uniaxial and triaxial static creep

testing, fatigue resistance test on beam asphalt specimens, creep compliance test, indirect tensile resilient modulus test, and other tests [ITC 2004]. Figure 5.16 shows a general view of the Interlaken and Figure 5.17 shows the testing configuration. The system is fully computer controlled. Three 75 mm long Linear Variable Differential Transducers (LVDT's) were used on each sample to determine the deformations. All transducer measurements were monitored and recorded by computer.

Figure 5.16 General View of the Interlaken Universal Test Machine/Simple Performance Tester.

Figure 5.17 Dynamic Modulus Testing Setup in the Interlaken.

5.2.2 Sample Preparation

A proper specimen preparation for the dynamic modulus testing may require a significant number of trials. The procedure requires that the 150 mm diameter cylinders, prepared in the Superpave Gyratory Compactor (SGC), be cored to obtain 100 mm diameter specimens [Bonaquist 2003]. Figure 5.18 shows the coring system used in this research. Figure 5.19 shows cored specimens of the HL 3, SMA G, SP 19 D and SP 19 E mixes.

Figure 5.18 Coring System Used to Obtain 100 mm Cores from 150 mm Diameters SGC Cylinders.

Figure 5.19 Cored Specimens of the SMA G (#D1), SP 19 D (#57), SP 19 E (# 39) and HL 3 (#46) Mixes.

As the air voids of the core taken from the centre of the cylinder may be significantly lower than those of the entire cylinder (about 0.2 to 1.5 percent, depending on the type of mix), obtaining the specimens with the target air voids level of 6.0 ± 1.0 percent may be a relatively difficult task. Figure 5.20 shows a core of the SMA mix and an asphalt ring remaining from the coring operation. The surface of the core looks

tight, with low air voids while relatively large voids are visible in the outside surface of the ring. Table 5.5 shows the difference between the air voids of the SGC specimens and the air voids of the cores in the specimens used in the dynamic modulus test. The lowest average difference was that of the HL 3 mix (0.3 percent) and the highest difference was that of the SP 19 E mix (1.1 percent).

Figure 5.20 Core of the SMA G mix and the ring remaining after the coring.

Table 5.5 Summary of Dynamic Modulus Testing Specimen Densities and Air Voids.

Mix Type	Maximum Relative Density	SGC Cylinders		Cores		Voids Difference (%)
		Number	Air Voids (%)	Bulk Relative Density	Air Voids (%)	
HL 3	2.540	33	6.5	2.383	6.2	0.3
		34	6.6	2.382	6.2	0.4
		36	6.5	2.383	6.2	0.3
		Mean	6.5	2.383	6.2	0.3
SMA L	2.599	4	6.7	2.433	6.4	0.3
		7	6.6	2.433	6.4	0.2
		11	6.7	2.434	6.3	0.4
		Mean	6.7	2.433	6.4	0.3
SMA G	2.684	5	6.9	2.525	5.9	0.9
		6	6.8	2.520	6.1	0.7
		20	5.6	2.539	5.4	0.2
		Mean	6.4	2.528	5.8	0.6
SP 19 D	2.570	3	7.4	2.403	6.5	0.9
		4	7.3	2.407	6.3	1.0
		51	7.6	2.395	6.8	0.8
		Mean	7.5	2.402	6.5	0.9
SP 19 E	2.579	8	6.7	2.445	5.2	1.5
		22	7.0	2.418	6.2	0.7
		25	6.8	2.431	5.7	1.0
		Mean	6.8	2.431	5.7	1.1

5.2.3 Dynamic Modulus Testing Results

The testing was conducted at five different temperatures (-10 ºC, 4.4 ºC, 21.1 ºC, 37.8 ºC, and 54.4ºC) and six loading frequencies (0.1 Hz, 0.5 Hz, 1.0 Hz, 5.0 Hz, 10.0 Hz, and 25.0 Hz). The axial strains were ranging from 50 to 150 microstrains. The dynamic modulus (E*) and phase angle (ϕ) were determined for each mix. The dynamic modulus was calculated over the last five loading cycles using the following equation [AASHTO 2003]:

$$|E^*| = \sigma_0 / \varepsilon_0 \quad (5.1)$$

where:

σ_0 = average peak stress

ε_0 = average peak strain

The average peak stress was calculated as follows:

$$\sigma_0 = \bar{P} / A \quad (5.2)$$

where:

σ_0 = average peak stress

$\bar{P}$ = average peak load

A = area of specimen

The average peak strain was calculated as follows [AASHTO 2003]:

$$\varepsilon_0 = \bar{\Delta} / GL \quad (5.3)$$

where:

ε_0 = average peak strain

$\bar{\Delta}$ = average peak deformation

GL = gage length

The phase angle was calculated individually for each LVDT [AASHTO 2003]:

$$\phi = (t_i / t_p) * (360) \quad (5.4)$$

where:

ϕ = phase angle

t_i = average lag time between a cycle of stress (sec)

t_p = average time for a stress cycle (sec)

The dynamic modulus and phase angle were determined for a minimum of three specimens of each mix. Table 5.6 shows a summary of the dynamic modulus testing results for all five mixes.

Table 5.6 Summary of Dynamic Modulus Testing Results

Mix	Frequency (Hz)	Time (sec)	Average Modulus (kPa)				
			-10.0ºC	4.4ºC	21.1ºC	37.8ºC	54.4ºC
HL 3	25	0.04	29,035,597	18,234,080	8,517,013	3,677,663	1,771,922
	10	0.1	26,140,927	15,782,363	6,724,647	2,531,608	1,241,269
	5	0.2	23,758,520	14,155,470	5,632,195	2,001,509	1,062,556
	1	1	19,463,937	8,970,193	3,567,388	1,324,485	789,298
	0.5	2	17,024,643	8,410,651	2,903,347	1,139,086	723,110
	0.1	10	12,462,463	5,904,908	1,923,555	876,328	543,014
SMA L	25	0.04	28,328,933	17,781,917	8,991,958	3,787,753	1,635,066
	10	0.1	26,148,687	15,864,307	7,122,266	2,577,009	1,134,992
	5	0.2	22,299,133	14,503,093	6,005,836	2,018,145	939,640
	1	1	19,474,150	11,373,943	3,813,784	1,312,803	743,254
	0.5	2	16,197,897	10,030,364	3,115,649	1,124,041	698,482
	0.1	10	13,671,253	7,409,310	2,052,178	858,210	660,503
SMA G	25	0.04	21,880,647	14,303,734	5,971,156	2,475,618	1,401,389
	10	0.1	19,329,337	12,316,603	4,511,806	1,719,027	1,043,258
	5	0.2	17,532,513	10,777,247	3,689,282	1,406,425	903,193
	1	1	13,743,870	7,607,238	2,286,621	1,003,376	733,605
	0.5	2	12,003,197	6,335,759	1,868,067	902,241	683,879
	0.1	10	8,276,640	4,028,829	1,231,840	749,947	582,696
SP 19 D	25	0.04	30,403,193	21,183,310	11,078,390	5,898,574	2,975,443
	10	0.1	27,300,243	18,869,130	9,208,961	4,534,139	2,165,085
	5	0.2	25,117,033	17,367,207	8,078,782	3,780,130	1,806,861
	1	1	21,139,430	14,062,450	5,656,008	2,508,557	1,349,179
	0.5	2	18,947,950	12,641,303	4,764,570	2,127,961	1,224,906
	0.1	10	14,549,327	9,637,153	3,307,524	1,547,471	1,036,457
SP 19E	25	0.04	27,417,293	19,913,503	10,709,234	4,847,736	2,234,002
	10	0.1	24,465,313	17,316,047	8,545,018	3,457,608	1,695,693
	5	0.2	22,305,090	15,563,347	7,151,440	2,817,195	1,484,138
	1	1	18,038,760	11,729,560	4,506,336	1,957,403	1,242,169
	0.5	2	15,865,667	10,040,225	3,606,568	1,725,655	1,175,920
	0.1	10	11,332,473	6,810,045	2,272,055	1,370,845	1,088,088

At the specified range of the strain level (50 to 150 microstrains), the deformations of the HL 3 and SMA G mixes at a temperature of 54.4ºC were outside the range of the LVDT's. Therefore, the strain level was reduced to 40 microstrains. The specimens of these mixes exhibited a significant unrecoverable deformation (about 2.0 mm) during the dynamic modulus testing at the temperature of 54.4ºC and hair cracks were observed in some specimens after the testing.

The behaviour of asphalt materials depends on temperature and time of loading in the test. In order to compare test results of different mixes, a single master curve was formed for each mix. A master curve for the SP 19 D mix is shown in Figure 5.21 as an example. The data collected at different temperatures was shifted relative to the time of loading to form a single curve. The shift factor a(T) defines the required shift (as log of time) at a given temperature. The shift factor was calculated using the following equation [AASHTO 2003]:

$$t_r = t / a(T) \qquad (5.5)$$

where:

t_r = reduced time, time of loading at the reference temperature

t = time of loading, the reciprocal of the loading frequency

a(T) = shift factor as a function of temperature

T = temperature

The shift factor is shown in Figure 5.22. Figure 5.23 shows the master curves of all five mixes.

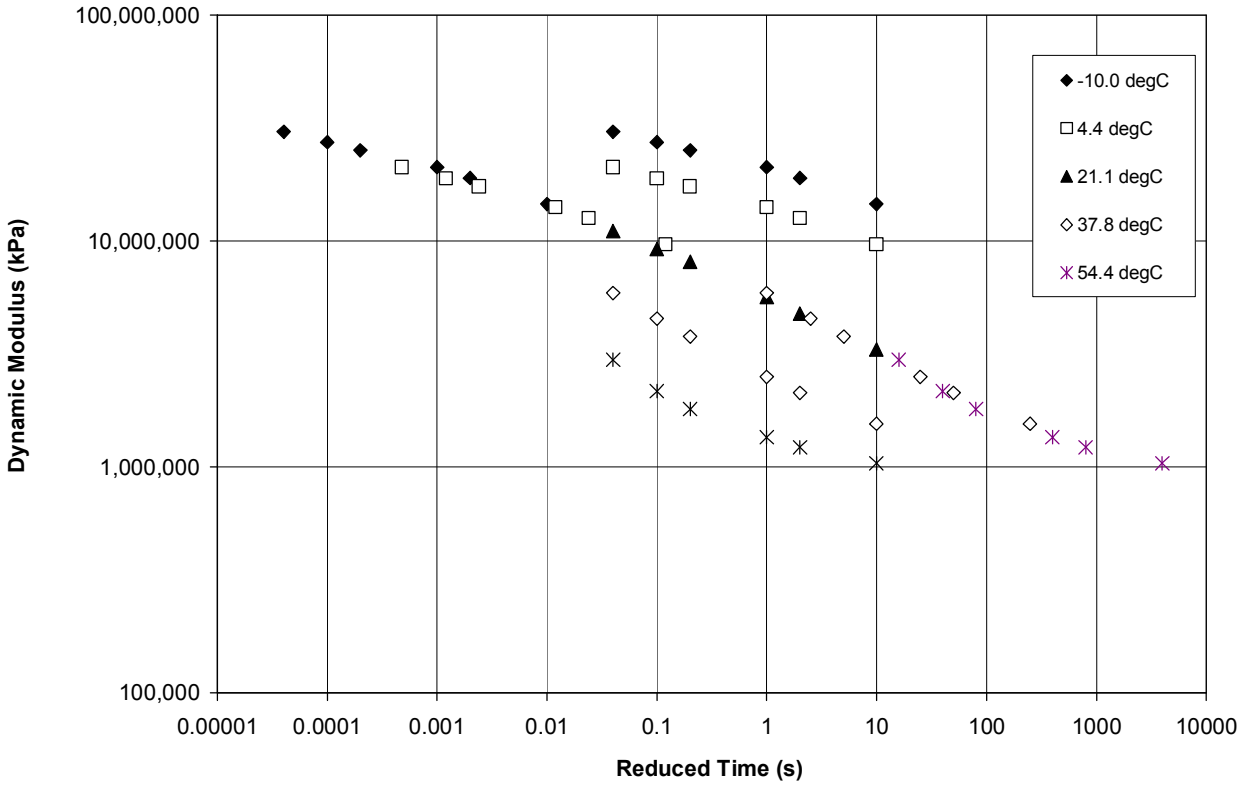

Figure 5.21 Master Curve of the SP 19 D Mix.

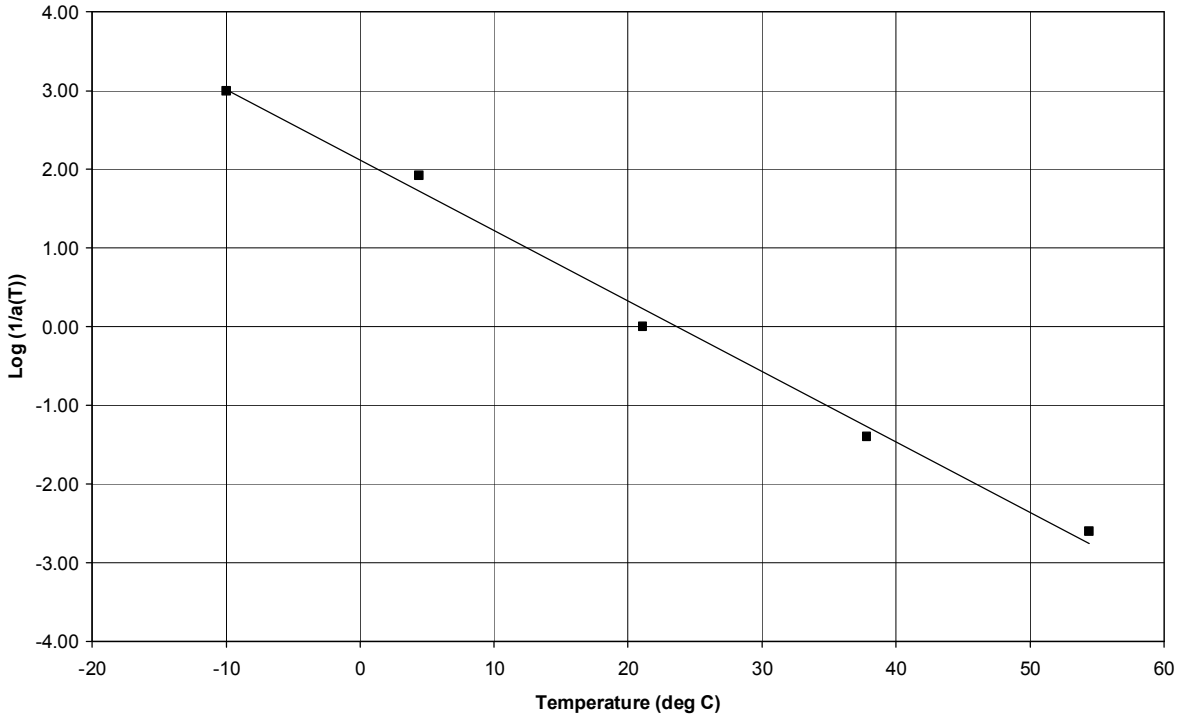

Figure 5.22 Shift Factor of the SP 19 D Mix.

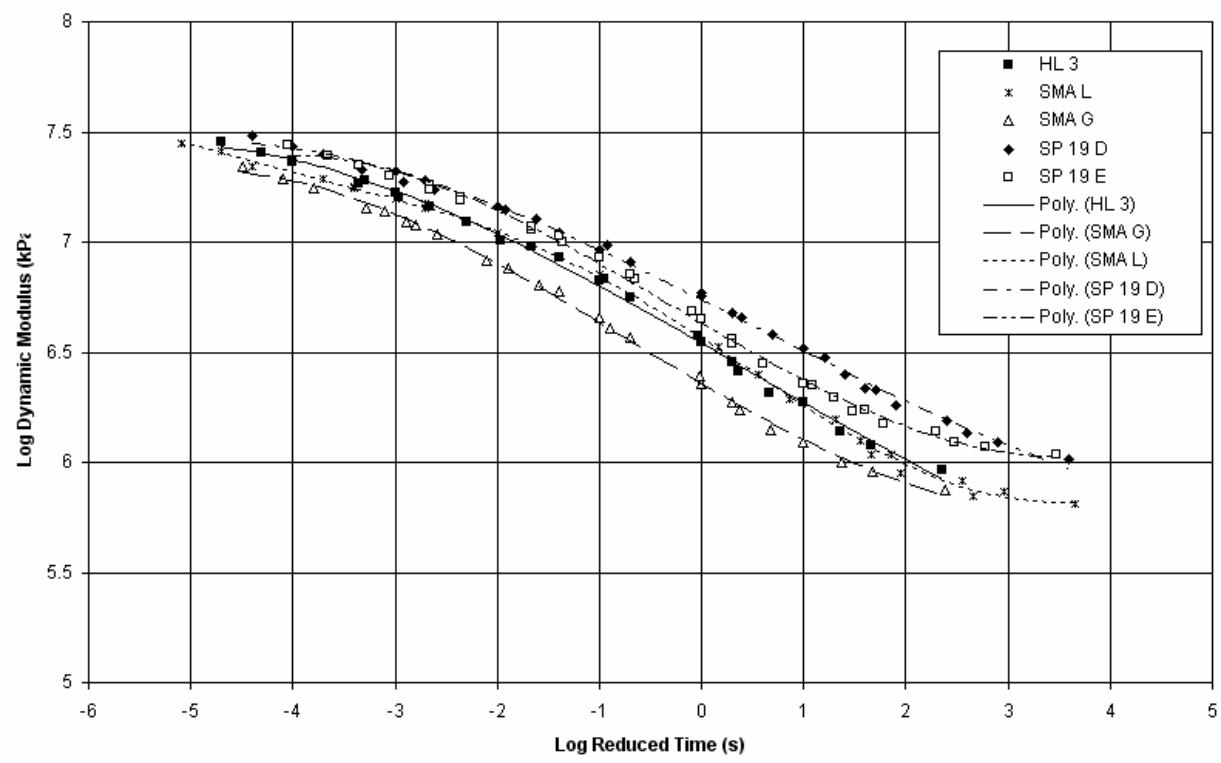

Figure 5.23 Master Curves of the HL 3, SMA L, SMA G, SP 19 D and SP 19 E Mixes.

The SMA G mix has the lowest dynamic modulus over the entire range of the loading time. The HL 3 and SMA L mixes have the dynamic modulus somewhat similar. The SP 19 D mix had generally the highest dynamic modulus, higher than the SP 19 E mix in the middle range of the loading time, although both mixes had similar modulus values at the high and low ends of the loading time.

5.3 PERFORMANCE GRADED ASPHALT CEMENT TESTING

The MEPDG requires testing of the asphalt cement complex shear modulus G* and the phase angle (δ) for Level 1 design [NCHRP 2004a]. The asphalt cement performance based grade is sufficient for Level 3 design. The complex shear modulus G* and the phase angle were determined in this research using the Dynamic Shear Rheometer (DSR) [AI 2003a]. The test data was also used to check if the asphalt cements meet the specified Superpave requirements. The asphalt cement testing was carried out on the Rolling Thin Film Oven (RTFO) residue. The results are summarized in Table 5.7. The DSR values were measured at temperatures of 15ºC, 25ºC, and 35ºC using an 8 mm parallel plate and 2.0 mm thick asphalt cement films; at temperatures of 46ºC, 60ºC, 70ºC and 80ºC, a 25 mm parallel plate was used and the film was 1.0 mm thick.

Table 5.7 Summary of Asphalt Cement Testing Results

PGAC 58-28 in HL 3							
Temperature, ºC	15	25	35	46	60	70	80
G*, kPa	4566.1	723.8	77.02	16.39	2.27	0.682	-
Phase Angle	57.1	67.1	70.5	79.5	84.7	86	-
G*/sin δ @ 58ºC	3.4						
PGAC 70-28 PMA in SMA L							
Temperature, ºC	15	25	35	46	60	70	80
G*, kPa	7200	426	96	26.4	7.33	2.31	0.684
Phase Angle	50.9	55	60.6	62.4	63.8	64.7	66.8
G*/sin δ @ 70ºC	2.6						
PG 70-28 (PMA) in SMA G							
Temperature, ºC	15	25	35	46	60	70	80
G*, kPa	1437.1	264.6	69.5	13.76	3.63	1.50	0.69
Phase Angle	56.3	60.7	57.7	60.8	61.9	64.6	68.6
G*/sin δ @ 70ºC	1.66 (2.5 @ 64 ºC)						
PGAC 64-28 in SP 19 D							
Temperature, ºC	15	25	35	46	60	70	80
G*, kPa	4460	630	170	44	7.53	1.94	0.52
Phase Angle	54.8	64.2	63.8	70.4	78.2	81.8	84
G*/sin δ @ 64ºC	5.4 (2.0 @ 70 ºC)						
PG 70-28 in SP 19 E							
Temperature, ºC	15	25	35	46	60	70	80
G*, kPa	4958.5	1150	282.5	59.2	14.48	6.12	2.73
Phase Angle	45.2	49.7	52.2	52.3	52.4	53.6	55.7
G*/sin δ @ 70ºC	7.6						

Table 5.8 compares the results of the asphalt cement testing with the Superpave specification. The specification requires that the G*/sin δ value at the upper grade temperature should be not less than 2.2 kPa. The PG 58-28 in the HL 3 mix, PG 70-28 in the SMA L mix and PG 70-28 in the SP 19 E mix meet their grade requirements. The asphalt cement in the SP 19 D mix meets the requirements for the PG 64-28 grade and is considered to be relatively close to meet the requirements for the PG 70-28 grade. The asphalt cement in the SMA G mix does not meet the requirements for the PG 70-28 grade but meets the requirements for the PG 64-28 grade. The G*/sin δ values of this asphalt cement is unusually low at other temperatures too.

Table 5.8 Comparison of Asphalt Cement Testing Results with Superpave Requirements.

Mix	Asphalt Cement Grade	RTFO Residue G*/sinδ (kPa)	
		Determined	Specified Minimum
HL 3	58-28	3.4	2.2 @ 58°C
SMA L	70-28	2.6	2.2 @ 70°C
SMA G	70-28	1.7 (2.5 @ 64ºC)	2.2 @ 70°C
SP 19 D	64-28	5.4 (2.0 @ 70ºC)	2.2 @ 64°C
SP 19 E	70-28	7.6	2.2 @ 70°C

5.4 TRIAXIAL REPEATED LOAD CREEP TESTING

5.4.1 Triaxial Repeated Load Creep Testing in Interlaken

The triaxial repeated load creep testing was carried out in order to investigate the visco-elasto-plastic behaviour of the asphalt mixes and to develop the material parameters needed in the finite element analysis. The Interlaken was used with the triaxial cell and pneumatic pressure system for the confinement [ITC 2004]. Figure 5.24 shows the Interlaken configuration for the triaxial test and Figure 5.25 shows the schematic diagram of the triaxial cell used in the repeated load creep test.

Figure 5.24 Interlaken Triaxial Test Configuration [ITC 2004] (temperature chamber is not shown).

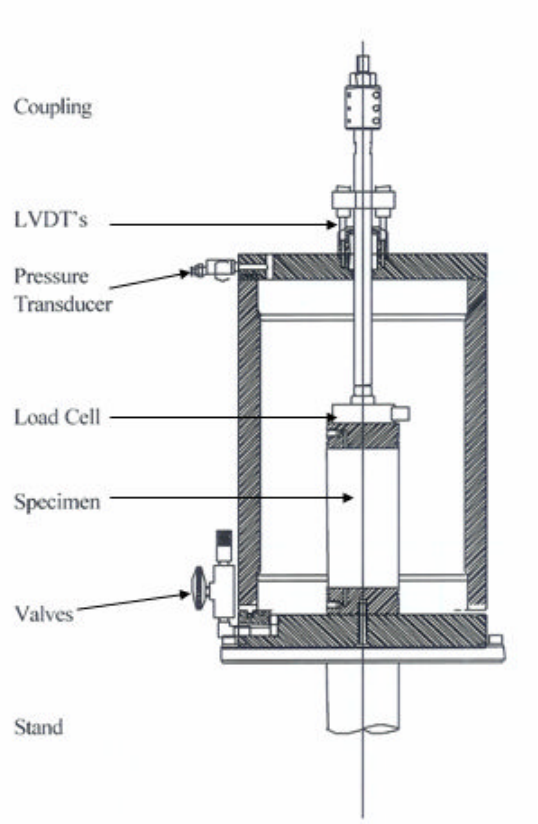

Figure 5.25 Schematic Diagram of Triaxial Cell [ITC 2004].

The triaxial repeated load creep and creep recovery tests were conducted. Each loading cycle consisted of two equal periods. During the first loading period, a constant loading deviatoric stress was applied. At the end of this period the load was removed, and a creep recovery was followed for the second period. The testing was carried out at a constant temperature of 50 ± 0.5ºC. Each specimen was conditioned at the testing temperature for at least six hours before the testing and the temperature was carefully checked using a thermometer and a thermocouple. Sample preconditioning was set at a 10 kPa deviatoric stress level maintained for a period of 5 minutes. Two axial LVDT's with a range from – 1.0 mm to + 1.0 mm were used with the triaxial cell. The time, load, air pressure, deviatoric stress and deformation were constantly monitored and recorded every 0.2 or 0.4 seconds.

The schematic of the stresses in the triaxial test is shown in Figure 5.26. The load measured by the load cell Q and the air pressure P is related to the principal stress by [U of Nottingham 1994]:

$$\sigma_{33} = Q/A + P \qquad (5.6)$$

where A is the cross-section area of the specimen.

$$\sigma_{22} = \sigma_{11} = P \quad (5.7)$$

The deviatoric stress σ is given by [U of Nottingham 1994]:

$$\sigma = \sigma_{33} - \sigma_{11} = Q/A \quad (5.8)$$

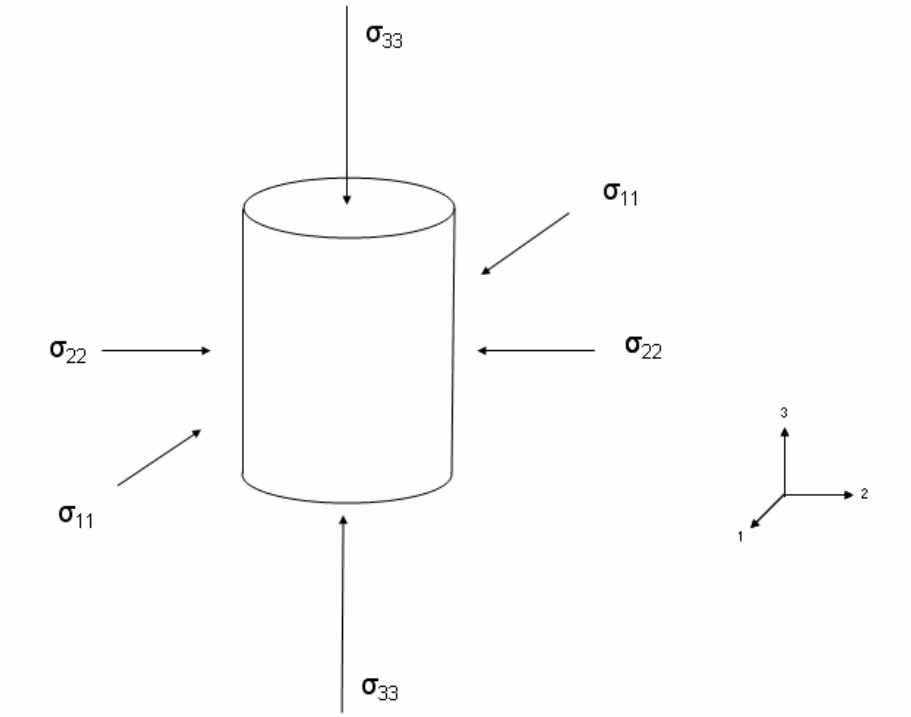

Figure 5.26 Schematic Showing Triaxial Coordinate System with Various Stresses.

Two sets of triaxial repeated load creep and creep recovery tests were completed for each asphalt mix. In Set 1, the specimens underwent 20 loading cycles. Each cycle consisted of one minute of creep under a constant deviatoric stress followed by one minute of creep recovery. In Set 2, the specimens underwent 3 loading cycles. Each cycle consisted of 30 minutes of creep under a constant deviatoric stress followed by 30 minutes of creep recovery. Both sets of tests were conducted at two deviatoric stress levels: 100 kPa; and 200 kPa. The confining pressure was 45 kPa for the test with the deviatoric stress of 100 kPa and 90 kPa for the test with the deviatoric stress of 200 kPa.

As the triaxial repeated load creep test is not a standard test preloaded in the Interlaken system, the Test Builder application software was used to develop separate programs to run the triaxial repeated load creep tests. The programs were developed with some assistance from the manufacturer of the Interlaken equipment.

5.4.2 Sample Preparation

The laboratory samples used for the triaxial repeated load testing were 100 mm diameter and 150 mm height cores obtained from the SGC cylinders. The procedure for the sample preparation was the same as for the dynamic modulus testing described in Section 5.2.2. Table 5.9 shows a summary of SGC cylinder and core densities and air voids. The target air voids level for the core samples was of 6.0 ± 1.0 percent. All of the core specimens were within the target limit.

Table 5.9 Summary of Creep Testing Specimens Densities and Air Voids

Mix Type	MRD	SGC Specimens		Cores		Air Voids Difference (%)
		Number	Air Voids (%)	BRD	Air Voids (%)	
HL 3	2.540	2	7.2	2.372	6.6	0.6
		32	6.3	2.392	5.8	0.4
		45	6.1	2.405	5.3	0.7
		46	6.4	2.393	5.8	0.6
		48	5.9	2.412	5.0	0.9
		49	6.1	2.402	5.4	0.6
		Mean	6.3	2.396	5.7	0.6
SMA L	2.599	4	6.7	2.433	6.4	0.3
		5	7.1	2.428	6.6	0.5
		11	6.7	2.434	6.3	0.4
		13	6.9	2.433	6.4	0.5
		14	7.1	2.424	6.7	0.4
		17	6.9	2.434	6.3	0.6
		Mean	6.9	2.431	6.5	0.5
SMA G	2.684	15	6.3	2.531	5.8	0.5
		16	5.9	2.536	5.5	0.4
		18	5.7	2.536	5.5	0.2
		20	5.6	2.539	5.4	0.2
		21	5.7	2.544	5.2	0.5
		Mean	5.8	2.537	5.5	0.4
SP 19 D	2.570	4	7.3	2.407	6.3	1.0
		50	7.2	2.411	6.2	1.0
		51	7.6	2.395	6.8	0.8
		52	7.0	2.406	6.4	0.6
		57	6.6	2.424	5.7	0.9
		58	7.1	2.404	6.5	0.7
		60	7.4	2.398	6.7	0.7
		Mean	7.2	2.406	6.4	0.8
SP 19 E	2.579	13	7.9	2.401	6.9	1.0
		22	7.0	2.418	6.2	0.7
		26	6.1	2.443	5.3	0.9
		27	6.7	2.436	5.5	1.2
		37	7.1	2.420	6.2	0.9
		Mean	7.0	2.424	6.0	0.9

5.4.3 Triaxial Repeated Load Creep Testing Results

The axial strain of the tested samples during the creep and creep recovery stages was calculated for each sample. Figures 5.27 and 5.28 show the deviatoric stress and axial strain, respectively, in the 20-cycle test conducted at a 100 kPa deviatoric stress level. Figures 5.29 and 5.30 show the deviatoric stress and axial strain, respectively, in the 3-cycle test conducted at a 100 kPa deviatoric stress level.

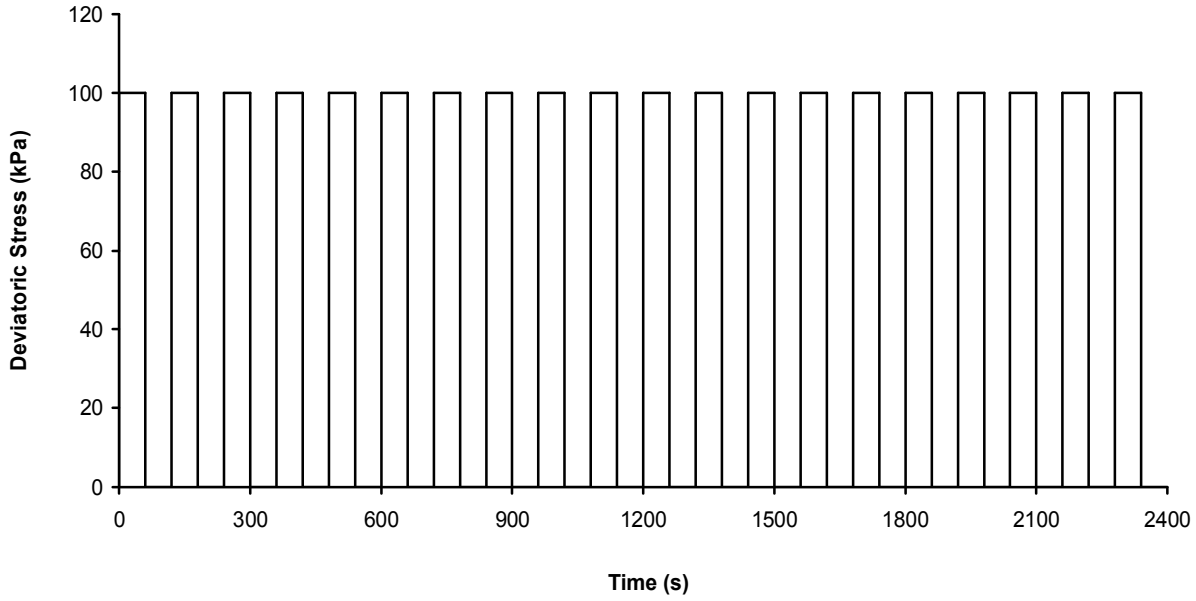

Figure 5.27 Deviatoric Stress in Triaxial Repeated Load Creep 20-Cycle Test, 100 kPa.

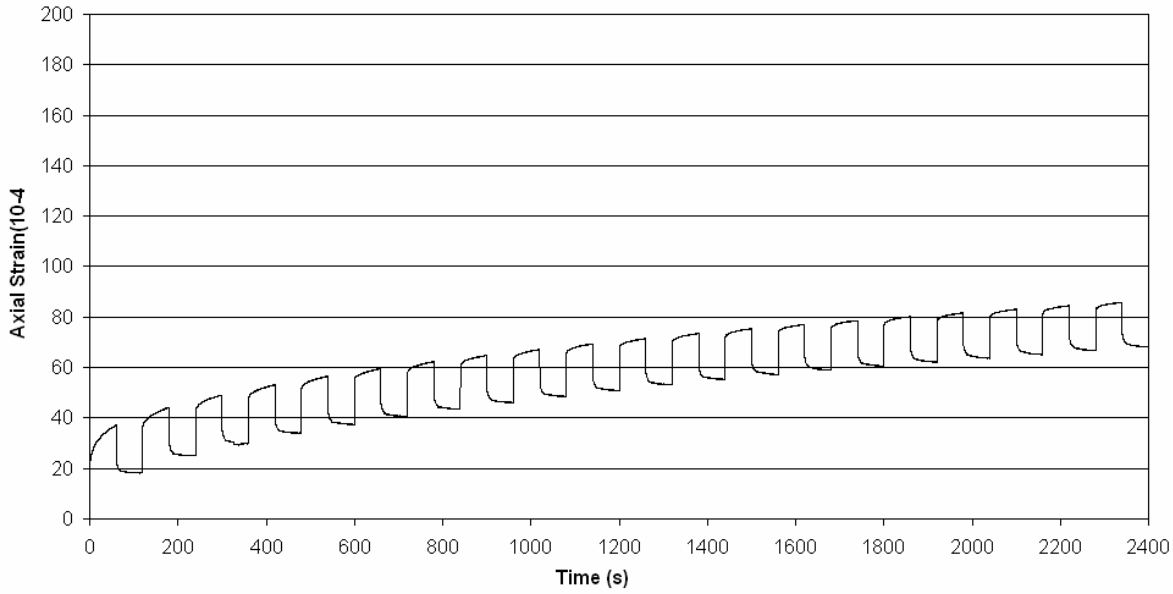

Figure 5.28 Axial Strain in Triaxial Repeated Load Creep 20-Cycle Test, 100 kPa, Sample 32, HL 3 Mix.

Error! Objects cannot be created from editing field codes.
Figure 5.29 Deviatoric Stress in Triaxial Repeated Load Creep 3-Cycle Test, 100 kPa.

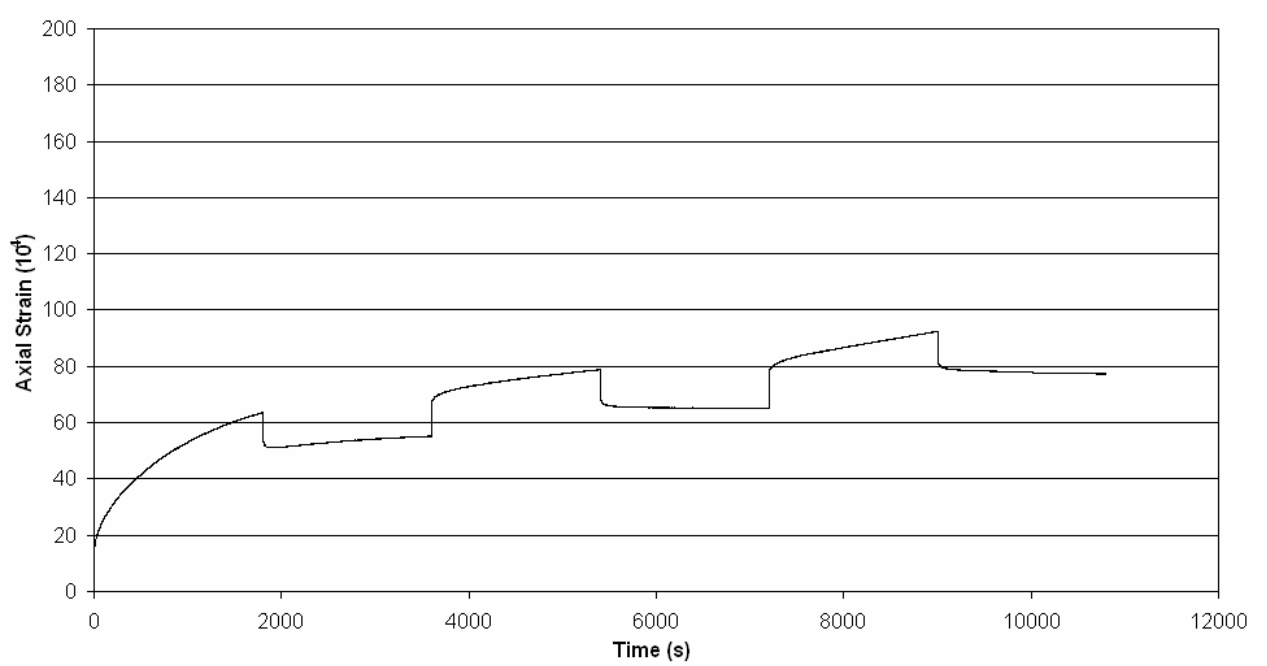

Figure 5.30 Axial Strain in Triaxial Repeated Load Creep 3-Cycle Test, 100 kPa, Sample 2, HL 3 Mix.

The plots of the axial strain in the 20-cycle and 3-cycle tests conducted at the 100 kPa and 200 kPa deviatoric stress levels for all five mixes are shown in Appendix B.

The analysis of the elastic, plastic, viscoelastic and viscoplastic behaviour of the asphalt mixes are described in Chapter Six, Asphalt Viscoplastic Behaviour.

5.5 SUMMARY

Four types of tests were conducted for this research:

Asphalt mix testing

1. Accelerated performance testing in terms of rutting resistance using the HWRT;
2. Dynamic modulus testing using the Interlaken system; and
3. Triaxial repeated load creep testing using the Interlaken system.

Asphalt cement testing

4. Shear modulus G* and phase angle δ of the asphalt cement

The SP 19 D mix exhibited the lowest rutting after 20,000 passes in the HWRT. The SP 19 E and SMA L mixes exhibited very similar rutting after 20,000 passes; their rutting was lower than those of the SMA G and HL 3 mixes. The HL 3 mix exhibited the highest rutting. Generally, both SMA mixes performed better in Phase 2 than the dense graded mixes.

The asphalt cements in the HL 3, SMA L and SP 19 E mixes met the Superpave requirements for their grades. The asphalt cement in the SMA G mix did not meet the requirements for the 70-28 grade. The asphalt cement in the SP 19 D mix met the requirements for the 64-28 grade; in fact it was close to meeting the requirements for the 70-28 grade.

In the triaxial repeated load creep and creep recovery test, the relationship between the axial strain and the time of loading and the deviatoric stress was investigated. The testing was conducted at 100 kPa deviatoric stress and the confining pressure of 45 kPa and 200 kPa deviatoric stress and 90 kPa confining pressure. Two sets of tests were carried out, each of different number of cycles and cycle time. The determined strain versus time and strain versus stress relationships are used in the asphalt mix visco-elasto-plastic behaviour analysis.

CHAPTER SIX
TASK TWO: ASPHALT VISCOPLASTIC BEHAVIOUR

The hot-mix asphalt plays a major role in asphalt pavement rutting. It is important to use a constitutive law that will take into account the behaviour occurring in in-situ service. This chapter is focused on the analyses of asphalt mix visco-elasto-plastic behaviour using the results from the triaxial repeated load creep and creep recovery testing.

6.1 ASPHALT MIX VISCO-ELASTO-PLASTIC BEHAVIOUR

The constitutive law for asphalt mixes can be expressed as [Perl 1983]:

$$\varepsilon_{ij} = \varepsilon_{ij} (\sigma_{ij}, t, N, T) \quad (6.1)$$

where:

ε_{ij} and σ_{ij} = strain and stress components, respectively
t = time
N = number of loading cycles
T = temperature

The triaxial repeated load creep and creep recovery test is used in this research for characterizing the visco-elsto-plastic behaviour of asphalt mixes, in particular to determine the elastic, plastic, viscoelastic and viscoplastic strain components. Figure 6.1 shows the deviatoric stress in the first cycle of the 20-cycle, 100 kPa test. Figure 6.2 shows the axial strain in the first cycle of the 20-cycle, 100 kPa test of Sample 22, SP 19 E mix.

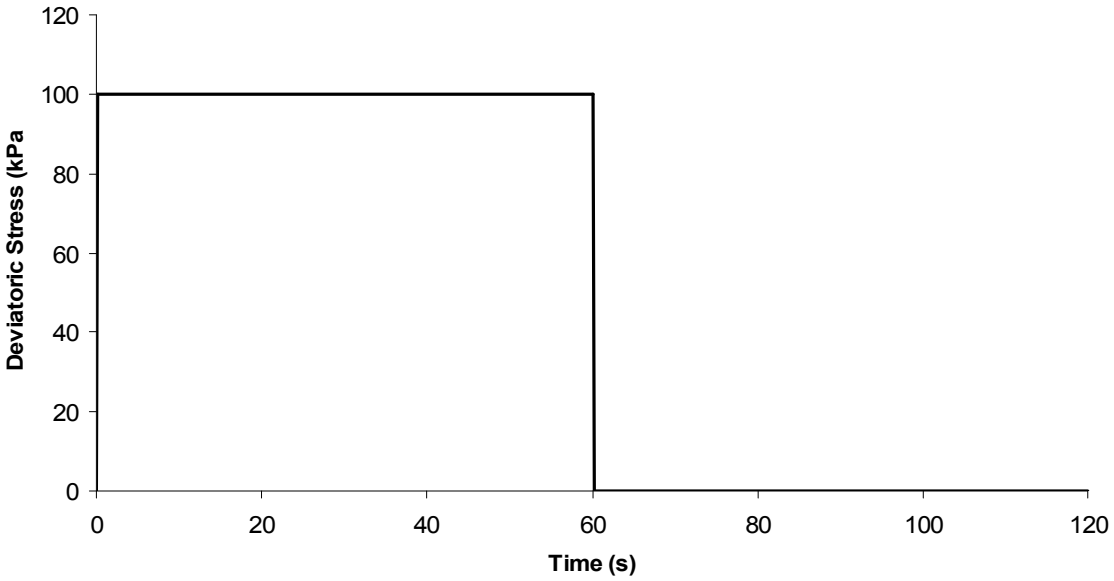

Figure 6.1 Deviatoric Stress in the First Cycle of the 20-Cycle, 100 kPa Test.

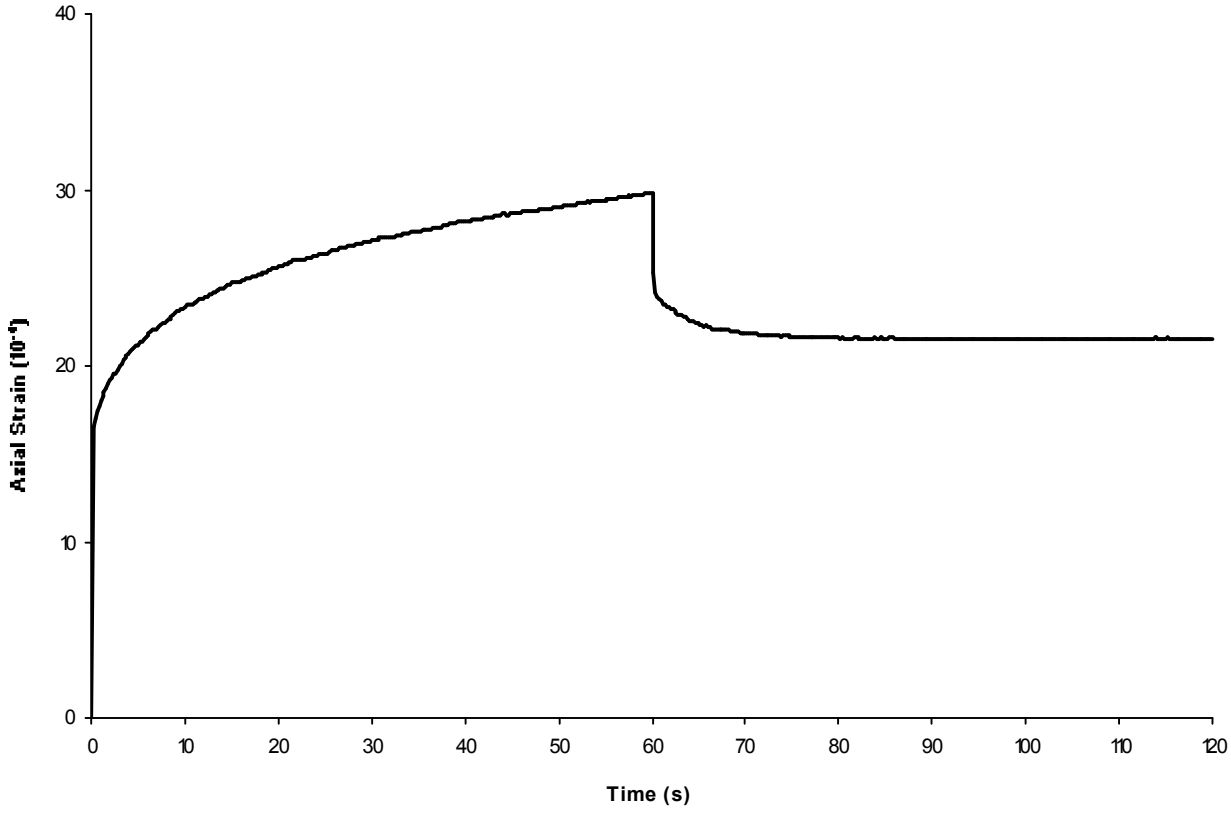

Figure 6.2 Axial Strain in the First Cycle of the 20-Cycle, 100 kPa Test, Sample 22, SP 19 E Mix.

The total strain (ε_t) in the creep and creep recovery test has recoverable and nonrecoverable elements. It can be broken down into four components [Von Quintus 1994]:

1. Elastic strain (ε_e) which is recoverable and time independent;
2. Plastic strain (ε_p) which is nonrecoverable and time independent;
3. Viscoelastic strain (ε_{ve}) which is recoverable and time dependent; and
4. Viscoplastic strain (ε_{vp}) which is nonrecoverable and time dependent.

$$\varepsilon_t = \varepsilon_e + \varepsilon_p + \varepsilon_{ve} + \varepsilon_{vp} \quad (6.2)$$

The total strain can also be expressed as [Perl 1983]:

$$\varepsilon_t(\sigma, t, N) = \varepsilon_e(\sigma) + \varepsilon_p(\sigma, N) + \varepsilon_{ve}(\sigma, t) + \varepsilon_{vp}(\sigma, t, N) \quad (6.3)$$

where:

σ = stress component
N = number of cycles
t = time of loading

These responses of the asphalt mixture can be determined in the creep and creep recovery test as follows [Von Quintus 1994]:

1. Elastic strain (ε_e) is defined as the instantaneous response occurring during recovery phase. It is equal to the instantaneous reduction in the total strain at the moment the load is removed;

2. The instantaneous response occurring during the loading contains the elastic (ε_e) and plastic (ε_p) components of the total strain ($\varepsilon_e + \varepsilon_p$). Therefore, by subtracting the elastic strain (ε_e) from the instantaneous loading strain, the plastic strain (ε_p) can be determined; and

3. The viscoelastic and viscoplastic strains are much more difficult to determine as they overlap during the loading stage ($\varepsilon_{ve} + \varepsilon_{vp}$) and are time dependant. However, the delayed response in the unloading phase consists of the viscoelastic strain (ε_{ve}) only. Therefore, the viscoplastic strain can be calculated by subtracting the elastic, plastic and viscoelastic strain from the total strain.

$$\varepsilon_{vp} = \varepsilon_t - \varepsilon_e - \varepsilon_p - \varepsilon_{ve} \quad (6.4)$$

The elastic, plastic, viscoelastic and viscoplastic components of the total strain in the first cycle of the 20-cycle, 100 kPa test of Sample 22, SP 19 E mix are shown in Figure 6.3

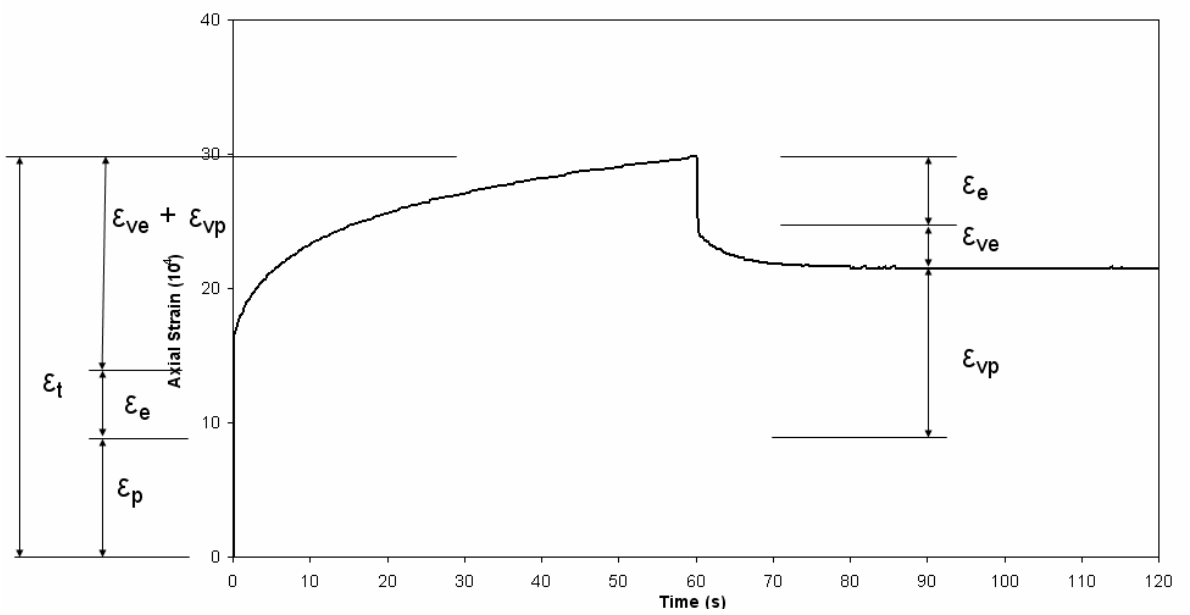

Figure 6.3 Elastic, Plastic, Viscoelastic and Viscoplastic Strains in the First Cycle of 20-Cycle, 100 kPa Test, Sample 22, SP 19 E Mix.

A spreadsheet was developed in Microsoft Excel to determine the strain components for the testing of all five mixes. The recoverable elastic and viscoelastic strains remain constant for all twenty cycles; they are independent of the number of cycles.

Figure 6.4 shows the plastic and viscoplastic strains in the 20-cycle, 100 kPa test of Sample 22 of the SP 19 E mix. The cumulative plastic strain curve flattens and becomes almost horizontal after about 400 seconds. The cumulative viscoplastic strain curve reaches a constant, relatively steep slope after about 600 seconds. It is an indication that the nonrecoverable deformation in the repeated load creep and creep recovery test depends mainly on the viscoplastic strain component, and that the plastic strain can be considered insignificant if larger number of pulses are applied. This confirms the observations by [Huang 1995].

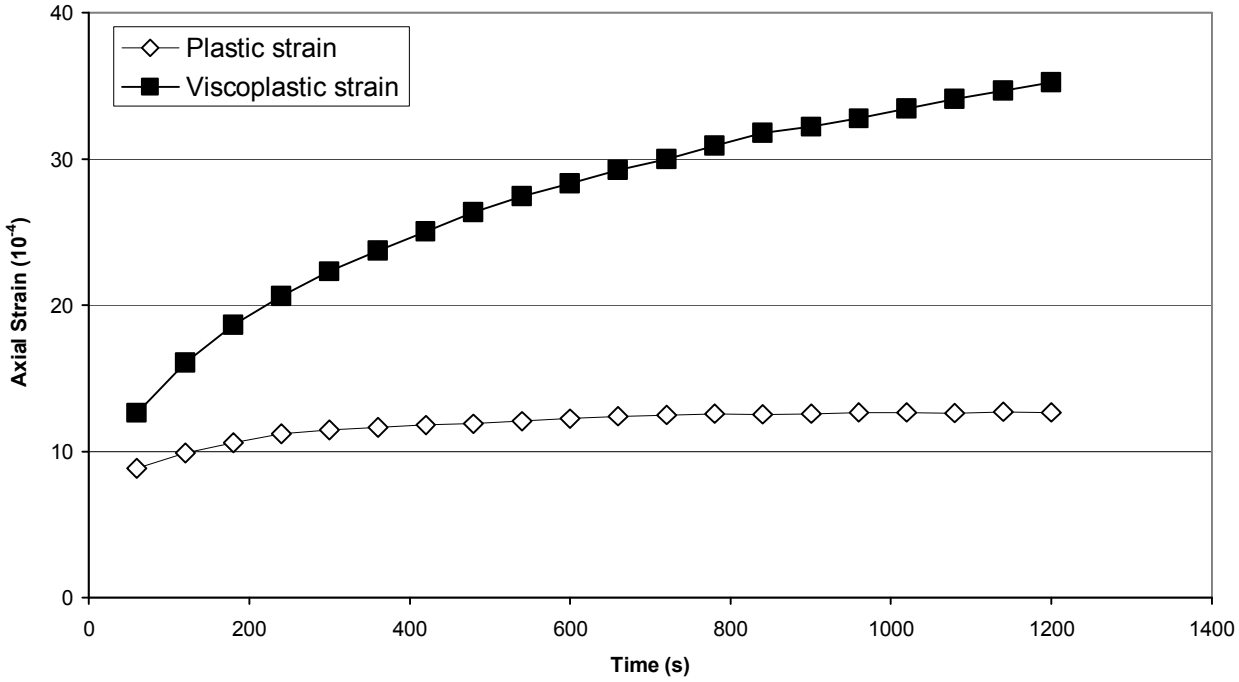

Figure 6.4 Plastic and Viscoplastic Strains in the 20-Cycle, 100 kPa Test, Sample 22, SP 19 E Mix.

6.2 CREEP PARAMETERS DEVELOPMENT

The viscoplastic axial strain versus time relationship for both deviatoric stress levels of 100 kPa and 200 kPa for the HL 3 mix is shown in Figure 6.5. The results from the 20-cycle and 3-cycle tests are included in this relationship.

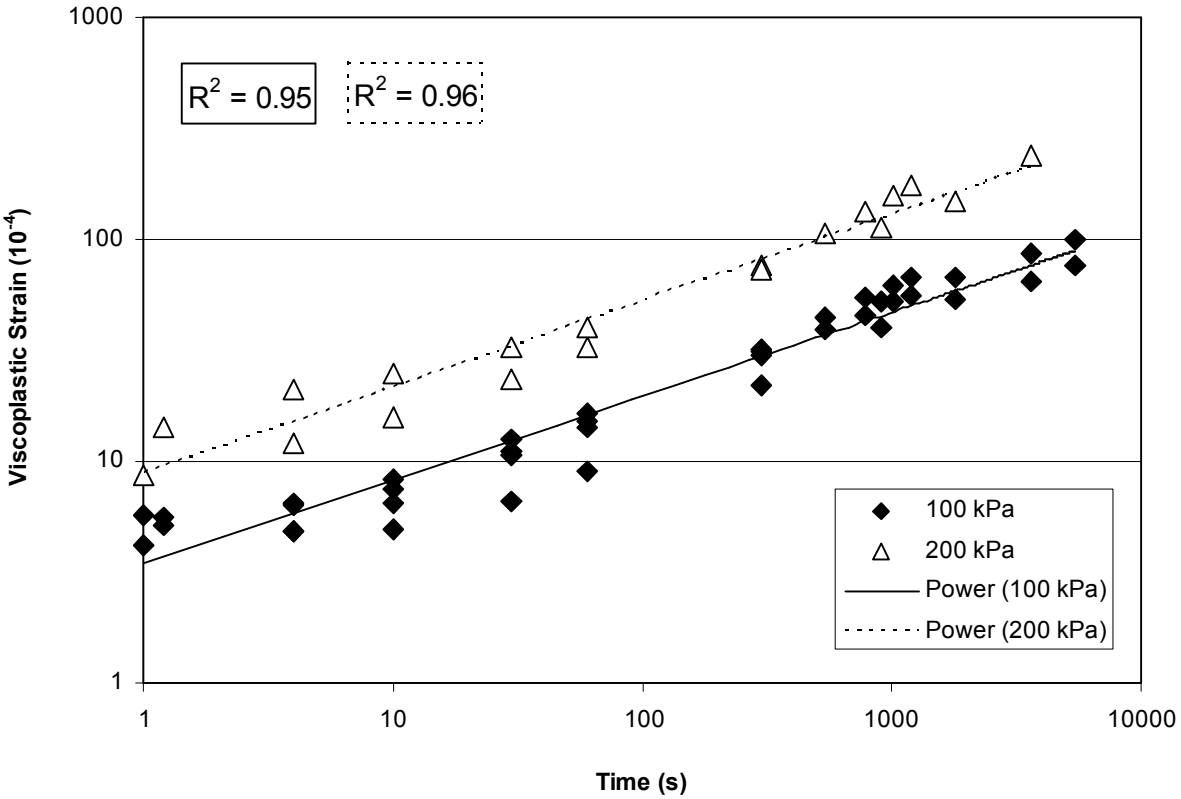

Figure 6.5 Viscoplastic Strain versus Time Relationship of the HL 3 Mix.

Because both lines in the plot exhibit similar slope, it can be concluded that the viscoplastic strain ε_{vp} is proportional to t^{β}. The slope β is 0.40. The viscoplastic strain is [Perl 1983]:

$$\varepsilon_{vp}(\sigma, t, N) = B(\sigma) \times t^{\beta} \tag{6.5}$$

and

$$B(\sigma) = \varepsilon_{vp}(\sigma, t, N) / t^{\beta} \tag{6.6}$$

The $\varepsilon_{vp} / t^{\beta}$ versus deviatoric stress relationship for the HL 3 mix is shown in Figure 6.6. It can be described by a second-order polynomial function [Perl 1983]:

$$B(\sigma) = b_1\sigma + b_2\sigma^2 \tag{6.7}$$

Therefore, the viscoplastic strain can be expressed as:

$$\varepsilon_{vp} = (b_1\sigma + b_2\sigma^2) \times t^{\beta} \tag{6.8}$$

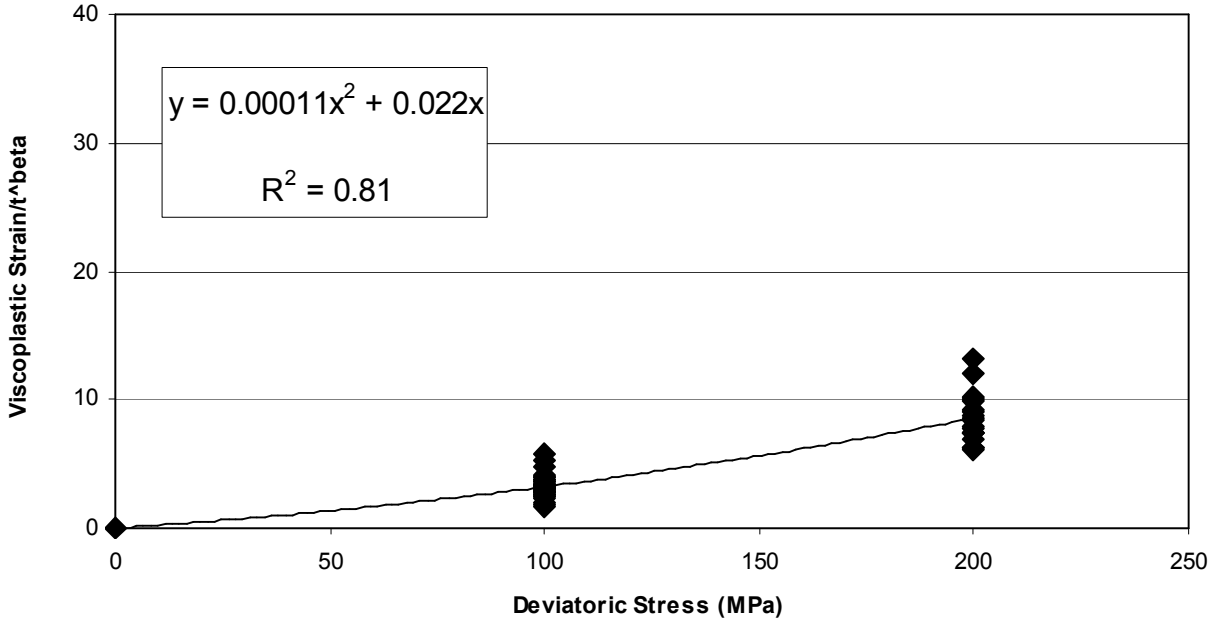

Figure 6.6 Viscoplastic Strain/t^{β} versus Deviatoric Stress Relationship of the HL 3 Mix.

As is the common practice among other researchers, the criteria for goodness of fit of statistical parameters can be based on the value of the coefficient of determination, R^2. The coefficient of determination is the correlation coefficient squared, and it tells the percentage of the variation in the dependent variable (Y), which is explained by the variation in the independent variable (X). The criteria used in this research are shown in Table 6.1 [Witczak 2002b, Tran 2004].

Table 6.1 Criteria for Goodness of Fit Statistical Parameters

Criteria	R^2
Excellent	≥ 0.90
Good	0.70 – 0.89
Fair	0.40 – 0.69
Poor	0.20 – 0.39
Very Poor	≤ 0.19

The relationship in Figure 6.6, represented by a second-order polynomial function, is considered to be good.

Figures 6.7 to 6.14 show the viscoplastic strain versus time and viscoplastic strain/t^{β} versus deviatoric stress relationships for the SMA L, SMA G, SP 19 D and SP 19 E mixes. The β, b_1 and b_2 parameters for all five mixes are summarized in Table 6.2. The viscoplastic strain versus time relationship is good for all

five mixes. The viscoplastic strain/t^{β} versus deviatoric stress relationship is good for the HL 3, SMA G, SP 19 D and SP 19 E mixes and fair for the SMA L mix.

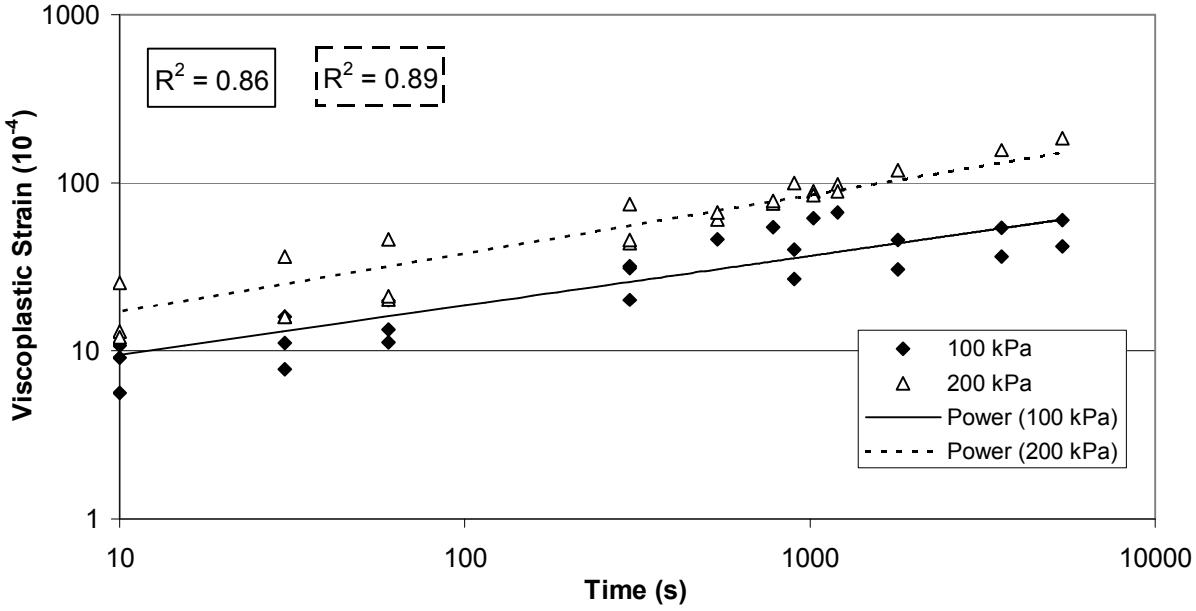

Figure 6.7 Viscoplastic Strain versus Time Relationship of the SMA L Mix.

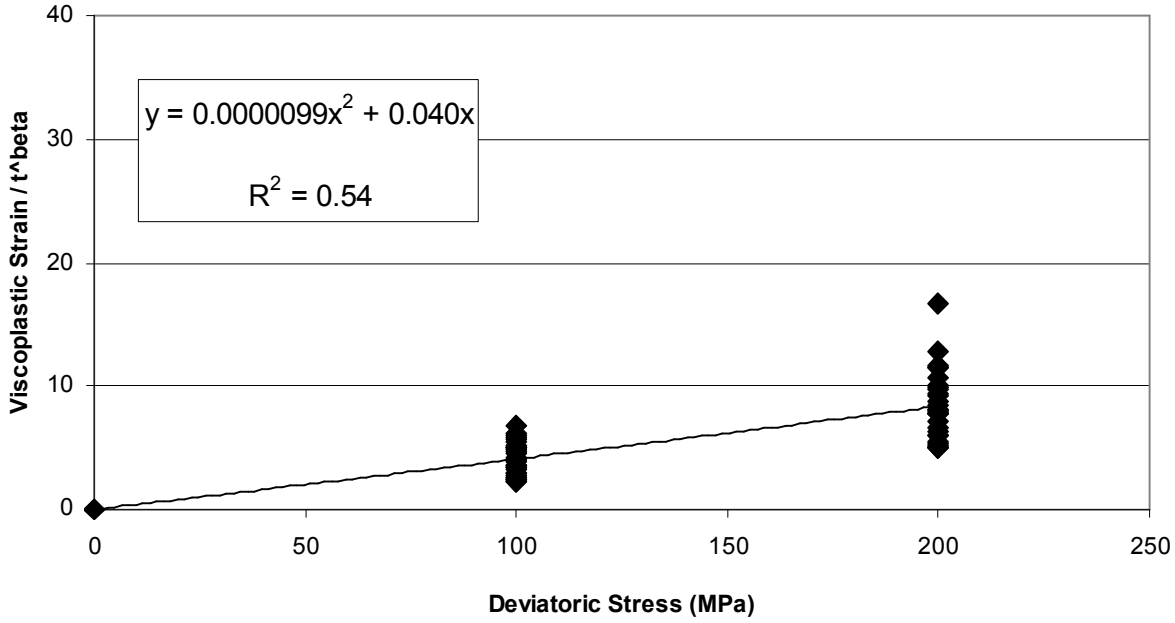

Figure 6.8 Viscoplastic Strain/t^{β} versus Deviatoric Stress Relationship of the SMA L Mix.

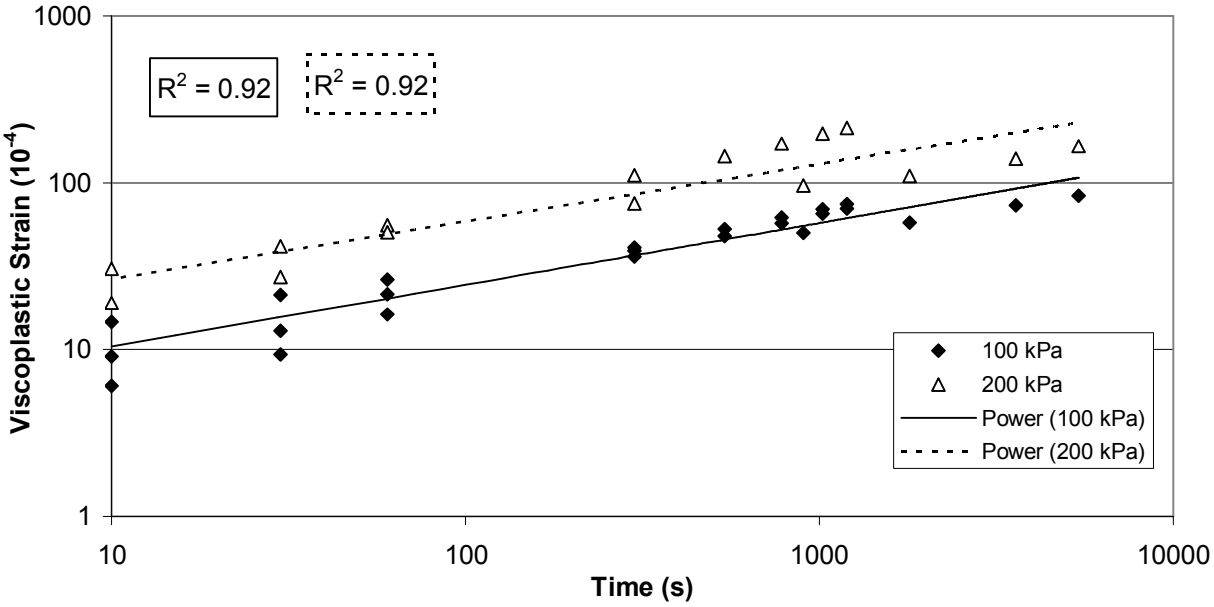

Figure 6.9 Viscoplastic Strain versus Time Relationship of the SMA G Mix.

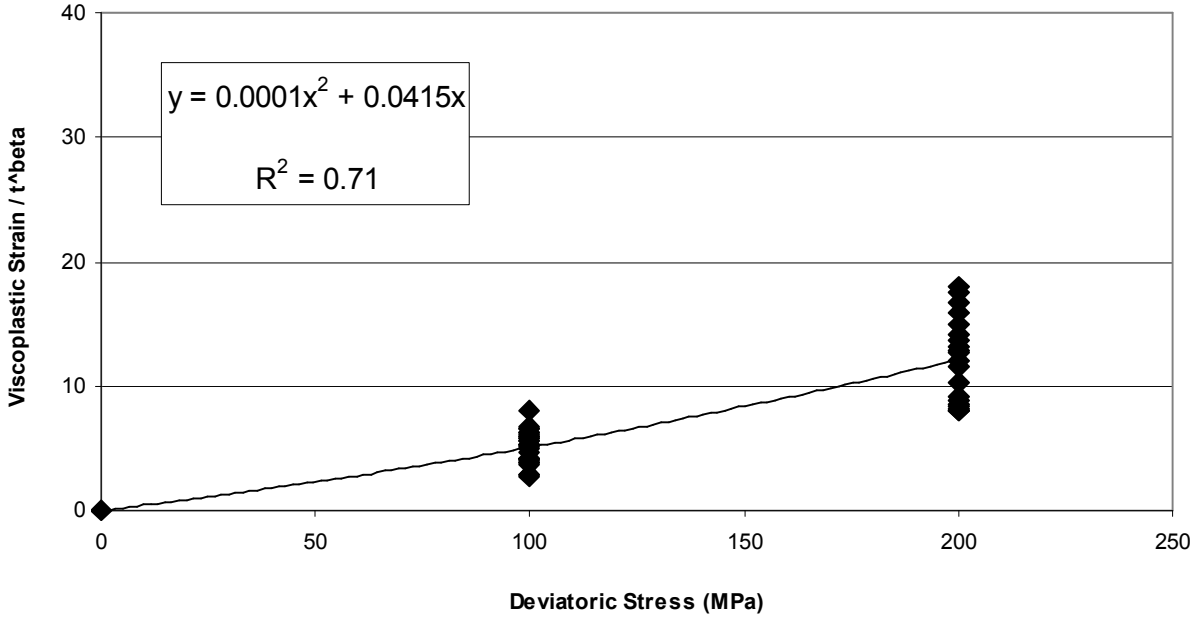

Figure 6.10 Viscoplastic Strain/t^{β} versus Deviatoric Stress Relationship of the SMA G Mix.

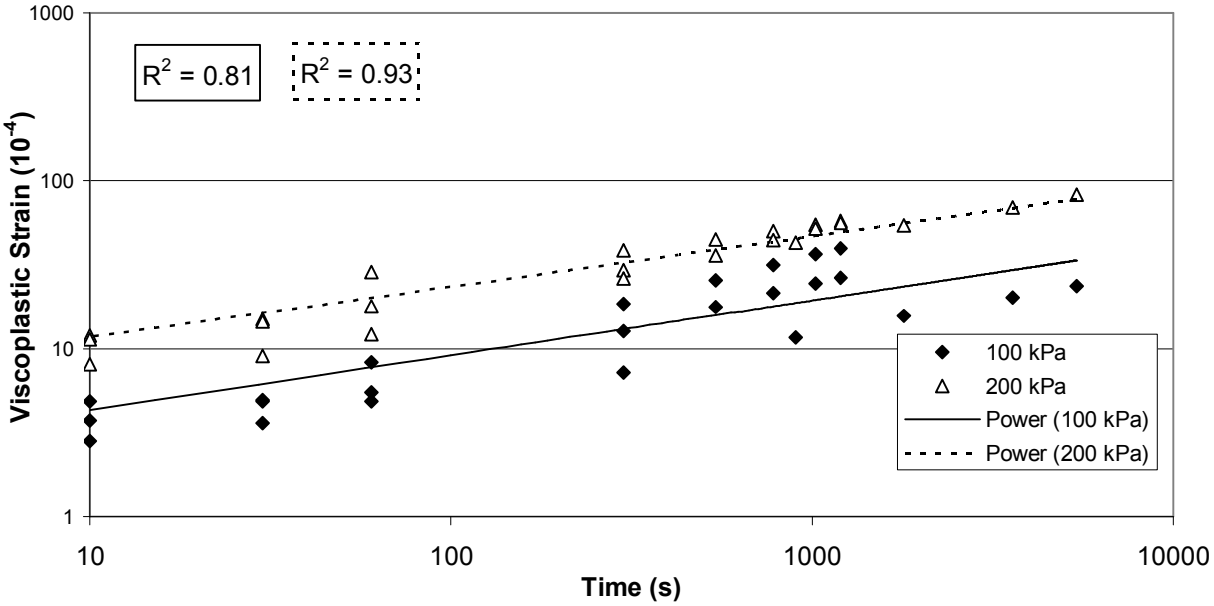

Figure 6.11 Viscoplastic Strain versus Time Relationship of the SP 19 D Mix.

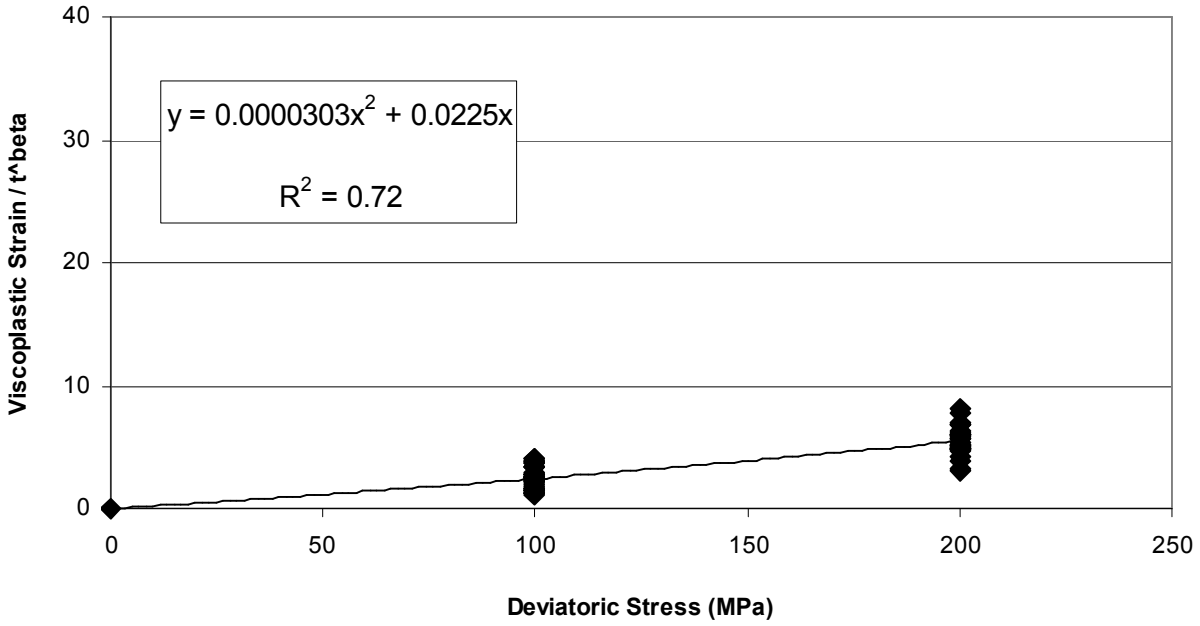

Figure 6.12 Viscoplastic Strain/t^{β} versus Deviatoric Stress Relationship of the SP 19 D Mix.

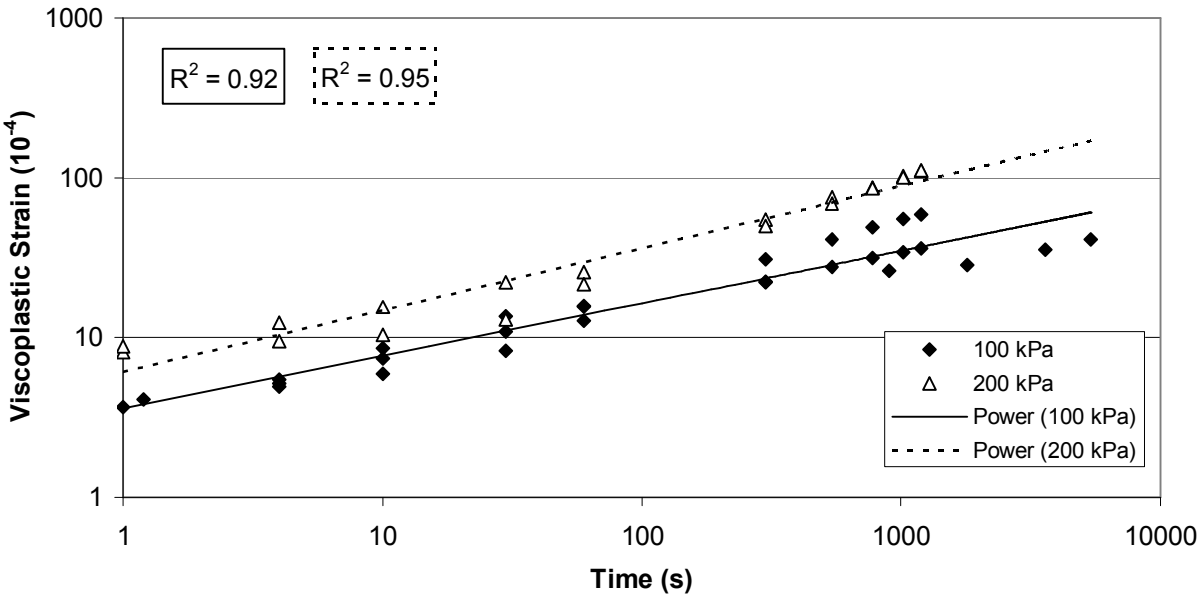

Figure 6.13 Viscoplastic Strain versus Time Relationship of the SP 19 E Mix.

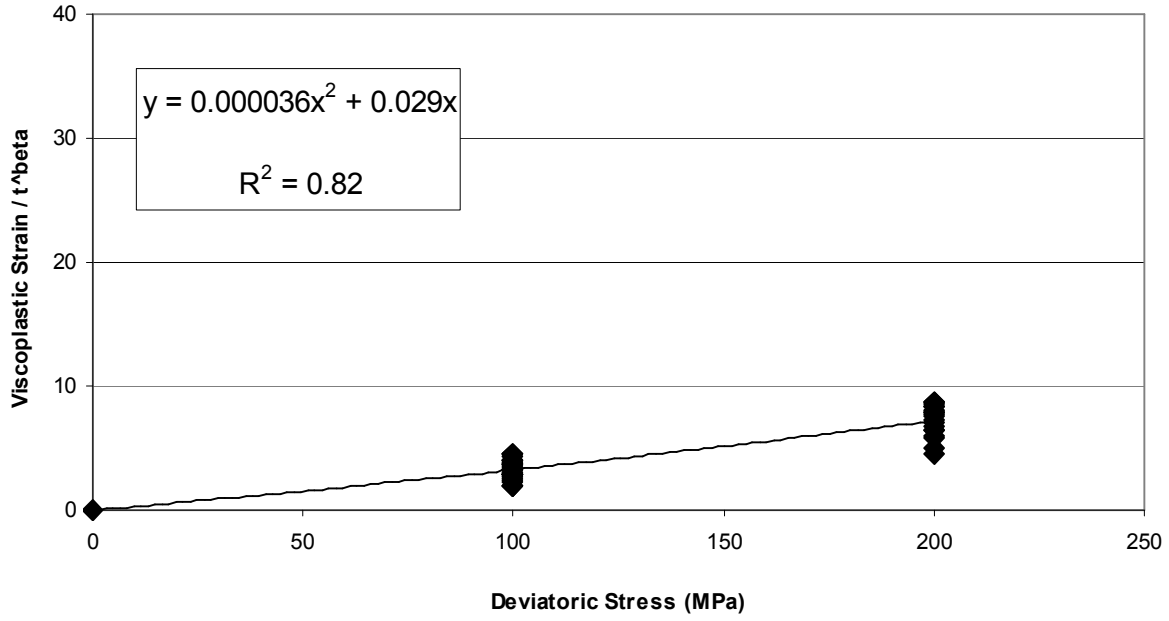

Figure 6.14 Viscoplastic Strain/t^{β} versus Deviatoric Stress Relationship of the SP 19 E Mix.

Table 6.2 Viscoplastic Parameters of the HL3, SMA L, SMA G, SP 19 D and SP 19 E Mixes.

Mix	Slope*			Function B(σ)			
	β	Relationship		b_1	b_2	Relationship	
		R^2	Category			R^2	Category
HL 3	0.40	0.78	good	0.0220	0.000110	0.81	good
SMA L	0.34	0.75	good	0.0400	0.000010	0.54	fair
SMA G	0.35	0.77	good	0.0415	0.000100	0.71	good
SP 19 D	0.32	0.71	good	0.0225	0.000030	0.72	good
SP 19 E	0.36	0.79	good	0.0290	0.000036	0.82	good

* Average slope for both stress levels.

The rate of the irrecoverable strain can be expressed as [Lai 1973]:

$$\dot{\varepsilon}_{vp}(t) = \beta(b_1\sigma + b_2\sigma^2)\, t^{\beta-1} \qquad (6.9)$$

A creep power law is available in ABAQUS, the finite element program that was used in this research. To define the creep model, the function in Equation 6.9 is expressed in a power law form. The creep power law model is as follows [Huang 1995, Hua 2000]:

$$\dot{\varepsilon}_{vp} = A\sigma^n t^m \qquad (6.10)$$

The A, n and m creep power law parameters for the five asphalt mixtures were developed using regression analysis. The parameters are given in Table 6.3.

Table 6.3 Asphalt Mixtures Creep Power Law Model Parameters.

Mix	Creep Model Power Law Parameters		
	A ($x10^{-8}$)	n	m
HL 3	14	1.48	-0.60
SMA L	113	1.04	-0.66
SMA G	42	1.31	-0.65
SP 19 D	32	1.20	-0.68
SP 19 E	47	1.20	-0.64

The presented parameters are used for the initial finite element modeling of the accelerated rutting performance testing in the HWRT using the ABAQUS program.

6.3 SUMMARY

Asphalt mix is a visco-elasto-plastic material over most of the in-service temperature range. The recoverable (elastic and viscoelastic) and nonrecoverable (plastic and viscoplastic) strain components are determined in the analyses. The viscoplastic strain component is the major contributor to the asphalt mixture rutting and only this component is used in the development of the material creep parameters.

The viscoplastic strain versus time and viscoplastic strain versus deviatoric stress relationships were analyzed. The A, n and m creep power law parameters were developed for all five mixes. They are used in the finite element modeling.

CHAPTER SEVEN
TASK THREE: FINITE ELEMENT MODELING

The finite element method is a very versatile analysis technique with the capabilities of two and three dimensional geometric modeling, nonlinear material characterization, plastic behaviour, and other sophisticated features. A commercially available finite element program, ABAQUS, is used in this research to model asphalt mix behaviour in the HWRT and to model pavement in-situ rutting performance.

7.1 ABAQUS MODELING

ABAQUS is a suite of powerful engineering simulation codes based on the finite element method. It can be used to solve relatively simple problems using linear analyses as well as complicated nonlinear problems. ABAQUS has an extensive library of finite elements and an extensive list of material models. In nonlinear analysis, ABAQUS automatically chooses the appropriate increments and convergence tolerances [ABAQUS 2004a].

The Complete ABAQUS Environment, ABAQUS/CAE [ABAQUS 2004B], was used in this research. ABAQUS/CAE has both, a pre-processor and a post-processor. In ABAQUS/CAE, an interface is included for creating, submitting, monitoring, and evaluating from ABAQUS/Standard simulations [ABAQUS 2004b].

ABAQUS requires the user to create geometry, select the material models and input the properties, select the required field and history output, assemble the instance, define required steps in the analysis including the time period for each step, define the boundary conditions and load type and magnitude, determine the finite element types, mesh the part, and submit the data for analysis. The results can be viewed in a graphical or tabular form [ABAQUS 2004b].

The critical step of any finite element simulation is to discretize the actual geometry of the structure using a collection of finite elements. Each finite element represents a discrete portion of the analyzed structure. The finite elements are joined by shared nodes. The collection of nodes and finite elements forms the mesh. The number of elements used in a particular mesh is referred to as the mesh density. In a stress

analysis, the displacement of the nodes is calculated by ABAQUS; once it is known, the stresses and strains in each finite element can be easily determined [Roberts 2003].

As the HWRT testing and dual wheel loading configurations are symmetrical, only half of the HWRT sample and only one wheel were included in the modeling; this allowed for a reduction in the number of elements and in the time required for each analysis.

With both the HWRT and pavement in-situ modeling, a two-dimensional plane strain modeling space was selected with deformable solid features. In doing so, the time of computations was also drastically reduced without significant loss in accuracy [Hua 2000]. The creep model available in the plasticity group was used for the rutting simulation and the A, n and m parameters were entered. The modulus of elasticity and Poisson's ratio were also entered for each mix.

The power law creep model is a relatively simple model but is considered appropriate for the problem at hand [Hua 2000, White 2002]. The time-hardening version of the creep model was used and is described as the time-hardening form [ABAQUS 2004a]:

$$\dot{\varepsilon}^{cr} = A\tilde{q}^{n}t^{m} \qquad (7.1)$$

where

$\dot{\varepsilon}^{cr}$ = uniaxial equivalent creep strain rate
$\tilde{q}$ = uniaxial equivalent deviatoric stress
t = total time
A, n and m = material parameters

For isotropic creep behaviour, $\tilde{q}$ is Mises equivalent stress. For physically reasonable behaviour, A and n must be positive and $-1 < m \leq 0$ [White 2002]. The asphalt mix parameters described in Chapter Six, Asphalt Viscoplastic Behaviour, meet these requirements and are used in the analysis.

As the temperature in the analysis is fixed at 50ºC, the parameters are developed from the triaxial repeated load creep test at 50ºC and the modulus of elasticity and Poisson's ratio determined at the same temperature are input into the program. If the creep model is used to describe the time dependant material behaviour, the repeated loading and continuous loading have the same effect on the predicted creep strain as long as the total loading times are the same [Hua 2000].

The CPE4R plane strain linear elements with reduced integration from the ABAQUS standard two-dimensional solid library is used in the simulation.

7.2 MODELING OF HWRT TESTING

7.2.1 Initial Modeling

The objective of the initial model is to describe the impact of HWRT on various asphalt mixes. As noted in Figure 7.1, the primary purpose of the model is to define what occurs in the asphalt sample during the HWRT test.

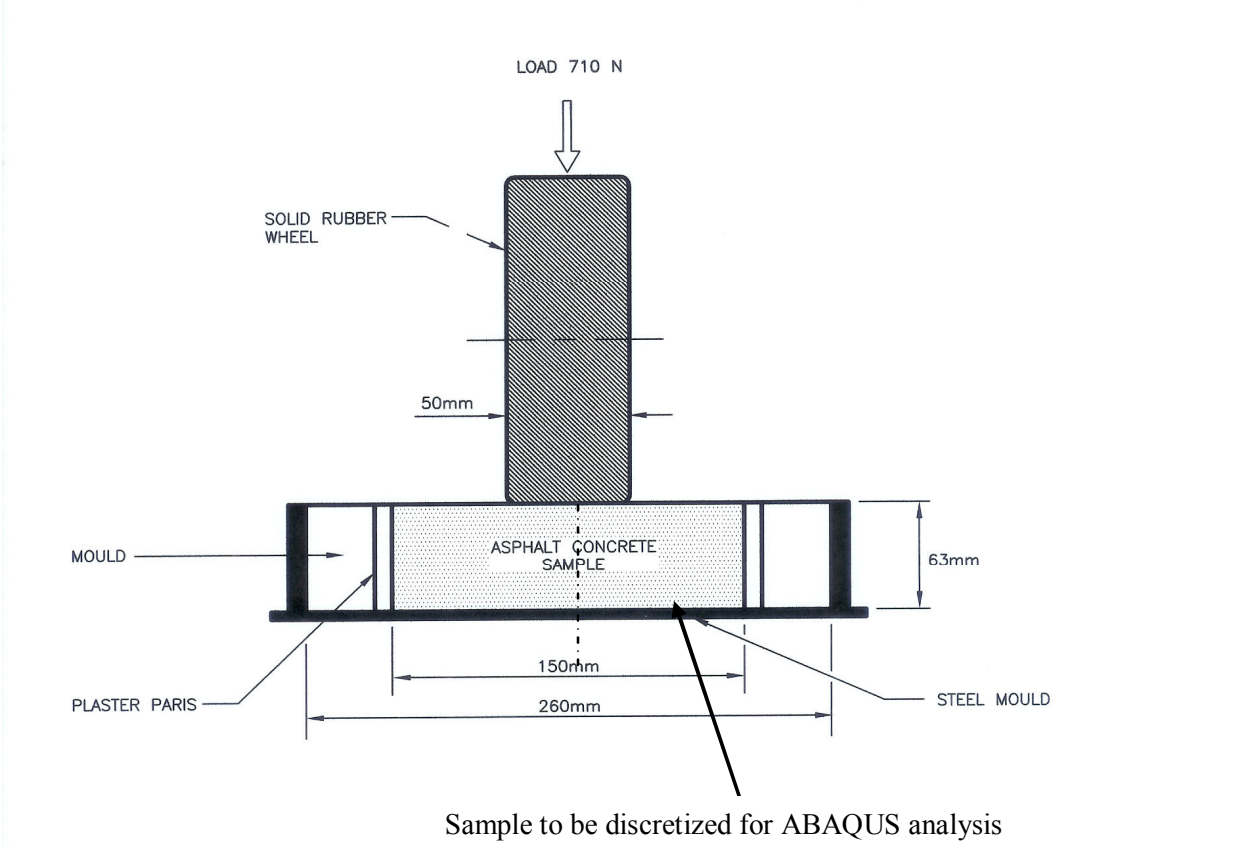

Figure 7.1 Schematic Rutting Resistance Testing in HWRT Used in ABAQUS Modeling.

A general schematic of the used finite element mesh is shown in Figure 7.2. The model has 504 elements, 550 nodes and 1,100 degrees of freedom.

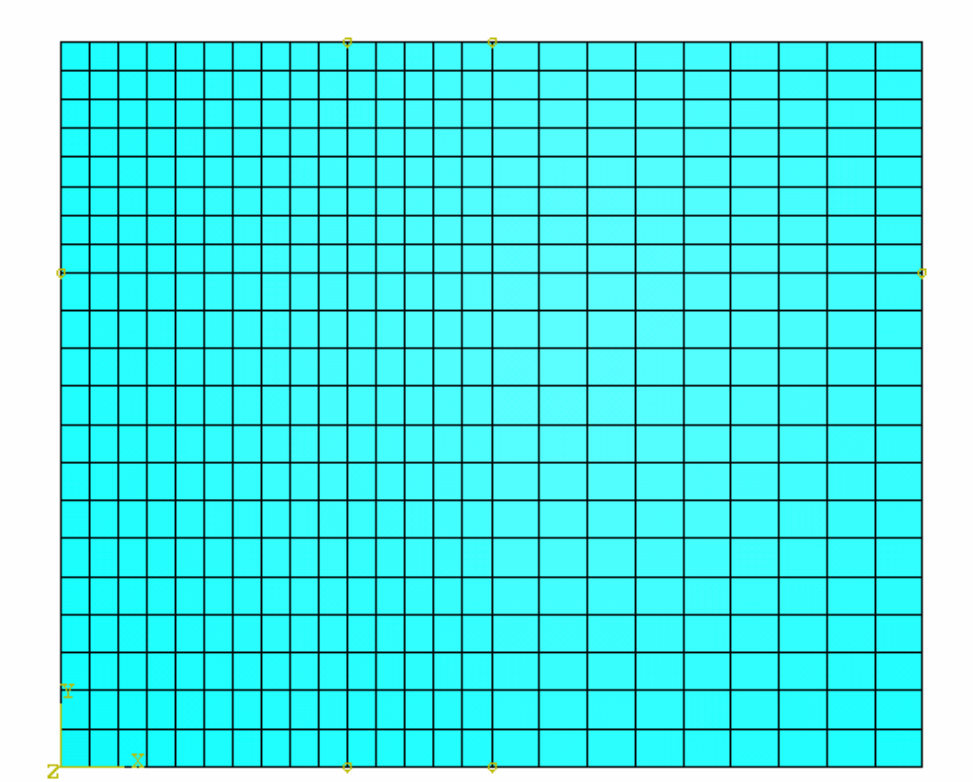

Figure 7.2 Schematic of Finite Element Mesh Used in HWRT Testing Simulation.

The modulus of elasticity at a temperature of 50ºC, used in the analysis, is obtained by the interpolation of the modulus at a frequency of 1 Hz from the testing described in Chapter Five, Material Characterization. The Poisson's ratio is calculated using the following formula given in MEPDG [NCHRP 2004a]:

$$\mu_{ac} = 0.15 + 0.35/1+e^{(-1.63+3.84x10^{-6}E_{ac})} \quad (7.2)$$

where:

μ_{ac} = Poisson's ratio of asphalt mix at a specific temperature

E_{ac} = modulus of asphalt mix at a specific temperature (psi)

The development of the creep parameters is described in Chapter Six, Asphalt Viscoplastic Behaviour. The elastic and initial creep parameters used in the simulation are shown in Table 7.1.

Table 7.1 Asphalt Mix Elastic and Creep Parameters.

Mix	Material Parameters				
	Elastic		Creep		
	Modulus kPa	Poisson's Ratio	A ($x10^{-8}$)	n	m
HL 3	950,000	0.41	14	1.48	-0.60
SMA L	800,000	0.42	113	1.04	-0.66
SMA G	800,000	0.42	42	1.31	-0.65
SP 19 D	1,600,000	0.39	32	1.20	-0.68
SP 19 E	1,400,000	0.40	47	1.20	-0.64

The footprint of the HWRT solid rubber wheel on the surface of asphalt mix samples, measured at a testing temperature of 50ºC, is shown in Figure 7.3. The average length of the wheel footprint of 28.5 mm is used to calculate the loading time and the contact pressure. For the load of 710 N applied in the HWRT testing, a uniform loading pressure of 500 kPa is used in the analysis.

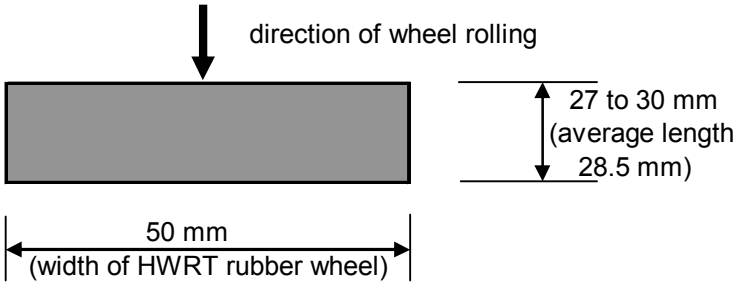

Figure 7.3 Footprint of HWRT Solid Rubber Wheel.

The test path in the HWRT is 230 mm long and typically, 53 ± 2 passes are completed in one minute. The time of loading is calculated using the following equation given in MEPDG [NCHRP 2004a]:

$$t = L_{eff} / 17.6\ v_s \qquad (7.3)$$

where:

t = time of loading (sec)

L_{eff} = effective length (inch)

v_s = operating speed (mph)

For the average wheel footprint length of 28.5 mm, the time of loading in one pass is about 0.14 sec. The time of lading conversion described by [Hua 2000] and shown in Figure 7.4 is used in this research. The T1-T2 time is 0.14 sec. and the T0-T1 and T2-T3 time periods are 0.07 sec. The converted loading time in one pass is 0.21 sec. The time of loading for 20,000 passes is 4,200 sec.

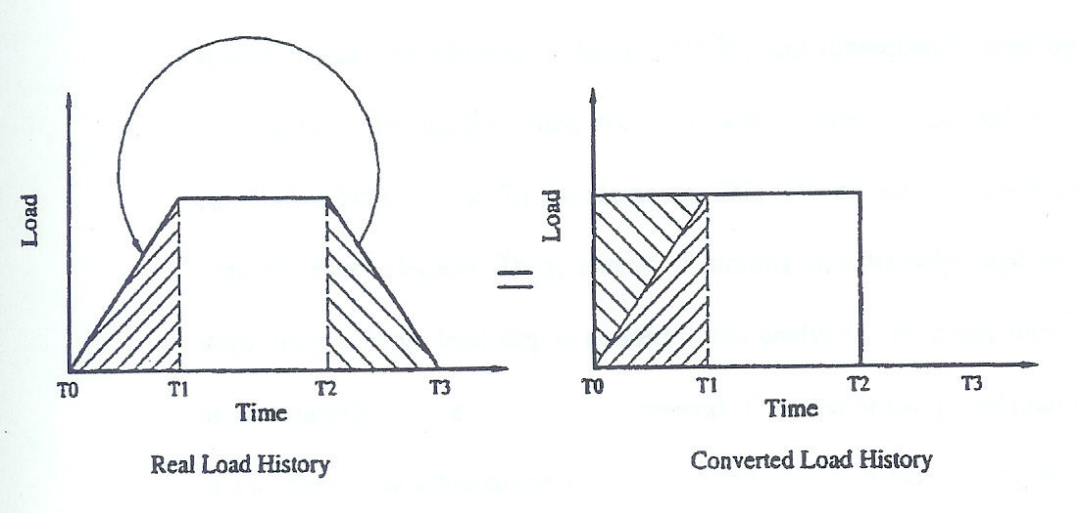

Figure 7.4 Load Duration Conversion [Hua 2000].

The boundary conditions and loading are shown in Figure 7.5. There are only vertical movements allowed along edge AB, and no vertical and horizontal movements are allowed along edges BC and CD. Loading of 500 kPa is applied along edge AE.

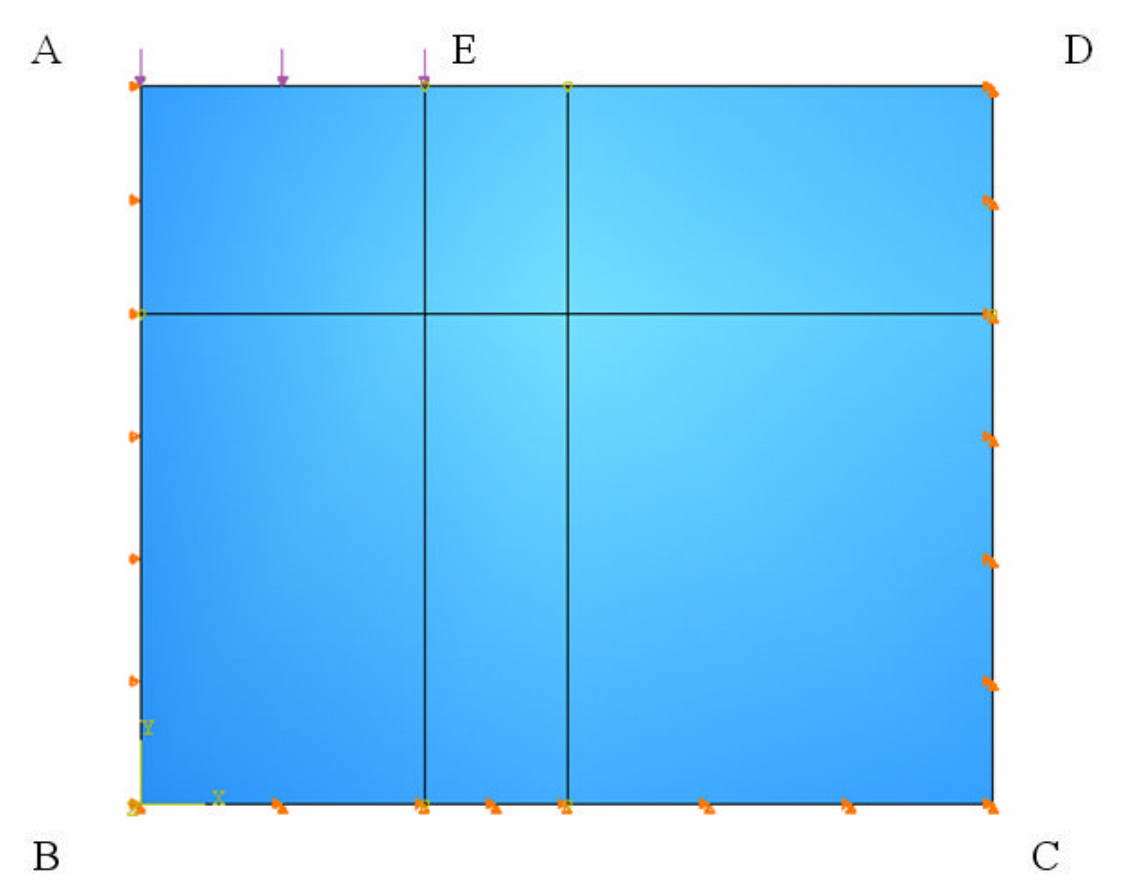

Figure 7.5 Boundary Conditions and Loading.

The Mises stress is used in the calculation of the creep rate in the creep model. Figures 7.6 and 7.7 show the Mises stresses in the HL 3 sample, calculated in ABAQUS at the end of the HWRT testing and in the triaxial repeated load creep testing, respectively. The Mises stress at the top of the sample in the HWRT test ranges from about 150 kPa to 230 kPa (with one point location of about 250 kPa). It is assumed that the deviatoric stress levels used in the repeated load creep testing of 100 kPa and 200 kPa is sufficient for the development of the creep parameters to be used in the simulation of the HWRT testing.

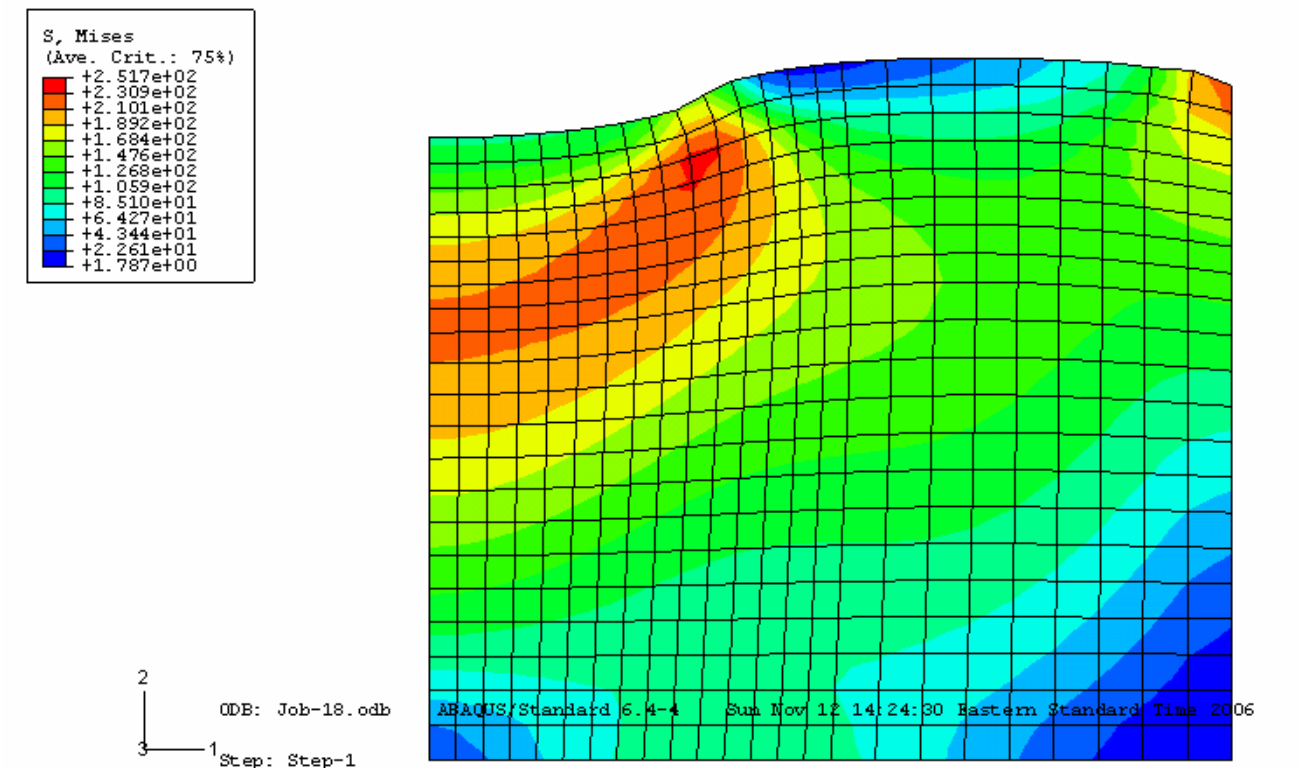

Figure 7.6 Mises Stress in HL 3 Sample after 20,000 Passes in HWRT Testing.

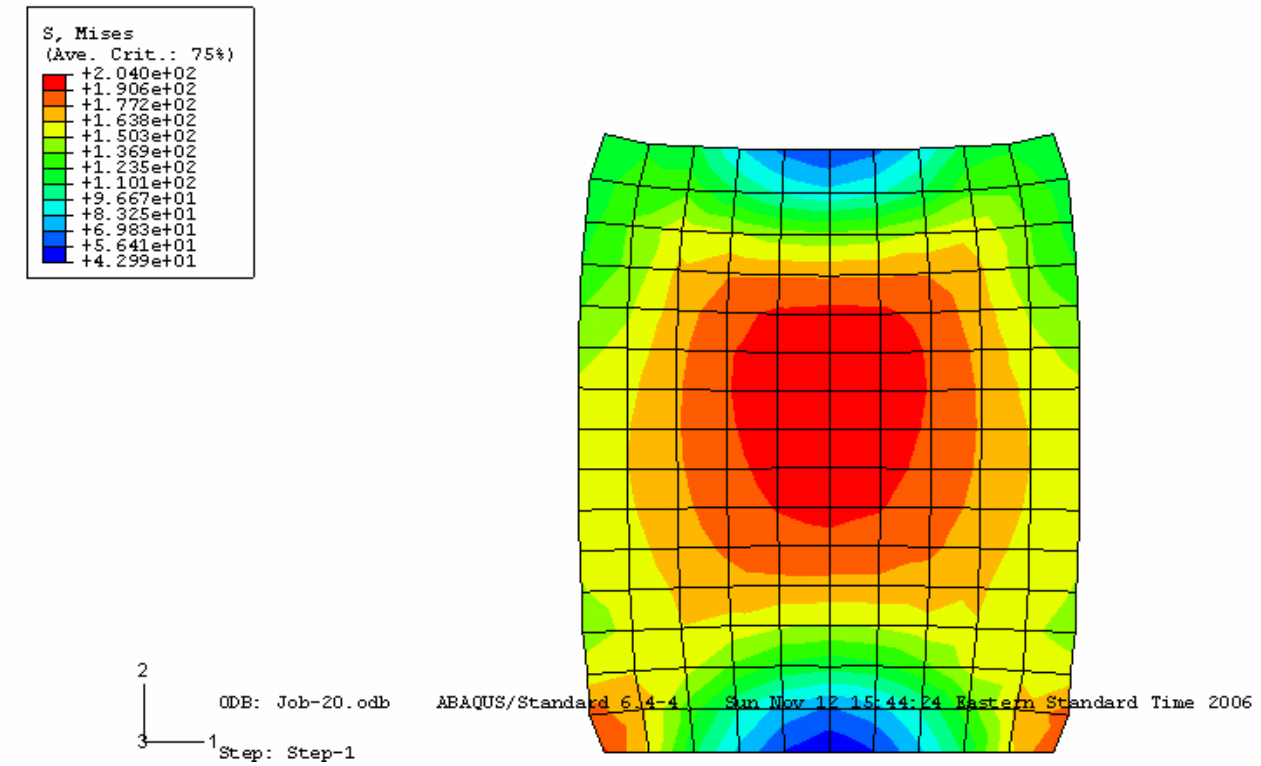

Figure 7.7 Mises Stresses in HL 3 Sample at the End of the 20th Cycle in the Triaxial Repeated Load Creep Test at 200 kPa Deviatoric Stress.

Figure 7.8 shows the deformed shape of the HL 3 sample after 20,000 passes predicted in the ABAQUS simulation. The selected deformation scale factor is 5.0. Figures 7.9 to 7.12 show the predicted deformed shapes of the SMA L, SMA G, SP 19 D and SP 19 E samples; U2 is the vertical deformation. The deformation scale factor is 5.0. There is some predicted upward deformation visible in the finite element modeling. Only the downward rutting is monitored and recorded during the HWRT testing. Although some upheavals were observed in the HWRT testing, they were not recorded.

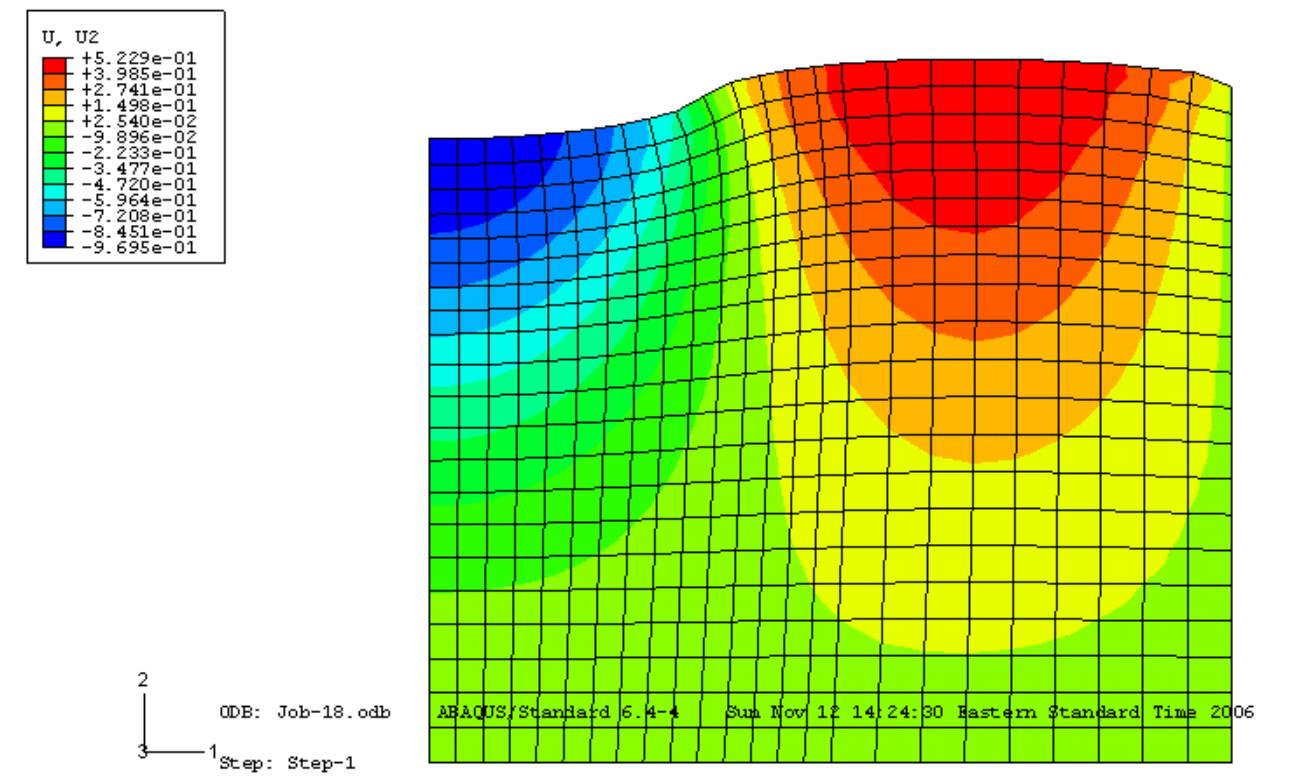

Figure 7.8 Predicted Deformed Shape of HL 3 Sample after 20,000 Passes.

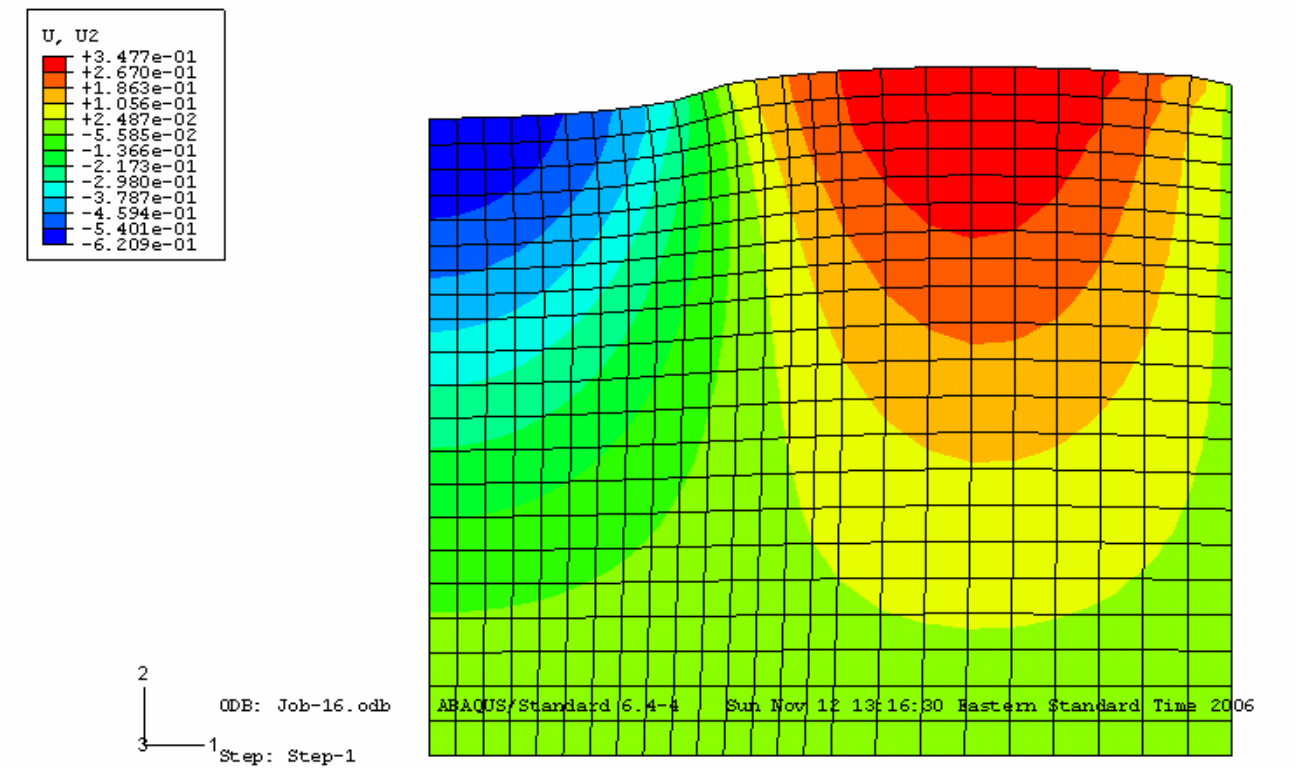

Figure 7.9 Predicted Deformed Shape of SMA L Sample after 20,000 Passes.

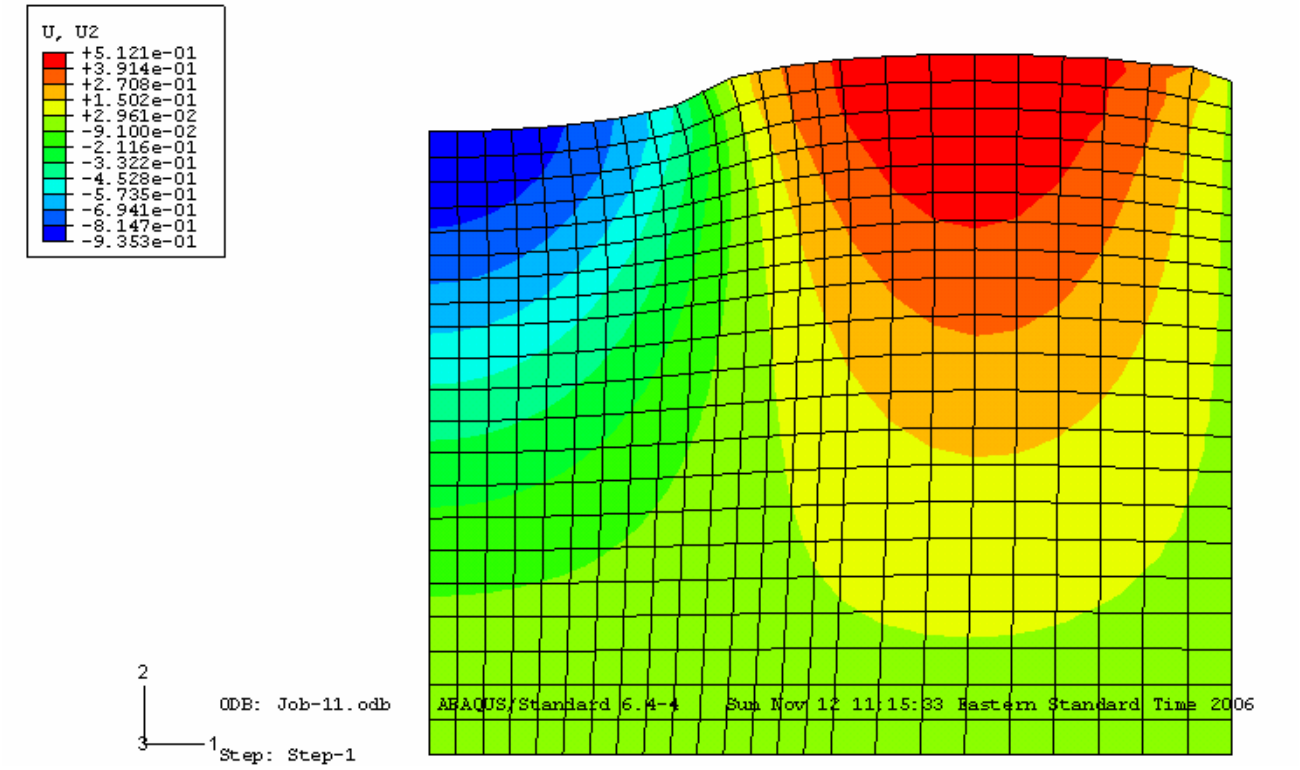

Figure 7.10 Predicted Deformed Shape of SMA G Sample after 20,000 Passes.

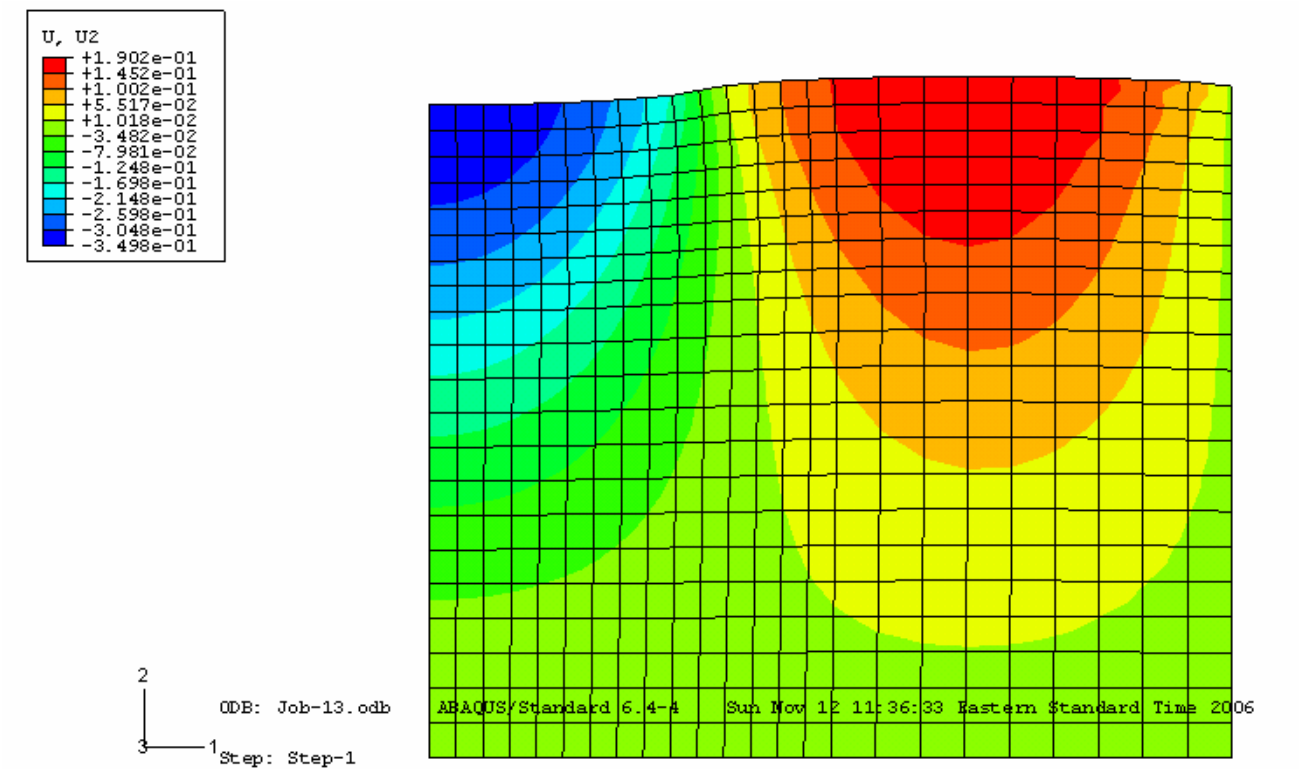

Figure 7.11 Predicted Deformed Shape of SP 19 D Sample after 20,000 Passes.

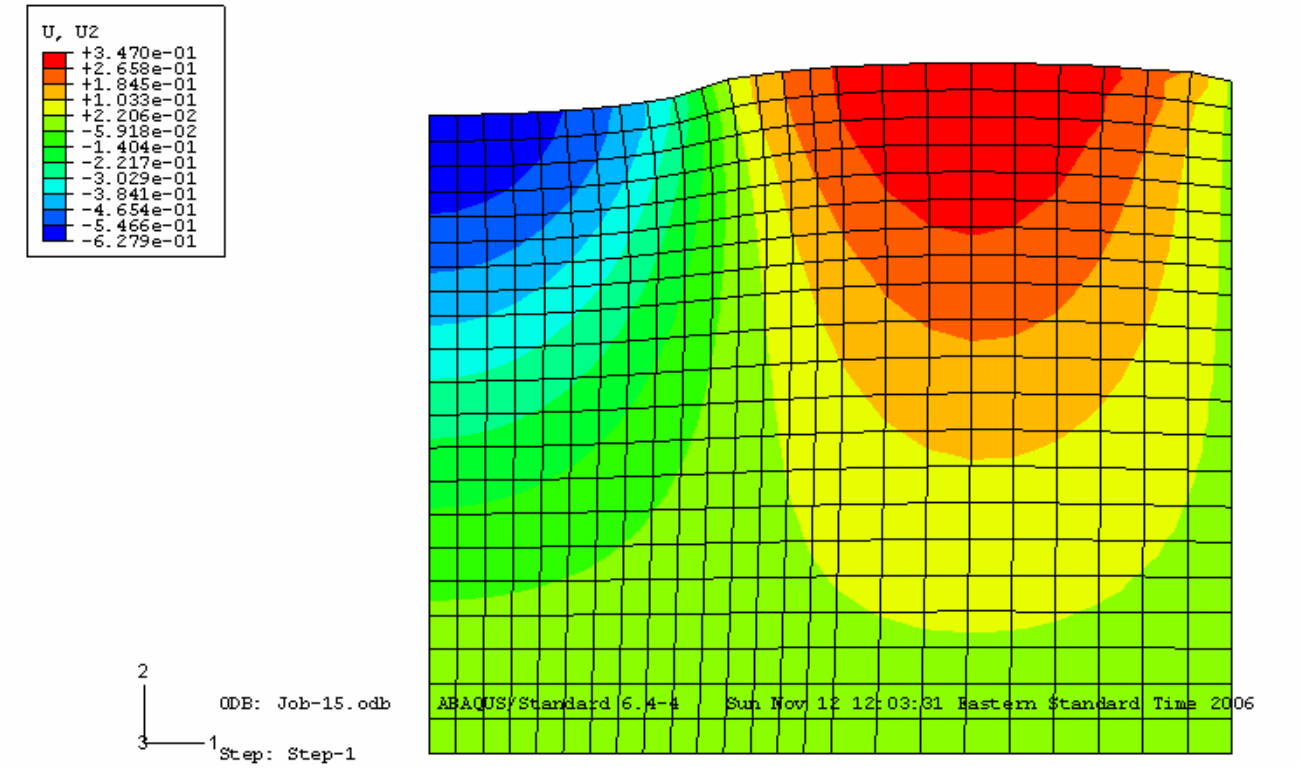

Figure 7.12 Predicted Deformed Shape of SP 19 E Sample after 20,000 Passes.

The rutting predicted in the ABAQUS simulations is compared with the measured rut depth in the HWRT testing as shown in Table 7.2 and Figure 7.13. The linear trend line for this relationship has R^2 of 0.83. The trend for the dense graded mixes (HL 3, SP 19 D and SP 19 E) only is better, as shown in Figure 7.14. The difference in the relationship for the dense graded mixes and the SMA mixes is due to the different mechanisms controlling the behaviour of the mixes as explained in Chapter Five, Mix Characterization. The predicted rutting was 1.9 to 3.1 times lower than the rutting measured in the HWRT laboratory testing. Mix ranking in the predicted rutting is the same as in the measured rutting.

Table 7.2 Comparison of Measured and Predicted Rutting after 20,000 Passes.

Mix	Rutting Measured in HWRT		Rutting Predicted in ABAQUS	
	Rut Depth (mm)	Ranking	Rut Depth (mm)	Ranking
HL 3	2.4	5	1.0	5
SMA L	1.5	2	0.6	2
SMA G	1.8	4	0.9	4
SP 19 D	1.1	1	0.4	1
SP 19 E	1.6	3	0.6	3

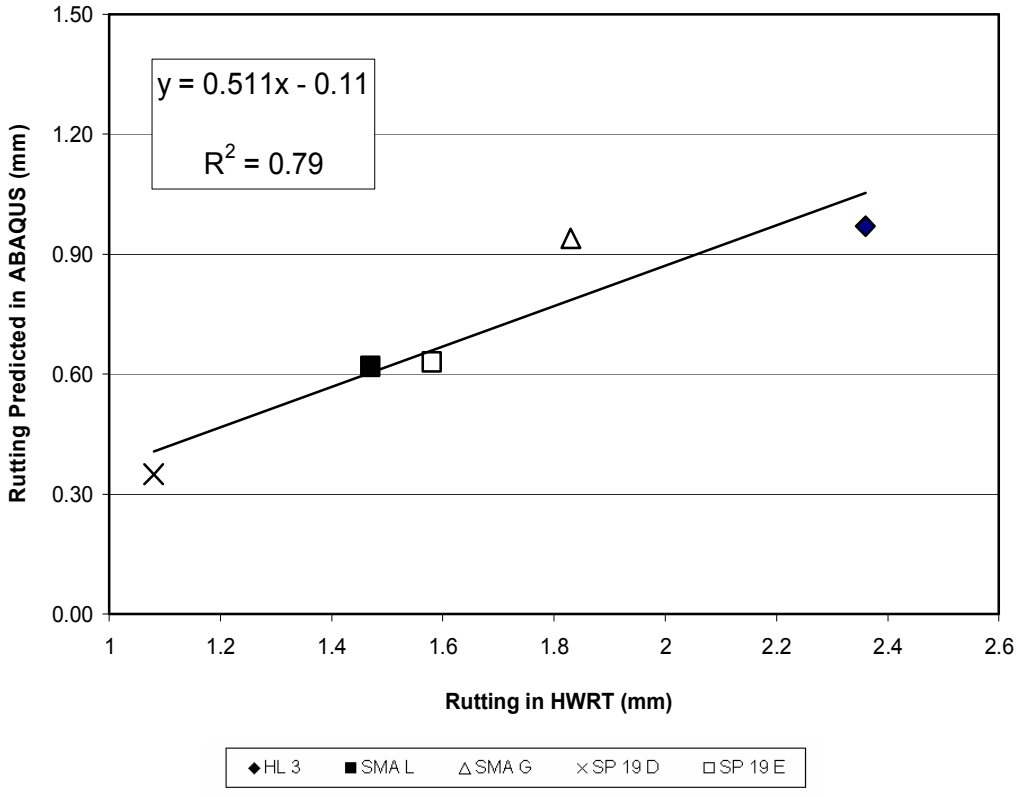

Figure 7.13 Relationship Between Measured and Predicted Rutting of HL 3, SMA L, SMA G, SP 19 E and SP 19 E Mixes.

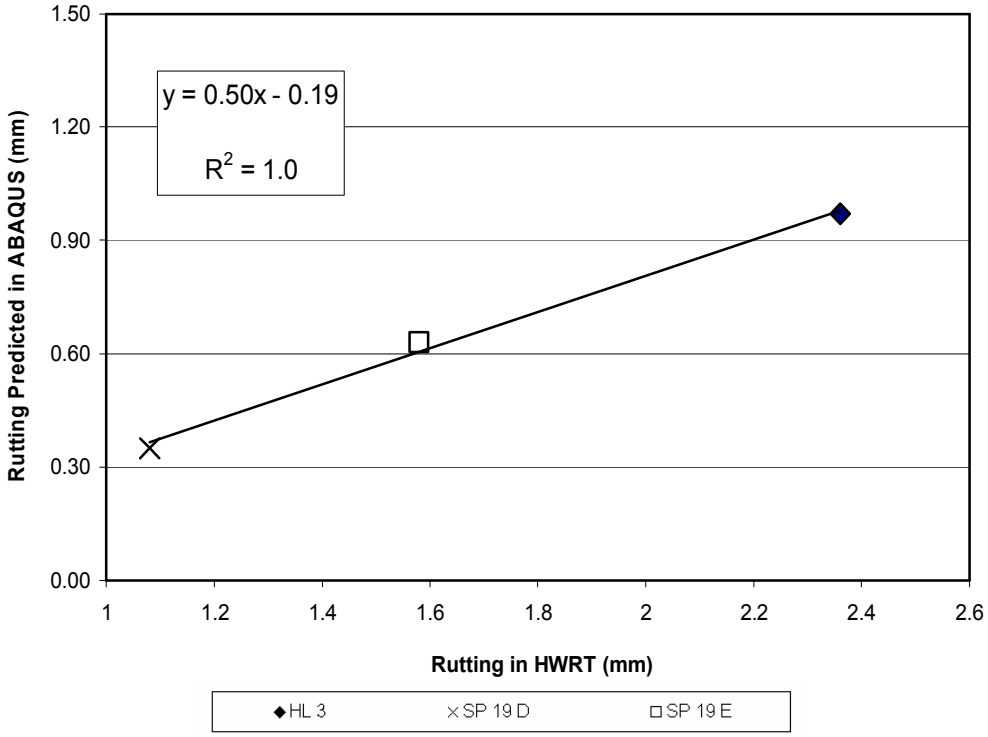

Figure 7.14 Relationship Between Measured and Predicted Rutting of the Dense Graded (HL 3, SP 19 D and SP 29 E) Mixes Only.

7.2.2 Axisymmetric and 3D Slice Analyses

In addition to the 2D plane strain ABAQUS simulation, additional analysis was carried out in axisymmetric 2D space. Also an analysis in three-dimensional (3D) space was carried out on a modeled slice of the HWRT sample.

A schematic of the axisymmetric 2D model is shown in Figure 7.15. The element mesh was the same as used in the 2D plane strain analysis. Figure 7.16 shows the deformed shape of the HL 3 sample after 20,000 passes predicted in the axisymmetric analysis. The deformed shapes of samples of the SMA L, SMA G, SP 19 D and SP 91 E mixes are shown in Appendix C.

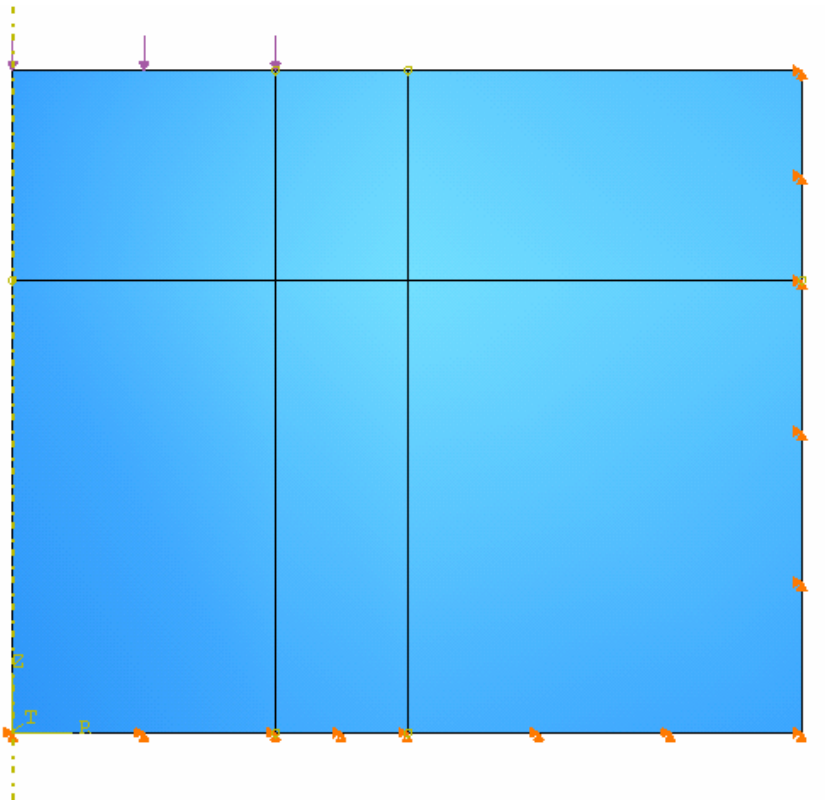

Figure 7.15 Schematic of Axisymmetric Model.

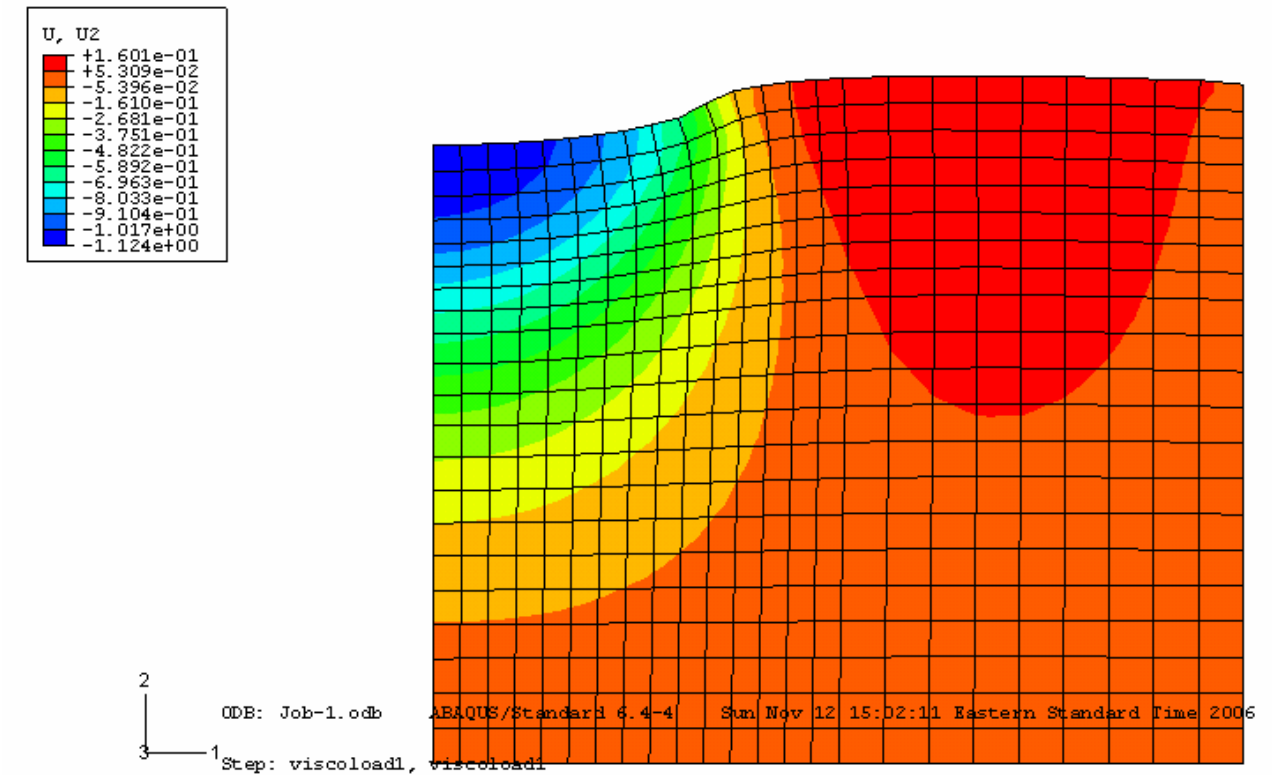

Figure 7.16 Deformed Shape of HL 3 Sample after 20,000 Passes Predicted in Axisymmetric Analysis.

A schematic of the 3D slice of the HWRT sample is shown in Figure 7.17. No side confinement was applied in the 3D slice model. A schematic of the element mesh is shown in Figure 7.18. Figure 7.19 shows the deformed shape of the HL 3 sample after 20,000 passes predicted in the 3D slice analysis. The deformed shapes of samples of the SMA L, SMA G, SP 19 D and SP 91 E mixes are shown in Appendix C.

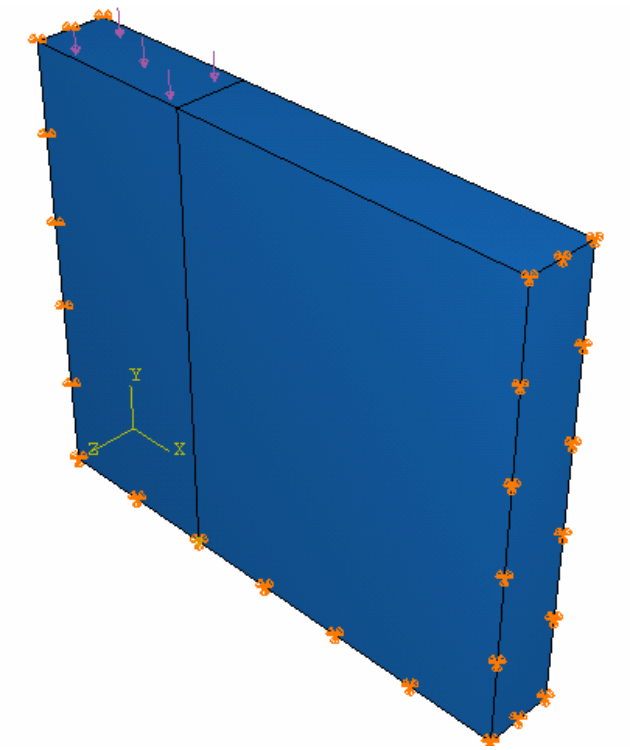

Figure 7.17 Schematic of 3D Slice of HWRT Sample.

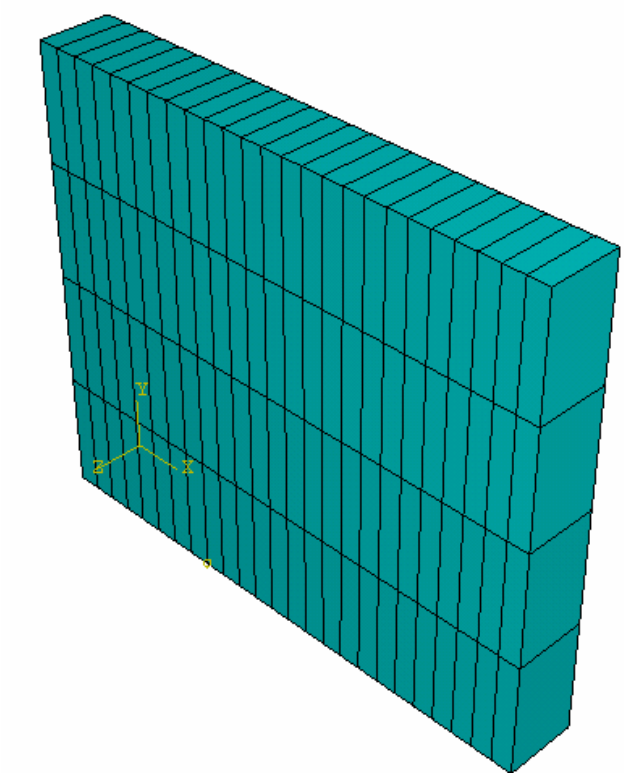

Figure 7.18 Schematic of Element Mesh of 3D Slice of HWRT Sample.

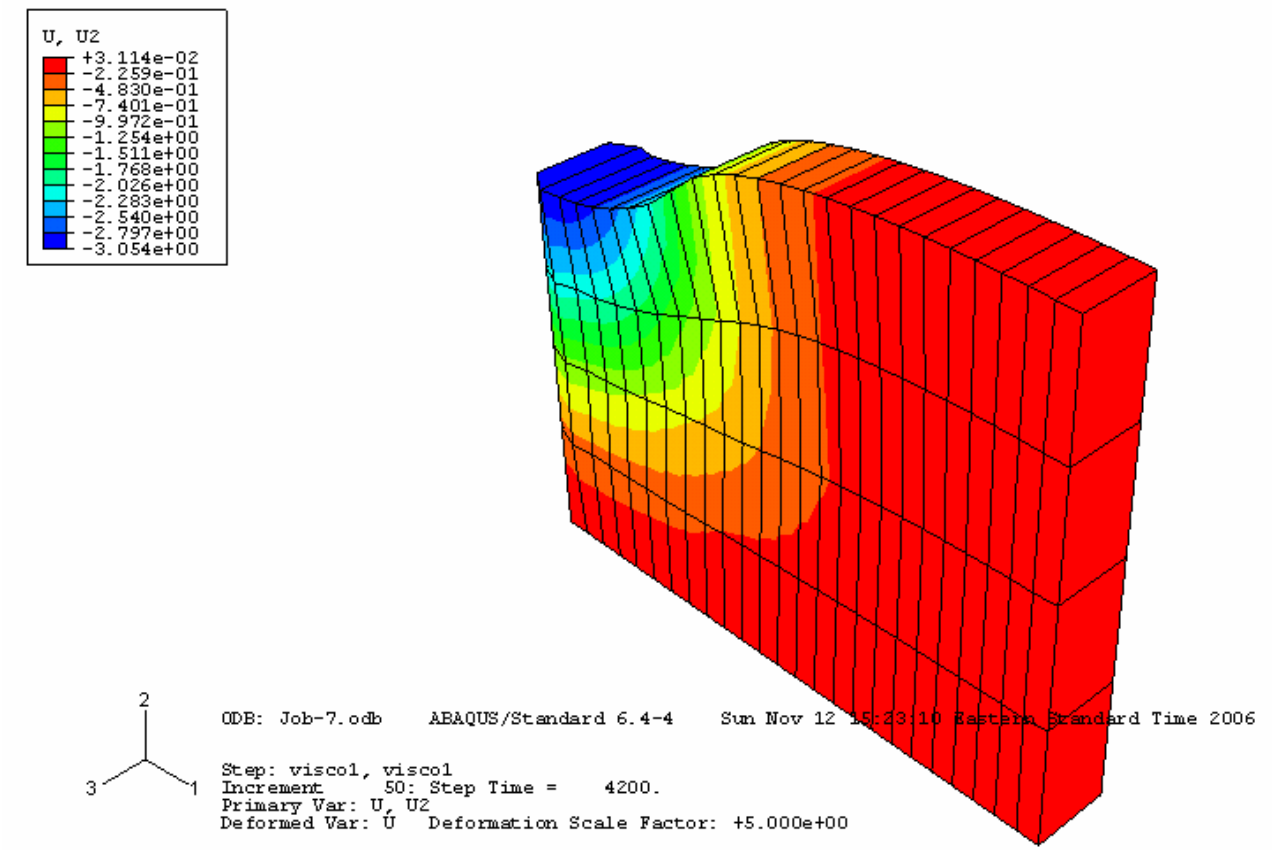

Figure 7.19 Deformed Shape of HL 3 Sample after 20,000 Passes Predicted in 3D Slice Analysis.

Table 7.3 shows a summary of measured deformations in the HWRT and predicted deformations in the 2D plane strain, axisymmetric 2D space and 3D slice analyses, including mix ranking and a factor of measured value over predicted value. As anticipated, the deformations predicted in the axisymmetric analyses are closer to the measured deformations than the predicted deformations in the plane strain analyses, with the factor of measured to predicted values ranging from 1.6 to 2.6. The deformations predicted in the 3D slice analyses are generally higher than the measured deformations with the factor of measured to predicted values ranging from 0.7 to 0.9; for the SP 19 D mix, the factor is 1.1. The ranking of the mixes is the same in all three types of finite element analysis and is the same as the ranking in the laboratory HWRT testing.

Table 7.3 Summary of Measured and Predicted Deformations ABAQUS 2D, Axisymmetric and 3D Slice Analyses.

Mix Type	Rutting in HWRT										
	Measured		Predicted in ABAQUS								
	mm	Mix Ranking	2D Plane Strain			Axisymmetirc 2D Space			3D Slice		
			mm	Factor*	Mix Ranking	mm	Factor*	Mix Ranking	mm	Factor*	Mix Ranking
HL 3	2.4	5	1.0	2.4	5	1.1	2.1	5	3.1	0.8	5
SMA L	1.5	2	0.6	2.4	2	0.7	2.0	2	1.5	0.8	2
SMA G	1.8	4	0.9	1.9	4	1.1	1.6	4	2.7	0.7	4
SP 19 D	1.1	1	0.4	3.1	1	0.4	2.6	1	0.9	1.1	1
SP 19 E	1.6	3	0.6	2.5	3	0.7	2.1	3	1.7	0.9	3

* Factor = measured value / predicted value.

Before the asphalt creep parameters developed in the laboratory creep testing are used in the pavement in-situ performance finite element analysis, it is considered necessary to calibrate them against the measured rutting in the HWRT testing.

7.2.2 Calibration Against Measured Rutting in HWRT

The rutting measured in the HWRT is used to calibrate the creep parameters, A, n and m. The ABAQUS predicted rut depth is compared with the measured rut depth at different cumulative times. The parameters are estimated by trial and error and adjusted until a good fit is obtained.

The n parameter is stress related. As the rut resistance testing in the HWRT is conducted at a constant loading stress of 500 kPa, the n parameter is fixed at the initial level shown in Table 7.1. Parameter A is the value of the y-axis intercept while parameter m is related to the slope of the strain-time relationship curve in a log-log scale [White 2002]. Initially only parameter A is adjusted to match the rutting depth

measured after 20,000 passes. Figures 7.20 to 7.24 compare the measured rut depth versus time relationship with rutting predicted in ABAQUS at the time of loading of about 1000, 1800, 2600, 3300 and 4200 sec.

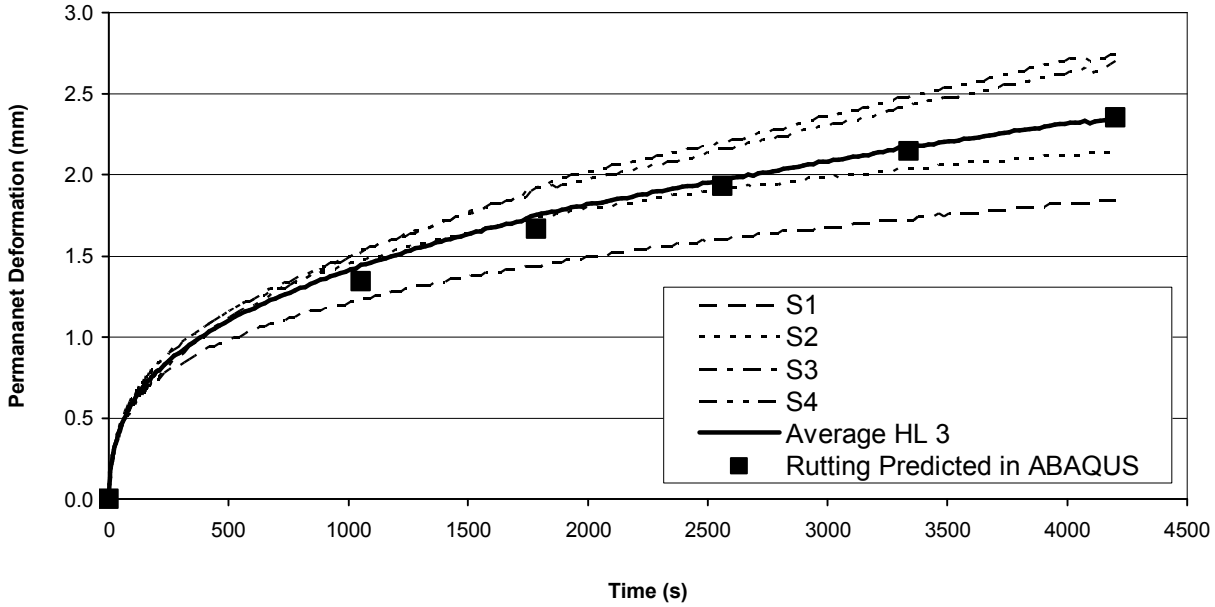

Figure 7.20 Rutting Measured in HWRT and Predicted in ABAQUS for the HL 3 Mix.

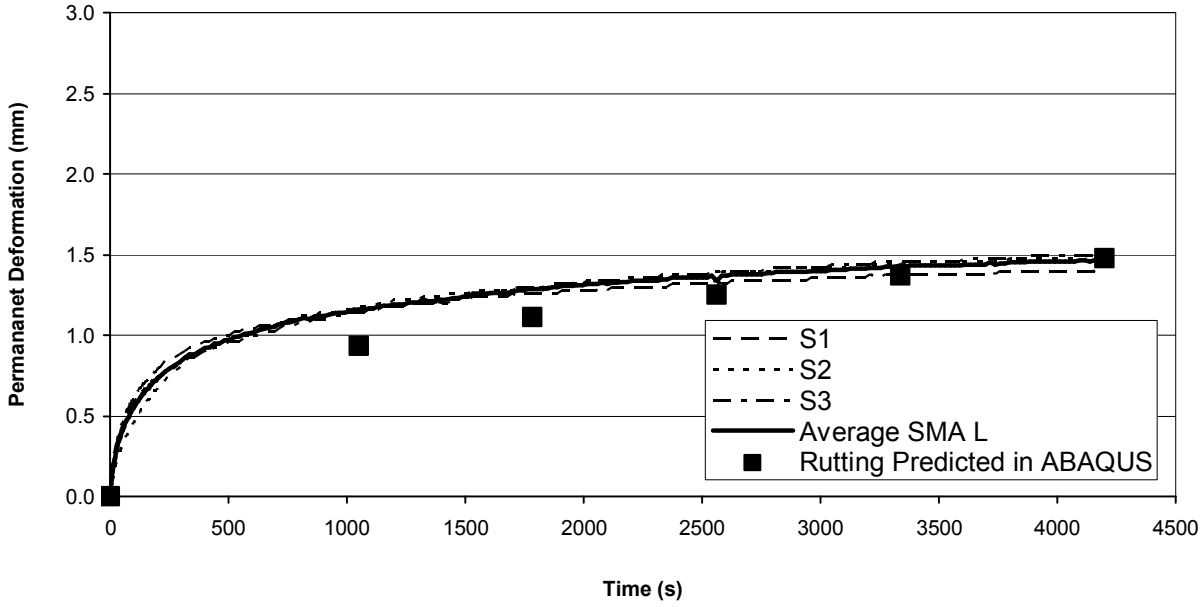

Figure 7.21 Rutting Measured in HWRT and Predicted in ABAQUS for the SMA L mix.

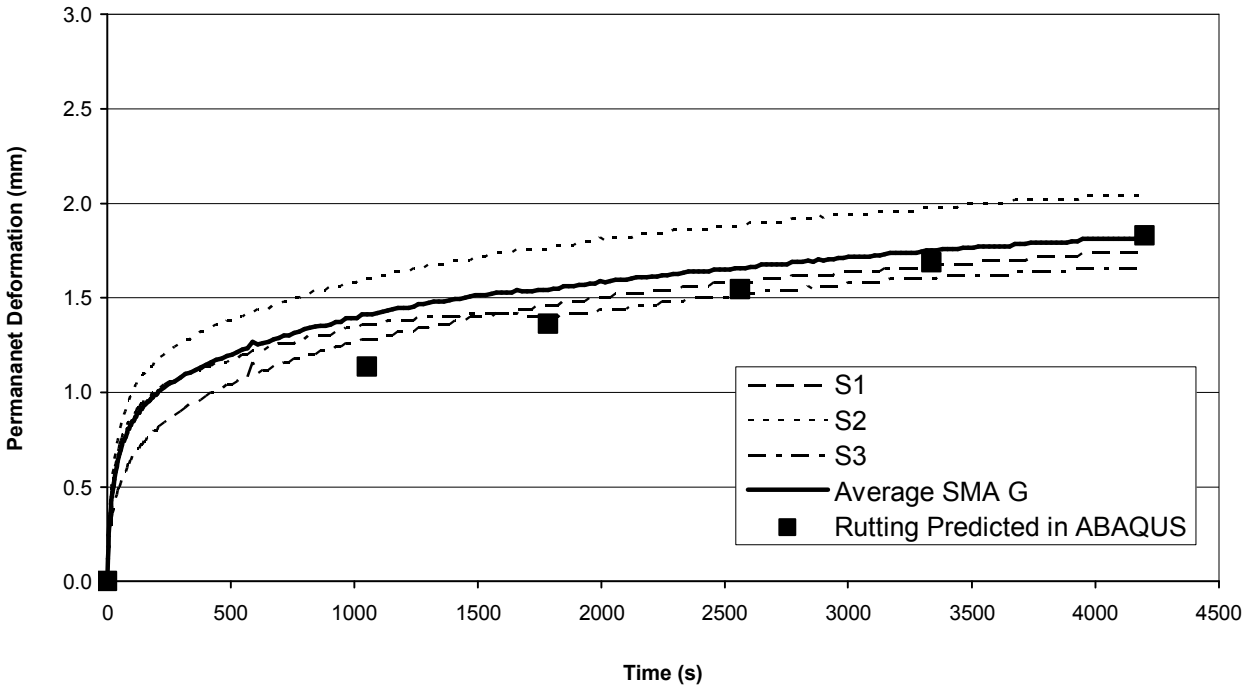

Figure 7.22 Rutting Measured in HWRT and Predicted in ABAQUS for the SMA G Mix.

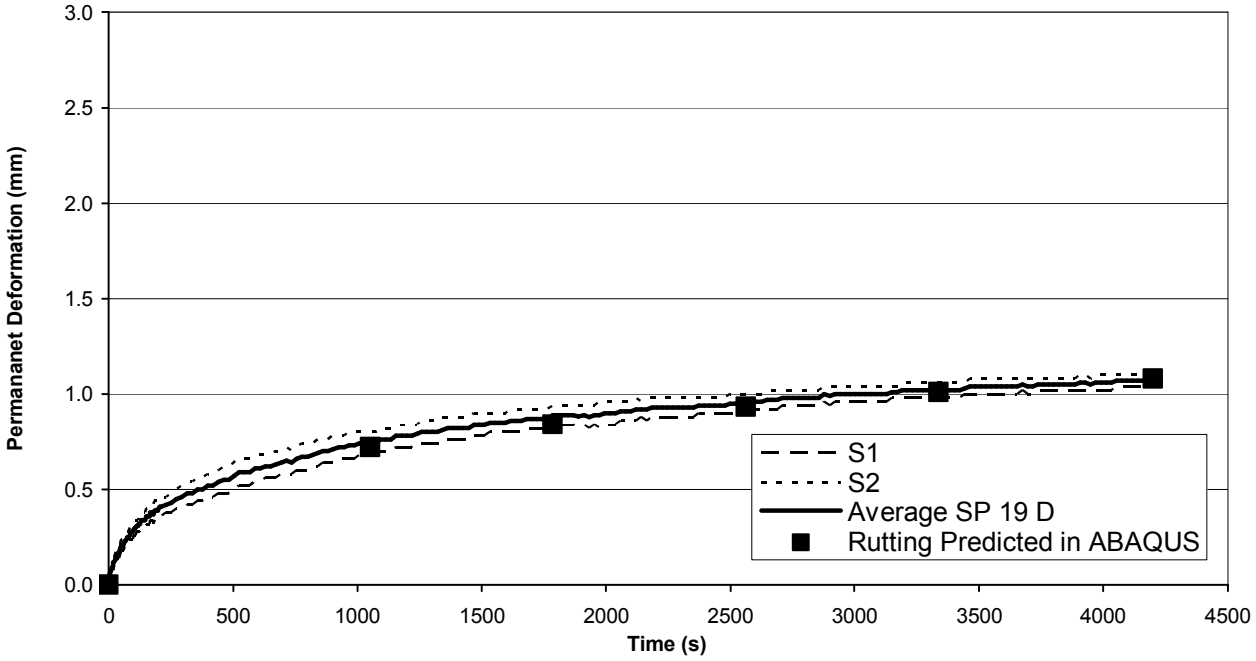

Figure 7.23 Rutting Measured in HWRT and Predicted in ABAQUS for the SP 19 D Mix.

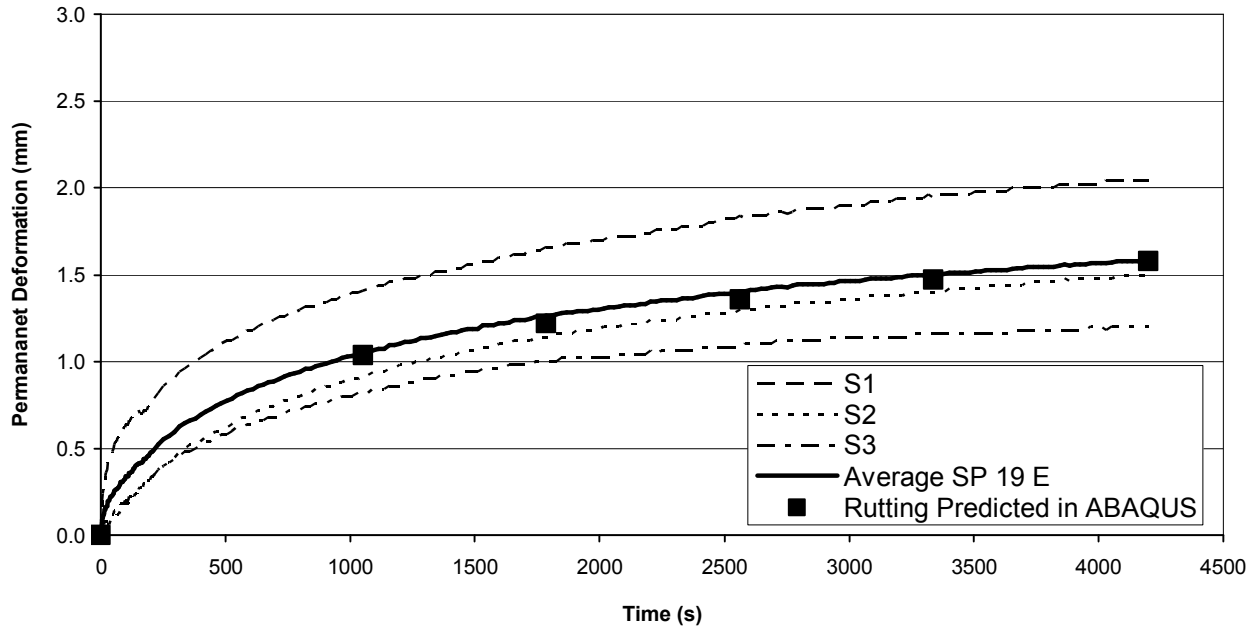

Figure 7.24 Rutting Measured in HWRT and Predicted in ABAQUS for the SP 19 E Mix.

After parameter A adjustment, the rutting predicted in ABAQUS overlaps the measured rutting in the dense graded mixes SP 19 D and SP 19 E. For the other three mixes, the adjustment of parameter m, controlling the slope, is also required. Only very small adjustment is required for the HL 3 mix; this small adjustment is likely due to relatively wide scatter of the HWRT testing results. However, for the SMA L and SMA G mixes much more significant adjustment is required. This is an indication that the power law model works very well for the dense graded mixes; however, it does not work very well for the SMA mixes that have a different mechanism controlling the behaviour of the mix. It is considered critical that the rutting model is calibrated against the measured rutting. The importance of proper model calibration was emphasized by [Chehab 2005]

Table 7.4 shows the final elastic and creep parameters. These values are used in the ABAQUS modeling of the pavement in-situ performance. Figures 7.25 to 7.27 show the measured rutting and rutting predicted in ABAQUS using the final parameters for the HL 3, SMA L and SMA G mixes. Table 7.5 shows the slopes and the intercepts in Phase 2 of rutting deformation.

Table 7.4 Final Material Parameters Used in ABAQUS Modeling

Mix	Material Parameters				
	Elastic		Creep		
	Modulus kPa	Poisson's Ratio	A ($x10^{-8}$)	n	m
HL 3	950,000	0.41	41	1.48	-0.63
SMA L	800,000	0.42	521	1.04	-0.80
SMA G	800,000	0.42	162	1.31	-0.79
SP 19 D	1,600,000	0.39	102	1.20	-0.68
SP 19 E	1,400,000	0.40	124	1.20	-0.64

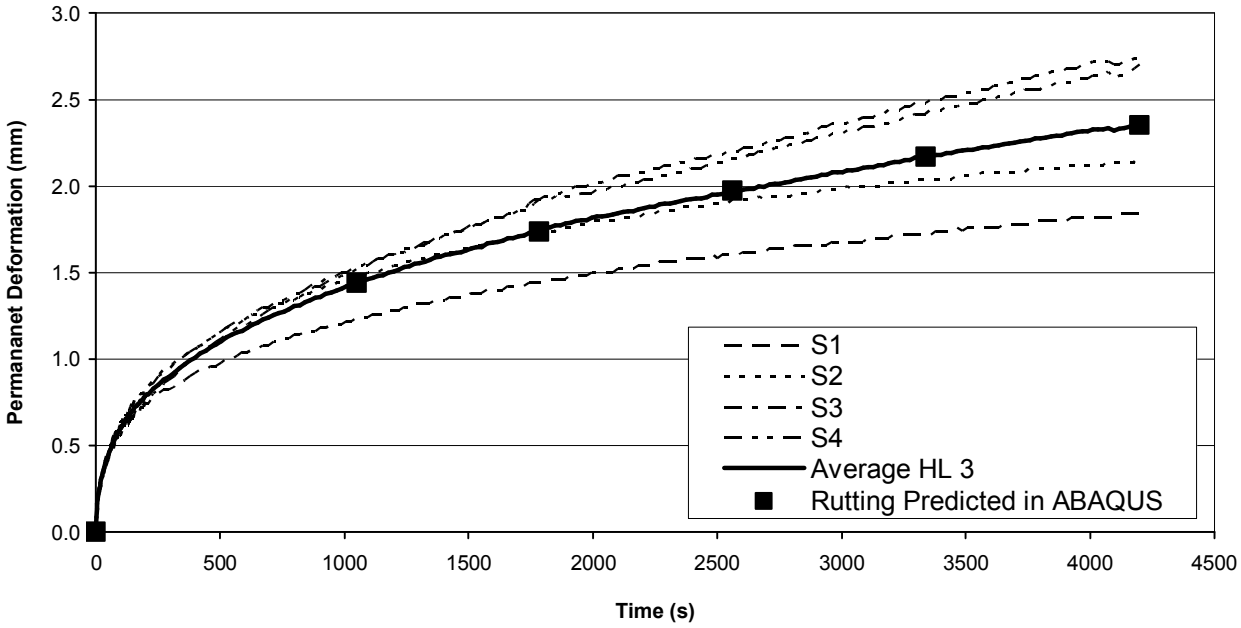

Figure 7.25 Measured and Predicted Rutting of the HL 3 Mix after Parameter m Adjustment.

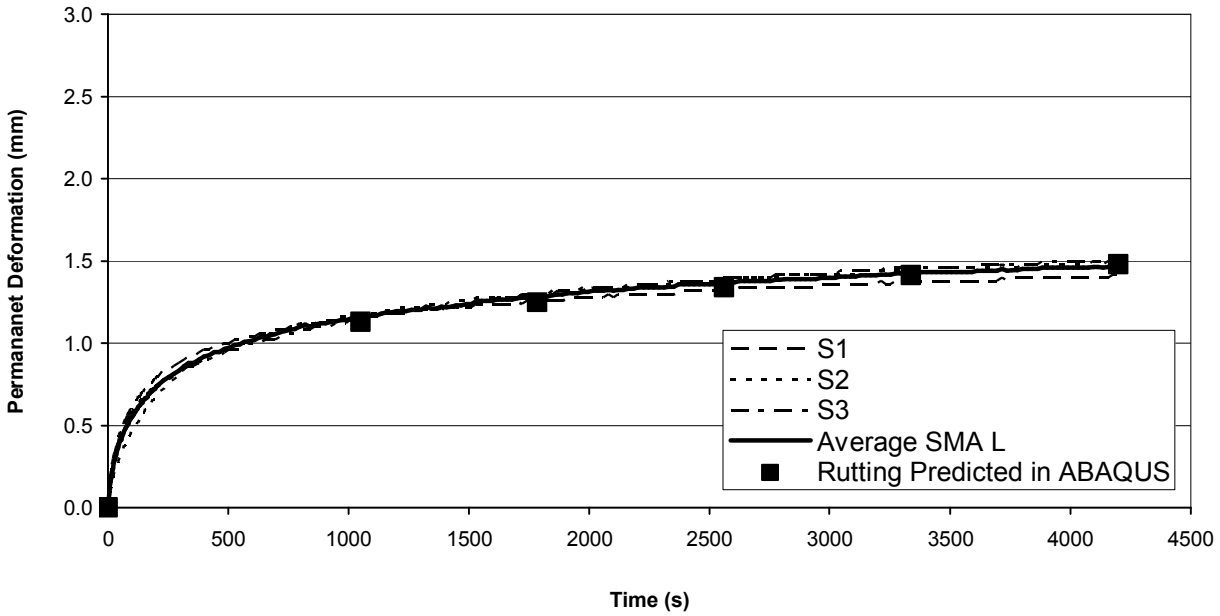

Figure 7.26 Measured and Predicted Rutting of the SMA L Mix after Parameter m Adjustment.

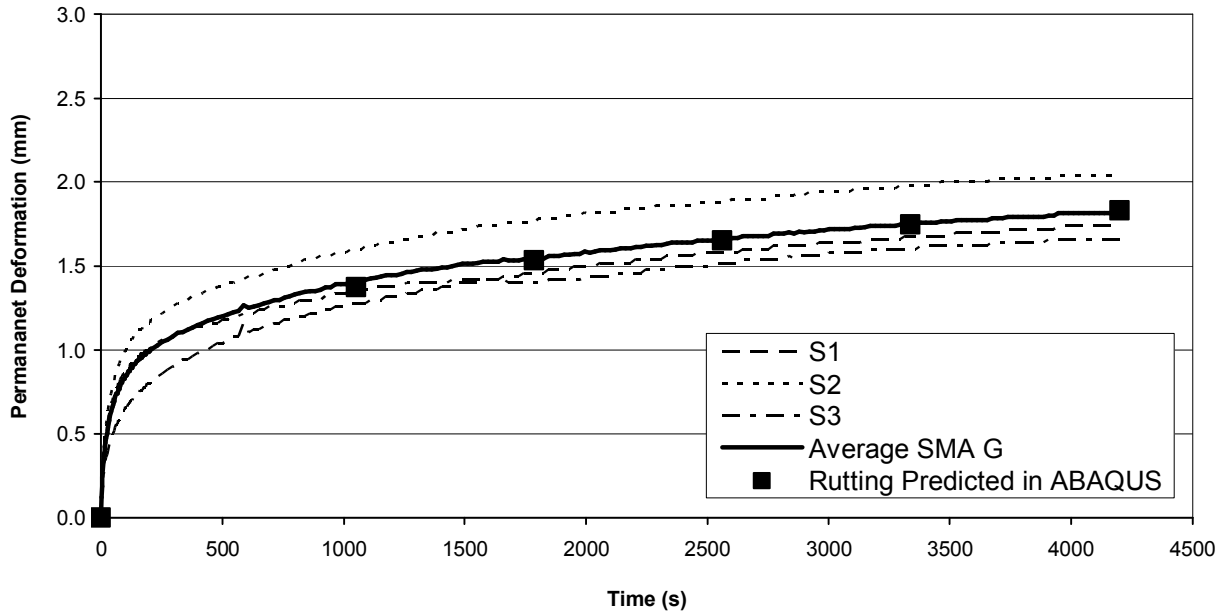

Figure 7.27 Measured and Predicted Rutting of the SMA G Mix after Parameter m Adjustment.

Table 7.5 Slopes and Intercepts for Measured and Predicted Rutting

Mix	Parameter			
	Slope		Intercept	
	HWRT	ABAQUS Simulation	HWRT	ABAQUS Simulation
HL 3	0.00025	0.00025	1.3	1.3
SMA L	0.00007	0.00009	1.1	1.2
SMA G	0.00011	0.00012	1.4	1.3
SP 19 D	0.00008	0.00009	0.7	0.7
SP 19 E	0.00015	0.00015	1.0	1.0

7.3 MODELING PAVEMENT IN-SITU PERFORMANCE

The objective is to model pavement in-situ performance in ABAQUS using the material parameters developed from the laboratory testing and HWRT testing analysis. Similarly to the HWRT modeling, 2D plane strain modeling is used. The rutting predicted in ABAQUS is compared with the rutting predicted in the MEPDG pavement design analysis in Chapter Eight and subsequently used to develop rutting criteria in the HWRT testing.

7.3.1 Loading Model

It is assumed in the model that a single 63 mm (2.5 inch) lift of asphalt is placed over a Portland cement concrete base so that rutting could occur only in the asphalt layer. It is also assumed that the layer of HMA is fully bonded with the underlaying Portland cement concrete layer so that no movement of the HMA layer can occur on the surface of the concrete base.

A dual wheel system of a standard axle load of 80 kN is used in the pavement in-situ performance analysis. The system is shown in Figure 7.28. A load of 20 kN is applied by each wheel in the system.

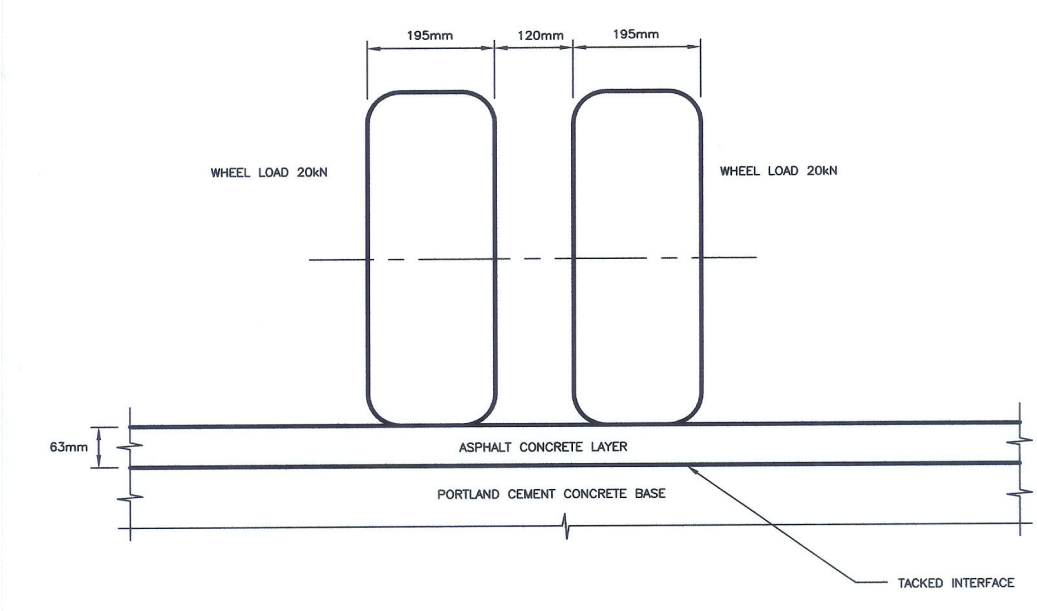

Figure 7.28 Dual Wheel System Used in Pavement In-Situ Performance Analysis.

Traditionally, tire-pavement contact stress is frequently assumed to be uniformly distributed over a circular contact area. However, recent studies have demonstrated that the tire-pavement stress is not uniformly distributed [Wang 2006]. The tire modeled in this research is a standard Goodyear G159A-11R22.5. The wheel load is applied through the tire treads to the surface of the asphalt layer. The actual footprint of the tire is shown in Figure 7.29. Because the contact area between the tire and the pavement is not exactly rectangular or circular, a new tire model is developed for the analysis based on the geometry of the tire footprint. It is shown in Figure 7.30. The wheel load is transferred to the pavement through five rectangular areas. The three middle areas are narrower and longer than the two outside areas. The different lengths of the areas are reflected in the 2D finite element analysis by using a longer time of loading for the middle three areas.

The contact pressure is not uniform. It ranges from 517 kPa (75 psi) for the outside areas to 586 kPa (85 psi) for the central area. The pressure in the remaining two areas in the middle is 552 kPa (80 psi).

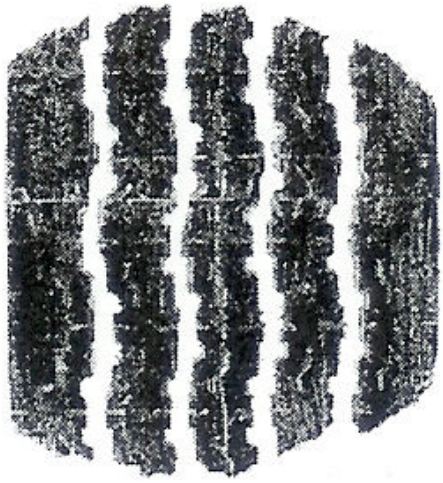

Figure 7.29 Goodyear Tire G159A-11R22.5 Footprint.

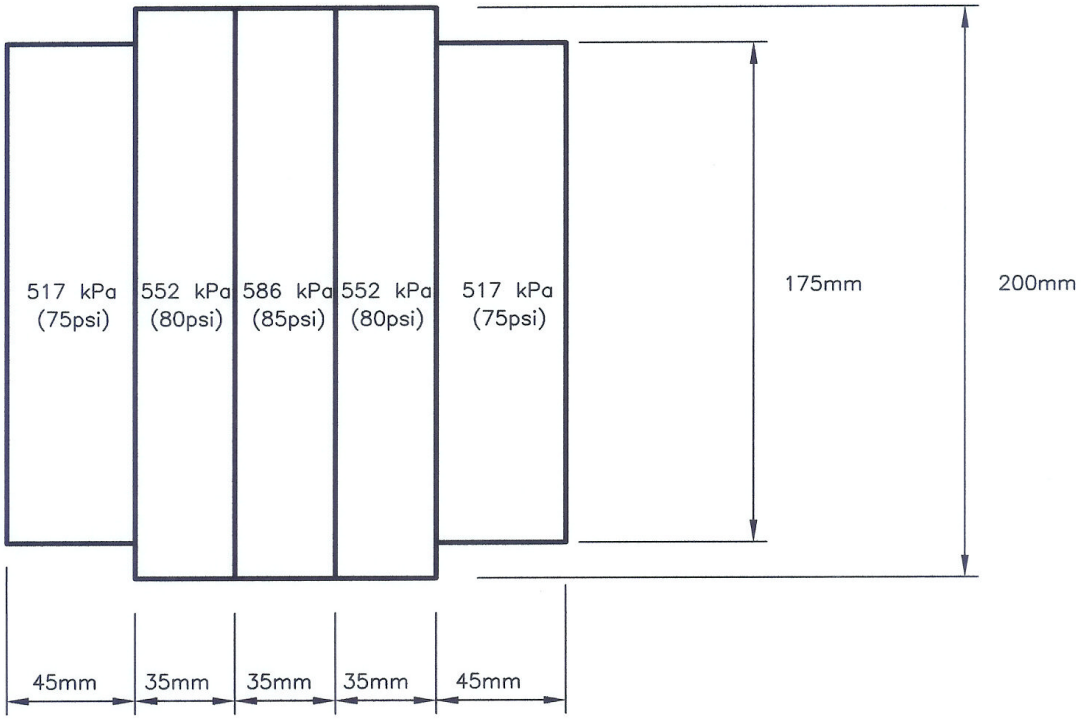

Figure 7.30 Wheel Tire Model Used in ABAQUS Simulation.

7.3.2 Parameters

The asphalt mixes' elastic and calibrated creep parameters, shown in Table 7.4, are used in the modeling of the in-situ pavement performance. The time of loading is calculated using equation 7.3. ABAQUS simulations are completed for 4 million, 10 million, 20 million and 30 million ESAL's traffic loading. The assumed average speed of commercial vehicles is 60 km/hour. It is also assumed that, for the typical Southern Ontario environment, asphalt pavements may rut during summer period with the starting point being at the end of spring and the rutting period can last potentially 5 months ending at the beginning of fall.

The effective time of loading in one tire pass for the 175 mm long outside tread areas, is 0.0126 sec. For the traffic loading of 30 million ESAL's applied over 20 years, the total loading time is 156,000 sec. As the three middle areas are longer by about 15 percent, an additional loading time of 24,000 sec is used for these areas. The loading time used in the ABAQUS simulations is given in Table 7.6.

Table 7.6 Loading Time Used in Pavement In-Situ Performance Simulation

Traffic Loading (ESAL's)	Time of Loading (sec)	
	Step 1	Step 2
4,000,000	21,000	3,200
10,000,000	52,000	8,000
20,000,000	104,000	16,000
30,000,000	156,000	24,000

7.3.3 Pavement In-Situ Performance Modeling

The definition of rutting used in the analysis is shown in Figure 7.31. The total rut depth is a sum of the downward rutting and the height of the upheaval. However, as the MEPDG methodology predicts only the downward rutting [NCHRP 2004b], only this part of the rut is used in the comparison of the ABAQUS predicted rutting with the MEPDG predicted rutting.

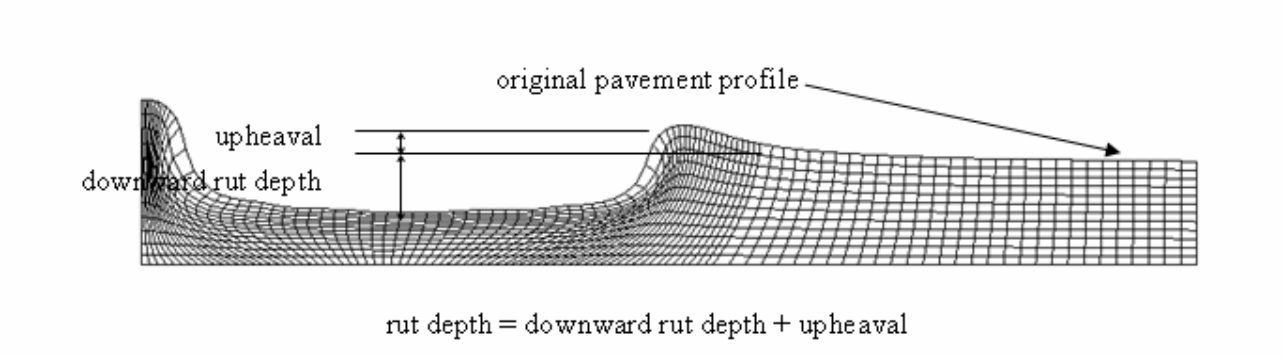

Figure 7.31 Rut Depth Definition Used in the Analysis.

The pavement model used in the analysis is shown in Figure 7.32. As the dual wheel system is symmetric, only half of the system is modeled. The distance between the two wheel tires in a dual wheel system is 120 mm. The density of the mesh under the load and directly next to it is twice the density in the 300 mm wide zone outside the loaded part. The contact pressure is as shown in the tire model.

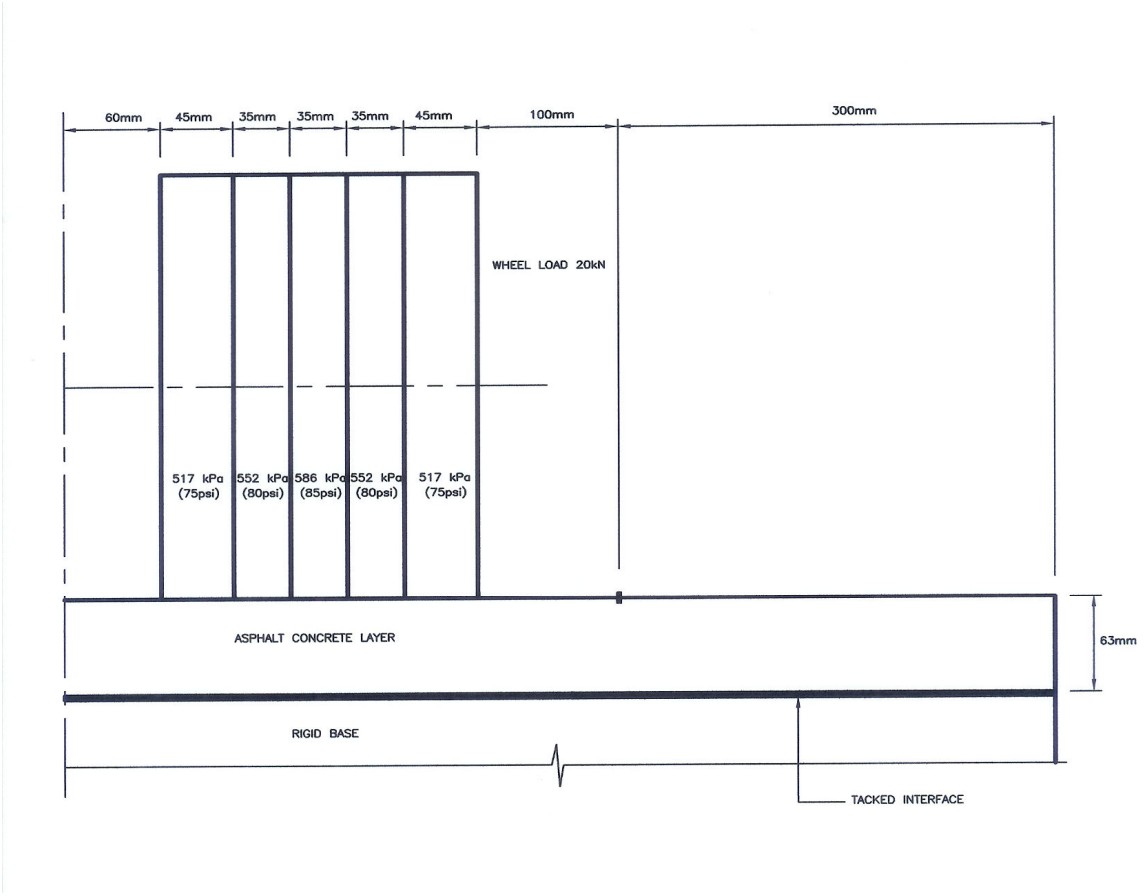

Figure 7.32 Schematic of Model Used for Pavement In-Situ Performance Simulation.

Figure 7.33 shows a general schematic of the finite element mesh used. The model has 1212 elements, 1326 nodes and 2652 degrees of freedom. The CPE4R plane strain linear elements with reduced integration are selected for the model from the ABAQUS standard two-dimensional solid library.

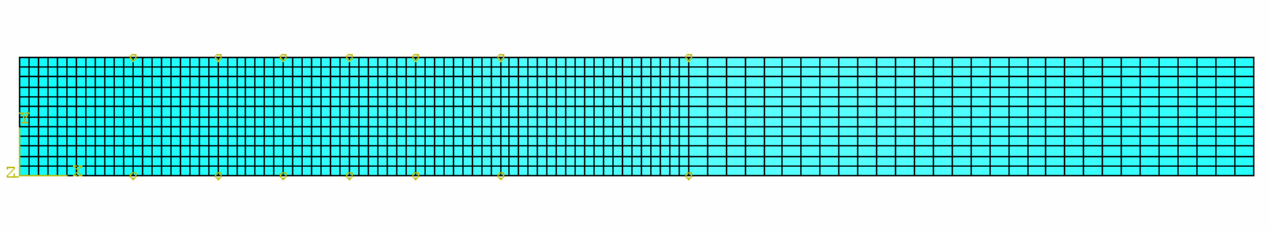

Figure 7.33 Schematic of Finite Element Mesh.

The boundary conditions are shown in Figure 7.34. There is no horizontal or vertical movement allowed at the bottom of the model and along the right edge of the model. Only vertical movement is allowed along the left edge of the model.

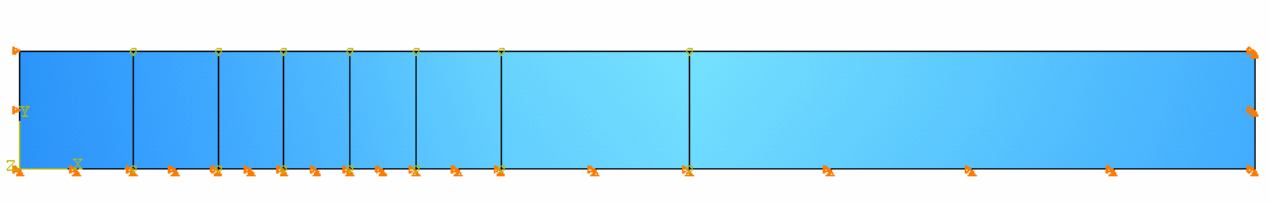

Figure 7.34 Boundary Conditions.

The loading model is shown in Figure 7.35 (Step 1) and Figure 7.36 (Step 2). In Step 1, the contact pressures shown in the tire model are applied over the entire tire width for a period of time based on the length of the outside areas of the tire model. In Step 2, the contact pressure is applied only in the three middle areas of the tire for an additional period. The loading times in Steps 1 and 2 are shown in Table 7.6.

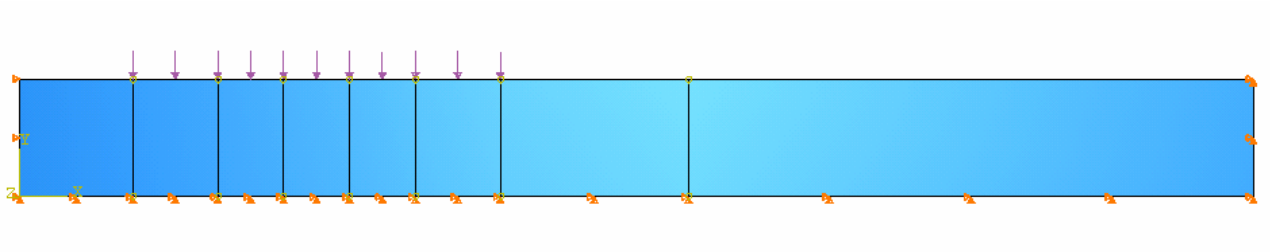

Figure 7.35 Step 1 Loading Model.

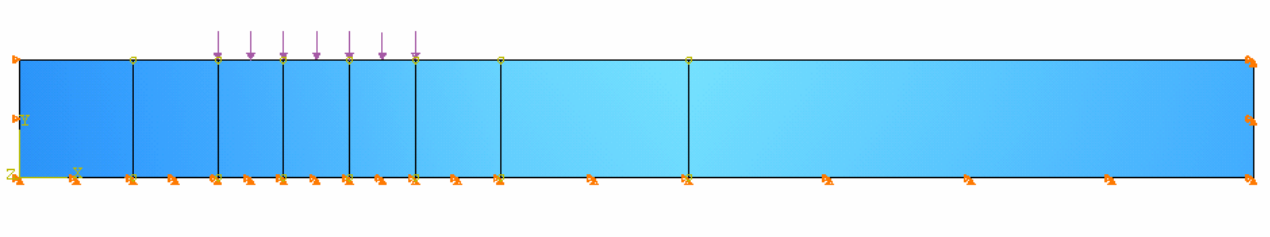

Figure 7.36 Step 2 Loading Model.

Figures 7.37 and 7.38 show the predicted deformed shapes of a pavement with HL 3 mix after application of 4 million and 30 million ESAL's, respectively. The depth of the downward rutting has increased from 4.0 mm for 4 million ESAL's to 8.3 mm for 30 million ESAL's. The height of the upheaval has increased from 3.6 mm for 4 million ESAL's to 7.5 mm for 30 million ESAL's. The total rut depth has increased from 7.6 mm for 4 million ESAL's to 15.5 mm for 30 million ESAL's. However, this total rut depth is without taking into account the distribution of the wheel movement in the wheel path, called the wheel wander.

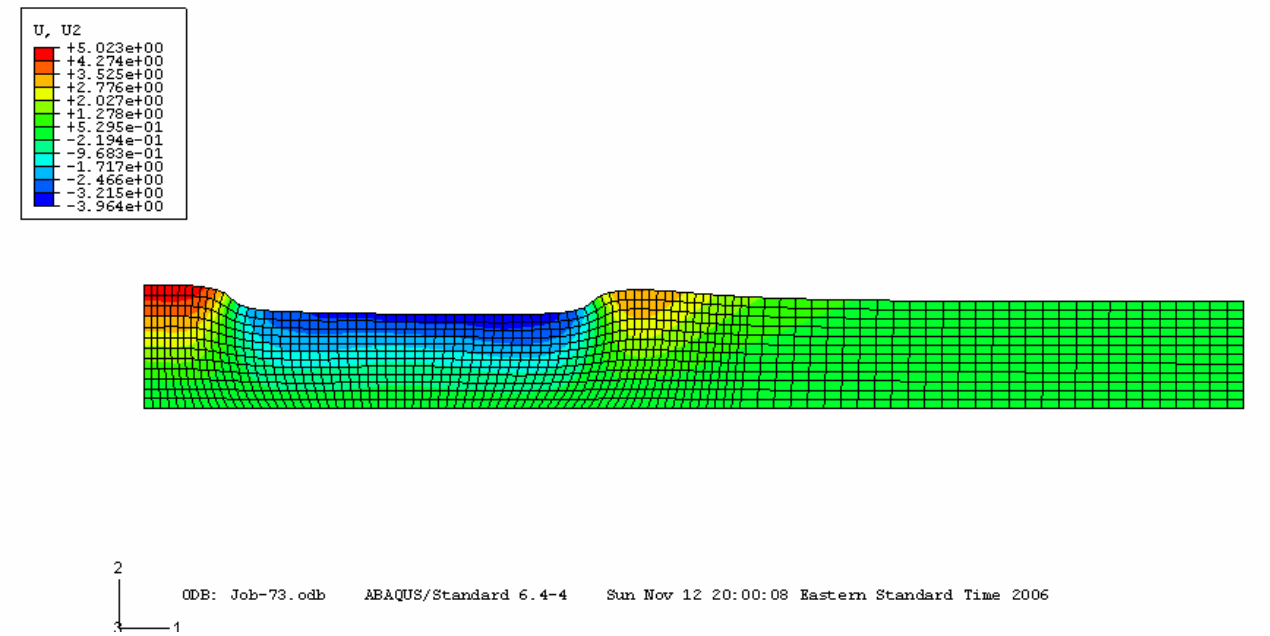

Figure 7.37 Deformed Shape of Pavement with the HL 3 Mix after 4 million ESAL's.

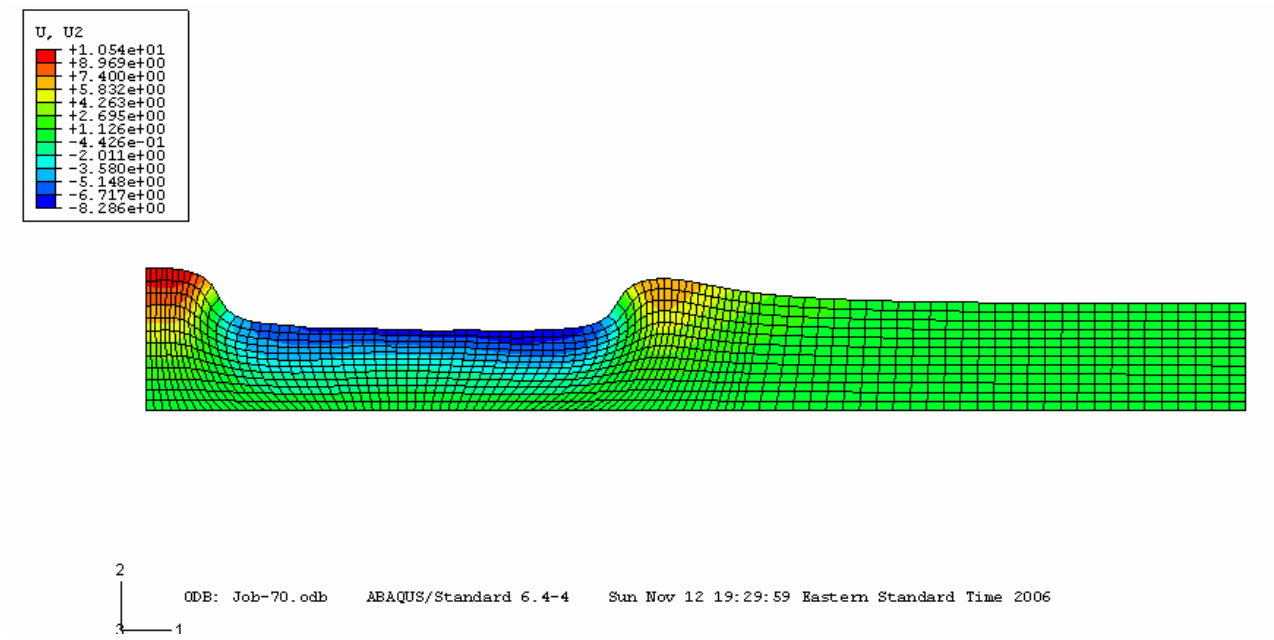

Figure 7.38 Deformed Shape of Pavement with the HL 3 Mix after 30 million ESAL's.

Figures 7.39 to 7.42 show the deformed shapes of pavements with the SMA L, SMA G, SP 19 D and SP 19 E mixes after 30 million ESAL's; U2 is the vertical deformation. The deformation scale factor of 2.0 is selected for all the deformed shape figures. The plots for all five mixes after 4 million, 10 million, 20 million and 30 million ESAL's are attached in Appendix D. Tables 7.7 to 7.10 show the downward rut depth, height of the upheaval and the total rut depth of pavements with all five mixes.

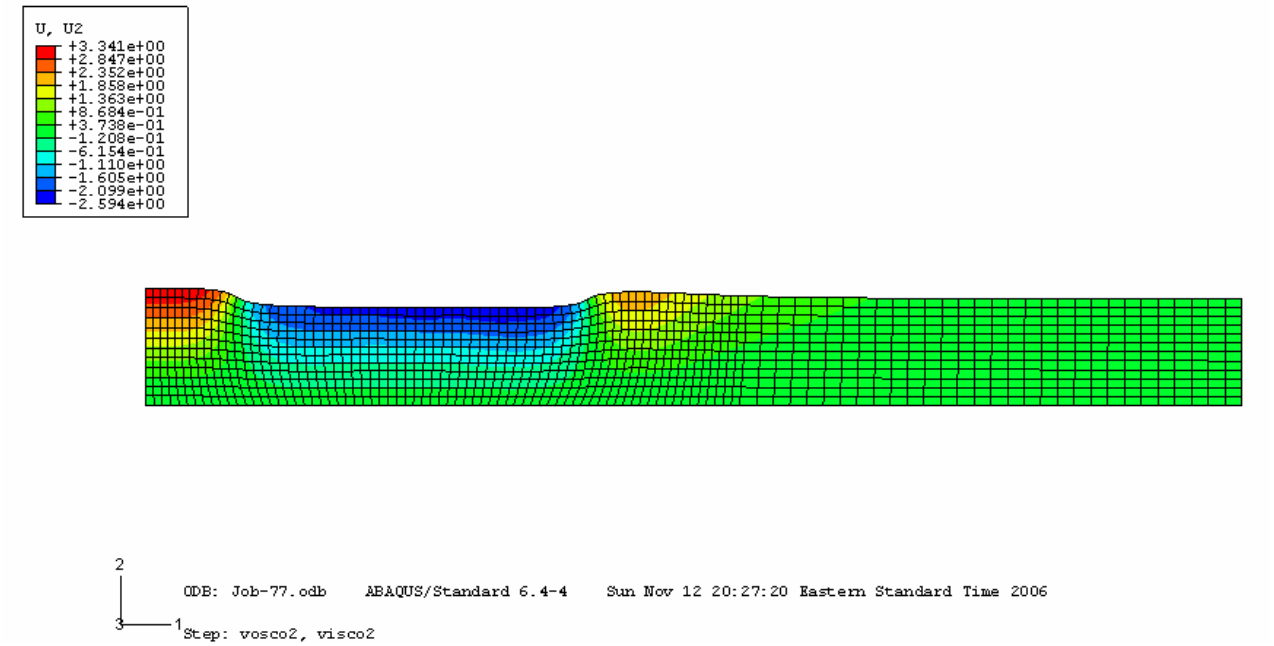

Figure 7.39 Deformed Shape of Pavement with the SMA L Mix after 30 million ESAL's.

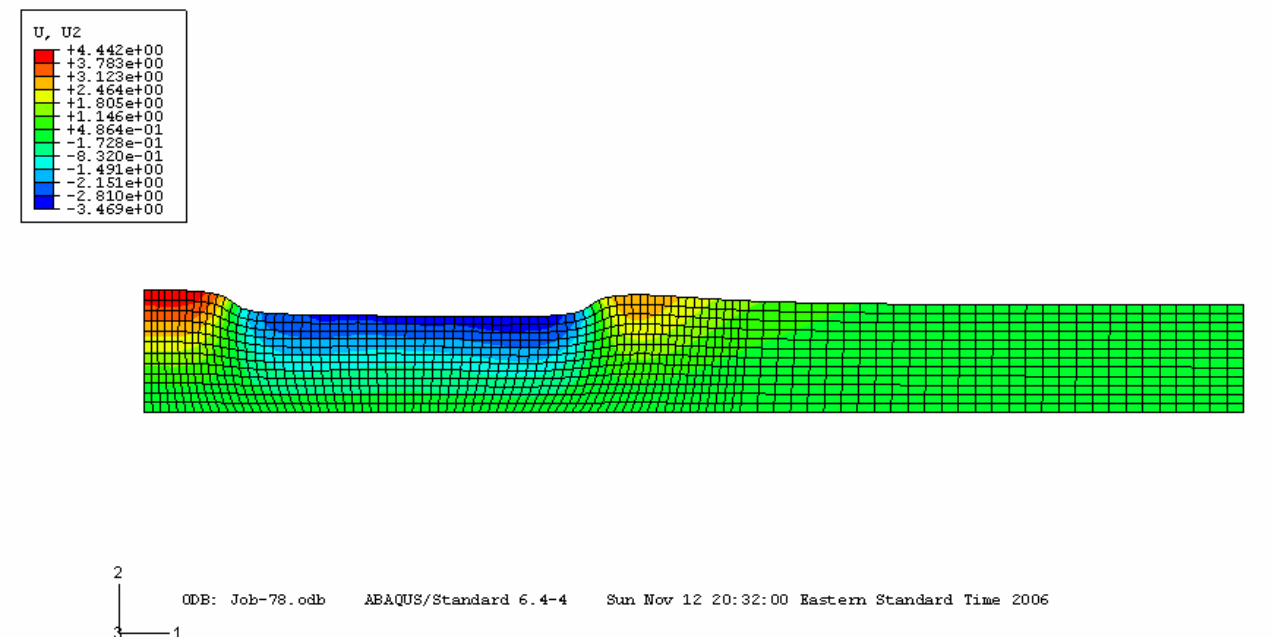

Figure 7.40 Deformed Shape of Pavement with the SMA G Mix after 30 million ESAL's.

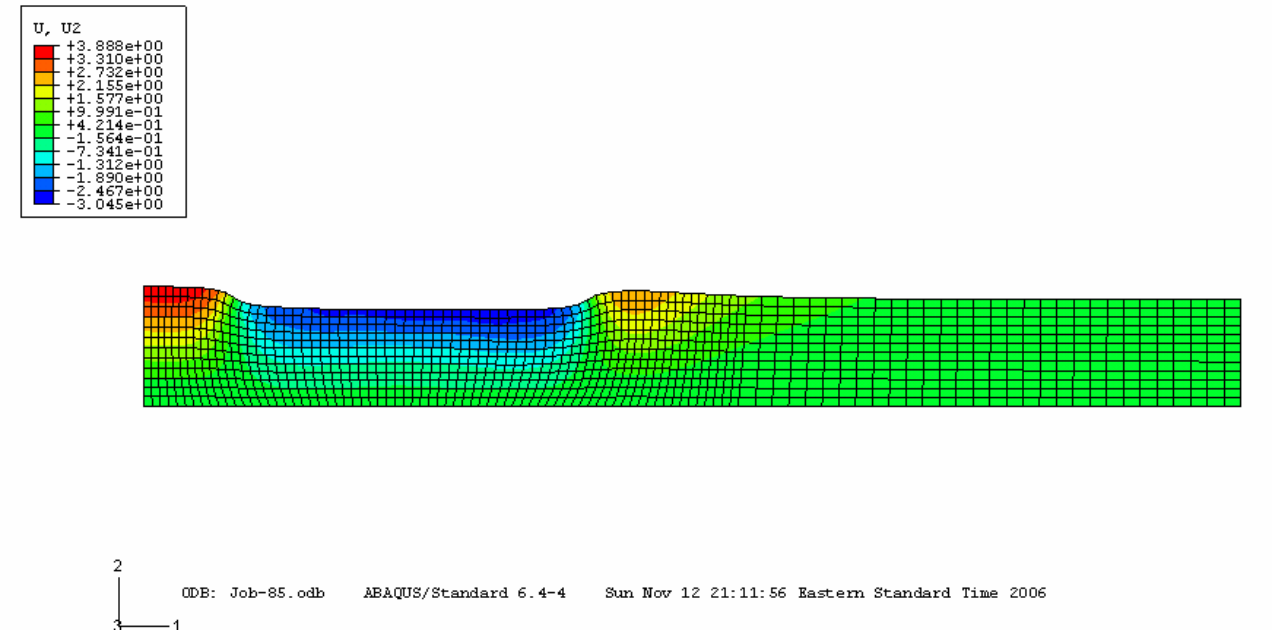

Figure 7.41 Deformed Shape of Pavement with the SP 19 D Mix after 30 million ESAL's.

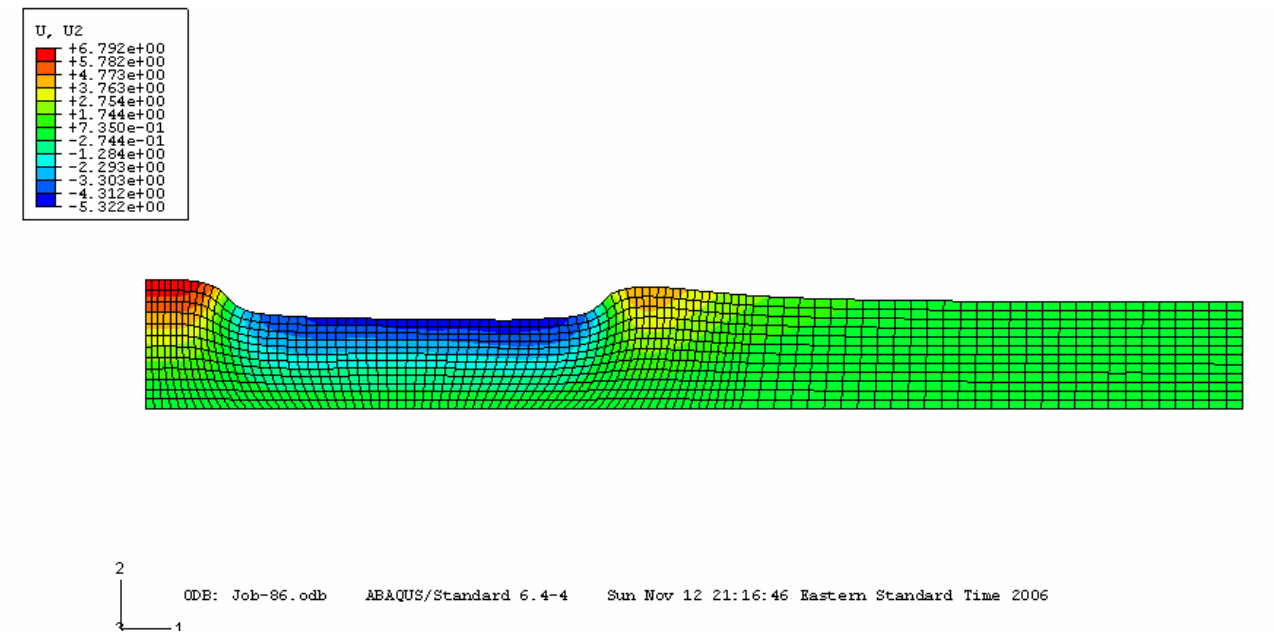

Figure 7.42 Deformed Shape of Pavement with the SP 19 E Mix after 30 million ESAL's.

Table 7.7 Predicted Pavement Rutting after 4 million ESAL's

Mix	Traffic Loading (million ESALs)	Pavement In-Situ Rutting Predicted in ABAQUS (mm)			Ranking
		Downward Rut Depth (-)	Average Upheaval (+)	Total Rut Depth	
HL 3	4.0	4.0	3.6	7.6	5
SMA L	4.0	1.7	1.5	3.2	2
SMA G	4.0	2.3	2.0	4.3	3
SP19D	4.0	1.6	1.4	3.0	1
SP19E	4.0	2.6	2.2	4.8	4

Table 7.8 Predicted Pavement Rutting after 10 million ESAL's

Mix	Traffic Loading (million ESALs)	Pavement In-Situ Rutting Predicted in ABAQUS (mm)			Ranking
		Downward Rut Depth (-)	Average Upheaval (+)	Total Rut Depth	
HL 3	10.0	5.5	5.0	10.5	5
SMA L	10.0	2.1	1.8	3.9	1
SMA G	10.0	2.8	2.4	5.2	3
SP19D	10.0	2.1	1.9	4.0	2
SP19E	10.0	3.6	3.1	6.7	4

Table 7.9 Predicted Pavement Rutting after 20 million ESAL's

Mix	Traffic Loading (million ESALs)	Pavement In-Situ Rutting Predicted in ABAQUS (mm)			Ranking
		Downward Rut Depth (-)	Average Upheaval (+)	Total Rut Depth	
HL 3	20.0	7.1	6.4	13.5	5
SMA L	20.0	2.4	2.0	4.4	1
SMA G	20.0	3.2	2.8	6.0	3
SP19D	20.0	2.7	2.3	5.0	2
SP19E	20.0	4.6	4.0	8.6	4

Table 7.10 Predicted Pavement Rutting after 30 million ESAL's

Mix	Traffic Loading (million ESALs)	Pavement In-Situ Rutting Predicted in ABAQUS (mm)			Ranking
		Downward Rut Depth (-)	Average Upheaval (+)	Total Rut Depth	
HL 3	30.0	8.3	7.5	15.5	5
SMA L	30.0	2.6	2.2	4.8	1
SMA G	30.0	3.4	3.1	6.5	3
SP19D	30.0	3.0	2.6	5.6	2
SP19E	30.0	5.3	4.6	9.9	4

7.3.4 Wheel Wander and Additional Analysis

As the wheel tire wanders within the wheel path, it causes the upheaval outside the tire to migrate away from the wheel path [White 2002]. As a result, the uplift between the wheels and outside the tire will be substantially reduced (compressed). In a National Pooled Fund Study (PFS) at the Indiana Department of Transportation/Purdue University Accelerated Pavement Test Facility, rutting for the single-wheel-path loading (i.e. with no wander) was about 1.7 times that of rutting with 250 mm wander [White 2002]. A wander rut depth reduction factor of 1.7 is assumed in this research. Table 7.11 shows a summary of the predicted pavement rutting with wander reduction after 4 million, 10 million, 20 million and 30 million ESAL's. Figure 7.43 shows the predicted pavement rutting with wander reduction versus traffic loading relationship for all five mixes.

Table 7.11 Summary of Predicted Total Pavement Rutting With Wheel Wander Reduction

Mix	Predicted Pavement Rut Depth with Wheel Wander Reduction (mm)							
	4.0 million ESAL's		10.0 million ESAL's		20.0 million ESAL's		30.0 million ESAL's	
	Rut Depth (mm)	Ranking	Rut Depth (mm)	Ranking	Rut Depth (mm)	Ranking	Rut Depth (mm)	Ranking
HL 3	4.5	5	6.2	5	7.9	5	9.1	5
SMA L	1.9	2	2.3	1	2.6	1	2.8	1
SMA G	2.5	3	3.1	3	3.5	3	3.8	3
SP19D	1.8	1	2.4	2	2.9	2	3.3	2
SP19E	2.8	4	3.9	4	5.1	4	5.8	4

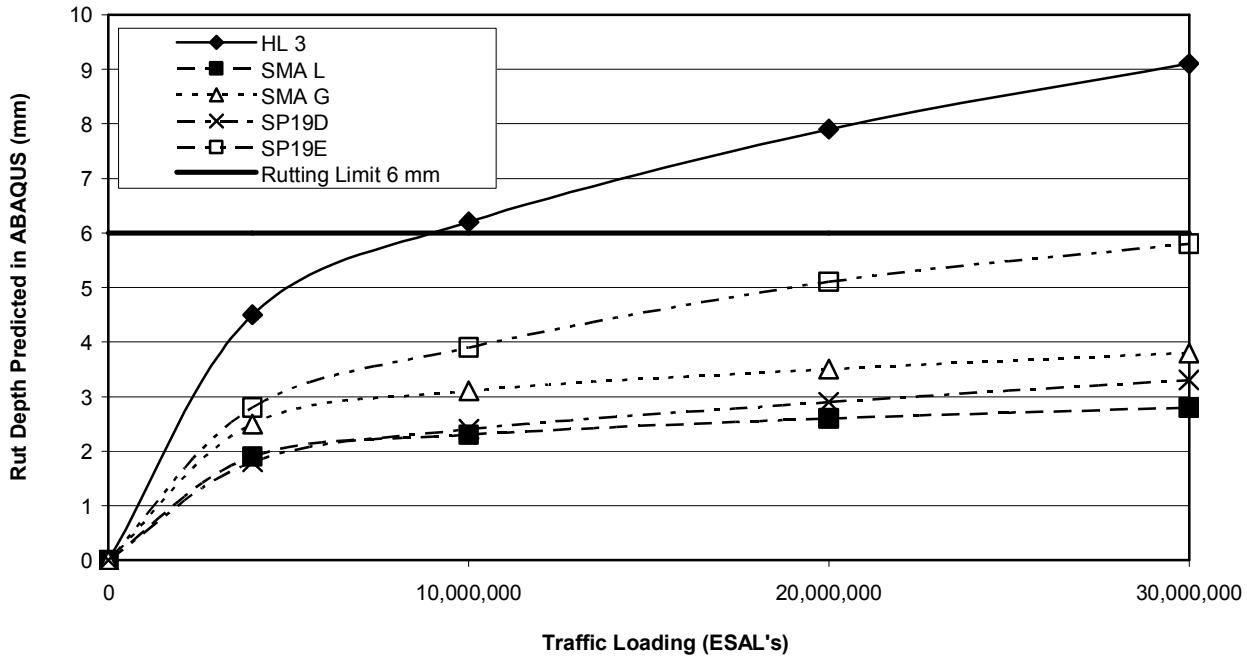

Figure 7.43 Predicted Rutting with Wander Reduction versus Traffic Loading Relationships.

Table 7.12 shows the slopes and intercepts of the predicted rutting with wander reduction versus traffic loading.

Table 7.12 Predicted Rutting Versus Traffic Loading Relationships

Mix	Relationship		R^2
	Slope	Intercept	
HL 3	14.5×10^{-8}	4.8	0.99
SMA L	2.5×10^{-8}	2.1	0.99
SMA G	3.5×10^{-8}	2.8	0.99
SP 19 D	4.5×10^{-8}	2.0	1.00
SP 19 E	9.5×10^{-8}	3.0	0.98

The rutting failure criterion for asphalt portion of the pavement structure was assumed as 6.0 mm, the same as used by [White 2002]. Table 7.13 compares the predicted pavement rutting of all five mixes after 30 million ESAL's with the rutting failure criterion. Only the HL 3 mix does not meet this requirement. However, the HL 3 mix is typically used on low to medium volume roads in Ontario designed to carry less that 3.0 million ESAL's. The pavement predicted rutting for this mix after 4.0 million ESAL's is 4.5 mm, which means that the mix meets the performance requirements at this traffic level.

Table 7.13 Predicted Pavement Rutting versus Performance Requirement

Mix	Predicted Pavement Rutting With Wander Reduction After 30 million ESAL's	Rutting Failure Criterion for Asphalt Layer (mm)
HL 3	9.1*	6
New SMA	2.8	6
Old SMA	3.8	6
SP19D	3.3	6
SP19E	5.8	6

* HL 3 does not meet the requirements. However, in practice this mix is not used on high volume facilities.

In additional analysis, the rutting of pavements with SMA L and SMA G mixes after 30 million ESAL's was predicted in ABAQUS using the initial m parameter. The results are shown in Table 7.14. These values are compared with the values from the ABAQUS simulation using the calibrated m parameters. Table 7.15 shows the ranking of all mixes based on the rutting predicted in ABAQUS using the initial and calibrated m parameters. This ranking is compared with the ranking in the MEPDG pavement performance analysis in Chapter Eight, Asphalt Pavement and Mix Performance.

Table 7.14 Predicted Rutting of SMA Mixes Using Initial m Parameter

Mix	Traffic Loading (million ESALs)	Predicted Pavement Field Rutting Using ABAQUS (mm)			Assumed Wander Reduction Factor	Anticipated Rut Depth (mm)
		Downward Rut Depth (-)	Average Upheaval (+)	Total Rut Depth Without Wander		
SMA L	30.0	4.8	3.7	8.5	1.7	5.0
SMA G	30.0	5.8	5.1	10.9	1.7	6.4

Table 7.15 Mix Ranking in Pavement Predicted In-Situ Performance

Mix	Ranking after 30 million ESAL's	
	Using Initial m Parameter For SMA Mixes	Using Final m Parameter For SMA Mixes
HL 3	5	5
New SMA	2	1
Old SMA	4	3
SP19D	1	2
SP19E	3	4

In the ranking with the initial m parameter, the dense graded mix SP 19 D is the best, followed by the SMA L mix, SP 19 E mix and the SMA G mix; the HL 3 mix is the poorest. When the m parameter is calibrated against the measured rutting in the HWRT, the ranking had changes and the SMA mixes perform much better. The SMA L mix is now the best, the SP 19 D mix is the second, the SMA G mix is the third, followed by the SP 19 E mix; the HL 3 mix is again the poorest.

The SMA mixes are known for their excellent resistance to rutting and cracking [Brown 1997, Kennepohl 1999, Perraton 2001]. If the creep power law is used for SMA mixes modeling, the m parameter derived from the repeated load creep tests should be calibrated against the measured rutting in the HWRT testing to better reflect the behaviour of the mix.

The performance of the SP 19 D is very good in the laboratory testing and ABAQUS modeling in this research. The mix exhibits high dynamic modulus and excellent resistance to rutting in the HWRT testing. The SP 19 D mix is a lean (i.e. with lower asphalt cement content), fine-graded Superpave mix incorporating only 4.35 percent asphalt cement, quarried coarse aggregate and a high percentage of manufactured sand. The excellent performance of this mix questions the conventional belief that coarse mixes offer better resistance to rutting. Kandhal, for instance, concluded in a research described in [Kandhal 2002] that there was no significant difference between the rutting resistance of coarse- and fine-graded Superpave mixes.

Although the SP 19 D mix exhibits excellent resistance to rutting, its cracking endurance is not known and may be of concern. This mix is considered to be a good comparison mix for research purposes;

however, its practical application would require a thorough investigation if it were to be used on high volume facilities.

7.4 SUMMARY

Viscoplastic deformation is the major contributor to hot-mix asphalt rutting. The ABAQUS finite element program is used for simulation of the asphalt mix accelerated rutting performance in the HWRT testing and pavement in-situ performance. Two-dimensional plane strain models are used in both simulations. Additional analyses of HWRT testing are completed in ABAQUS axisymmetric 2D space and on a 3D slice. Initially, the material elastic (modulus of elasticity and Poisson's ratio) and creep (A, n and m) parameters developed from the laboratory dynamic modulus and triaxial repeated load creep and creep recovery testing are used. The creep power law and continuous loading time are used in the finite element modeling.

Although there is a reasonable linear relationship between the predicted and the laboratory measured rutting, the predicted values are several times lower that the measured ones. The adjustment of parameter A for all mixes and parameter m for SMA mixes is necessary. The calibrated parameters are used in the finite element pavement in-situ performance simulation.

CHAPTER EIGHT
TASK FOUR: ASPHALT PAVEMENT AND MIX PERFORMANCE

The objective of this chapter is to compare the asphalt pavement in-situ performance predicted using ABAQUS finite element program with the new Mechanistic-Empirical Pavement Design Guide (MEPDG). Also, it emphasizes the significance of the laboratory accelerated rutting performance testing and recommends the performance criteria for this testing.

8.1 MEPDG PAVEMENT DESIGN ANALYSIS

The MEPDG, formerly known as the AASHTO 2002 Guide, was developed in the United States for the National Cooperative Highway Research Project (NCHRP) under the 1-37A project. In the MEPDG methodology, the strains and stresses caused by the application of a wheel load are computed and then used in empirical formulas to calculate pavement structural distresses under a designed number of load applications [NCHRP 2004b]. The MEPDG includes a procedure for predicting asphalt pavement rutting. The use of mechanistic-empirical approach to pavement design used in MEPDG may be particularly important for pavements in warm locations and designed for high traffic levels because the most commonly used conventional empirical AASHTO 93 pavement design methodology [AASHTO 1993] overestimates performance (underestimates distresses) in these locations [Carvalho 2006].

Figure 8.1 shows the overall design process for asphalt pavements in MEPDG [NCHRP 2004b]. The required input includes traffic, foundation, climate and material properties. As there was no climatic model for the Province of Ontario available during the course of this research, the climatic model from New York Upper State is used in the analyses. A default load spectrum is used with a number of vehicles adjusted accordingly to obtain the required level of traffic loading.

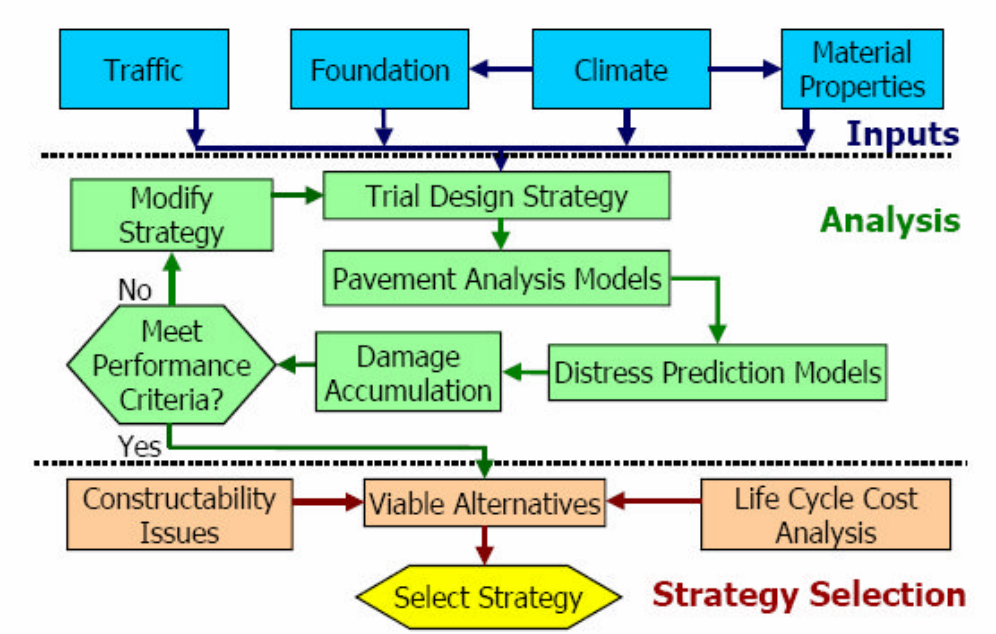

Figure 8.1 MEPDG Overall Design Process for Asphalt Pavement [NCHRP 2004b].

The required material properties depend on the level of design. In Level 1 design, the required input for the asphalt layers is based on dynamic modulus measured at various temperatures and loading rates. Level 1 design would be used for freeway design. The dynamic modulus master curve is used in the performance prediction. The input for the asphalt binder includes Superpave binder test data. For Levels 2 and 3, the dynamic modulus is calculated using the Witczak predictive model [NCHRP 2004b]. Levels 2 and 3 would be used for lower volume facilities and sites where specific data is not available. The required properties include gradation information (percent retained on 3/4 sieve, 3/8 sieve and # 4 sieve), and PG grade for asphalt cement. Levels 1, 2 and 3 also require asphalt general information: volumetric effective binder content; air voids; and reference temperature. The asphalt pavement rutting model included in MEPDG is described earlier in Chapter Two, Literature Review.

The analyses in this chapter are focused on actual design and associated rutting in the asphalt layer. The pavement structure assumed for the analyses is given in Table 8.1.

Table 8.1 Pavement Structure Assumed for MEPDG Analyses.

Layer Type	Thickness*
Hot-Mix Asphalt	63 mm (2.5 in.)
PC Concrete	250 mm (10 in.)
Granular Base	300 mm (12 in.)
Subgrade	-

* The required input in MEPDG is in imperial units.

Initially, attempts were made to use Level 1 analysis and the measured dynamic modulus values described earlier in Chapter Five, Material Characterization. However, an email correspondence with Dr. Mohamed EL-Basyouny from Arizona State University, one of the developers of the guide, revealed that there are still corrections to be done in MEPDG, particularly in Level 1 analysis. Dr. Mohamed El-Basyouny warned that there was an error in the jointed Portland cement pavement (JPCP) analysis that was being fixed. This is likely why the rutting calculation for asphalt mix placed over JPCP concrete did not work. A copy of the email correspondence is attached in Appendix E. Therefore, only Level 3 analyses are completed for all five asphalt mixes. The measured dynamic modulus is only used for comparison. The material parameters used in the MEPDG Level 3 analyses are listed in Table 8.2.

Table 8.2 Material Parameters Used in MEPDG Level 3 Analyses.

Mix	Asphalt Layer Parameters							
	Gradation				PGAC Grade	Volume of Effective Binder (%)	Air Voids (%)	Total Unit Weight (pcf)*
	Retaining on Sieves			Passing Sieve				
	19 mm	9.5 mm	4.75 mm	75 µm				
HL 3	0.0	14.0	40.0	3.7	58-28	11.5	6.2	146
SMA L	0.0	28.9	74.6	9.1	70-28	12.9	6.4	152
SMA G	0.0	34.3	75.0	8.0	64-28	13.4	5.8	158
SP 19 D	2.8	31.8	39.8	4.2	70-28	9.0	6.5	151
SP 19 E	3.0	36.8	62.0	3.8	70-28	9.7	5.7	151

* The required input in MEPDG is in imperial units.

The Level 3 analyses are completed for the traffic loading equivalent of 20 and 30 million ESAL's. A summary of the rut depth is given in Table 8.3. The table also shows the ranking of the asphalt mixes performance in terms of their resistance to rutting.

The rutting predicted for the SP 19 D mix of 6.6 mm after the traffic of 30 million ESAL's is the smallest and the mix is ranked as the best. The SP 19 E mix with the rutting of 8.3 mm is ranked as number two. The rutting of the SMA mixes' is high: 11.0 mm for SMA L, and the mix is ranked as number three; and 12.2 mm for SMA G, and the mix is ranked as number four. The HL 3 mix is ranked as number five with the highest rutting of 12.7 mm.

Table 8.3 Summary of Asphalt Pavement Rutting Analysis in MEPDG.

Mix	Pavement Rut Depth Predicted in AASHTO 2002 (mm) Traffic Loading (million ESAL's)		Asphalt Mix Rutting Performance Ranking
	20	30	
HL 3	10.4	12.7	5
New SMA	9.0	11.0	3
Old SMA	10.0	12.2	4
SP19D	5.4	6.6	1
SP19E	6.7	8.3	2

The rutting predicted for the SMA mixes is much higher than would be typically anticipated for this mix type. An email correspondence with Dr. Mohamed El-Basyouny from Arizona State University revealed that the current MEPDG rutting models are calibrated for dense graded mixes only and, if used for SMA mixes, give higher rutting than observed in the field. The models might need to be adjusted for the SMA. A copy of the email correspondence is attached in Appendix E.

In the MEPDG model, asphalt rutting potential depends mainly on the dynamic modulus of the asphalt mix, i.e. the lower the modulus, the higher the rutting potential. The SMA is known for its relatively low modulus; its rutting resistance is based mainly on the stone-on-stone contact. By contrast, the rutting resistance of the dense graded mixes relies mainly on the asphalt cement/fine aggregate matrix. Therefore, the models that work well with the dense graded mixes will likely not work with the gap graded SMA mixes.

Figure 8.2 shows the dynamic modulus master curves for all five mixes, developed during the laboratory testing described in Chapter Five, Material Characterization. The modulus of the SMA G mix is the lowest. The moduli of the HL 3 and SMA L mixes are generally almost the same for almost the entire range of frequencies; they are lower than those of the SP 19 D and SP 19 E mixes. The SP 19 D mix has

the highest modulus. The ranking of the mixes in the MEPDG analyses is generally similar to the ranking of their dynamic modulus ranking.

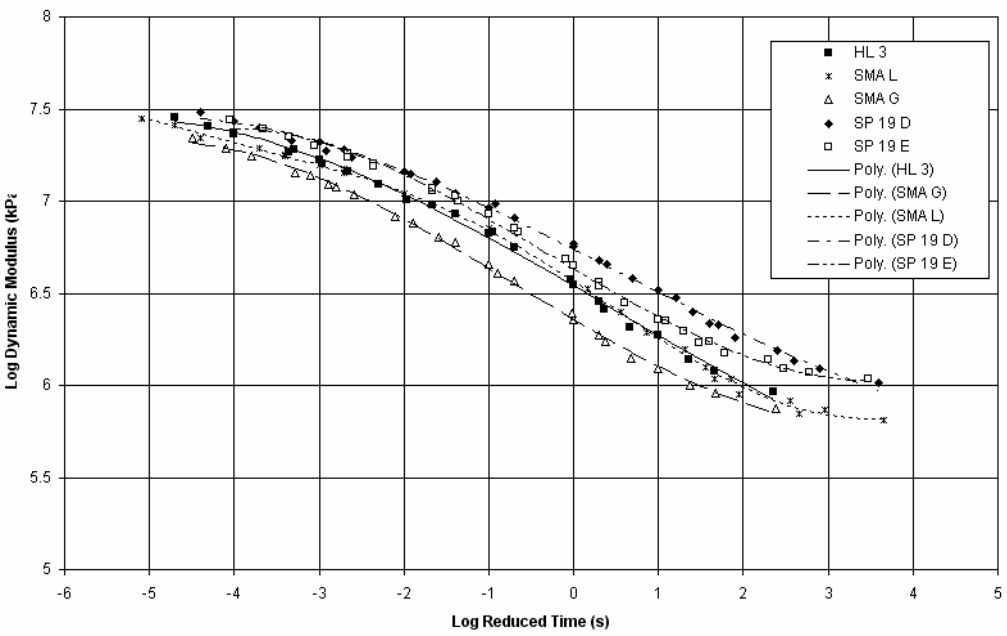

Figure 8.2 Master Curves of HL 3, SMA L, SMA G, SP 19 D and SP 19 E Mixes.

8.2 COMPARISON OF MEPDG AND ABAQUS PREDICITIONS

Tables 8.4 and 8.5 compare the rutting predicted by the ABAQUS finite element modeling and the rutting predicted by the MEPDG analyses after 20 and 30 million ESAL's. The rutting relationship for the dense graded HL 3, SP 19 D and SP 19 E mixes forms almost a straight line while the two SMA mixes do not match this relationship. Figure 8.3 shows this relationship for 30 million ESAL's traffic loading only. Figure 8.4 shows the relationship for the dense graded HL 3, SP 19 D and SP 19 E mixes only. The relationship for the dense graded mixes only is good.

Table 8.4 Comparison of Rutting Predicted in ABAQUS and MEPDG
After 20 Million ESAL's.

Mix	Rutting Predicted After 20 million ESALs			
	ABAQUS		MEPDG	
	Rut Depth (mm)	Ranking	Rut Depth (mm)	Ranking
HL 3	7.1	5	10.4	5
SMA L	2.4	1	9.0	3
SMA G	3.2	3	10.0	4
SP19D	2.7	2	5.4	1
SP19E	4.6	4	6.7	2

Table 8.5 Comparison of Rutting Predicted in ABAQUS and MEPDG
After 30 Million ESAL's.

Mix	Rutting Predicted After 30 million ESALs			
	ABAQUS		MEPDG	
	Rut Depth (mm)	Ranking	Rut Depth (mm)	Ranking
HL 3	8.3	5	12.7	5
SMA L	2.6	1	11.0	3
SMA G	3.4	3	12.2	4
SP19D	3.0	2	6.6	1
SP19E	5.3	4	8.3	2

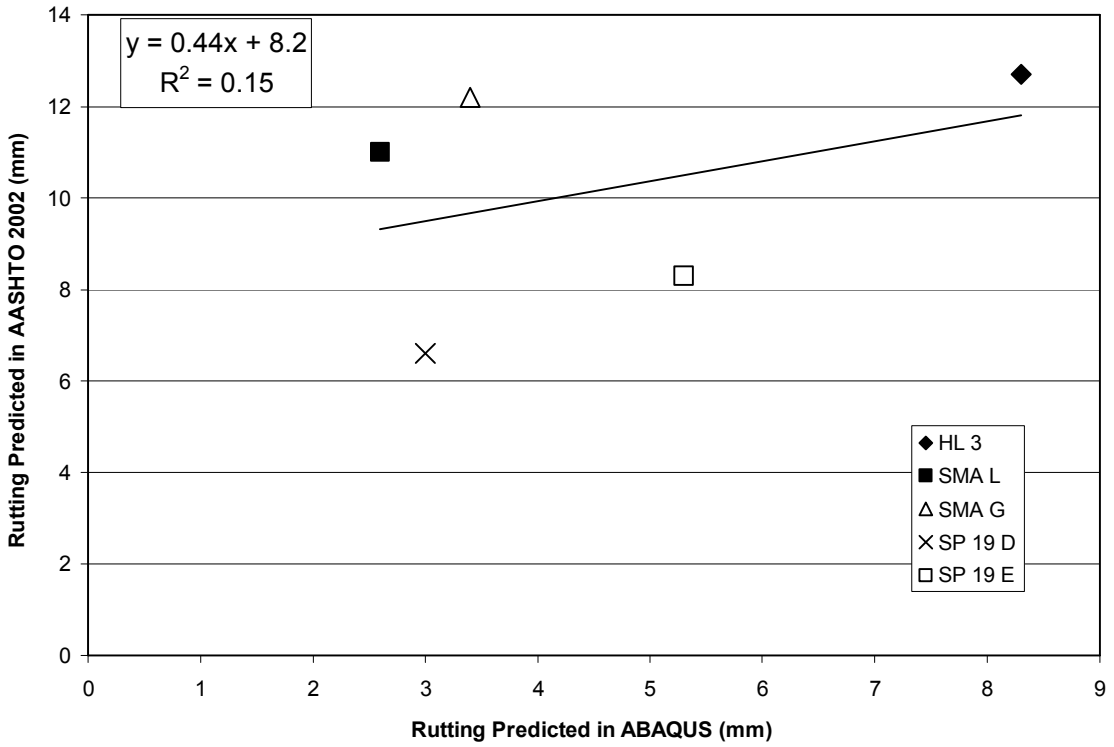

Figure 8.3 Comparison of Rutting Predicted in ABAQUS and MEPDG for HL 3, SMA L, SMA G, SP 19 D and SP 19 E Mixes after 30 million ESAL's.

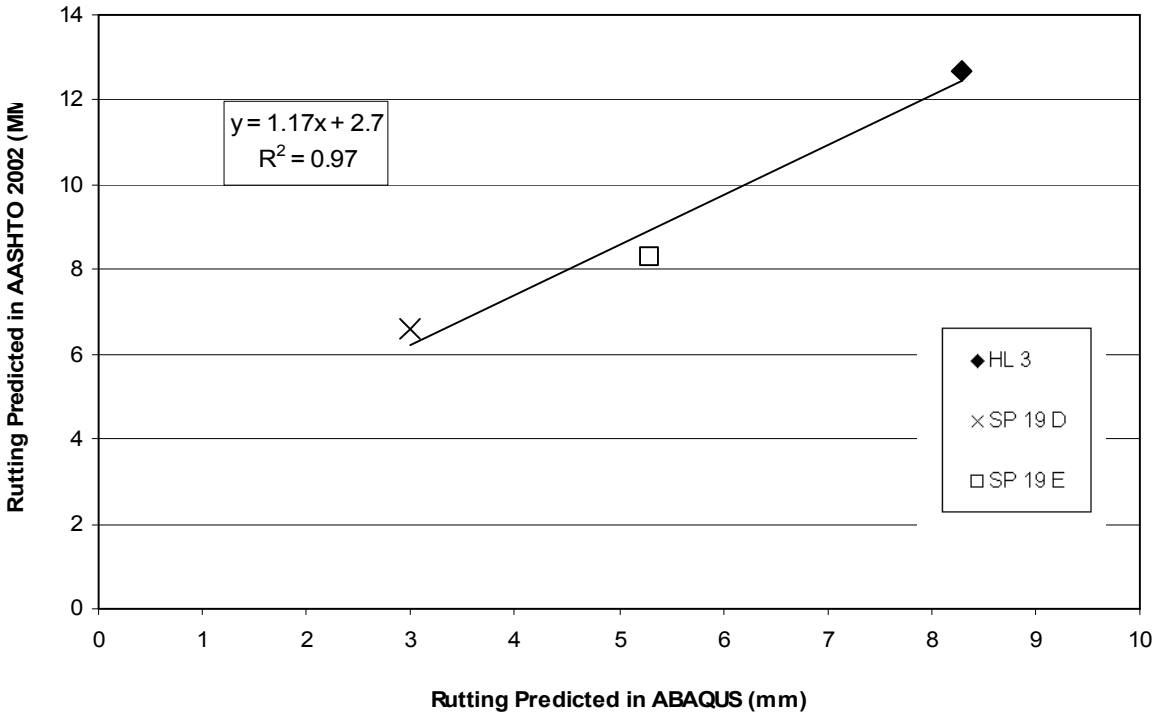

Figure 8.4 Comparison of Rutting Predicted in ABAQUS and MEPDG for HL3, SP 19 D and SP 19 E Mixes after 30 million ESAL's.

Table 8.5 shows the asphalt mix ranking in ABAQUS modeling using the initial and final parameters and MEPDG pavement analyses after 30 million ESAL's. The predicted performance of the SMA mixes in ABAQUS is much better than in MEPDG, particularly after parameter m was calibrated against the measured rutting in HWRT testing.

Table 8.5 Mix Ranking in ABAQUS and MEPDG.

Mix	Ranking		
	ABAQUS		MEPDG
	Using Initial m Parameter	Using Final m Parameter	
HL 3	5	5	5
SMA L	2	1	3
SMA G	4	3	4
SP19D	1	2	1
SP19E	3	4	2

Table 8.6 shows the dense graded mixes' ranking in the HWRT laboratory testing, ABAQUS modeling and MEPDG pavement analyses. The SMA mixes are excluded from this comparison. All three methods rank the dense graded mixes in the same order: SP 19 D is the best; SP 19 E is the second; and HL 3 is the poorest one.

Table 8.6 Ranking of Dense Graded Mixes in HWRT Testing, ABAQUS Modeling and MEPDG Analysis.

Mix	Mix Ranking		
	HWRT	ABAQUS	MEPDG
HL 3	3	3	3
SP 19 D	1	1	1
SP 19 E	2	2	2

The ranking of all five mixes, including SMA L and SMA G, in the ABAQUS simulation and HWRT laboratory testing is discussed in Chapter Seven, Finite Element Modeling.

8.3 RUTTING RESISTANCE CRITERIA IN HWRT TESTING

The link between laboratory testing and potential field performance of asphalt mixes is very important to improve asphalt pavement life-cycle performance. The asphalt mixes placed on larger paving projects should be examined for their rutting resistance at the mix design stage. This would limit costly pavement maintenance and repairs and reduce associated traffic interruptions. There have been numerous attempts to form this missing link by developing laboratory equipment and procedures for accelerated asphalt mix performance testing. The HWRT is one of the loaded wheel testers developed for this purpose [Colley 2000, Yildrim 2001].

Although the HWRT is assumed to somewhat simulate road conditions, particularly if the rubber wheel is used, it is an empirical test. However, when properly correlated to a specific site's conditions, it has the potential to allow the user agency the option of pass/fail or "go/no go" criteria and to rank the mixes in terms of their rutting resistance. It is important that the performance criteria used in asphalt mix screening are based on the anticipated pavement traffic loading. This research provides the data that can be used for performance criteria development.

The results of the rutting resistance testing in the HWRT described in Chapter Five, Material Characterization and the results of the ABAQUS analysis described in Chapter Seven, Finite Element Modeling are used in the criteria development. The rutting predicted in ABAQUS for SMA L, SMA G, SP 19 D and SP 19 E mixes is less than the failure limit of 6.0 mm after 30 million ESAL's. The assumed failure limit for asphalt portion of the pavement of 6.0 mm is the same as used by [White 2002]. The rutting predicted for the HL 3 mix is 4.5 mm (below the specified limit) after 4 million ESAL's and 9.1 mm (well above the specified limit) after 30 million ESAL's. The criteria are based on an assumption that if the rutting predicted in ABAQUS for a particular mix is less than the failure limit of 6.0 mm, the rutting measured in the HWRT is acceptable (below the maximum allowable limit) for this mix. Table 8.4 shows the recommended rutting resistance criteria for the testing in the HWRT.

Table 8.7 Recommended Criteria for Rutting Performance Testing in HWRT.

Traffic Loading		Maximum Allowable Rut Depth in HWRT Testing (mm)	
Level	Million ESAL's	10,000 passes	20,000 passes
High	> 30.0	< 1.6	< 1.8
Medium	3.0 – 30.0	< 1.9	< 2.3
Low	< 3.0	< 2.1	< 2.8

The criteria for the low volume roads are based on the performance of the HL 3 mix. The criteria for the high volume roads are based on the performance of the SMA mixes and the SP 19 D and SP 19 E mixes. The unusually high values of rutting in HWRT of Set 1 samples of SP 19 E mix (1.72 mm after 10,000 passes and 2.04 mm after 20,000 passes) and Set 2 samples of SMA G mix (1.82 mm after 10,000 passes and 2.06 mm after 20,000 passes) are ignored in the development of the rutting criteria. The criteria for the medium traffic loading level are the middle values.

The recommended criteria are based on a limited amount of testing and should be considered as initial only. More testing in HWRT would be required to confirm the initial criteria. This should also include testing mixes representing the middle traffic range from 3 to 30 million ESAL's.

The HWRT can be used at the mix design stage in the pass/fail assessment, new materials evaluation, quality control and failure investigation. The ability of the HWRT to adequately predict the magnitude of rutting for a particular pavement structure has not been determined and is not the objective of the testing. Another important use of the HWRT is for calibration of the material parameters, developed in the laboratory creep or other testing, against the measured results of accelerated performance testing, as described in this thesis.

8.4 PAVEMENT FIELD PERFORMANCE

The five asphalt mixes used in this research were obtained from paving contractors in Ontario in fall 2004 and summer 2005. The objective was to obtain typical asphalt mixes used in paving projects across the province. There was a general request by the mix suppliers that the name of the contractor, mix designer, source of materials and the location of mix placement should remain confidential. Therefore, only limited mix design information is included in this thesis and no official pavement performance monitoring plan was prepared.

Complete pavement performance field monitoring would require a significant budget, would have to be carried out over an extended period of time and would require reliable construction, traffic loading and environmental data. The mixes supplied by the contractors for this research are new and obtained from plant production; during the time frame of this research, the pavements incorporating the mixes have been in service for a short period of time (about 1 year). Only short visual inspections were completed on these road sections to check for the presence of any visible rutting. Rutting less that 1.0 mm deep is not

considered to be significant (or measurable). The observations from these inspections are summarized below:

Section with HL 3 mix – this mix is placed as the surface course on a minor arterial urban road. There is no traffic data available for this road section; however, the traffic loading is anticipated to be less than 1,500,000 ESAL's over a period of 20 years, and no heavy commercial truck is anticipated on this road. At the time of inspection, the pavement had been in service for only one year. There was no measurable rutting observed on the pavement during inspection.

Section with SMA L mix – this mix is placed as the surface course on one of the busiest highways in Ontario. This section of the highway is anticipated to take a traffic loading of more than 30,000,000 ESAL's over a period of 20 years. During the time of inspection, the pavement had been in service for less than one year (less than one summer). The pavement was in excellent condition with no measurable rutting observed during inspection.

Section with SMA G mix - this mix is placed on one of the busiest highways in Ontario. This section of the highway is anticipated to take a traffic loading of more than 30,000,000 ESAL's over a period of 20 years. Two site inspections have been completed on this section to date. During the first inspection, after about one year of service, some SMA G mix densification was observed. The measurements with a 2 m long straight edge indicated that the asphalt has densified to a depth of 1.0 to 2.0 mm. At the time of the second inspection, the pavement had been in service for slightly more than 1.5 years. The asphalt seemed to tighten up and no additional measurable densification was observed.

Section with SP 19 D mix – this mix is placed on a highway that is anticipated to carry about 10,000,000 ESAL's over a period of 20 years. The SP 19 D mix is placed as the binder course. No surface rutting was observed on this section during an inspection 1 year after construction.

Section with SP 19 E mix – this mix is placed as a binder course on a busy highway in Ontario. This section of the highway is anticipated to take a traffic loading of more than 30,000,000 ESAL's over a period of 20 years. One inspection was completed on this section about 1 year after construction. No measurable surface course rutting was observed on this section.

8.5 SUMMARY

The rutting predicted in the ABAQUS finite element modeling is compared in this chapter with the predicted rutting using the new mechanistic-empirical pavement method of pavement design, MEPDG, Level 3.

The relationship between predicted rutting using both methods is good for the dense graded mixes only (HL 3, SP 19 D and SP 19 E). The two SMA mixes do not match this relationship. The ranking of the three dense graded mixes in the HWRT laboratory testing, ABAQUS modeling and MEPDG analyses is the same. The performance of both SMA mixes in the ABAQUS finite element modeling is much better than in the MEPDG analyses.

The criteria for asphalt mix accelerated rutting resistance testing in the HWRT are recommended for three traffic loading levels: low, medium; and high. They can be used at the mix design stage in the pass/fail mix assessment, new materials evaluation, quality control and failure investigations.

CHAPTER NINE
CONCLUSIONS AND RECOMMENDATIONS

The purpose of this chapter is to summarize the major findings of the research and provide recommendations on future direction.

9.1 CONCLUSIONS

The results presented provide the methodology for asphalt mix rutting potential analysis. They include material characterization and asphalt mix behaviour analysis, finite element modeling and asphalt pavement and mix performance comparison.

9.1.1 Objectives

The objectives of this research are to investigate the nonlinear visco-elasto-plastic nature of asphalt mix in order to define the strain component that is the major contributor to asphalt rutting, to determine the laboratory testing method to measure the necessary characteristics, and to determine the material parameters required in the analysis for asphalt mixes rutting. Also, it is important to compare the pavement in-situ performance predicted using the finite element method with laboratory measured rutting using wheel track tester. This then forms the basis for the development of the rutting performance criteria in the wheel track testing.

9.1.2 Material Characterization and Asphalt Mix Behaviour

Testing in the HWRT is a suitable method for determining the rutting potential of asphalt mixes. It can be used not only to rank the mixes or as a pass/fail mix screening tool, but also to define the nature of rutting. However, the HWRT accelerated rutting performance test is empirical and is not designed to be used for asphalt pavement rutting prediction.

Dense grade mixes tested in the HWRT exhibit relatively small initial densification and then gradually reach a constant rutting slope. SMA mixes exhibit relatively high initial densification and then quickly reach a constant rutting slope that is typically flatter than that of the dense graded mixes.

The HWRT is able to screen the mixes in terms of their rutting potential. The conventional HL 3 Marshall mix, that incorporates a softer grade asphalt cement than other mixes, crushed gravel and natural sand, exhibits the highest potential to rutting. Other dense graded mixes incorporating higher grade asphalt cements, quarried coarse aggregate and crushed or manufactured sand exhibit much better rutting resistance. The SMA mixes exhibit very good to excellent resistance to rutting, particularly in the second half of the test between 10,000 and 20,000 passes. After the initial densification, the stone-on-stone mechanism is triggered and the deformation curve becomes relatively flat.

Asphalt mix deformation has recoverable (elastic and viscoelastic) and nonrecoverable (plastic and viscoplastic) components. The triaxial repeated load creep and creep recovery test conducted at various stress levels allows the measurement of all four components. The viscoplastic strain is the major contributor to asphalt mix rutting. The asphalt mix parameters A, n and m can be developed from the triaxial repeated load creep and creep recovery test results analysis.

Each asphalt mix has a unique set of parameters: elastic – modulus of elasticity and Poisson's ratio; and creep – A, n and m. Although the parameters should be calibrated against a measured permanent deformation, it is important that they are based on the results of laboratory testing. The rutting measured in the accelerated HWRT testing provides suitable performance data for the calibration of the creep parameters.

9.1.3 Finite Element Modeling

The finite element method is an effective tool for modeling the nonlinear viscoplastic behaviour of asphalt. The asphalt performance in the HWRT testing and pavement in-situ rutting can be modeled using a commercially available finite element program, ABAQUS. The creep power law model included in the ABAQUS library is suitable for material behaviour characterization.

There is a good linear relationship between the rutting predicted in the finite element modeling and the rutting measured in the accelerated performance testing. However, the predicted rutting is two to three times lower than the measured rutting, and a calibration is required. Parameter A should be adjusted to match the total rut depth for all five mixes. Parameter m should be adjusted for SMA mixes to match the slope of the measured and predicted rutting curves.

The deformations in the additional ABAQUS axisymmetric 2D space analyses are closer to the measured values than the deformations in the 2D plane strain analyses. The deformations in the 3D slice analysis are somewhat higher than the measured values.

If the calibrated parameters are used in the pavement in-situ service finite element modeling, the excellent rutting resistance of the SMA mixes is reflected in the analysis. The predicted rutting of SMA mixes is generally better, or at least equal, than that of a good quality dense graded mixes.

Two-dimensional modeling is suitable for asphalt performance modeling in the wheel tester as well as for the pavement in-situ performance. One of the benefits of using the creep model in the finite element modeling is that the total cumulative time of loading can be utilized in the analysis. This allows the computation time for repetitive loading analysis to be relatively short.

The shape and pattern of the tire may have a significant impact on the rutting. A simple tire model that reflects a typical shape of the tire footprint and contact pressure distribution is developed in this research.

The impact of the wheel wander on the depth of the asphalt layer rutting may be significant. The wheel will basically reshape the upheaval part of the deformation, thus reducing the total depth. The wheel wander reduction factor determined in other research is used in the calculation of the anticipated pavement in-situ rutting.

9.1.4 Asphalt Pavement and Mix Performance Comparison

The pavement in-situ rutting determined in the MEPDG Level 3 analysis is compared with rutting predicted in ABAQUS finite element simulation. The pavement structure models used in the ABAQUS simulation and MEPDG analysis are the same, consisting of a layer of hot-mix asphalt placed over a Portland cement concrete base; the pavement rutting is limited to the asphalt layer only.

The relationship between the predicted rut depth in MEPDG and ABAQUS is good for the dense graded mixes. However, the predicted performance of the SMA mixes in the ABAQUS analysis is much better than in the MEPDG analyses. In the MEPDG prediction model, asphalt layer rutting depends mainly on the value of the dynamic modulus and asphalt cement viscosity. Both SMA mixes exhibit relatively low dynamic modulus, lower than that of the dense graded mixes, and this is likely the cause of their relatively poor performance in the MEPDG analyses.

It is important that the asphalt mixes being used on larger paving projects are examined for their rutting resistance at the mix design stage. The use of good, rutting resistant mixes would limit costly asphalt pavement maintenance and repair operations, and reduce traffic interruptions. The accelerated rutting performance testing in the HWRT is one of the small-scale wheel tracking devices developed for this purpose. The results of this research are used for the development of the asphalt mix performance criteria in the HWRT testing. The criteria correlate to low, medium and high traffic loading levels.

9.2 RECOMMENDATIONS

The following recommendations are presented based on the results of this research:

- There is significant progress in the pavement technology available to pavement engineers. The industry has moved from conventional methods of asphalt mix design and testing toward the Superpave methodology. The equipment available allows the engineering parameters of asphalt mixes to be determined quickly using reliable methodology. This research presents an effective way of investigating asphalt mixes rutting resistance and predicting pavement in-situ rutting performance. This includes the use of the triaxial repeated load creep and creep recovery test to characterize the strain components of asphalt mixes, as well as using FEM for nonlinear viscoplastic analysis. It is recommended that the described method be used not only as a research tool, but also for new or improved materials evaluation, for pavement failure investigation, and for comprehensive mix behaviour analysis at the design stage for more complex paving projects;

- Use the accelerated rutting performance testing in loaded wheel testers not only to rank the mixes or for the mix pass/fail screening, but also to analyze the rate of rutting for particular mix types and to calibrate the predicted performance in finite element or other types of analysis against laboratory measured rutting. However, it should be recognized that wheel tracking is an empirical test and its purpose is not to directly predict pavement in-situ rutting performance;

- Care should be exercised in evaluating the performance of SMA mixes. Although the mixes have relatively low elastic modulus, their resistance to rutting is excellent. They can exhibit relatively high initial densification until the stone-on-stone contact in the mix is triggered;

- Use the dry test and the solid rubber wheel in the HWRT testing if the investigation is focused on rutting only. In a typical HWRT wet test, where the samples are immersed in hot water, stripping may play an important role and bias the results;

- Use the initial rutting performance criteria developed in this research if the accelerated rutting performance testing is conducted. The rutting criteria are related to traffic loading levels;

- The developed A, n and m parameters for dense graded and SMA mixes can be used for general pavement in-situ performance analysis and laboratory testing simulations. However, every asphalt mix has its own set of parameters and care should be exercised when using these parameters for conditions and mixes other than those used in this research; and

- The analyses in this research are based on somewhat limited laboratory testing (number of specimens) and a limited number of mixes. It is recommended that the development of permanent deformation in asphalt mixes be examined more thoroughly by conducting the triaxial repeated load creep and creep recovery testing on larger number of specimens and using a wider range of deviatoric stress. Also, it is suggested that the testing be conducted at various temperatures to investigate its impact on the rate of rutting. The additional testing should include a mix that is typically used for a medium traffic level. When the correction of the MEPDG is completed and the SMA models are adjusted, it is recommended to run the Level 1 analyses to verify the predicted rutting.

REFERENCES

[AASHTO 1993] AASHTO, "Guide for Design of Pavement Structures", American Association of State Highways and Transportation Officials, 1993.

[AASHTO 2003] American Association of State Highway and Transportation Officials, "Standard Test Method for Determining Dynamic Modulus of Hot-Mix Asphalt Concrete Mixtures", AASHTO Designation: TP 62-03, 2003.

[ABAQUS 2004a] ABAQUS Inc., "ABAQUS Version 6.5, Analysis User's Manual", 2004.

[ABAQUS 2004b] ABAQUS Inc., "ABAQUS Version 6.5, ABAQUS/CAE User's Manual", 2004.

[AI 1992] Asphalt Institute , "Computer Program CAMA, Version 2.0, Computer-Assisted Asphalt Mix Analysis, User's Manual", Lexington, Kentucky, 1992.

[AI 2003a] Asphalt Institute, Superpave, Performance Graded Asphalt Binder Specification and Testing, Superpave Series No. 1, (SP-1), Asphalt Institute, Lexington, Kentucky, 2003.

[AI 2003b] Asphalt Institute, Superpave, Superpave Mix Design, Superpave Series No. 2 (SP-2), Asphalt Institute, Lexington, Kentucky, 2003.

[Anderson 2003] Anderson R.M., Turner P.A., Peterson R.L. and Mallick R.B., "Relationship of Superpave Gyratory Compaction Properties to HMA Rutting Behaviour", National Cooperative Highway Research Program, NCHRP Report 478, Transportation Research Board, Washington, D.C., 2003.

[Bonaquist 2003] Bonaquist F. R., Christensen D.W., Stump W., "Simple Performance Tester for Superpave Mix Design: First –Article Development and Evaluation", National Cooperative Highway Research Program, NCHRP Report 513, Transportation Research Board, Washington, D.C., 2003.

[Brown 1990] Brown F. S., "Basic Concept, Bituminous Pavements Lecture Notes", University of Nottingham, 1990.

[Brown 1992] Brown E.R and Cross S. A., "A National Study of Rutting in Hot Mix Asphalt (HMA) Pavements", Association of Asphalt Paving Technologists, Proceedings, 61, 535-582, 1992.

[Brown 1997a] Brown E. R., Mallick R. B., Haddock J. E. and Bukowski J., "Performance of Stone Matrix Asphalt (SMA) Mixtures in the United States", National Center for Asphalt Technology, NCAT Report 97-1, Auburn, Alabama, 1997.

[Brown 1997b] Brown F. S., "Achievements and Challenges in Asphalt Pavement Engineering", 8th International Conference on Asphalt Pavements, Seattle, 1997.

[Brown 2001a] Brown E. R., Kandhal S. P. and Zhang J., "Performance Testing for Hot Mix Asphalt", National Center for Asphalt Technology, NCAT Report 01-05, Auburn, Alabama, 2001.

[Brown 2001b] Brown E. R., Kandhal S. P. and Zhang J., "Performance Testing for Hot Mix Asphalt (Executive Summary)", National Center for Asphalt Technology, NCAT Report 01-05A, Auburn, Alabama, 2001.

[Brown 2002] Brown E.R., Cooley L.A., Hanson D., Lynn C., Powell B., Prowell B., Watson D., "NCAT Test Track Design, Construction, and Performance", National Center for Asphalt Technology, NCAT, Auburn University, 2002.

[BS 2003] BS "Bituminous mixtures – Test methods for hot-mix asphalt, Part 22: Wheel Tracking", British Standard, BS EN 12697-22:2003, 2003.

[Buchanan 2005] Buchanan S. and Smith B. J., "Performance Evaluation of Hot-Mix Asphalt Using Rotary Loaded Wheel Testing", Transportation Research Board Annual Meeting, Washington, D.C., 2005.

[Carvalho 2006] Carvalho R. L. and Schwartz C. W., "Comparison of Flexible Pavement Designs: AASHTO Empirical Versus NCHRP Report 1-37A Mechanistic-Empirical", Transportation Research Board Annual Meeting, Washington, D.C., 2006.

[CEN 2004] European Committee for Standardisation, CEN, "Bituminous Mixtures – Test Method for Hot Mix Asphalt – Part 22: Wheel Tracking Test", prEN 12697-22 Standard, 2004.

[Chandrupatla 2002] Chandrupatla T.R., Belegundu A.D., Introduction to Finite Elements in Engineering, Prentice Hall, New Jersey, 2002.

[Chehab 2005] Chehab G.R. and Galal K.A., "The M-E Design Guide: A Case Study on HMA Overlays over Fractured PCC Slabs", Journal of the Association of Asphalt Paving Technologists, Volume 74, 2005.

[Collop 2003] Collop A., McDowell G. R. and Lee Y., "Modeling the Behaviour of an Idealised Asphalt Mixture Using the Distinct Element Method", Transportation Research Board Annual Meeting, Washington, D.C., 2004.

[Cooley 2000] Cooley L. A., Kandhal S. P., Fee F. and Epps A., "Loaded Wheel Testers in the United States: State of the Practice", National Center for Asphalt Technology, NCAT Report 2000-4, Transportation Research E-Circular No. E-C016, Auburn, Alabama, 2000.

[Coree 1998] Coree H. B. and VanDerHorst K., "SUPERPAVE Compaction", Transportation Conference Proceedings, Center for Transportation Research and Education, Iowa State University, Ames, Iowa, 1998.

[Cross 2001] Cross S. A. and Voth D. M., "Effects of Sample Preconditioning on Asphalt Pavement Analyzer (APA) Wet Rut Depths", Transportation Research Board Annual Meeting, Washington, D.C., 2001.

[Desai 2000a] Desai C.S., Mechanics of Materials and Interfaces, The Disturbed State Concept, CRC Press, 2000.

[Desai 2000b] Desai C.S., "Unified Disturbed State Constitutive Model for Asphalt Concrete", 14th Engineering Mechanics Conference, Austin, Texas, 2000.

[Desai 2002] Desai C.S., "Mechanistic Pavement Analysis and Design Using Unified Material and Computer Models", Department of Civil Engineering and Engineering Mechanics, The University of Arizona, Key Note Paper, Third International Symposium, 3D Finite Element for Pavement Analysis, Design and Research, Amsterdam, The Netherlands, 2002.

[DSC 2002] DSC Consulting and Software, "Pavement Analysis Including Microcracking, Fracture, Reflection Cracking, Etc.", DSC-SST2D and DSC-SST3D Programs, 2002.

[Emery 1990] Emery J.J., "Asphalt Pavement Rutting Experience in Canada", Proceedings of Canadian Technical Asphalt Association, 1990.

[Erkens 2002] Erkens M. J. G. S., Liu X., Scarpas T., Molenar A. A. A. and Blaauwendraad J., "Modeling of Pavement Materials – Numerical and Experimental Aspects", American Society of Civil Engineers, 15th ASCE Engineering Mechanics Conference, New York, 2002.

[Epps 02] Epps J. A., Seeds S., Schulz T., Alavi S., Ashmore C., Monismith C. L., Deacon J. A., Harvey J. T. and Leahy R., "Recommended Performance-Related Specification for Hot-Mix Asphalt Construction: Results of the Westrack Project", Transportation Research Board, National Research Council, National Cooperative Highway Research Program, NCHRP Report 455, Washington, D.C., 2002.

[Faheem 2005] Faheem A. F., Bahia H. U. and Ajideh H., "Estimating Results of a Proposed Simple Performance Test for Hot-Mix Asphalt from Superpave Gyratory compactor Results", Transportation Research Board Annual Meeting, Washington, D.C., 2005.

[FHWA 2002] U.S. Department of Transportation, Federal Highway Administration, "Hamburg Wheel Tracking Device", FHWA, Turner-Fairbank Highway Research Center, T-FHRC Publication, 2002.

[Haas 1975] Haas R. and Meyer F. R. P., "Cyclic Creep of Bituminous Materials Under Transient High Volume Loads", Transportation Research Board, TRR No. 549, 1975.

[Haas 1994] Haas R., Hudson W. and Zaniewski W, Modern Pavement Management, Krieger Publishing Company, Florida, 1994.

[Haas 1997] Haas R., et al., Pavement Design and Management Guide, Transportation Association of Canada, Ottawa, 1997.

[Hall 1999] Hall K. D. and Williams S. G., "Acquisition and Evaluation of Hamburg Wheel-Tracking Device", National Technical Information Service, MBTC FR-1044, Springfield, Virginia, 1999.

[Harman 2003] Harman T., "Overview, Understanding the Performance of Modified Asphalts in Mixtures", Presentation, Federal Highway Administration, 2003.

[Harvey 2002] Harvey T. J., Hoover P. T., Coetzee F. N. and Monismith L. C., "Rutting Evaluation of Asphalt Pavements Using Full-Scale Accelerated Load and Laboratory Performance Tests", Presented for the 2002 Federal Aviation Administration Airport Technology Transfer Conference, 2002.

[Hein 2004] Hein D. and Olidis C., "Guide for the Mechanistic-Empirical Design of New and Rehabilitated Pavement Structures, Material Characterization, Is Your Agency Ready?", Transportation Association of Canada, Annual Conference in Quebec City, 2004.

[Hua 2000] J. Hua, "Finite Element Modeling and Analysis of Accelerated Pavement Testing Devices and Rutting Phenomenon", Ph.D. Thesis, Purdue University, 2000.

[Huang 1995] Huang H., "Analysis of Accelerated Pavement Tests and Finite element Modeling of Rutting Phenomenon", Ph.D. Thesis, Purdue University, 1995.

[Huang 2001] Huang B., Mohammad L.N., Rasoulian M., "3-D Numerical Simulation of Asphalt Pavement at Louisiana Accelerated Loading Facility (ALF)", Transportation Research Record, National Research Council, Washington, D.C., 2001.

[ITC 2004] ITC Interlaken, "Interlaken Soil and Asphalt Test System, Interlaken Technology Corporation Manual", 2004.

[Kaloush 2001] Kaloush K. E. and Witczak W. M., "Simple Performance Test for Permanent Deformation of Asphalt Mixtures", Transportation Research Board Annual Meeting, Washington, D.C., 2001.

[Kandhal 1998] Kandhal S. P., Mallick B. R. and Brown R. E., "Hot Mix Asphalt For Intersections in Hot Climates", National Center for Asphalt Technology, NCAT Report No. 98-06, Auburn, Alabama, 1998.

[Kandhal 2001] Kandhal S. P. and Mallick R.B., "Effects of Mix Gradation on Rutting Potential of Dense-Graded Asphalt Mixtures", Transportation Research Board, National Research Council, Transportation Research Record No. 1767, Washington, D.C., pp. 146-151, 2001.

[Kandhal 2002a] Kandhal S. P. and Cooley A. L. Jr. "Evaluation of Permanent Deformation of Asphalt Mixtures Using Loaded Wheel Tester", National Center for Asphalt Technology, NCAT Report 02-08, Auburn, Alabama, 2002.

[Kandhal 2002b] Kandhal S. P. and Colley L. A., "Coarse Versus Fine-Graded Superpave Mixtures: Comparative Evaluation of Resistance to Rutting", Transportation Research Board, Washington, D.C., 2002.

[Kandhal 2003] Kandhal S. P. and Cooley A.L., Jr., "Accelerated Laboratory Rutting Tests: Evaluation of the Asphalt Pavement Analyzer", National Cooperative Highway Research Program, NCHRP Report 508, Transportation Research Board, Washington, D.C., 2003.

[Kennepohl 1999] Kennepohl G., Aurilio V., Uzarowski Ll, Emery J. and Luim P., "Ontario Experience with SMA and Performance To Date", Proceedings, Canadian Technical Asphalt Association, pp. 495-516, 1999.

[Lai 1973] Lai J., Anderson D., "Irrecoverable and recoverable Nonlinear Viscoelastic Properties of Asphalt Concrete", Transportation Research Record 468, National Research Council, Washington D.C., p 73-88, 1973.

[LTRC 2004] Louisiana Transportation Research Center, LTRC, "Comparative Performance of Rubber Modified Hot Mix Asphalt Under ALF Loading", Technical Summary Report 374, 2004.

[Lu 2006] Lu Q. and Harvey T. J., "Evaluation of Hamburg Wheel Tracing Device Test by Laboratory and Field Performance Data", Transportation Research Board Annual Meeting, Washington, D.C., 2006.

[Maupin 1999] Maupin G.W., "A Case Study of the Design, Installation, and Early Performance of a Nineteen-Millimeter Superpave Mix", Virginia Transportation Research Council, Charlottesville, Virginia, 1999.

[Meyer 1977] Meyer R.P. F. and Haas C.G. R., "A Working Design Subsystem for Permanent Deformation in Asphalt Pavements", Proceedings, Fourth International Conference on the Structural Design of Asphalt Pavements, Vol. 1, Ann Arbor, 519-528, 1977.

[Monismith 1999] Monismith L. C., Brown F. S., "Developments in the Structural Design and Rehabilitation of Asphalt Pavement over Three Quarters of a Century", Asphalt Paving Technology, 75th Anniversary Historical Review and Index of Journals 1975-1999, Volume 68A, 1999.

[Monismith 2000] Monismith L. C., Harvey J. T., Long F. and Weissman S., "Tests to Evaluate Stiffness and Permanent Deformation Characteristics of Asphalt/Binder-Aggregate Mixes, A Critical Discussion", Technical Memorandum, TM-UCB PRC-2000-1, 2000.

[MTO 2002] Ontario Ministry of Transportation, "Material Specification for Hot Mix Asphalt", Ontario Provincial Standard Specification, OPSS 1150, 2002.

[MTO 2004] Ontario Ministry of Transportation, "Material Specification for Superpave and Stone Mastic Asphalt Mixtures", Ontario Provincial Standard Specification, OPSS 1151, 2004.

[NCHRP 2003] National Cooperative Highway Research Program, "Refining the Calibration and Validation of Hot Mix Asphalt Performance Models: An Experimental Plan and Database", Research Results Digest, Number 284, 2003.

[NCHRP 2004a] National Cooperative Highway Research Program, "Guide for Mechanistic-Empirical Design of New and Rehabilitated Pavement Structures", NCHRP, Part 2 – Design Inputs, Chapter 2 Material Characterization", 2004.

[NCHRP 2004b] National Cooperative Highway Research Program, "Guide for Mechanistic-Empirical Design of New and Rehabilitated Pavement Structures", NCHRP, Part 3 – Design Analysis, Chapter 3 Design of New and Reconstructed Flexible Pavements", 2004.

[NCHRP 2004c] National Cooperative Highway Research Program, "Guide for Mechanistic-Empirical Design of New and Rehabilitated Pavement Structures", NCHRP, Appendix RR: Finite Element Procedures for Flexible Pavement Analysis", 2004.

[Novak 2004] Novak M., Birgisson B., Roque R. and Choubane B., "Effects of One-Way and Two-Way Directional Heavy Vehicle Simulator Loading on Rutting in Hot-Mix Asphalt Pavements", Transportation Research Board Annual Meeting, Washington, D.C., 2004.

[O'Flaherty 2002] O'Flaherty C.A., Highways: The Location, Design, Construction & Maintenance of Pavements, 4th Edition, Butterworth Heinemann, 2002.

[Ottosen 1992] Ottosen N. and Peterson H., Introduction to the Finite Element Method, Prentice Hall Europe, 1992.

[Perl 1983] Perl M., Uzan J., Sides A., "Visco-Elasto-Plastic Constitutive Law for a Bituminous Mixture Under Repeated Loading", Transportation Research Record 911, National Research Council, Washington, D.C., p 21-27, 1983.

[Perraton 2001] Perraton D., Carter A., Tremblay D. and Langlois P., "Rheological Properties, Thermal Cracking and Rutting Resistance of Stone Matrix Asphalt", Proceedings, Canadian Technical Asphalt Association, 46, pp. 423-450, 2001.

[Powell 2003] Powell R.B., "Laboratory Performance Testing for the NCAT Pavement Test Track", Transportation Research Board Annual Meeting, Washington, D. C., 2003.

[Roberts 2003] Roberts F.L., Mohammad L.N., Oin H. and Huang B., "Comparative Performance of Rubber Modified Hot Mix Asphalt Under ALF Loading", Federal Highway Administration, Report No. FHWA/LA/03/374, 2003.

[Rothenburg 1992] Rothenburg L., Bobowicz A. and Haas C. G. R., "Micromechanical Modeling on Asphalt Concrete in Connection with Pavement Rutting Problems", Proceedings of the 7th International Conference on Asphalt Pavements, Design, Volume One, Derry and Sons Ltd, 1992.

[Sadasivam 2004] Sadasivam S., Khosla N. P. and Maplass G. A., "NCSU Wheel Tracking Device: Its Ability to Predict Rutting of Superpave Mixes", Transportation Research Board Annual Meeting, Washington, D.C., 2004.

[Sadd 2002] Saad M. H., Dai Q., Parameswaran V. and Shukla A., "Microstructural Simulation of Asphalt Materials: Modeling and Experimental Verification", American Society of Civil engineers, 15th Engineering Mechanics Conference, New York, 2002.

[Saleh 2002] Saleh M. F., Steven B. and Alabaster D., "Three Dimensional Nonlinear Finite Element Model to Simulate the Pavement Response in the Canterbury Accelerated Pavement Testing Facility (CAPTIF)", Transportation Research Board Annual Meeting, Washington, D.C., 2003.

[Scarpas 1997] Scarpas A., Van Gurp C. A. P. M., Al-Khoury R. and Erkens S. M. J. G., "Finite Element Simulation of Damage Development in Asphalt Concrete Pavements", Proceedings of 8th International Conference on Asphalt Pavements, University of Washington, Seattle, 1997.

[Schwartz 2005] Schwartz C., "Evaluation of Witczak Dynamic Modulus Prediction Model", Transportation Research Board Annual Meeting, Washington, D.C., 2005.

[Shah 2004] Shah A., McDaniel R. and Gallivan V., "Evaluation of Mixtures Using Dynamic Modulus Tester: Results and Practical Considerations", Journal of the Association of Asphalt Paving Technologists, Volume 73, 2004.

[Sivasubramaniam 2004] Sivasubramaniam S., Galal K. A., Noureldin A. S., White T. D. and Haddock J. E., "Modeling Permanent Deformation Using Laboratory, Proto-type, and In-Service Accelerated Pavement Testing", Transportation Research Board Annual Meeting, Washington, D.C., 2004.

[Spencer 1988] Spencer A.J.M., Continuum Mechanics, Longman Scientific & Technical, 1988.

[Sukumaran 2004] Sukumaran B., "Three Dimensional Finite Element Modeling of Flexible Pavements", Federal Aviation Administration (FAA), 2004 FAA Worldwide Airport Technology Transfer Conference, Atlantic City, Mew Jersey, USA, 2004.

[Tashman 2004] Tashman L., Masad E., Little A. and Zbib H., "Identification of Hot Mix Asphalt Permanent Deformation Using Triaxial Strength Tests and Microtexture-Based Viscoplastic Continuum Model", Transportation Research Board Annual Meeting, Washington, D.C., 2004.

[Texas DOT 2003] Texas Department of Transportation, Pavement Construction Specifications, Draft 10/03/03, 2003.

[Texas DOT 2004] Texas Department of Transportation, "Tex-242-F, Hamburg Wheel-tracking Test", Texas DOT Online Manual System, 200-F, Bituminous Test Procedures Manual, Chapter 38, 2004.

[Texas DOT 2005] Texas Department of Transportation, "Tex-231-F, Static Creep Test", 200-F, Bituminous Test Procedures Manual, 2005.

[Tighe 2003] Tighe L. S., Jeffray A., Kennepohl G., Haas R. and Matheson M., "Field Experiments in CPATT's Long Term Program of Pavement Research", Transportation Association of Canada, Annual Conference in St. John's, Newfoundland and Labrador, 2003.

[Timm 2003] Timm D. H. and Newcomb D., "Calibration of Flexible Pavement Performance Equations for Mn/ROAD", Transportation Research Board Annual Meeting, Washington, D.C., 2003.

[TRAC 1990] Washington State Transportation Center (TRAC) Workbook, "Section 3, Fundamentals of Mechanistic-Empirical Design", 1990.

[Tran 2004] Tran N.H. and Hall K.C., "Evaluating the Predictive Equation in Determining Dynamic Modulus of Typical Asphalt Mixtures Used in Arkansas", Journal of the Association of Asphalt Paving Technologists, Volume 73, 2004.

[Uddin 2000a] Uddin W., "Simulation of Falling Weight Deflectometer for In-Situ Material Characterization of Highway and Airport Pavements", 6th International LS-DYNA Users Conference, Michigan, 2000.

[Uddin 2000b] Uddin W and Ricalde L., "Nonlinear Material Modeling and Dynamic Finite Element Simulation of Asphalt Pavements", Fourteen Engineering Mechanics Conference, Department of Civil Engineering, The University of Texas at Austin, Austin, Texas, 2000.

[Uddin 2002] Uddin W. and Garza S., "3D-FE Simulation and Dynamic Response Analysis of FWD Impact on Asphalt Pavements", International Conference on Highway Pavement Data, Analysis and Mechanistic Design Applications, 2002.

[Ullidtz 1998] P. Ullidtz, Modelling Flexible Pavement Response and Performance, Polyteknisk Forlag, Narayana Press, Gylling, 1998.

[U of Nottingham 1994] University of Nottingham, "MSc Highway Engineering/MSc Transport Engineering, Soil Mechanics for Highway Engineers, Lecture Notes", 1994.

[Uzarowski 2004] Uzarowski L., Paradis M. and Lum P., "Accelerated Performance Testing of Canadian Asphalt Mixes Using Three Different Wheel Rut Testers", Transportation Association of Canada, TAC, Annual Conference in Quebec City, Quebec, 2004.

[Van Dommelen 2002] Van Dommelen A. E., Houben L. J. M., Molenar A. A. A. and Visser A. F. H. M., "Full Scale Testing and Modeling of Permanent Deformation in Asphalt Pavements", Paper Published by International Journal of Pavements, Volume 1, Number 1, 2002.

[Von Quintus 1994] Von Quintus H.L., "Performance Prediction Models In the Superpave Mix Design System", Strategic Highway Research Program, SHRP-A-699, Washington, D.C., 1994.

[Walker 1999] Walker D. and Buncher M., "Intersection Strategy", Asphalt Institute, Lexington, Kentucky, 1999.

[Wang 2006] Wang F. and Machemehl R. B., "Mechanistic-Empirical Study of Effects of Truck Tire Pressure on Pavement: Measured Tire-Pavement Contact Stress Data", Transportation Research Board Annual Meeting, Washington, D.C., 2004.

[White 2002] White T.D., Haddock J.E., Hand A. J. T. and Fang H., "Contributions of Pavement Structural Layers to Rutting of Hot Mix Asphalt Pavements", Transportation Research Board, National Research Council, National Cooperative Highway Research Program, NCHRP Report 468, Washington, D.C., 2002.

[White 2003] White T., Hua J. and Galal K. "Analysis of Accelerated Pavement Tests", Transportation Research Board Annual Meeting, Paper CS8-7, Washington, D.C., 2003.

[Witczak 2001] Witczak W. M., "Superpave / 2002 Design Guide Performance Prediction Modeling", Presentation at Canadian Technical Asphalt Association (CTAA) and Canadian User Producer Group for Asphalt (CUPGA) Meeting, Toronto, 2001.

[Witczak 2002a] Witczak M.W., Kaloush K.E. and Von Quintus H., "Pursuit of the Simple Performance Test for Asphalt Mixture Rutting", Association of Asphalt Paving Technologists, Proceedings, 71, pp. 671-679, 2002.

[Witczak 2002b] Witczak M.W., Kaloush K., Pelinen T., El-Basyouny M. and Von Quintus H., "Simple Performance Test for Superpave Mix Design", National Cooperative Highway Research Program, NCHRP Report 465, Transportation Research Board, Washington, D.C., 2002.

[Witczak 2005] Witczak M., "Simple Performance Tests: Summary and Recommended Methods and Database", National Cooperative Highway Research Program, NCHRP Report 547, Transportation Research Board, Washington, D.C., 2005.

[Yandell 1997] Yandell W. O. and Behzadi G., "Performance Prediction of Accelerated Loading Facility (ALF) Trials Using Elastic, Visco-Elastic and Elasto-Plastic Analysis", Proceedings of 8th International Conference on Asphalt Pavements, University of Washington, Seattle, 1997.

[Yildrim 2001] Yildrim Y. and Kennedy W. T., "Correlation of Field Performance to Hamburg Wheel Trucking Device Results", Federal Highway Administration Report No. FHWA/TX-04/0-4185-1, 2001.

[Yoder 1975] Yoder E.J., Witczak M.W., Principles of Pavement Design, Second Edition, John Wiley & Sons, Inc., 1975.

[Zhang 2002] Zhang J. and Kandhal S. P., "Comparison of Fundamental and Simulative Test Methods for Evaluating Permanent Deformation of Hot Mix Asphalt" Transportation Research Board Annual Meeting, Washington, D.C., 2002.

[Zhu 2001] Zhu L. Y., Fwa T. F. and Liu Y., "Rutting Potential Evaluation of Asphalt Mixtures by Repeated-Load Creep Test", Transportation Research Board Annual Meeting, Washington, D.C., 2002.

[Zienkiewicz 1968] Zienkiewicz O.C., Cheung Y.K., The Finite Element Method in Structural Continuum Mechanics, McGraw-Hill Publishing Company Limited, 1968.

APPENDIX A

AIR VOIDS IN HWRT SPECIMENS

Table A1 Summary of Air Voids in HWRT Specimens

Mix	Specimen Number	Air Voids (%)
HL 3	62	6.3
	63	6.3
	66	6.0
	69	6.0
	71	6.7
	72	6.5
	73	6.9
	74	6.9
	75	6.5
	76	6.8
	78	6.5
	79	6.8
	Mean	6.5
	Standard Deviation	0.3
SMA L	1	6.4
	2	6.7
	5	6.9
	7	6.8
	9	6.9
	10	6.4
	12	6.8
	14	6.9
	16	7.0
	17	6.6
	18	7.0
	19	6.8
	Mean	6.8
	Standard Deviation	0.2
SMA G	109	6.5
	112	6.3
	113	6.1
	119	6.1
	120	6.2
	121	6.0
	124	6.7
	125	6.0
	126	6.1
	127	6.4
	128	6.3
	131	6.2
	Mean	6.2
	Standard Deviation	0.2

Table A1 (continued)
Summary of Air Voids in HWRT Specimens

Mix	Specimen Number	Air Voids (%)
SP 19 D	84	6.4
	87	6.7
	91	6.4
	92	6.7
	93	6.8
	94	6.7
	96	6.6
	97	6.2
	98	6.8
	99	6.1
	100	6.3
	101	6.7
	Mean	6.5
	Standard Deviation	0.2
SP 19 E	82	6.1
	89	6.9
	102	6.9
	110	6.8
	111	6.9
	114	6.6
	115	6.8
	116	7.0
	133	6.5
	134	6.4
	135	7.0
	136	6.8
	Mean	6.7
	Standard Deviation	0.3

APPENDIX B

ASPHALT MIXES AXIAL STRAIN PLOTS

HL 3 Mix, 100 kPa

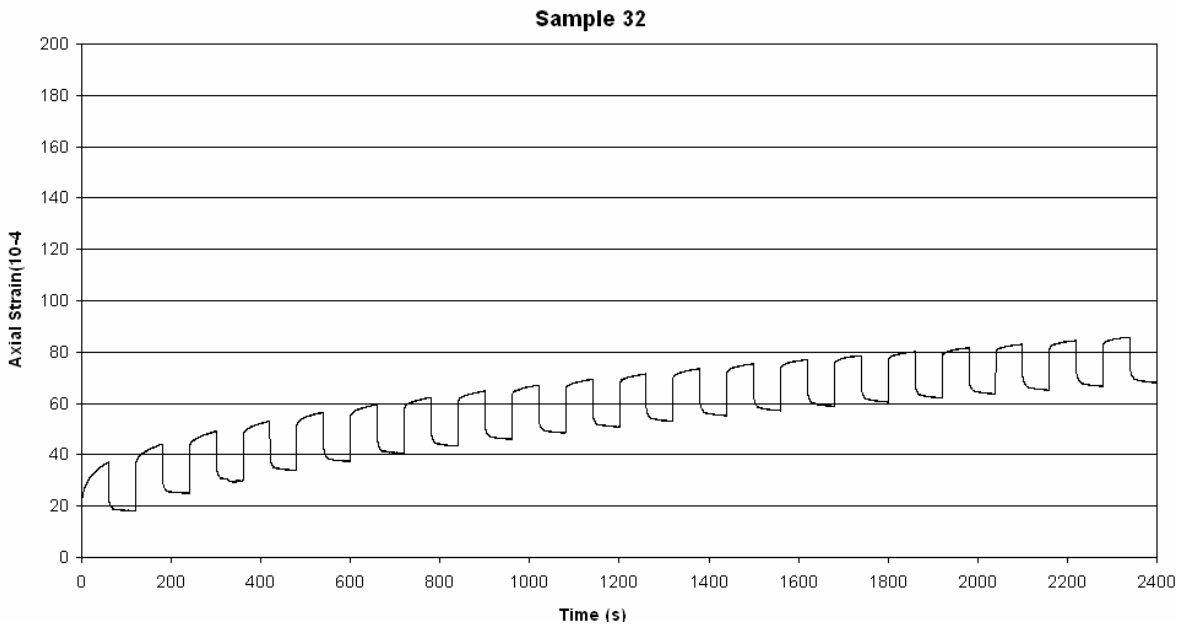

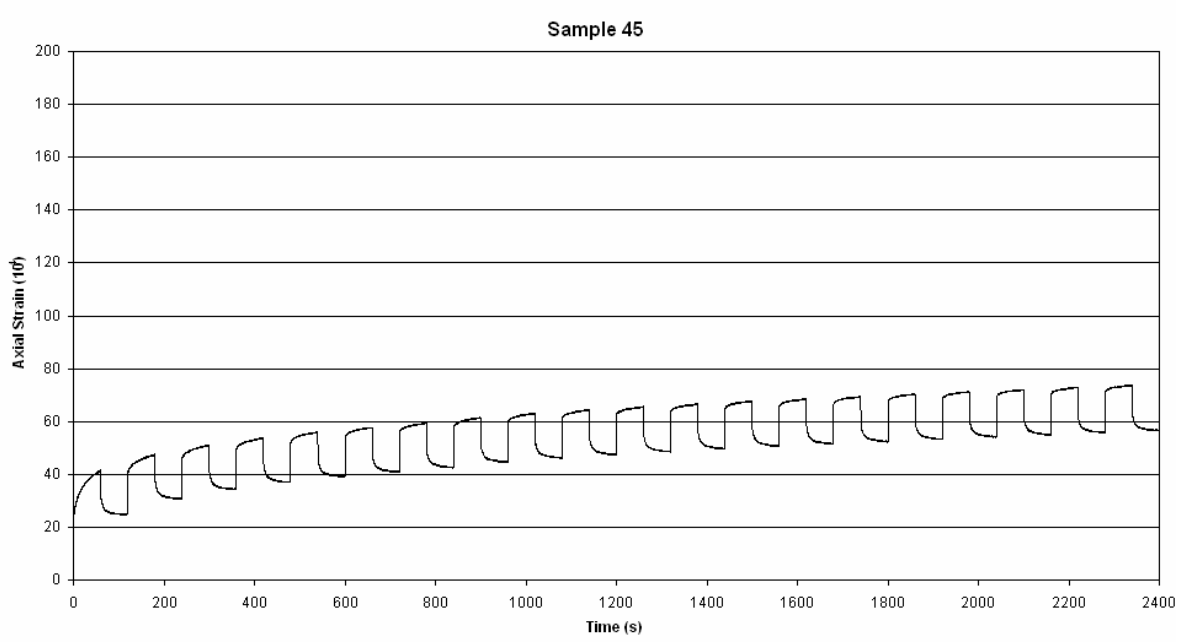

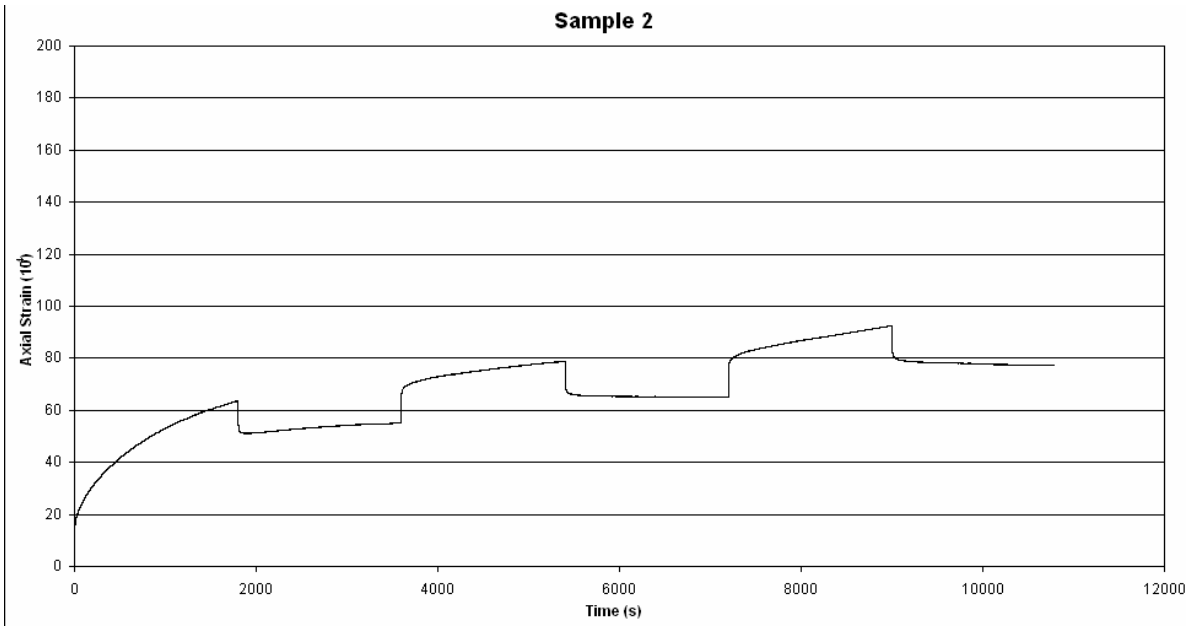
Sample 2
Axial Strain (10⁻⁴)
200
180
160
140
120
100
80
60
40
20
0
0
2000
4000
6000
8000
10000
12000
Time (s)

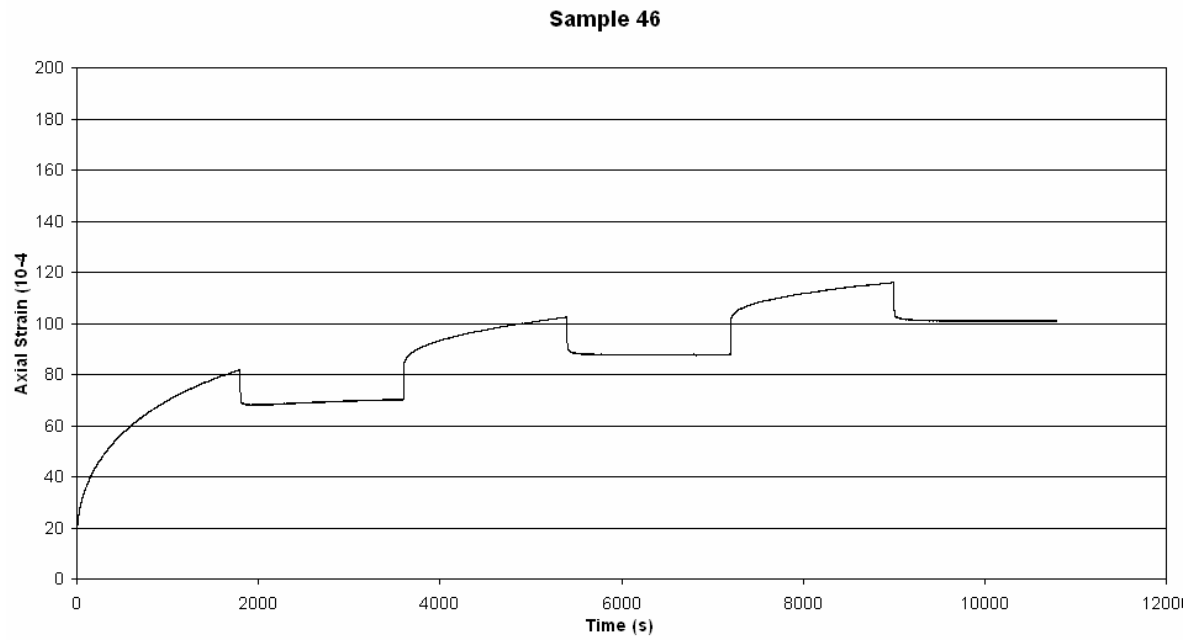
Sample 46
Axial Strain (10-4
200
180
160
140
120
100
80
60
40
20
0
0
2000
4000
6000
8000
10000
12000
Time (s)

HL 3, 200 kPa

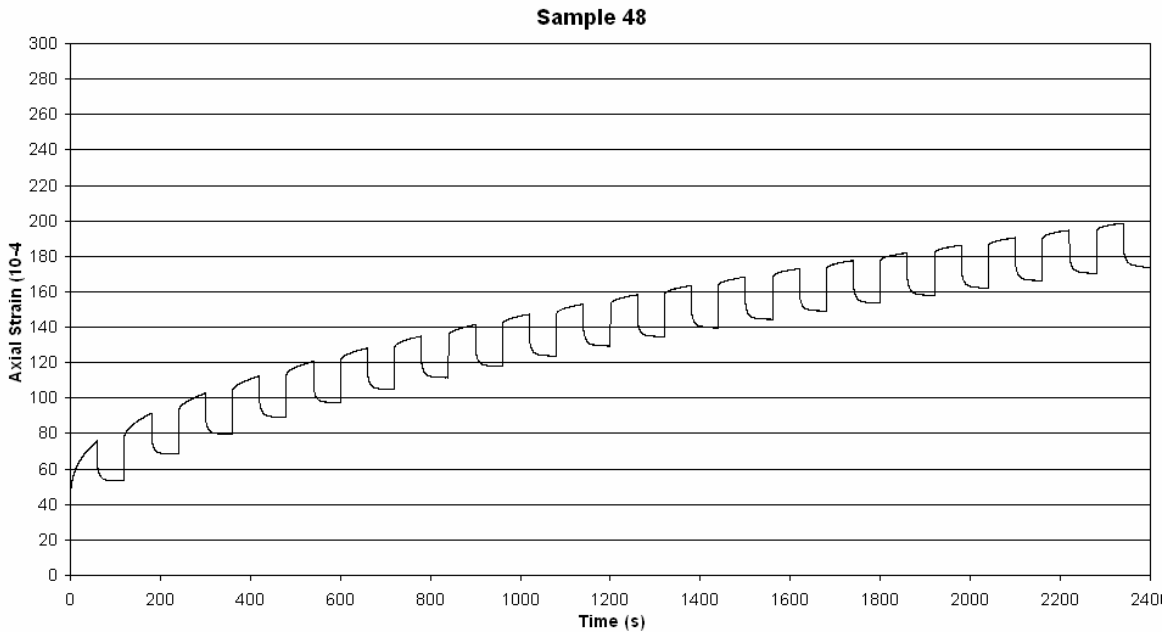
Sample 48
Axial Strain (10-4
Time (s)
0
20
40
60
80
100
120
140
160
180
200
220
240
260
280
300
0
200
400
600
800
1000
1200
1400
1600
1800
2000
2200

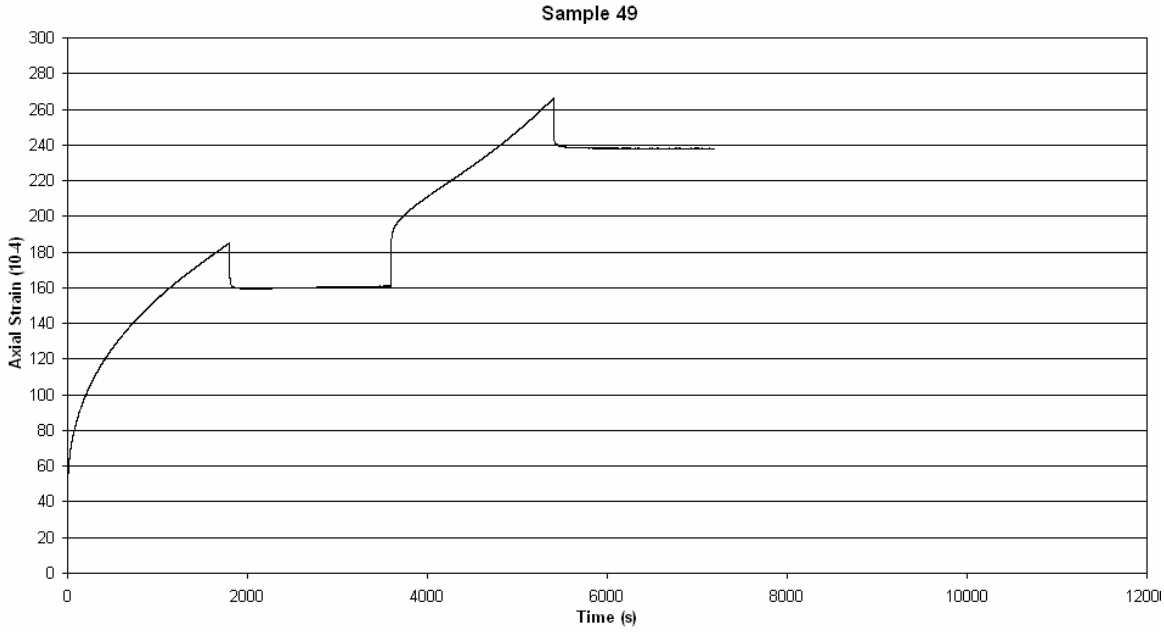
Sample 49
Axial Strain (10-4)
Time (s)
0
20
40
60
80
100
120
140
160
180
200
220
240
260
280
300
0
2000
4000
6000
8000
10000

SMA L, 100 kPa

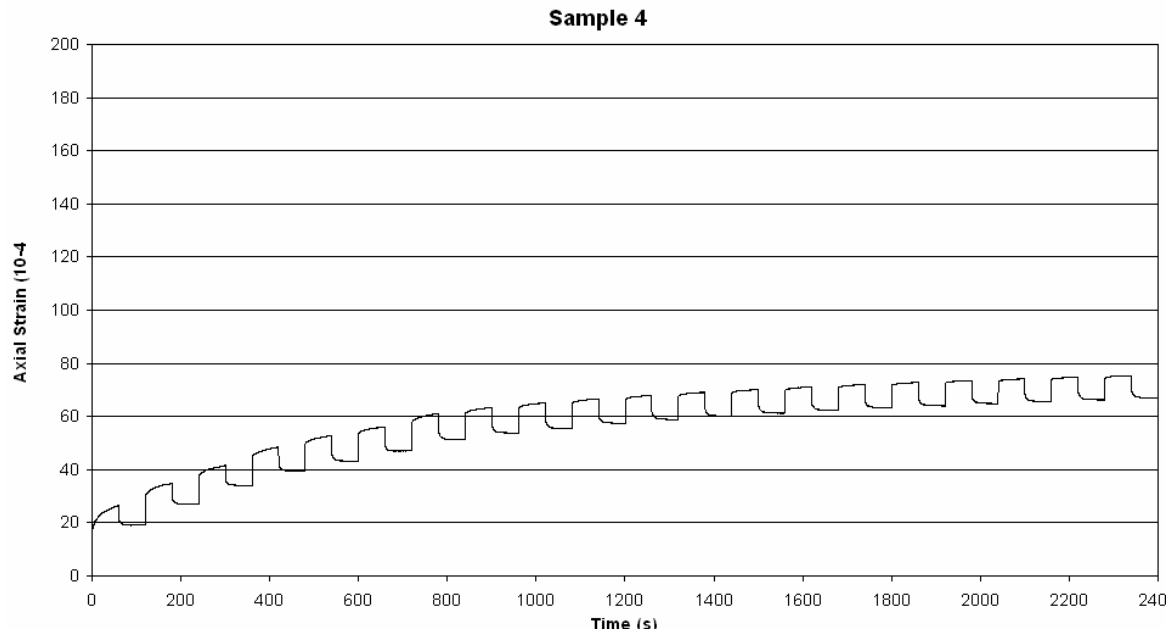
Sample 4
Axial Strain (10-4
200
180
160
140
120
100
80
60
40
20
0
0
200
400
600
800
1000
1200
1400
1600
1800
2000
2200
240
Time (s)

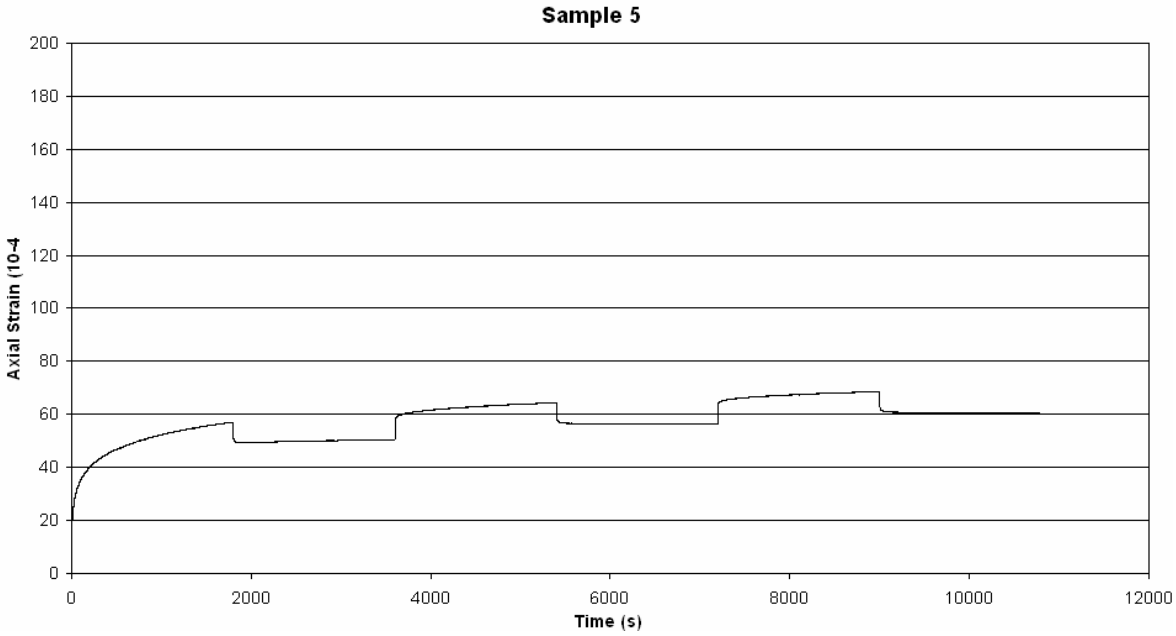
Sample 5
Axial Strain (10-4
200
180
160
140
120
100
80
60
40
20
0
0
2000
4000
6000
8000
10000
12000
Time (s)

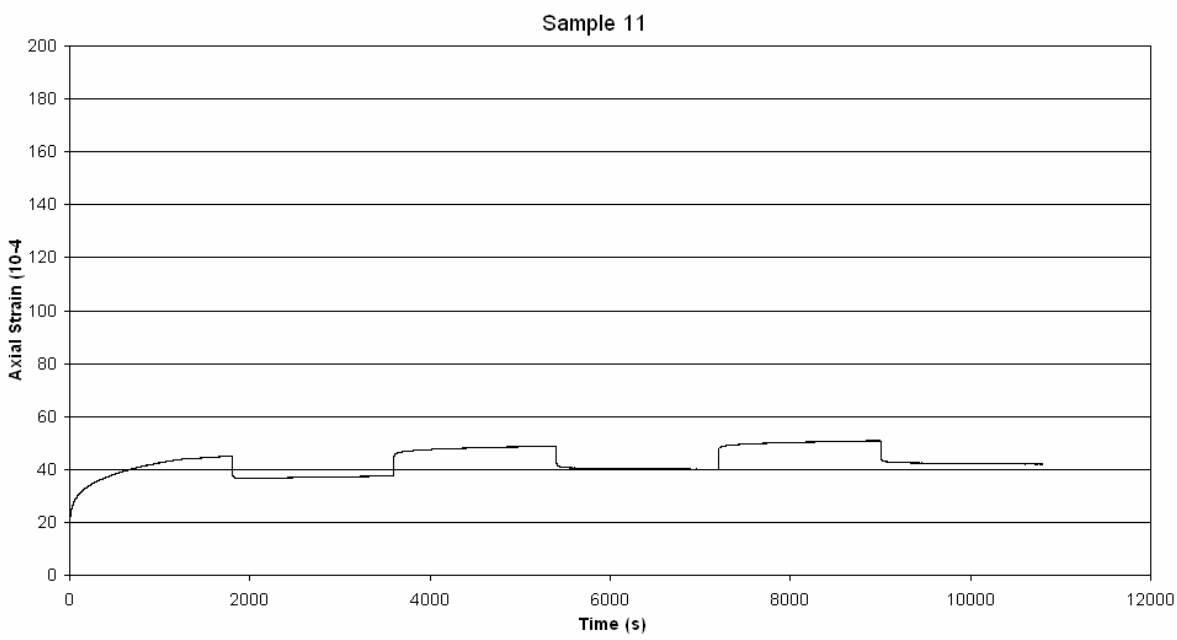
Sample 11
Axial Strain (10-4
Time (s)
0
20
40
60
80
100
120
140
160
180
200
0
2000
4000
6000
8000
10000
12000

SMA L, 200 kPa

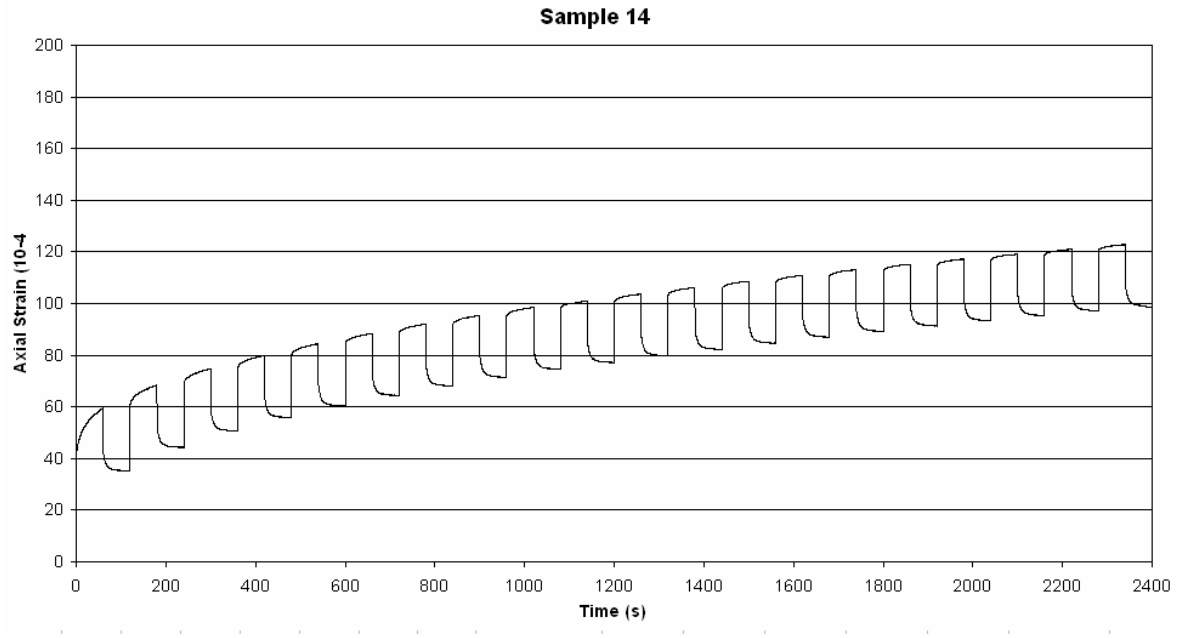
Sample 14
Axial Strain (10-4
Time (s)
0
20
40
60
80
100
120
140
160
180
200
0
200
400
600
800
1000
1200
1400
1600
1800
2000
2200
2400

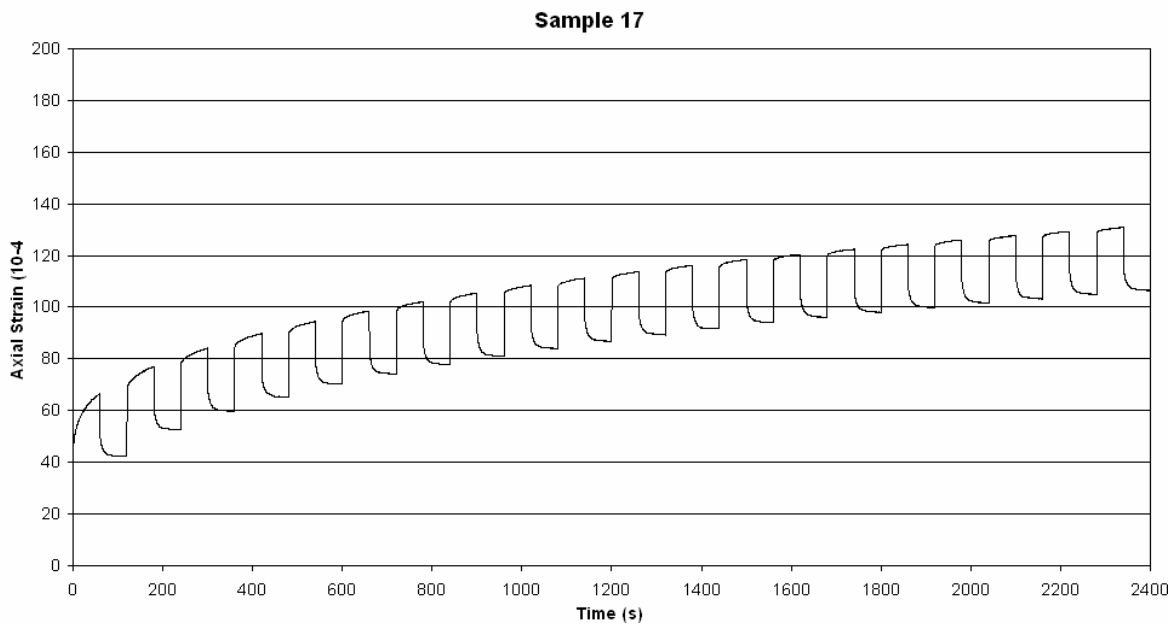
Sample 17
Axial Strain (10-4
Time (s)
0
20
40
60
80
100
120
140
160
180
200
0
200
400
600
800
1000
1200
1400
1600
1800
2000
2200
2400

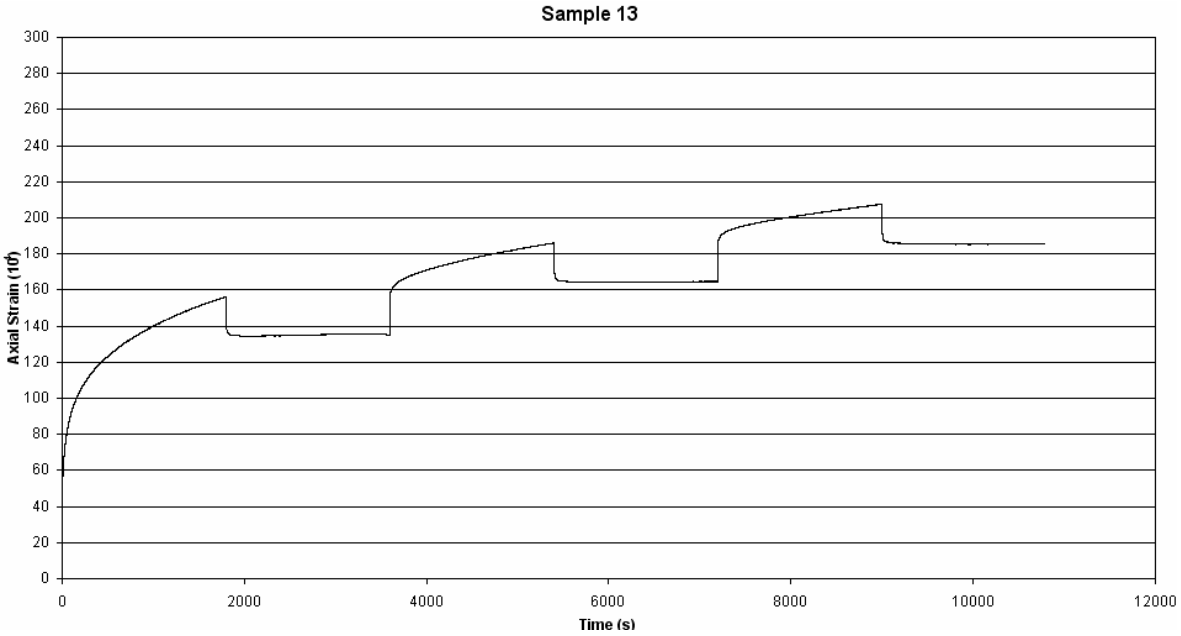
Sample 13
Axial Strain (10-4)
Time (s)
0
20
40
60
80
100
120
140
160
180
200
220
240
260
280
300
0
2000
4000
6000
8000
10000
12000

SMA G, 100 kPa

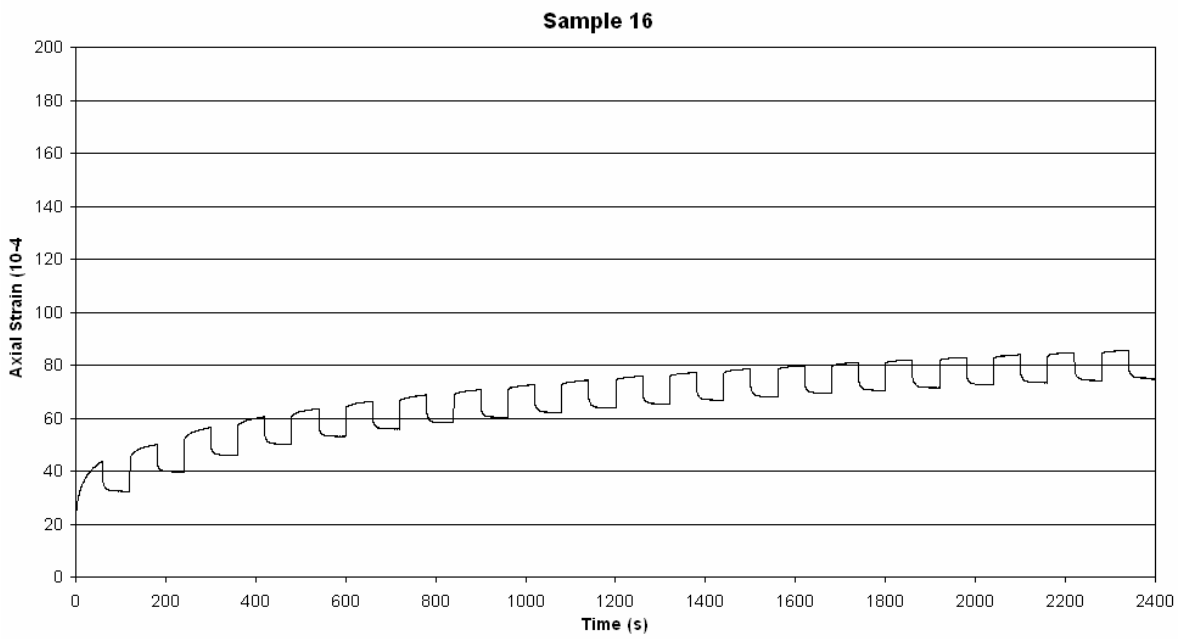
Sample 16
Axial Strain (10-4
Time (s)
0
20
40
60
80
100
120
140
160
180
200
0
200
400
600
800
1000
1200
1400
1600
1800
2000
2200
2400

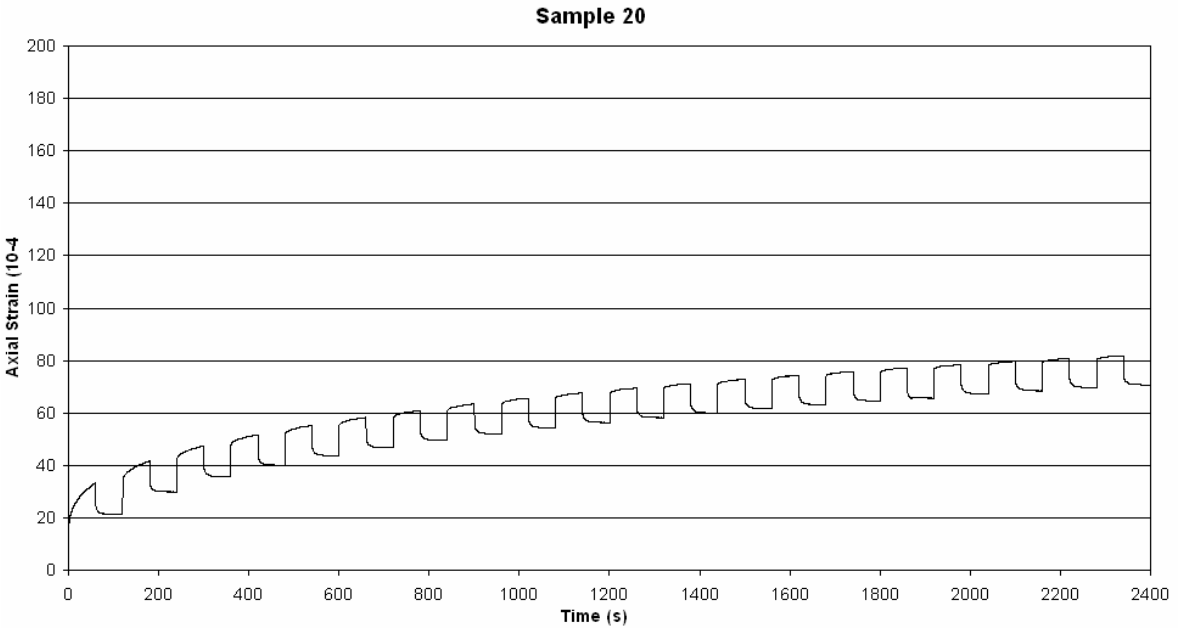
Sample 20
Axial Strain (10-4
Time (s)
0
20
40
60
80
100
120
140
160
180
200
0
200
400
600
800
1000
1200
1400
1600
1800
2000
2200
2400

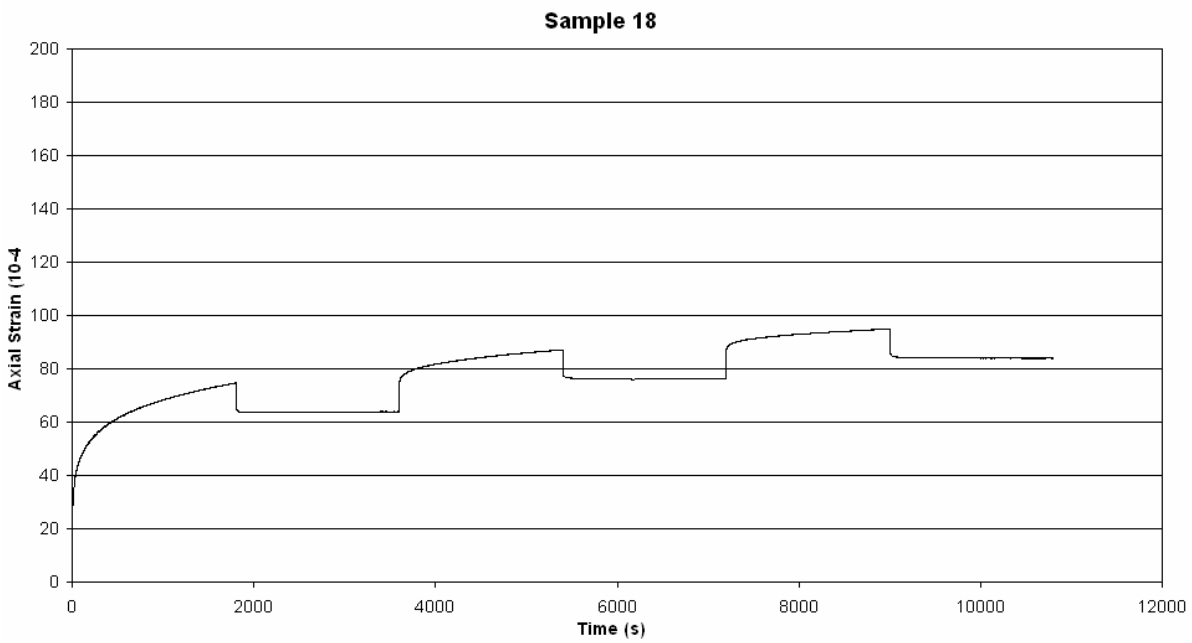
Sample 18
Axial Strain (10-4
Time (s)
0
20
40
60
80
100
120
140
160
180
200
0
2000
4000
6000
8000
10000
12000

SMA G, 200 kPa

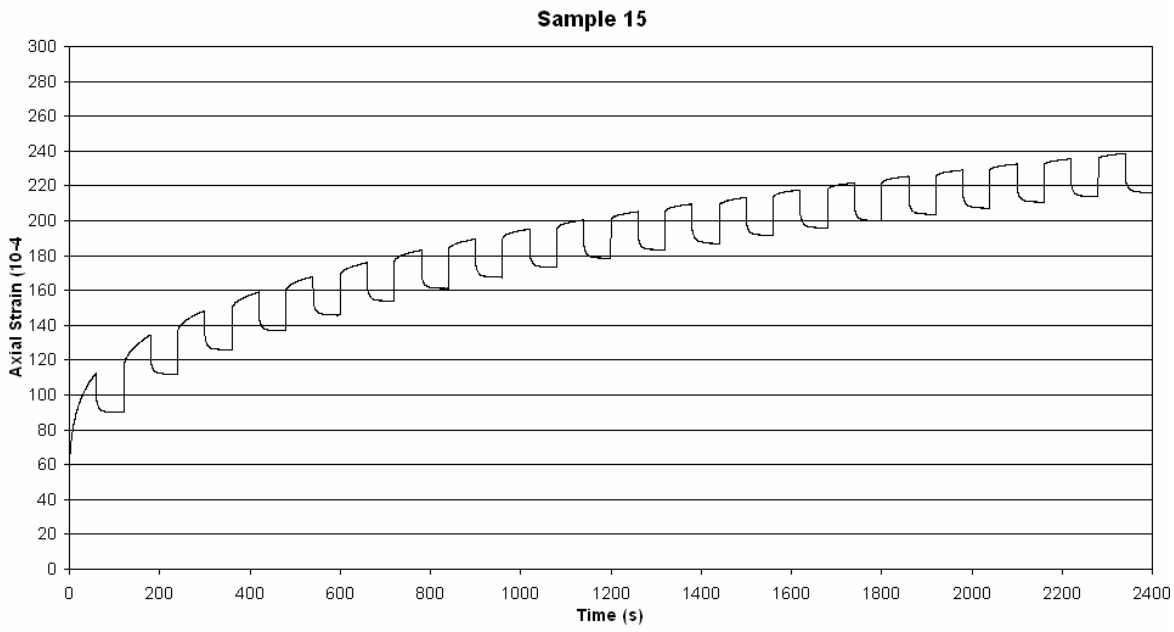
Sample 15
Axial Strain (10-4
Time (s)
0
20
40
60
80
100
120
140
160
180
200
220
240
260
280
300
0
200
400
600
800
1000
1200
1400
1600
1800
2000
2200
2400

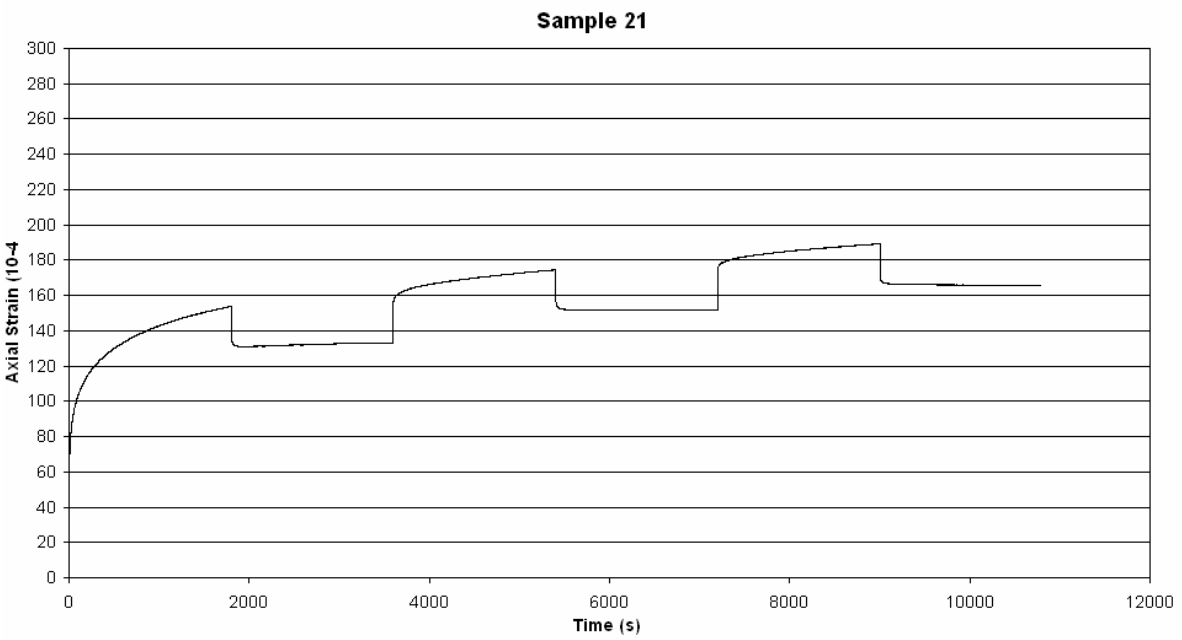

SP 19 D, 100 kPa

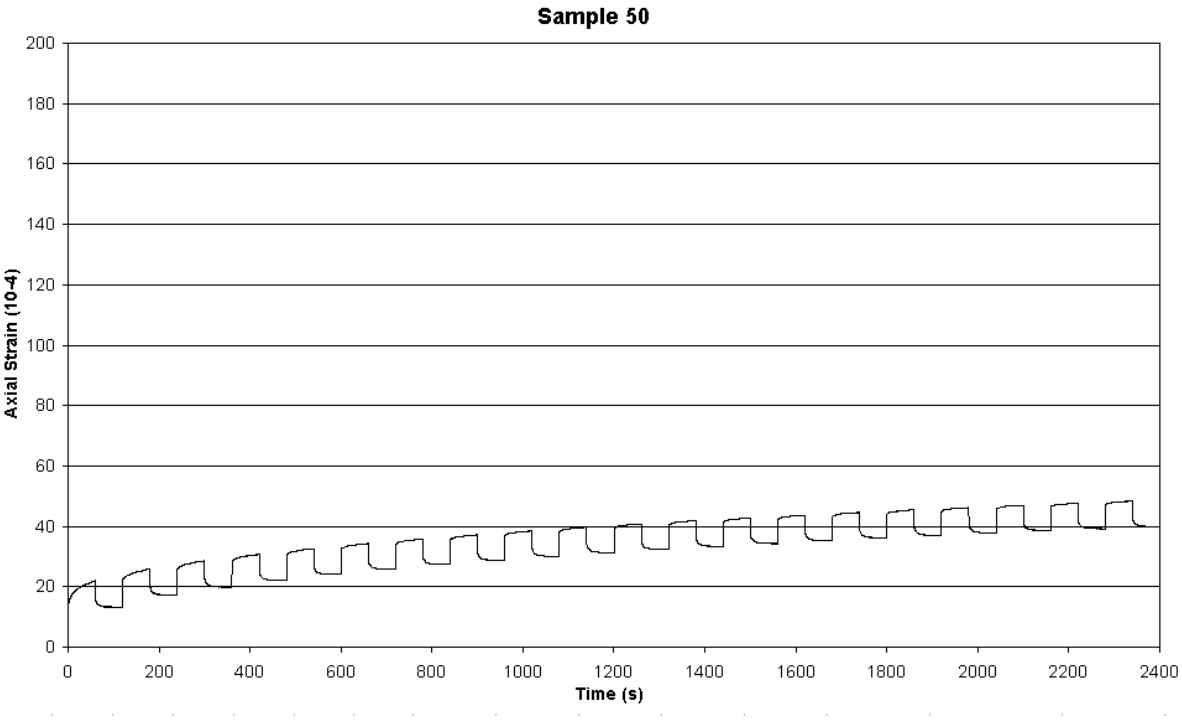

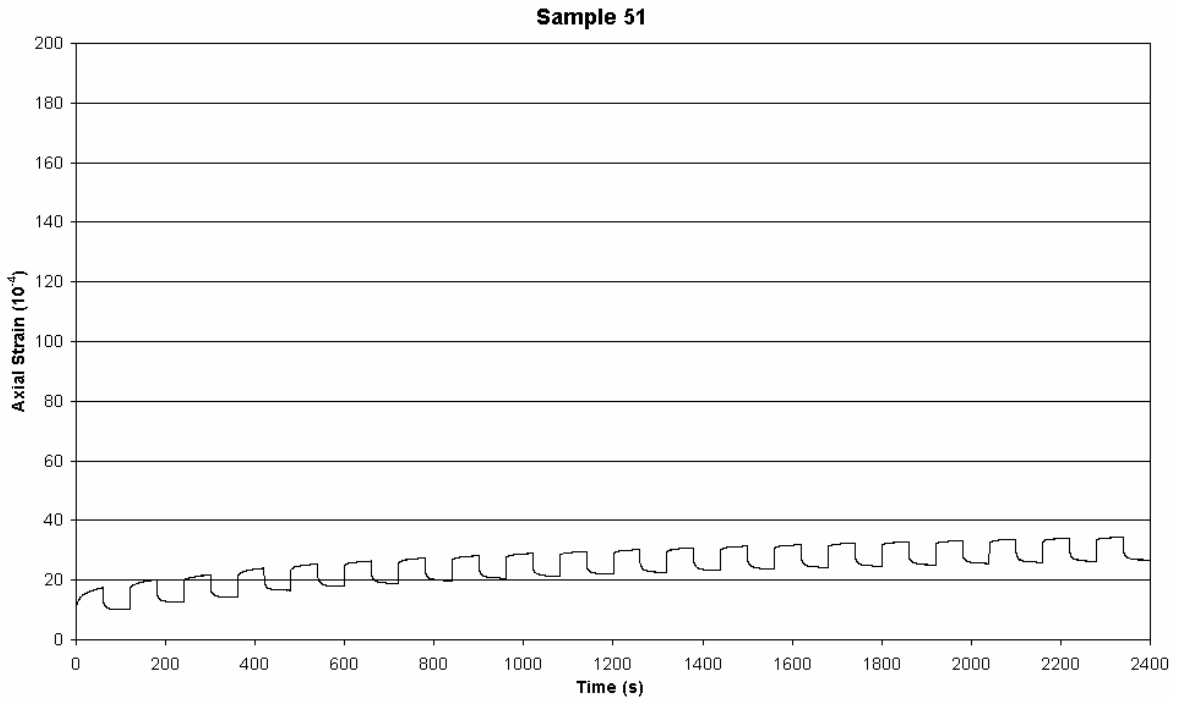
Sample 51
Axial Strain (10-4)
Time (s)
0
20
40
60
80
100
120
140
160
180
200
0
200
400
600
800
1000
1200
1400
1600
1800
2000
2200
2400

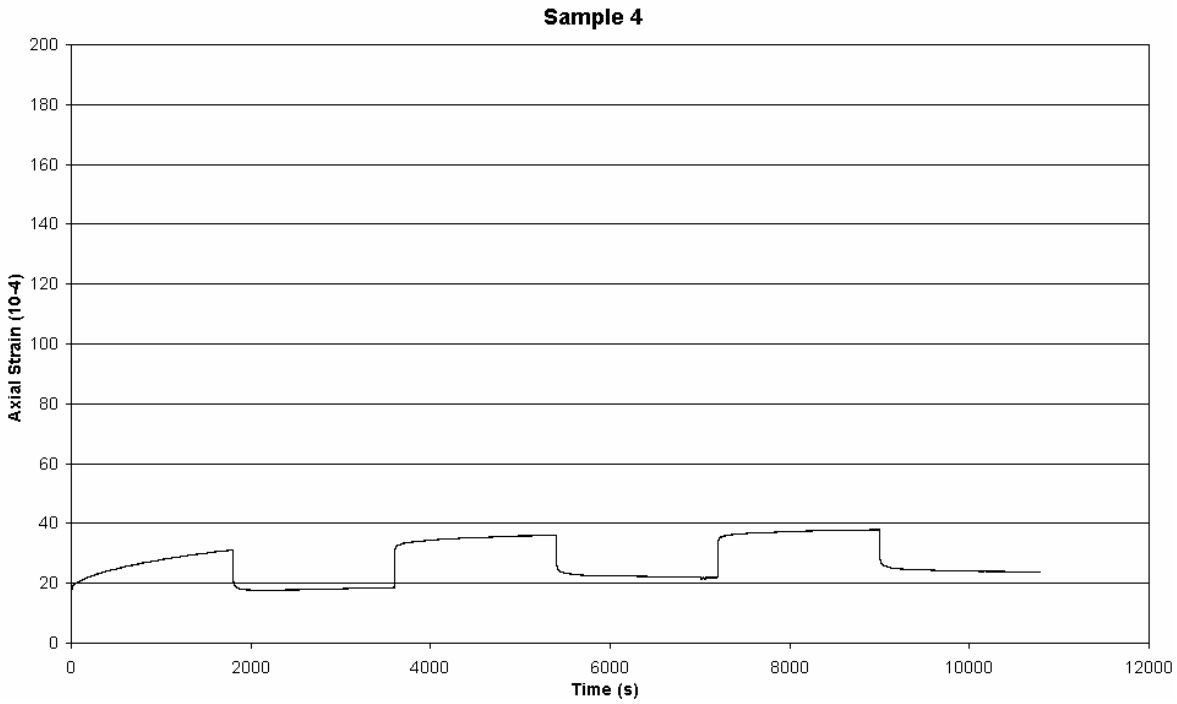
Sample 4
Axial Strain (10-4)
Time (s)
0
20
40
60
80
100
120
140
160
180
200
0
2000
4000
6000
8000
10000
12000

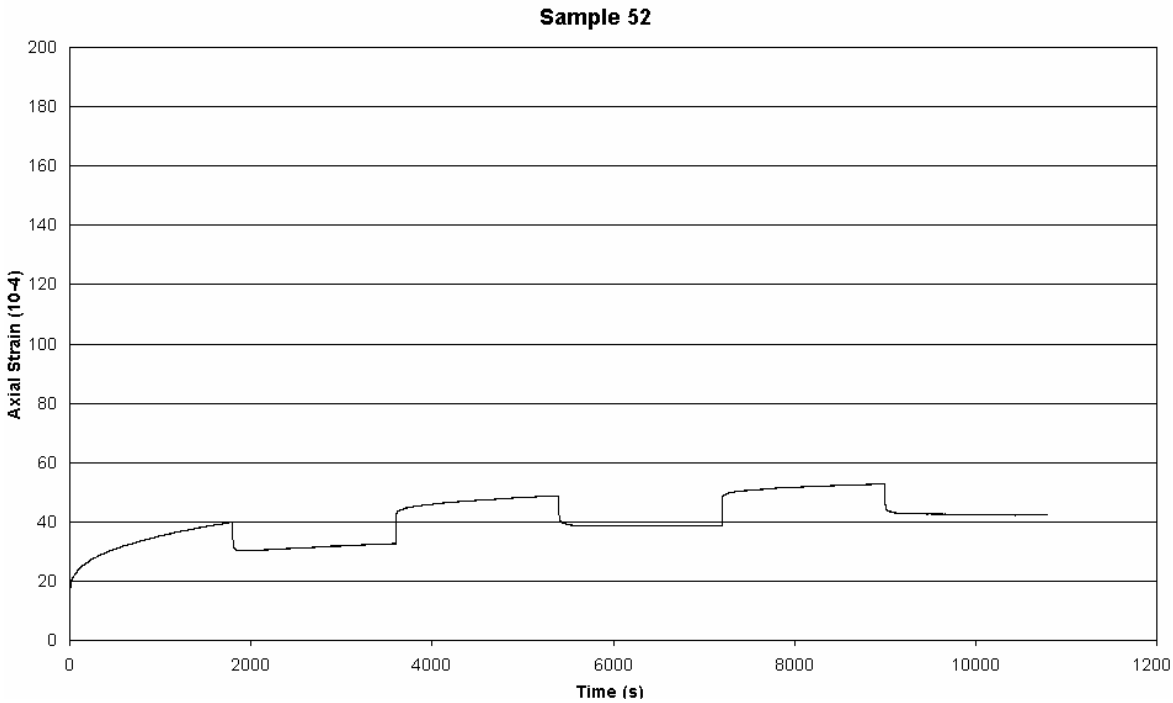

SP 19 D, 200 kPa

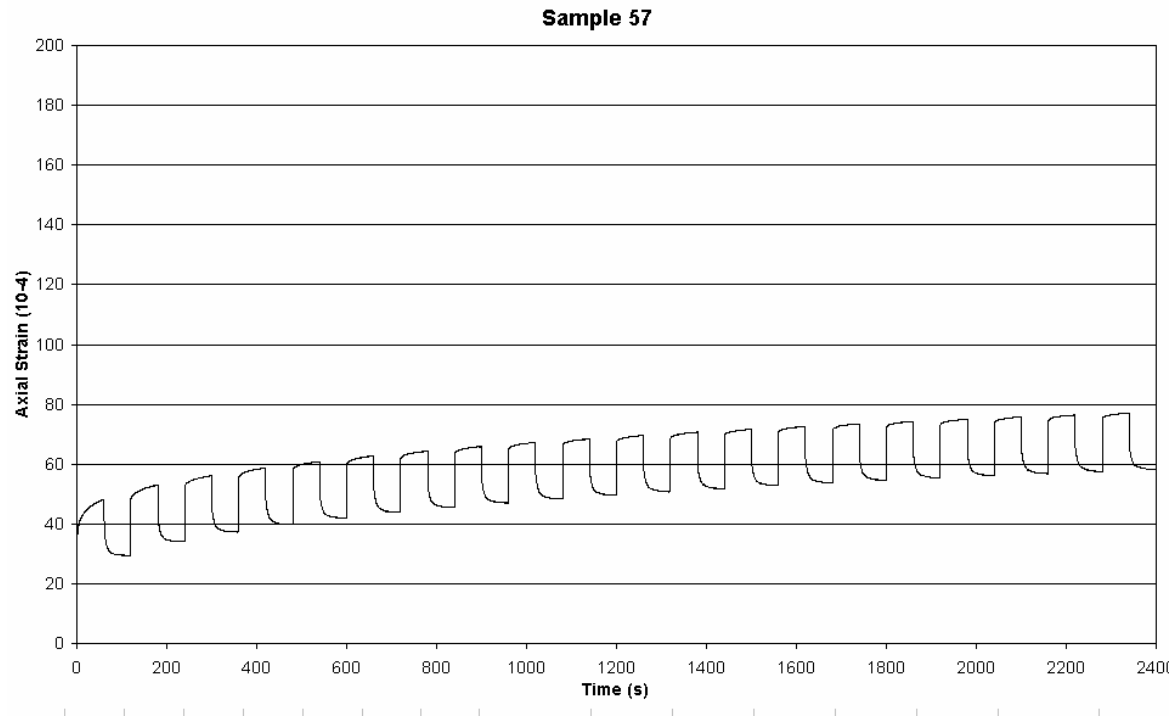

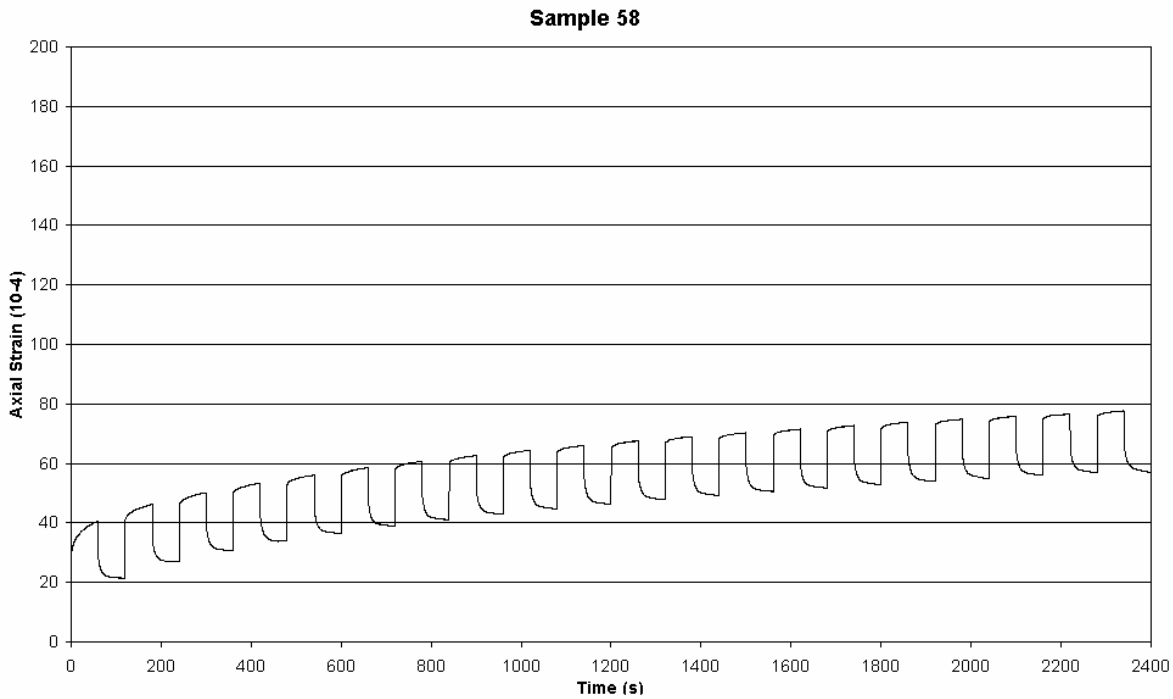
Sample 58
Axial Strain (10-4)
Time (s)
0
20
40
60
80
100
120
140
160
180
200
0
200
400
600
800
1000
1200
1400
1600
1800
2000
2200
2400

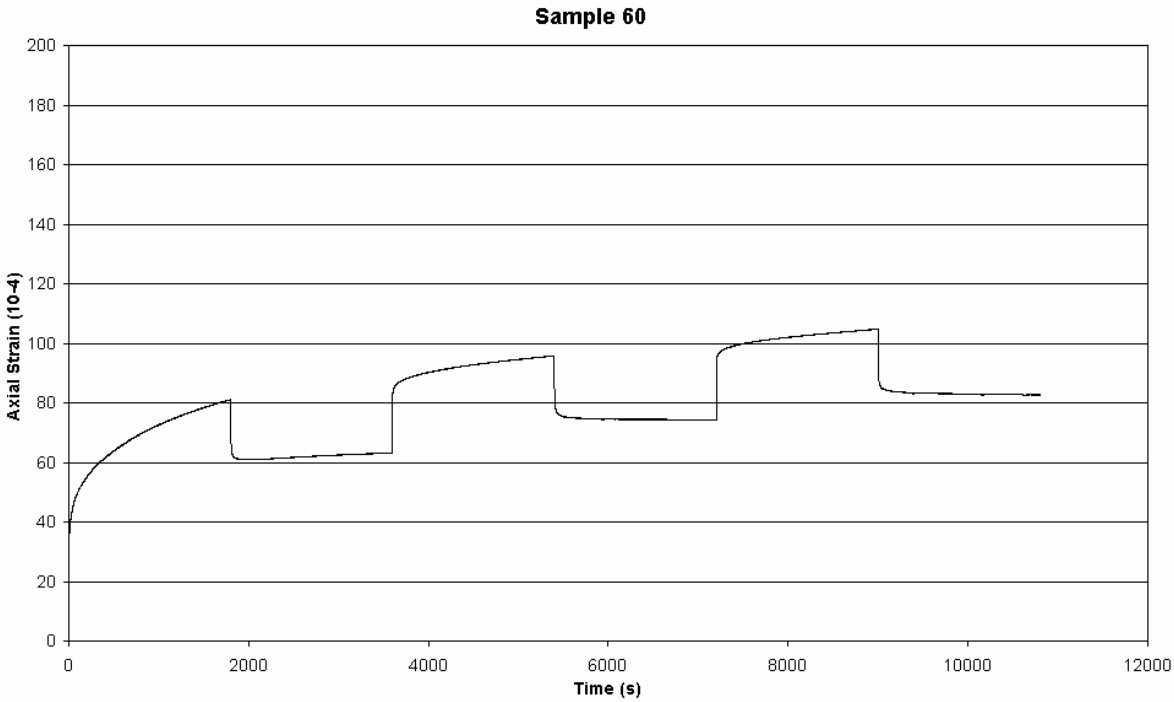
Sample 60
Axial Strain (10-4)
Time (s)
0
20
40
60
80
100
120
140
160
180
200
0
2000
4000
6000
8000
10000
12000

SP 19 E, 100 kPa

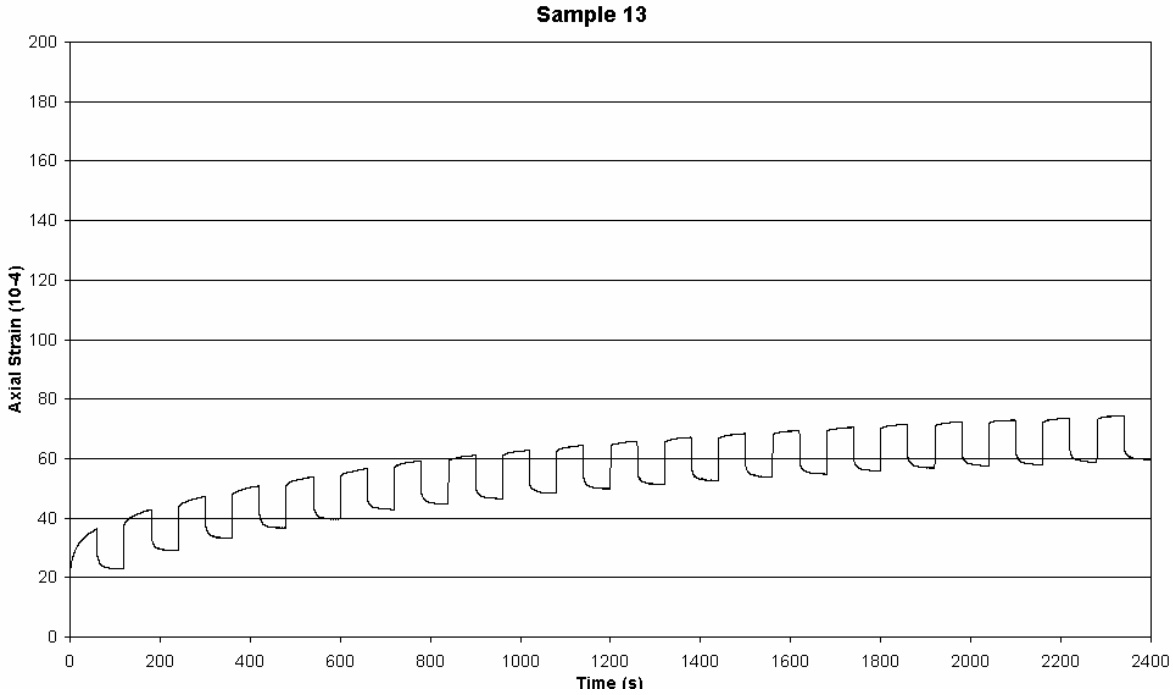

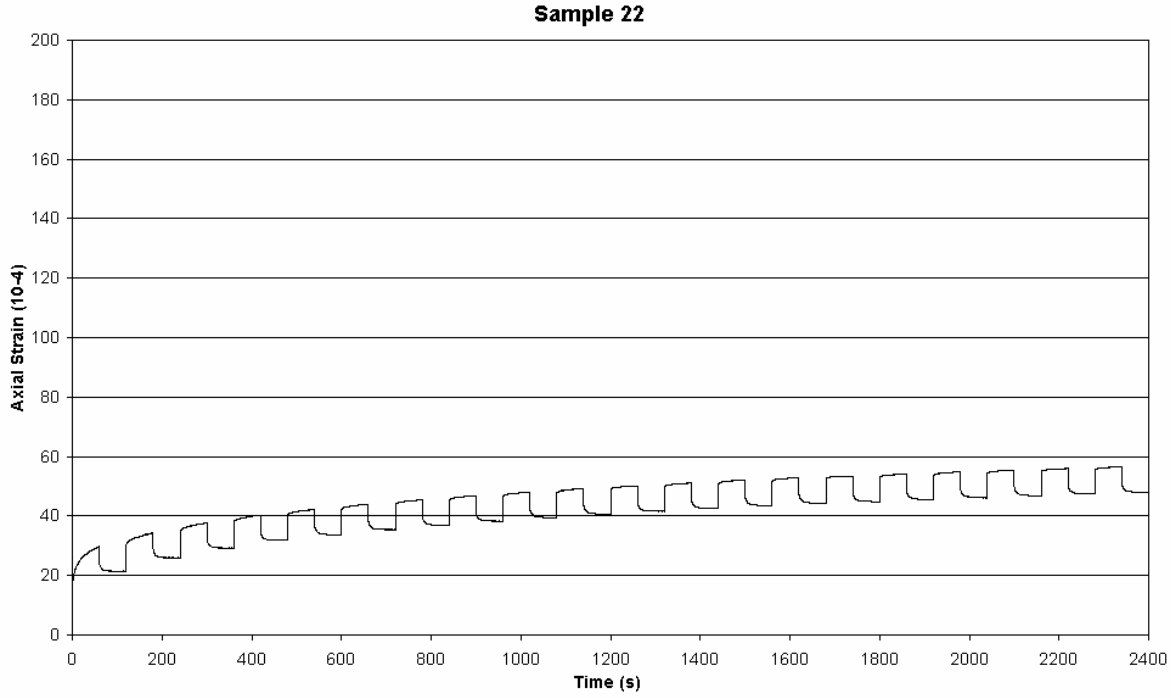

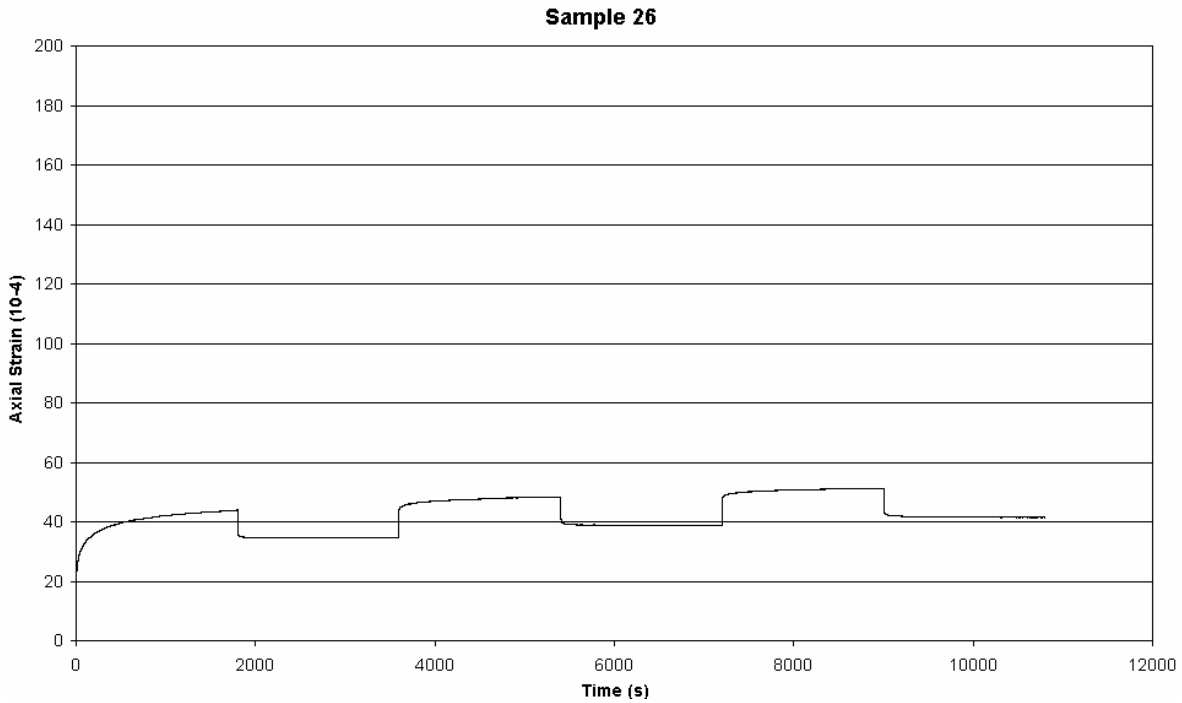

SP 19 E, 200 kPa

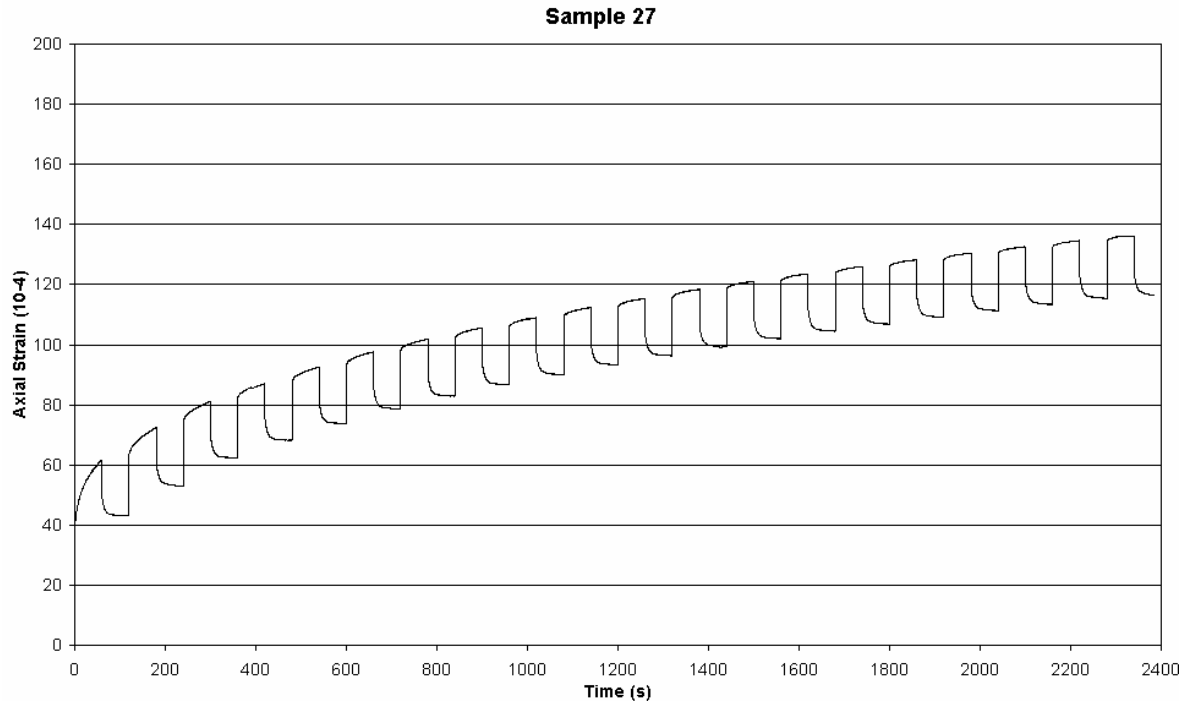

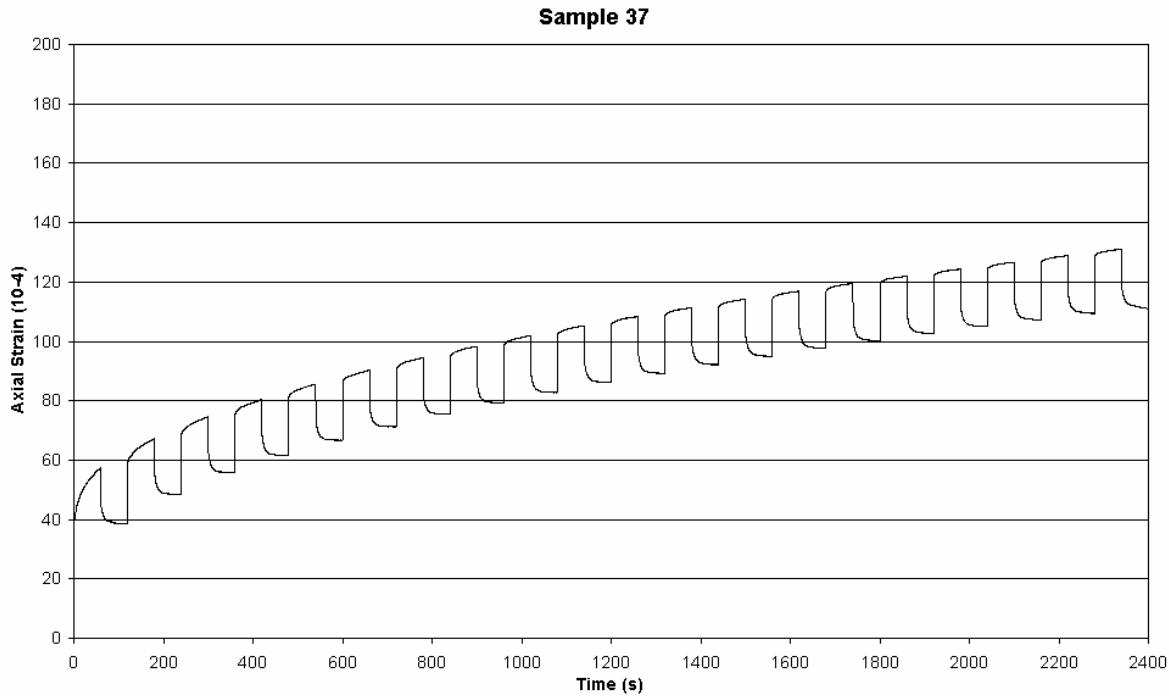
Sample 37
Axial Strain (10-4)
Time (s)
0
20
40
60
80
100
120
140
160
180
200
0
200
400
600
800
1000
1200
1400
1600
1800
2000
2200
2400

APPENDIX C

ABAQUS HWRT TEST MODELING PLOTS

HWRT Test Axisymmetric 2D Space Modeling Using Initial Parameters

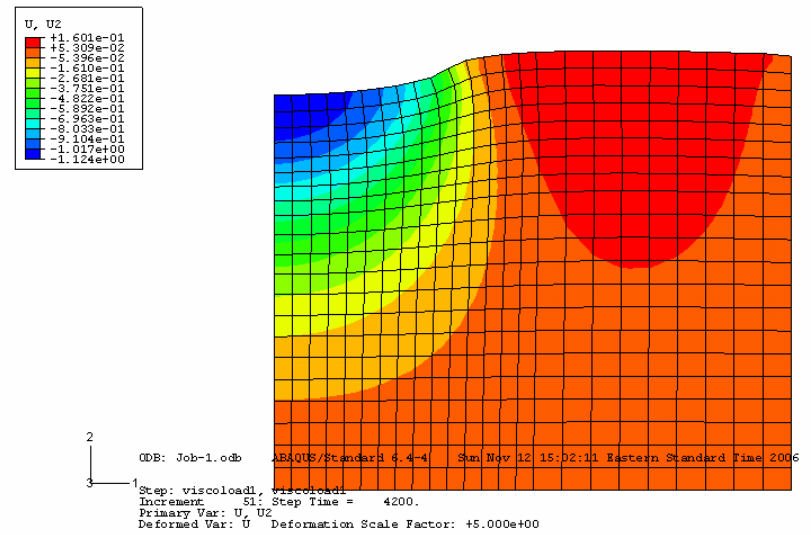

Figure C1 Deformed Shape of HL 3 Sample after 20,000 Passes Predicted in ABAQUS Axisymmetric 2D Space Simulation Using Calibrated Parameters.

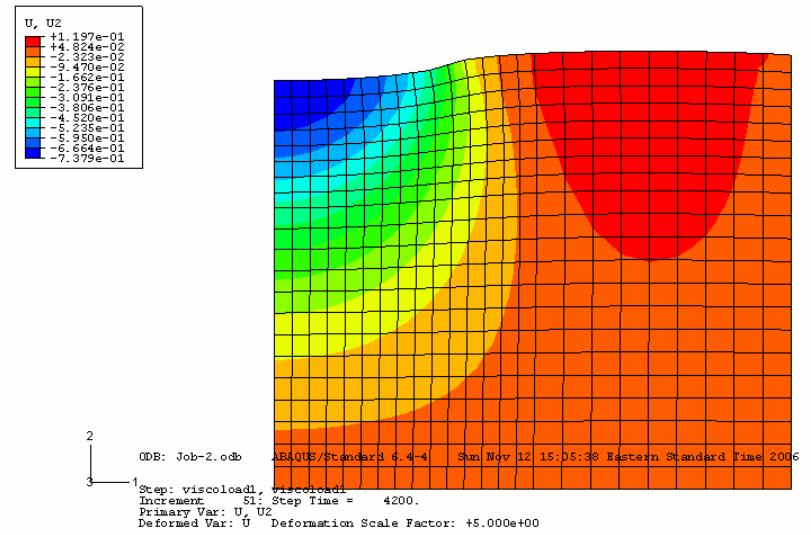

Figure C2 Deformed Shape of SMA L Sample after 20,000 Passes Predicted in ABAQUS Axisymmetric 2D Space Simulation Using Calibrated Parameters.

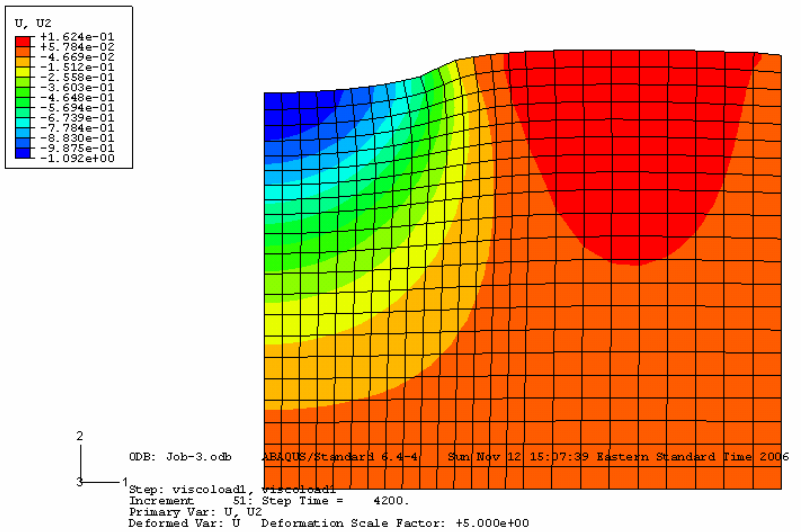

Figure C3 Deformed Shape of SMA G Sample after 20,000 Passes Predicted in ABAQUS Axisymmetric 2D Space Simulation Using Calibrated Parameters.

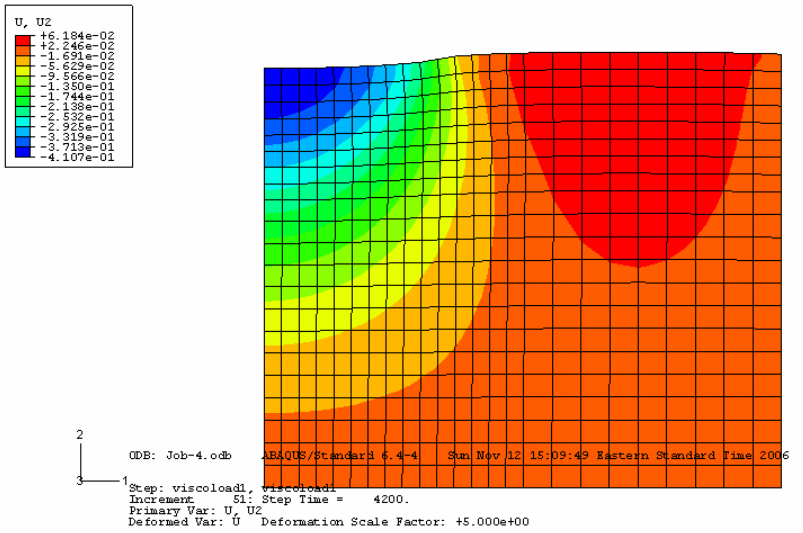

Figure C4 Deformed Shape of SP 19 D Sample after 20,000 Passes Predicted in ABAQUS Axisymmetric 2D Space Simulation Using Calibrated Parameters.

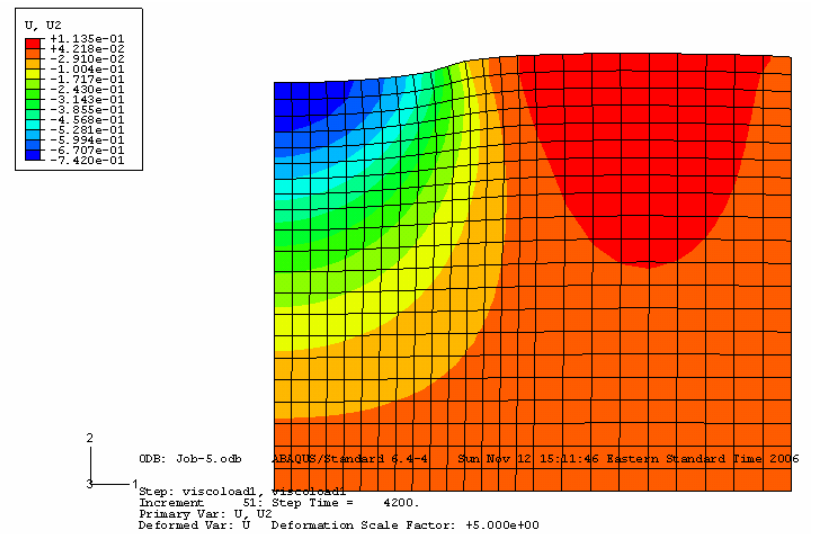

Figure C5 Deformed Shape of SP 19 E Sample after 20,000 Passes Predicted in ABAQUS Axisymmetric 2D Space Simulation Using Calibrated Parameters.

HWRT Test 3D Slice Modeling Using Initial Parameters

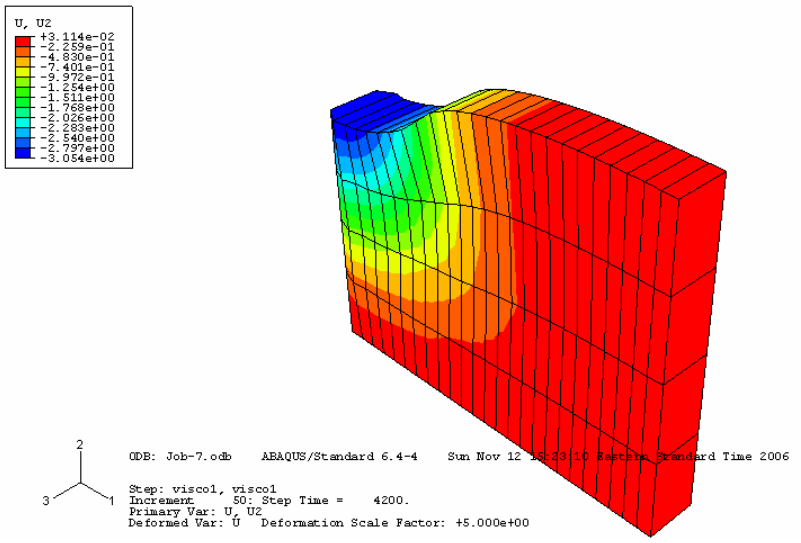

Figure C6 Deformed Shape of HL 3 Sample after 20,000 Passes Predicted in ABAQUS 3D Simulation Using Calibrated Parameters.

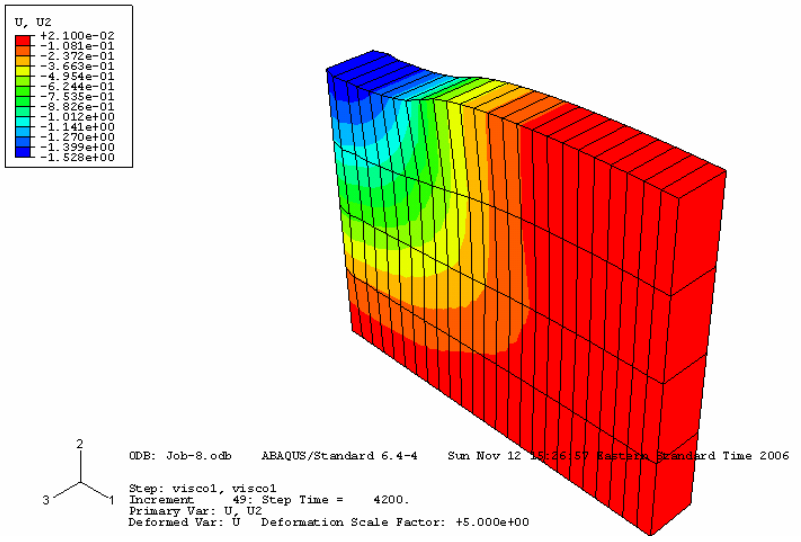

Figure C7 Deformed Shape of SMA L Sample after 20,000 Passes Predicted in ABAQUS 3D Simulation Using Calibrated Parameters.

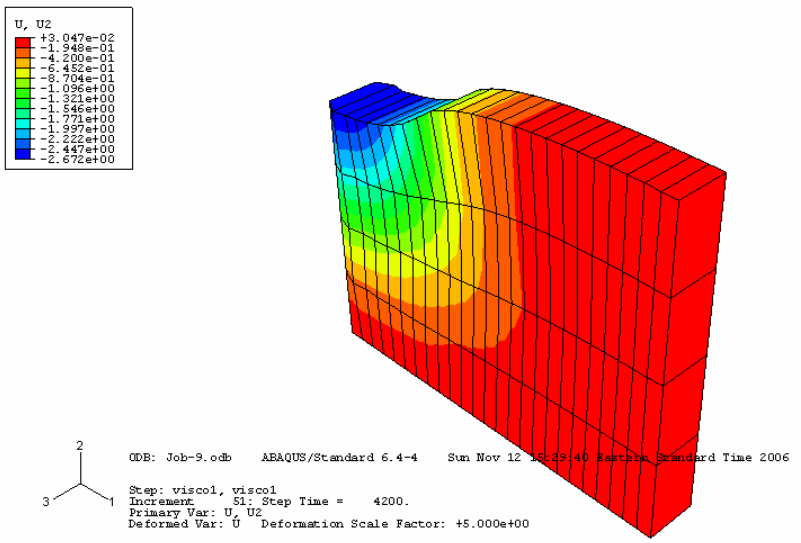

Figure C8 Deformed Shape of SMA G Sample after 20,000 Passes Predicted in ABAQUS 3D Simulation Using Calibrated Parameters.

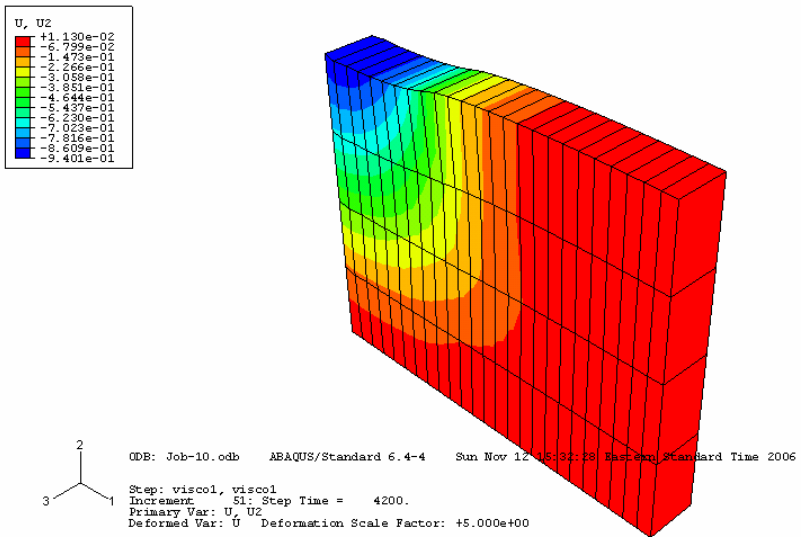

Figure C9 Deformed Shape of SP 19 D Sample after 20,000 Passes Predicted in ABAQUS 3D Simulation Using Calibrated Parameters.

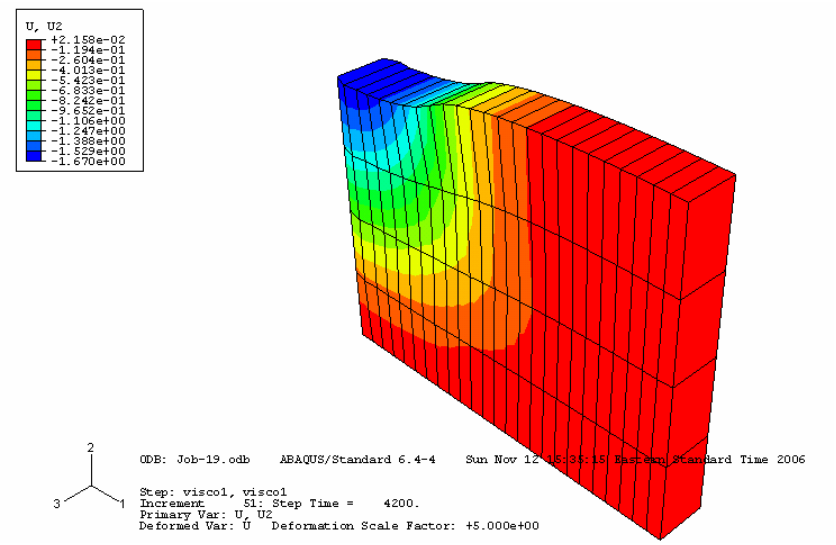

Figure C10 Deformed Shape of SP 19 E Sample after 20,000 Passes Predicted in ABAQUS 3D Simulation Using Calibrated Parameters.

HWRT Test 2D Plane Strain Modeling Using Initial Parameters

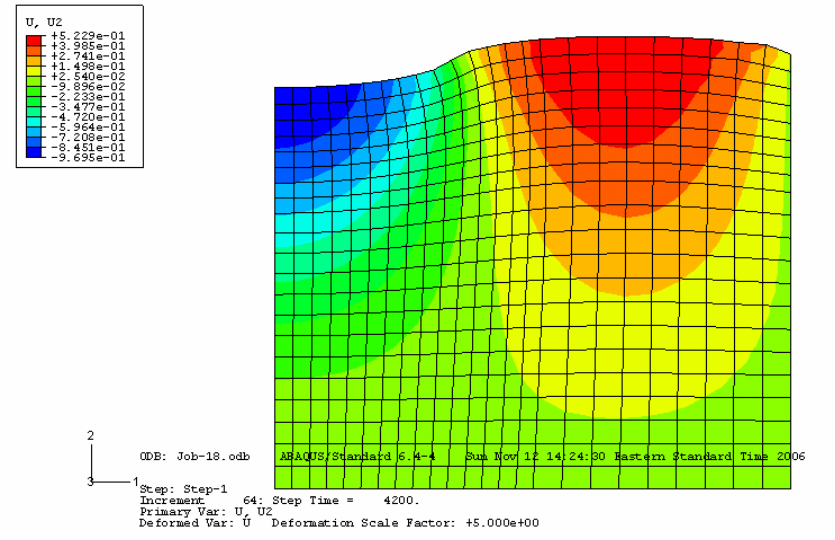

Figure C11 Deformed Shape of HL 3 Sample after 20,000 Passes Predicted in ABAQUS Simulation Using Calibrated Parameters.

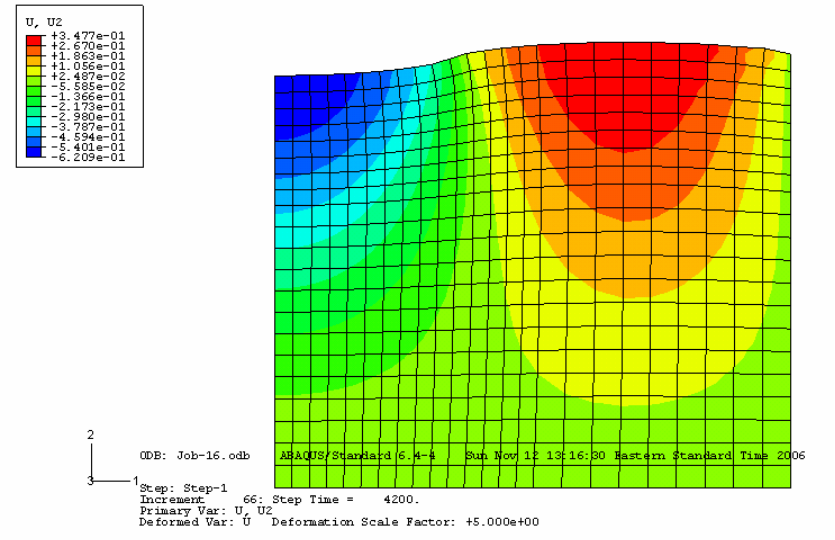

Figure C12 Deformed Shape of SMA L Sample after 20,000 Passes Predicted in ABAQUS Simulation Using Calibrated Parameters.

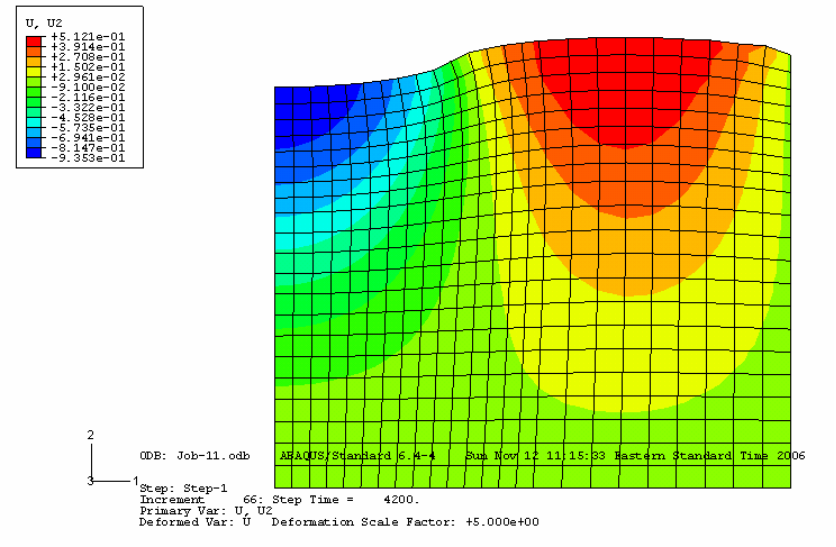

Figure C13 Deformed Shape of SMA G Sample after 20,000 Passes Predicted in ABAQUS Simulation Using Calibrated Parameters.

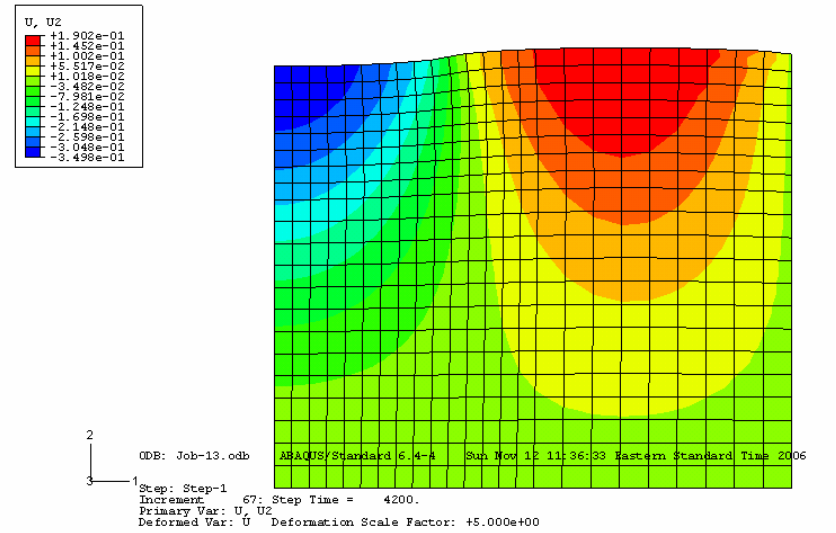

Figure C14 Deformed Shape of SP 19 D Sample after 20,000 Passes Predicted in ABAQUS Simulation Using Calibrated Parameters.

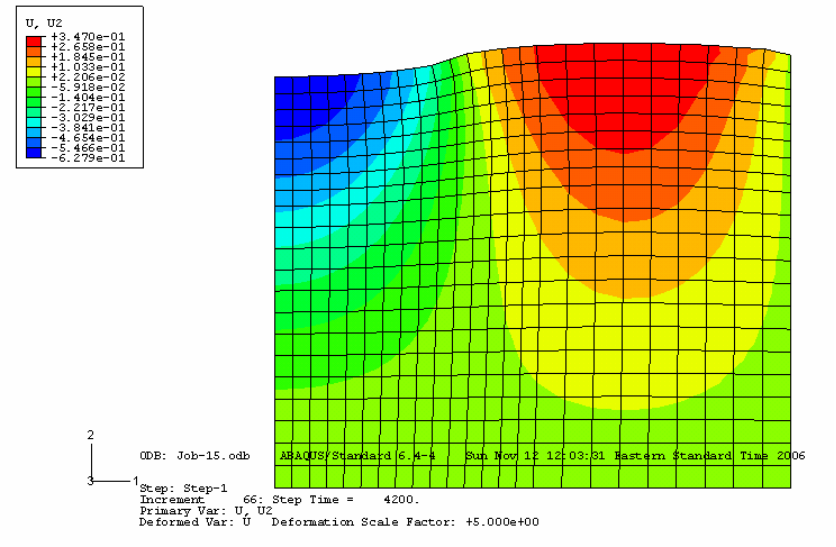

Figure C15 Deformed Shape of SP 19 E Sample after 20,000 Passes Predicted in ABAQUS Simulation Using Calibrated Parameters.

APPENDIX D

ABAQUS PAVEMENT IN-SITU PERFOROMANCE MODELING PLOTS

HL 3 Mix

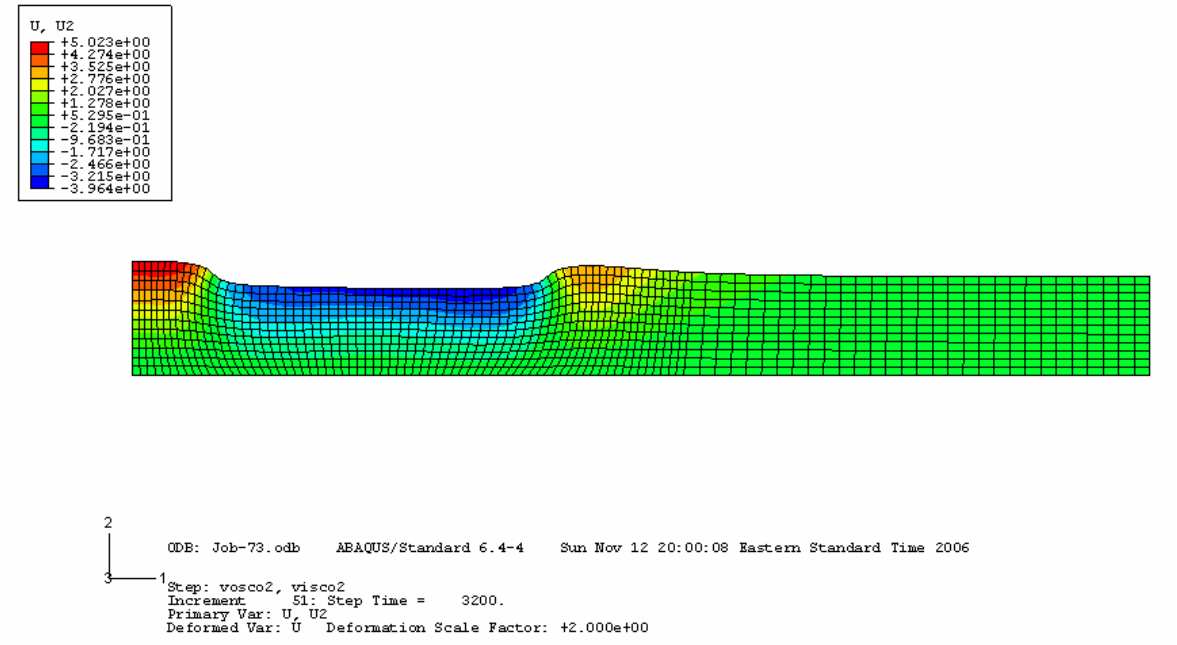

Figure D1 Predicted Deformed Shape of Pavement with HL 3 Mix after 4 million ESAL's.

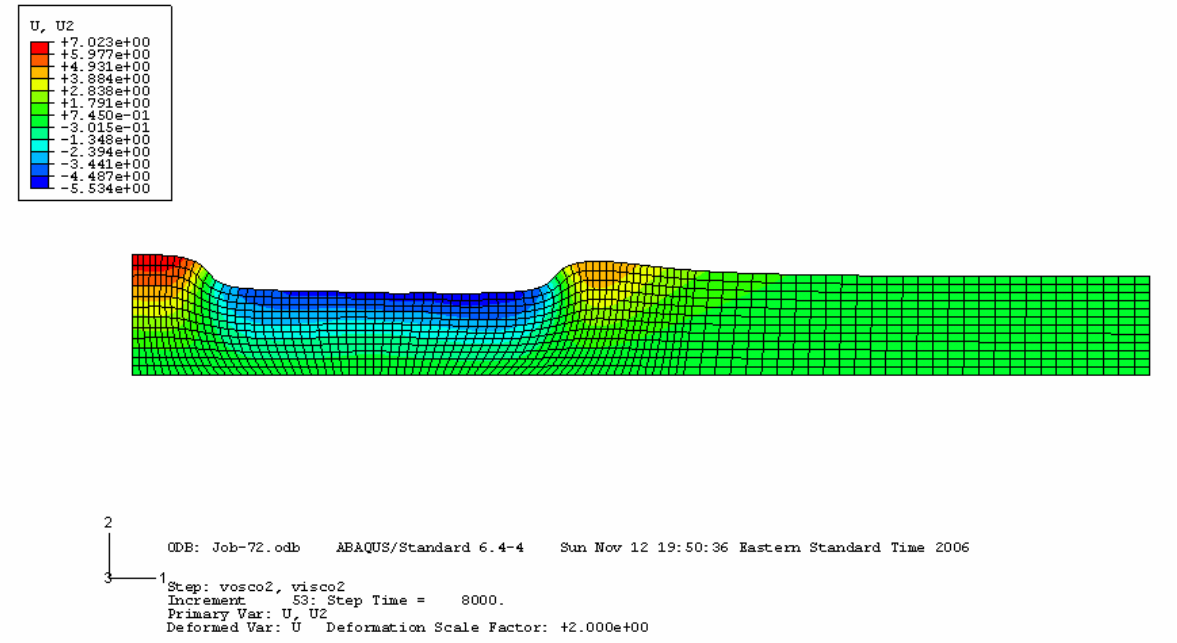

Figure D2 Predicted Deformed Shape of Pavement with HL 3 Mix after 10 million ESAL's.

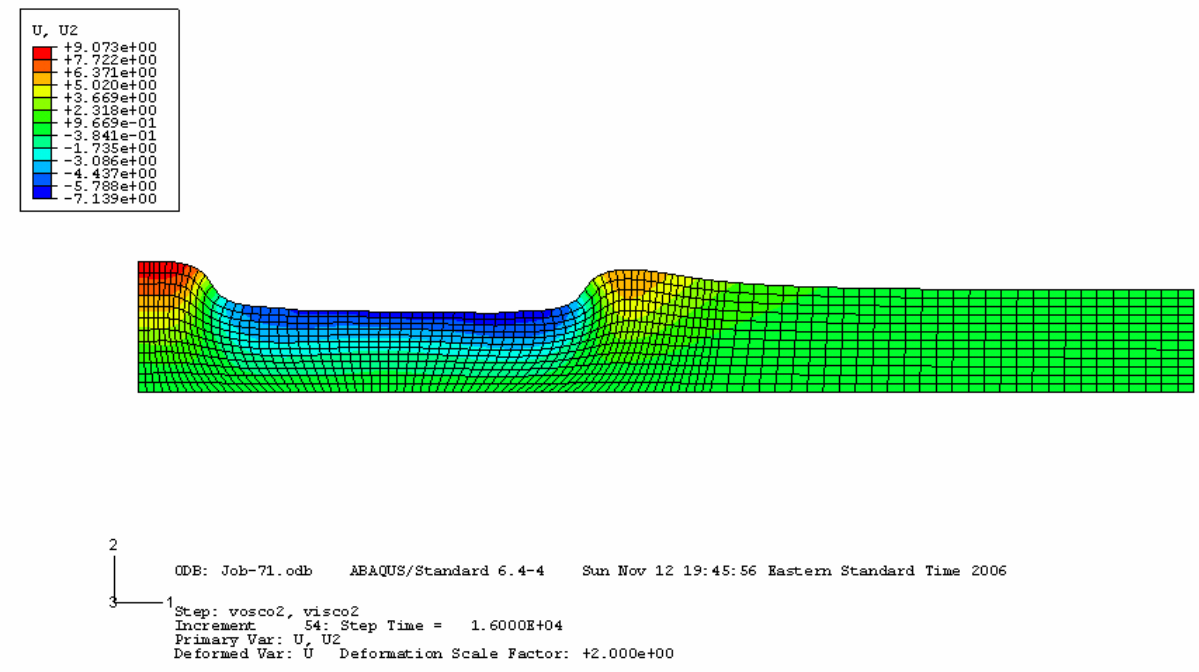

Figure D3 Predicted Deformed Shape of Pavement with HL 3 Mix after 20 million ESAL's.

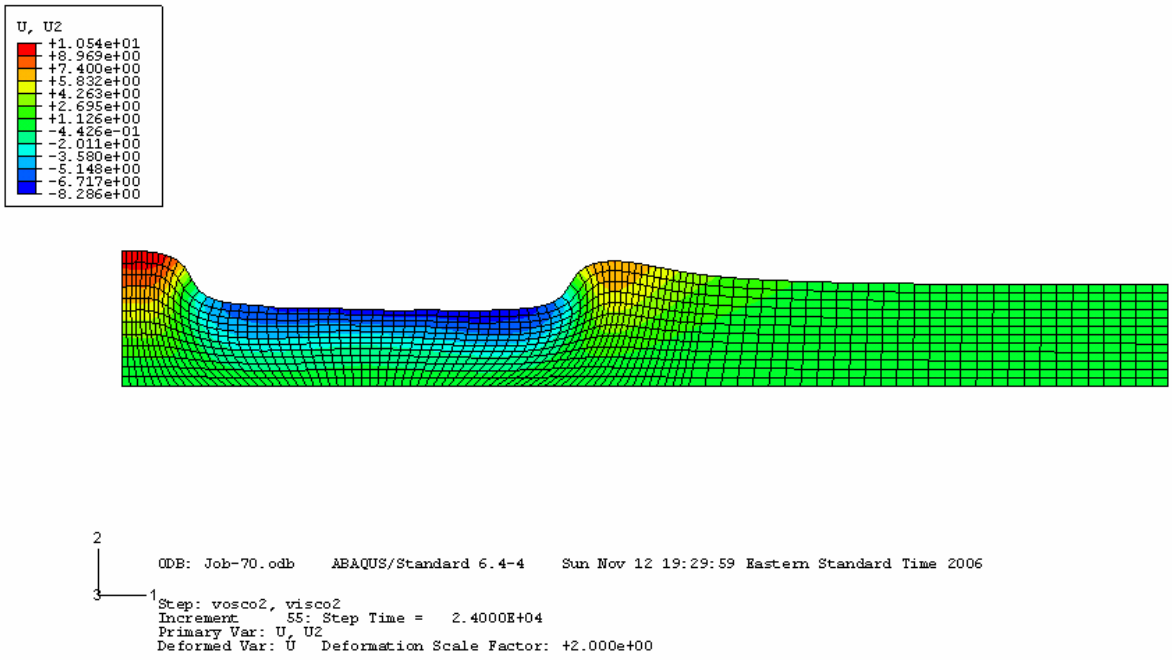

Figure D4 Predicted Deformed Shape of Pavement with HL 3 Mix after 30 million ESAL's.

SMA L Mix

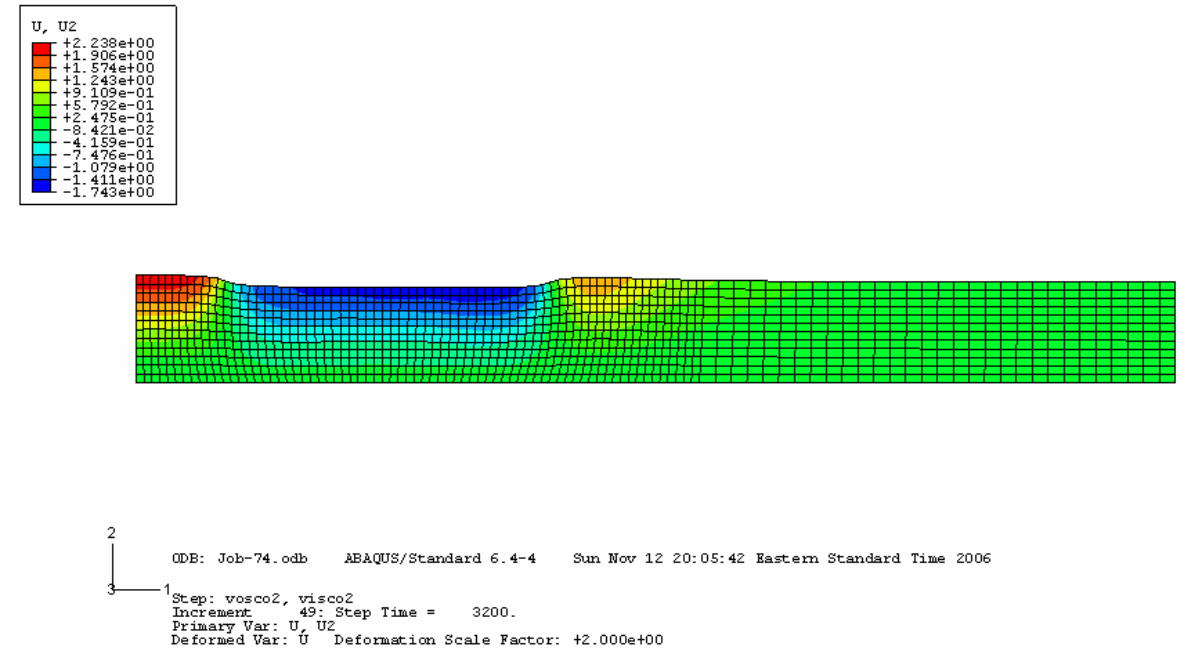

Figure D5 Predicted Deformed Shape of Pavement with SMA L Mix after 4 million ESAL's.

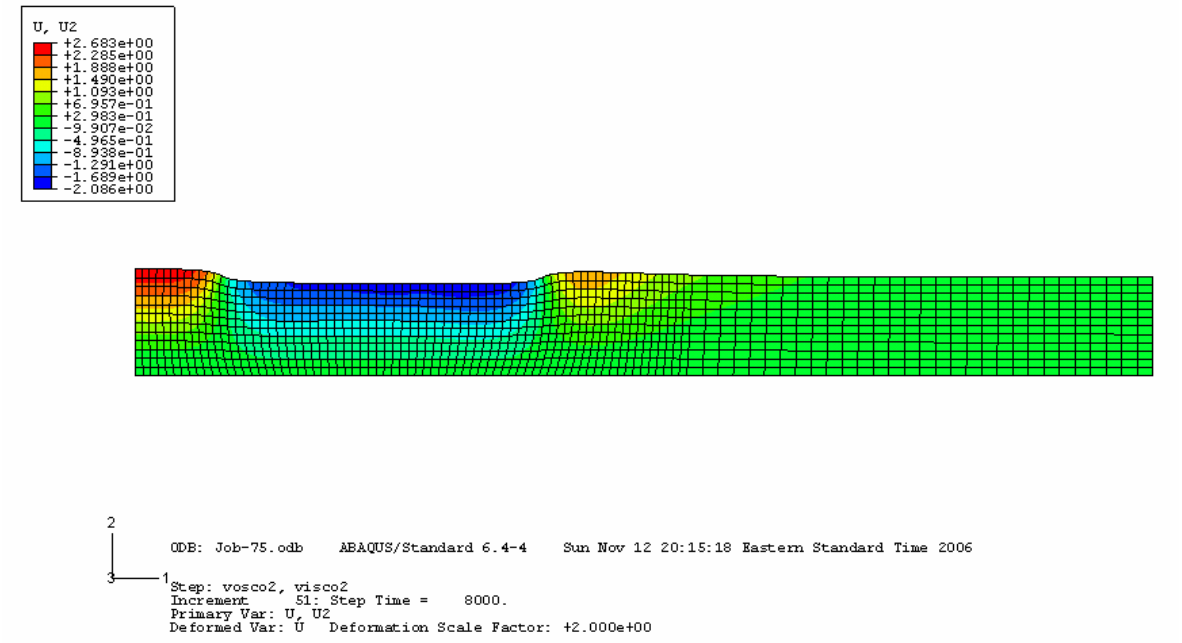

Figure D6 Predicted Deformed Shape of Pavement with SMA L Mix after 10 million ESAL's.

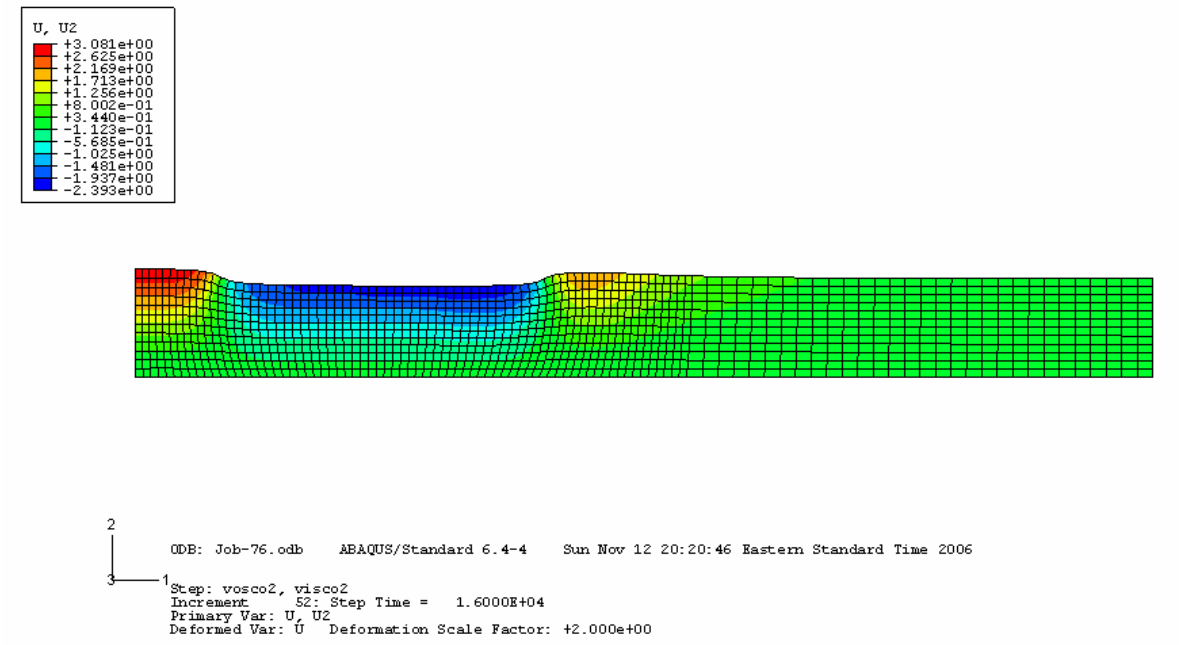

Figure D7 Predicted Deformed Shape of Pavement with SMA L Mix after 20 million ESAL's.

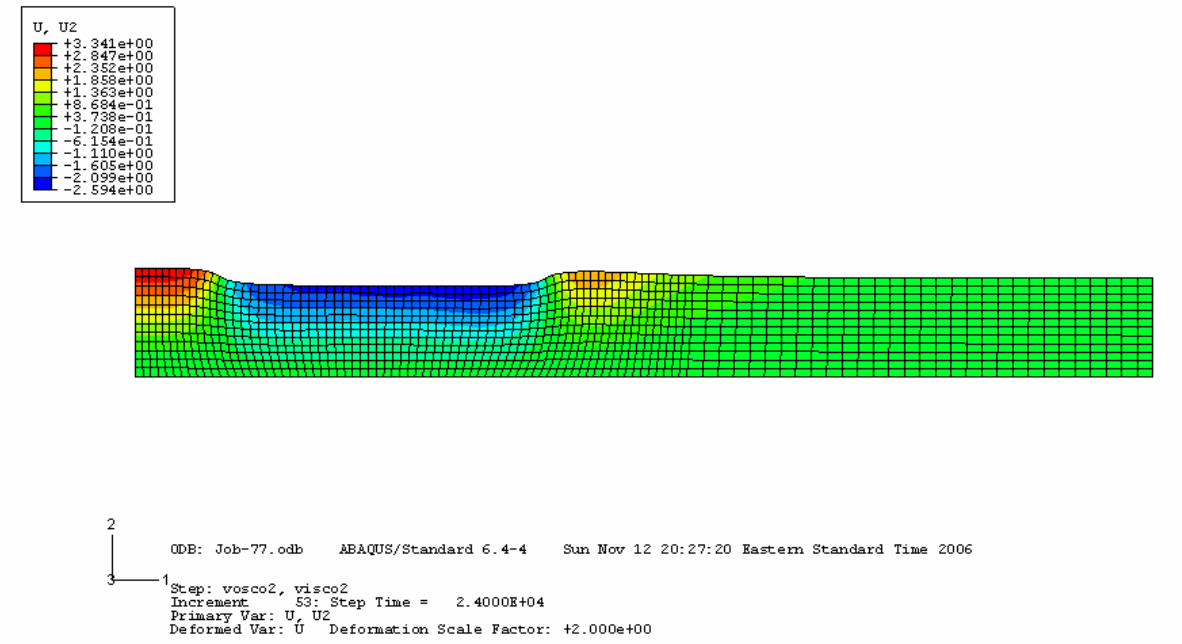

Figure D8 Predicted Deformed Shape of Pavement with SMA L Mix after 30 million ESAL's.

SMA G Mix

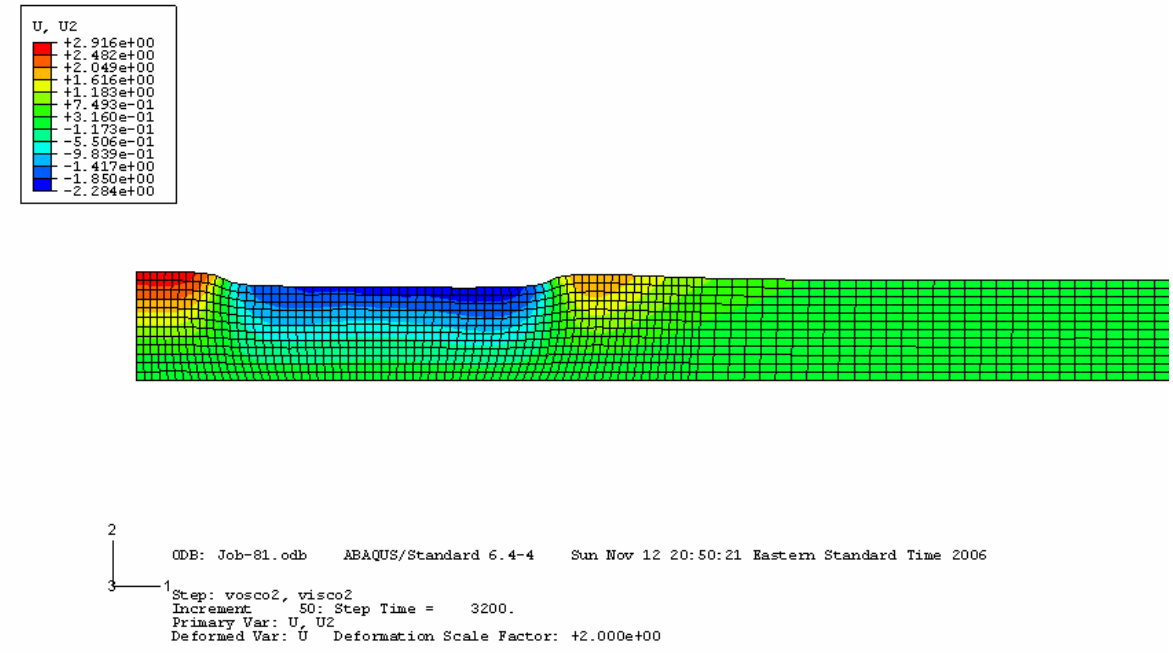

Figure D9 Predicted Deformed Shape of Pavement with SMA G Mix after 4 million ESAL's.

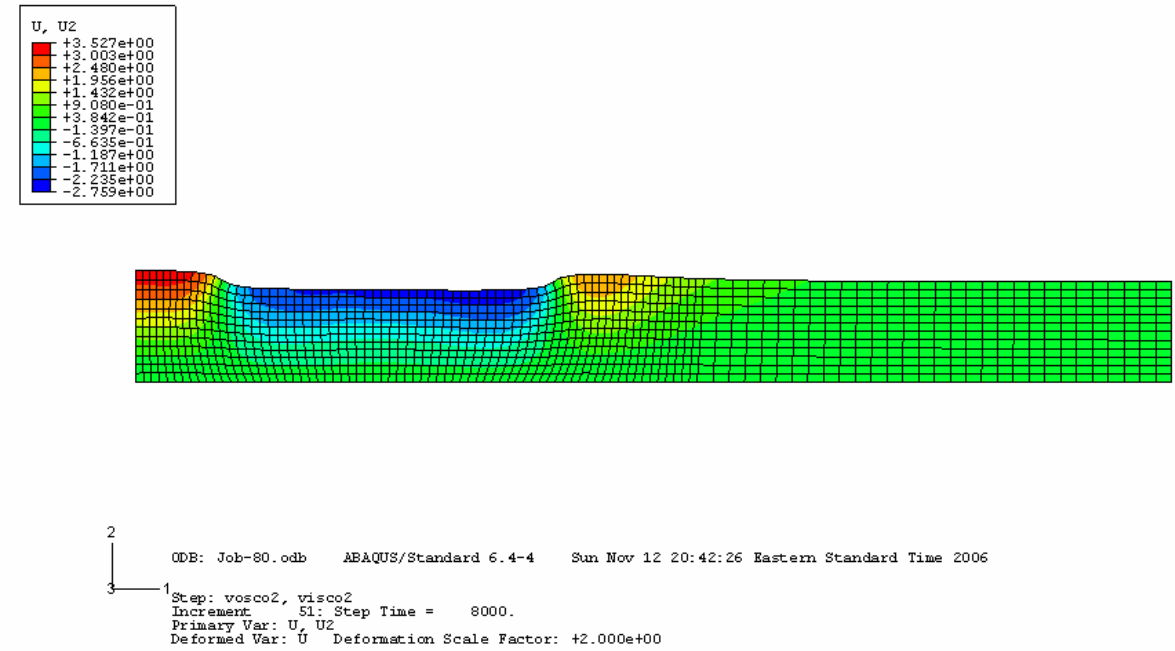

Figure D10 Predicted Deformed Shape of Pavement with SMA G Mix after 10 million ESAL's.

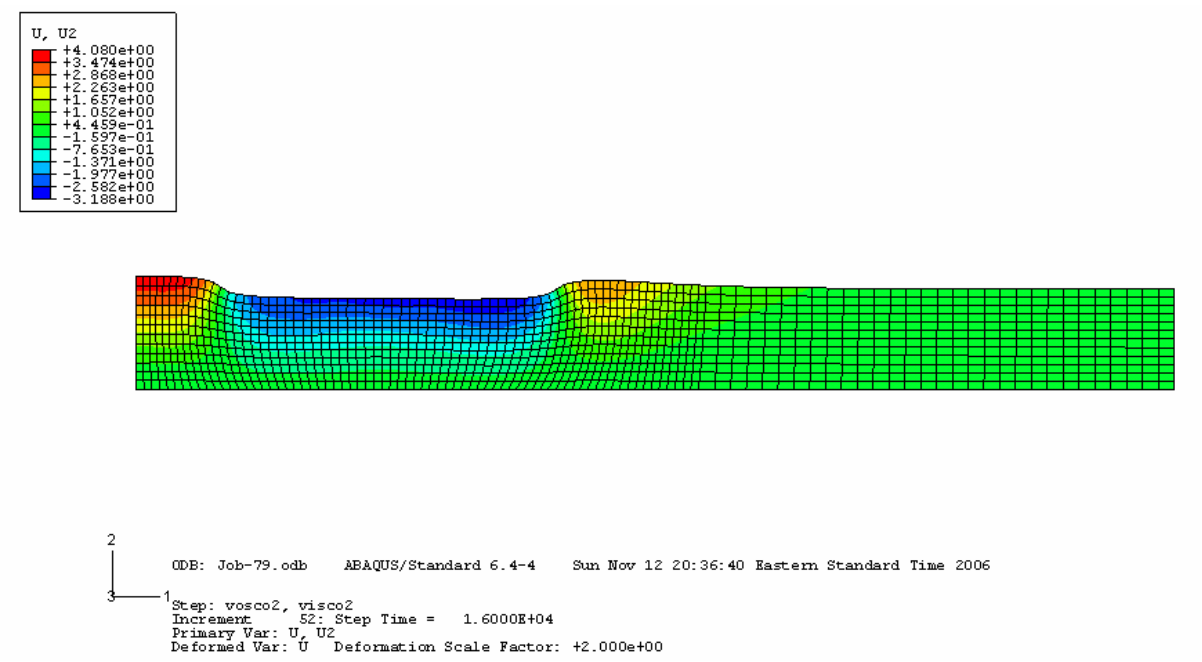

Figure B11 Predicted Deformed Shape of Pavement with SMA G Mix after 20 million ESAL's.

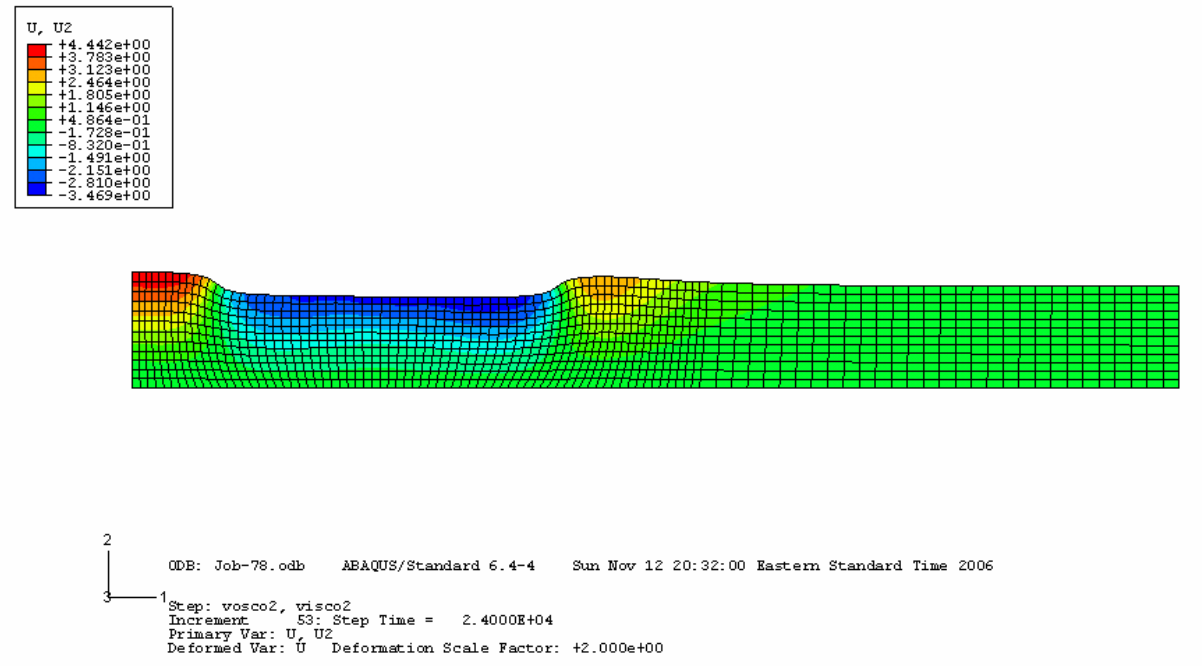

Figure B12 Predicted Deformed Shape of Pavement with SMA G Mix after 30 million ESAL's.

SP 19 D Mix

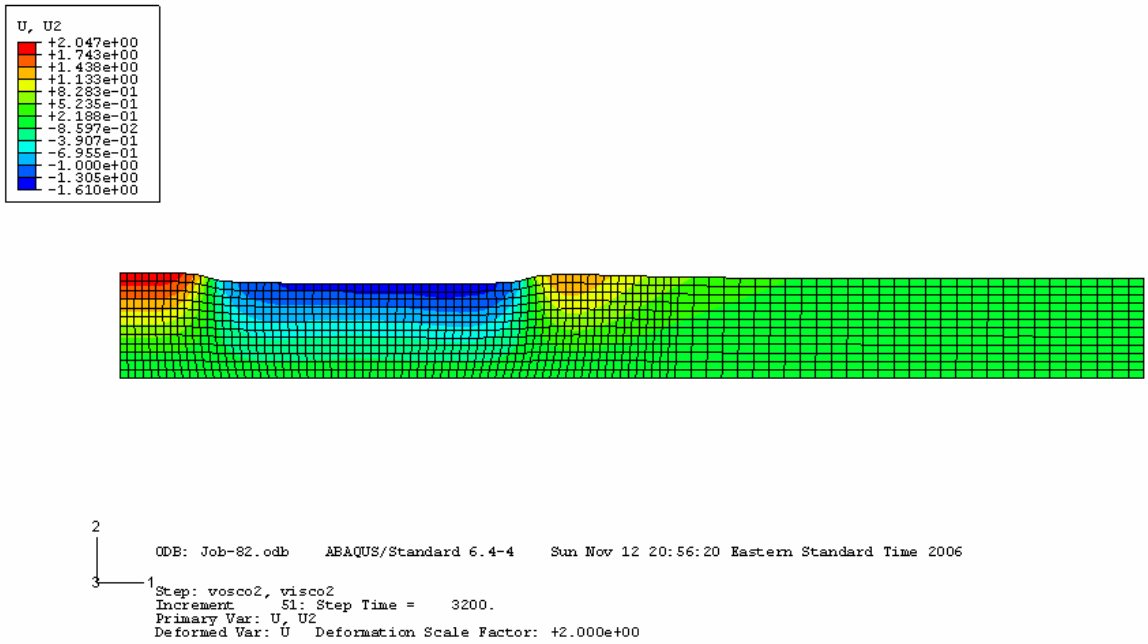

Figure D13 Predicted Deformed Shape of Pavement with SP 19 D Mix after 4 million ESAL's.

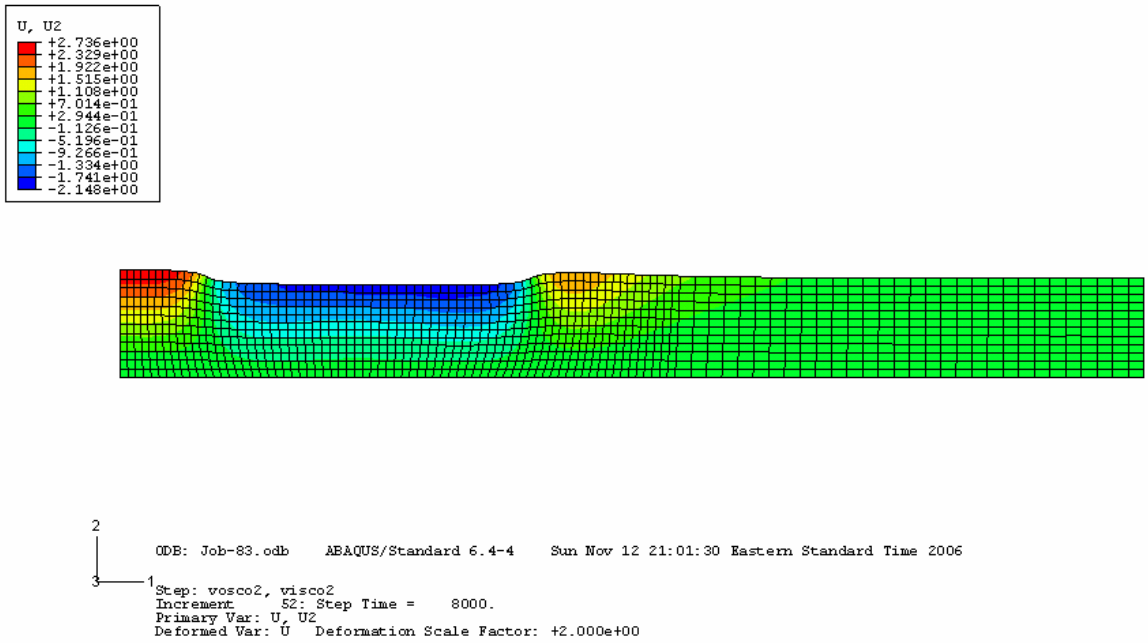

Figure D14 Predicted Deformed Shape of Pavement with SP 19 D Mix after 10 million ESAL's.

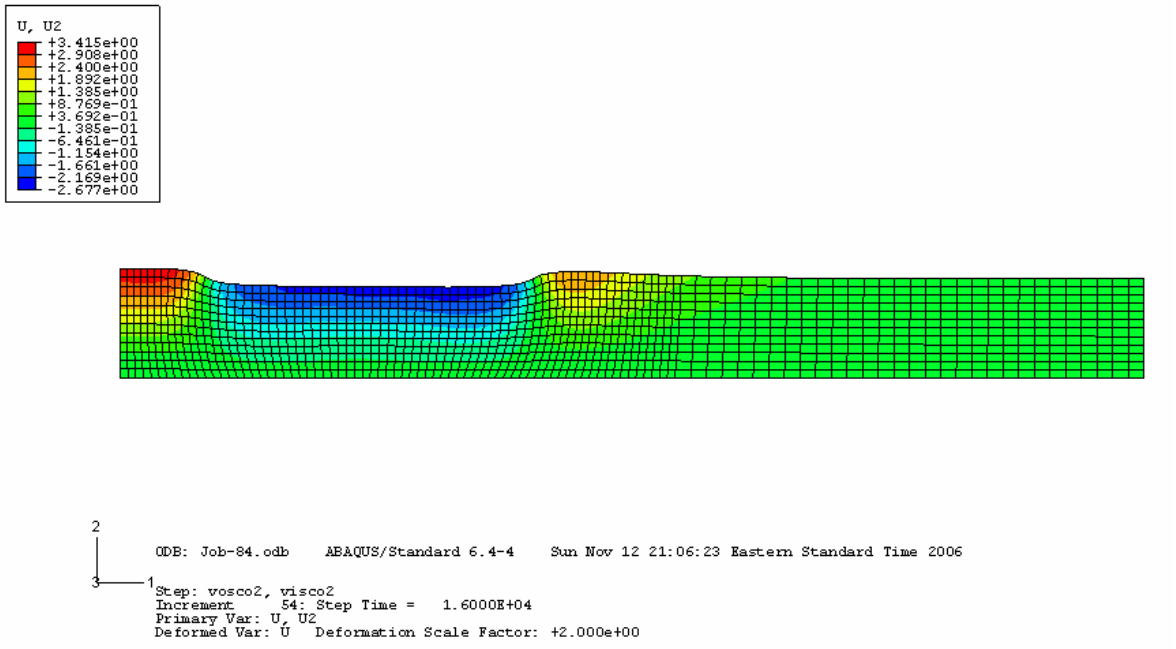

Figure D15 Predicted Deformed Shape of Pavement with SP 19 D Mix after 20 million ESAL's.

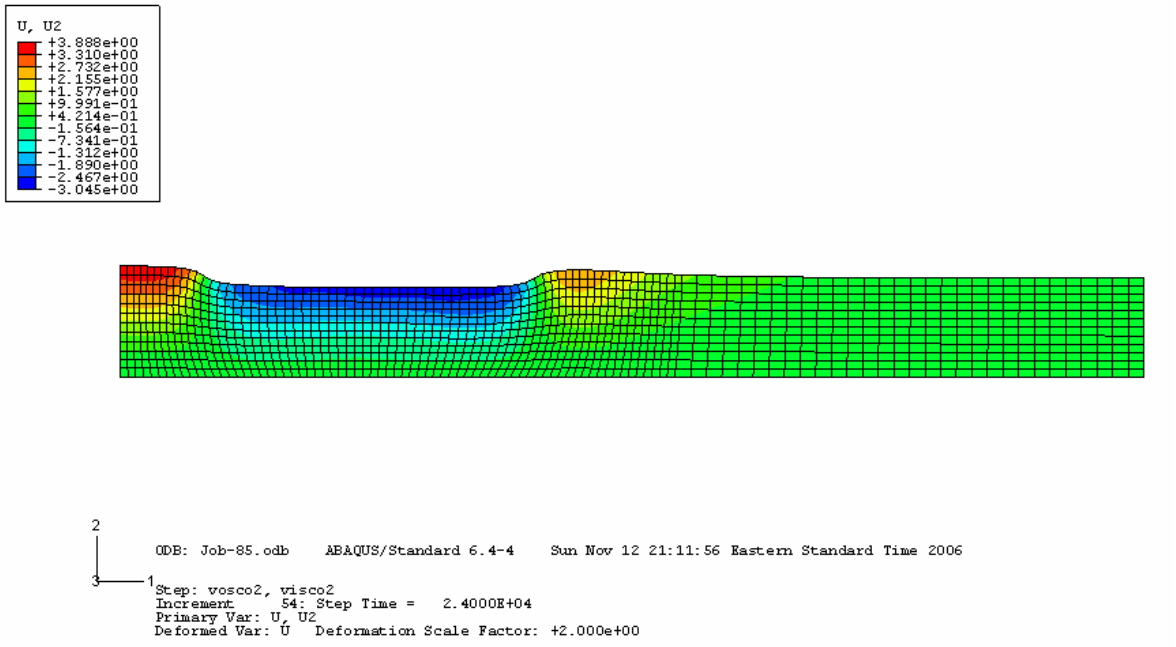

Figure D16 Predicted Deformed Shape of Pavement with SP 19 D Mix after 30 million ESAL's.

SP 19 E Mix

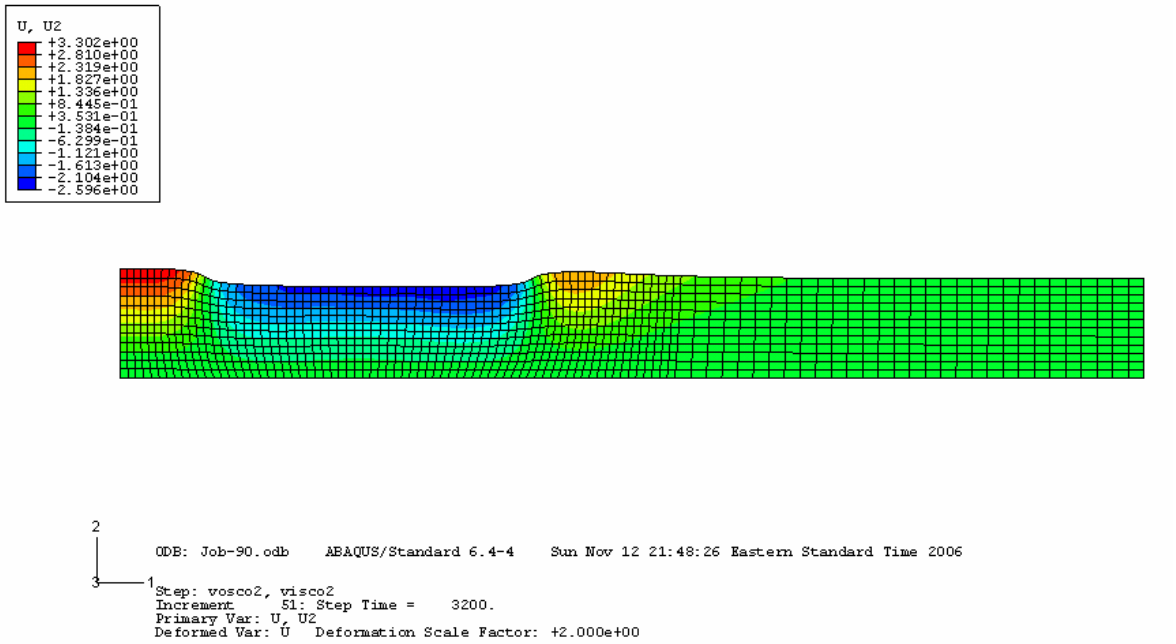

Figure D17 Predicted Deformed Shape of Pavement with SP 19 E Mix after 4 million ESAL's.

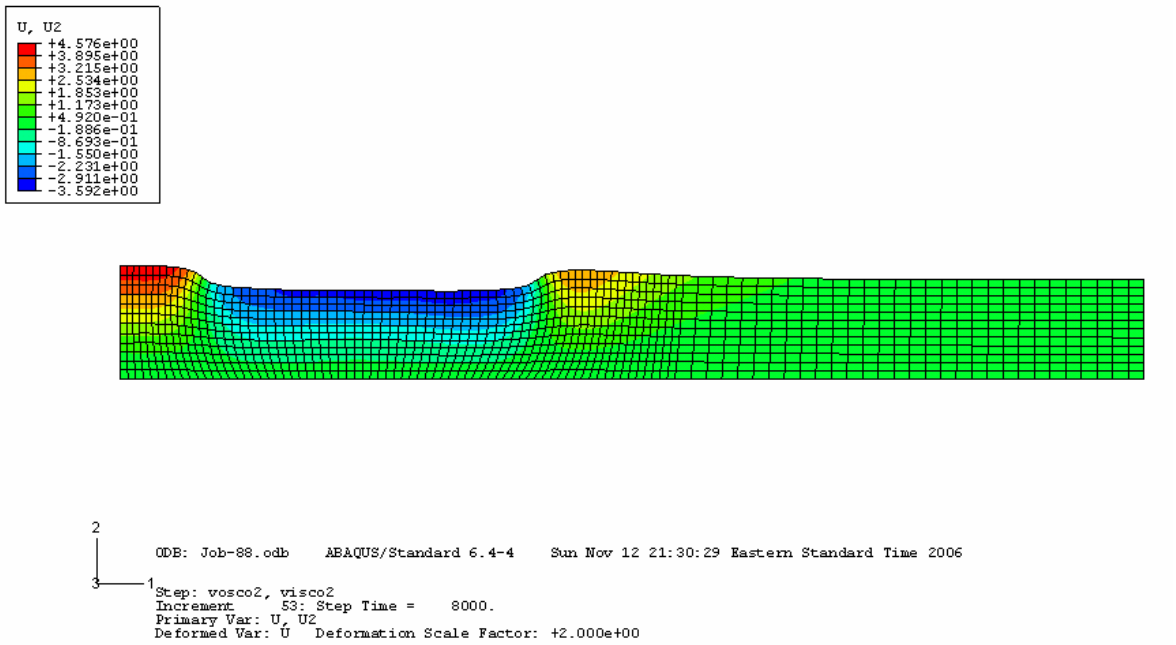

Figure D18 Predicted Deformed Shape of Pavement with SP 19 E Mix after

10 million ESAL's.

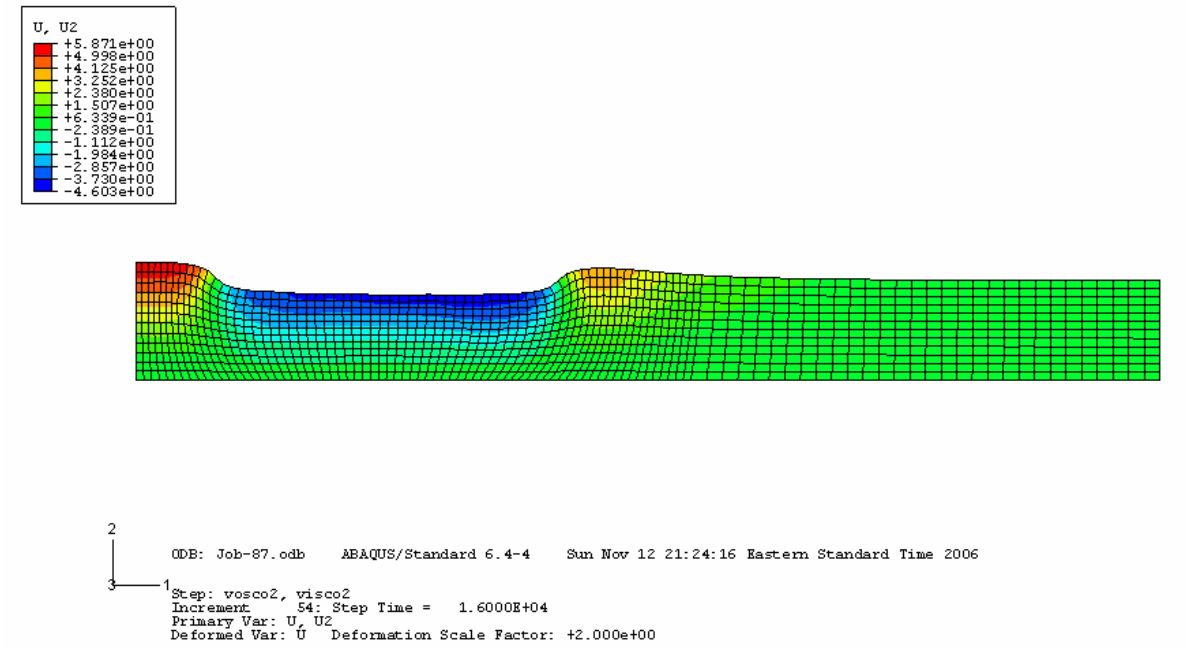

Figure D19 Predicted Deformed Shape of Pavement with SP 19 E Mix after 20 million ESAL's.

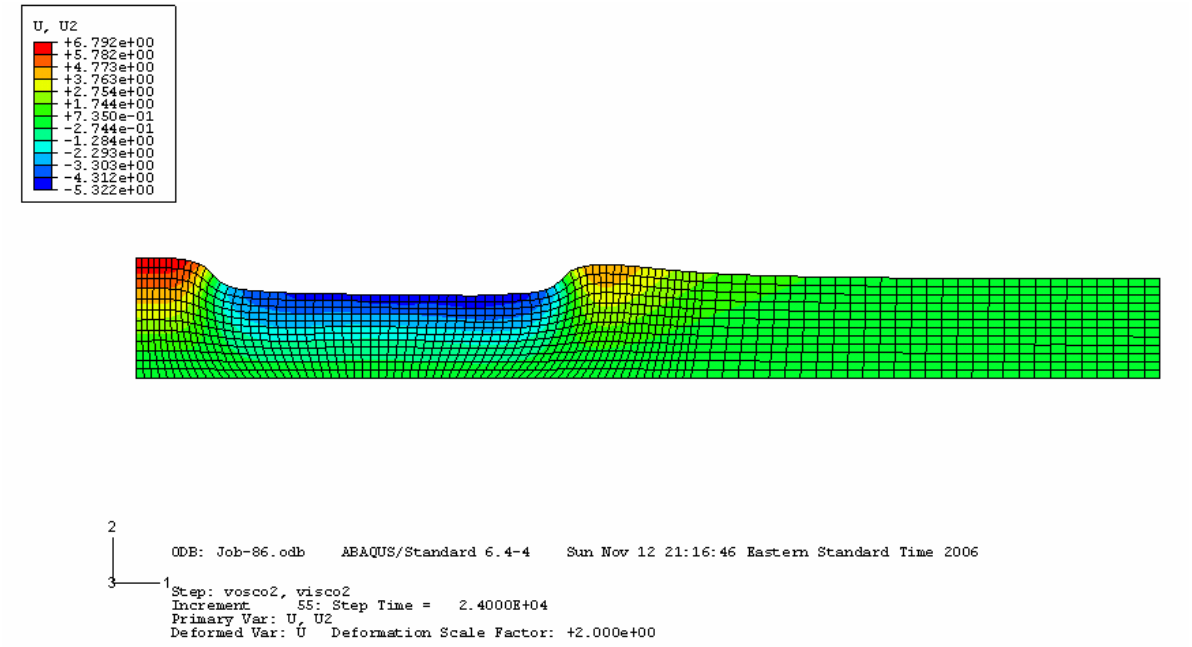

Figure D20 Predicted Deformed Shape of Pavement with SP 19 E Mix after 30 million ESAL's.

APPENDIX E

E-MAIL CORRESPONDENCE

From: Mohamed
To: 'Ludomir Uzarowski'
Sent: Tuesday, June 13, 2006 6:20 PM
Subject: RE: AASHTO 2002

G* units should be in Pa not KPa. The data you send me looked fine. If you regress them you would obtain an Ai of 8.67 and VTS -2.875 which is close to a PG 70-34 or PG 64-40. You should use Pa.

However, for the high rutting you are getting, I ran the section and I am not obtaining this significant rutting, in fact the rutting is about 0.1" after 20 years.

The thing is that you are running AC over JPCP, there is an error in the JPCP analysis and it is being fixed now.

The units for G* should be Pa, refer to the guide Part 2 chapter 2 for the equation used to convert G* and delta into viscosity.

Regards,

Mohamed El-Basyouny, Ph.D.
Assistant Professor, Research
Department of Civil and Environmental Engineering
Ira A. Fulton School of Engineering
Arizona State University
Tempe, Az 85287-5306
(480)727-6383

From: Ludomir Uzarowski [mailto:luzarowski@rogers.com]
Sent: Tuesday, June 13, 2006 3:16 PM
To: mohamed.elbasyouny@asu.edu
Subject: Fw: AASHTO 2002

Dear Dr. El-Basyouny,

Do you have any example dgp file for AASHTO 2002 Level 1 asphalt analysis? I have used my data entering G* in Pa and it does not work. When I entered the data in kPa it worked well. I am not able to find what mistake I am making.

Thank you for your help.
Ludomir Uzarowski

----- Original Message -----
From: Ludomir Uzarowski
To: mohamed.elbasyouny@asu.edu
Sent: Monday, June 12, 2006 3:26 PM
Subject: Re: AASHTO 2002

Dear Dr. El-Basyouny,

Thank you for your response. Should I enter G* in Pa, not kPa ? I have attached a dgp file for one of the mixes that I use in my analysis. In this pavement structure 2.5 inches of HMA is placed over 10 inches of PCC. If I enter the G* values in Pa, the program (Level 1) shows me that the rut depth will be 2 inches in Month 1. If I enter G* in kPa the rutting depth after 20 years is 0.10 inch. The mix is well known of very good resistance to rutting. I use 5 different mixes in my study and all of them exhibit the same rutting of 2 inches in Month 1 if I enter G* in Pa. I would very much appreciate your help.

Regards,
Ludomir Uzarowski

Ludomir Uzarowski, M.Sc., P.Eng.
Senior Pavement and Materials Engineer, Associate
Golder Associates Ltd.
100 Scotia Court
Whitby, Ontario
L1N 8Y6
Tel: 905-723-2727 Ext. 279
Fax: 905-723-2182
email: **Error! Hyperlink reference not valid.**
Web: **Error! Hyperlink reference not valid.**

----- Original Message -----
From: Mohamed
To: luzarowski@rogers.com
Cc: 'Harrigan, Ed'
Sent: Monday, June 12, 2006 1:24 PM
Subject: RE: AASHTO 2002

Dear Sir,

The Units used for G* is Pa not psi. It is an error in the output and it will be fixed in the new version.

As for SMA, the models are calibrated for dense graded mixes, we checked some SMA but it gave higher rutting than observed in the field. The models might need to be adjusted for the SMA.

If you want me to check your file, could you please send me your dgp file, there might be some other inputs which is causing the predicted rutting to be very high.

Best regards,

Mohamed El-Basyouny, Ph.D.
Assistant Professor, Research
Department of Civil and Environmental Engineering
Ira A. Fulton School of Engineering
Arizona State University
Tempe, Az 85287-5306
(480)727-6383

From: Harrigan, Ed [mailto:EHARRIGA@nas.edu]
Sent: Monday, June 12, 2006 4:43 AM
To: mohamed.elbasyouny@asu.edu
Subject: FW: AASHTO 2002

Hi, Mohamed.

Can you provide him with any help?

Thanks,

Ed

From: Ludomir Uzarowski [mailto:luzarowski@rogers.com]
Sent: Saturday, June 10, 2006 22:59
To: Harrigan, Ed
Subject: AASHTO 2002

Dear Dr. Harrigan,

I have run the AASHTO 2002 program, Internet version, a number of times in order to predict rutting performance of various asphalt mixes. I have noticed a discrepancy in the required G* input in Level 1 and 2 analysis that would like to bring to your attention and ask for clarification. The AASHTO 2002 program shows that I should enter G* values in Pa; however, after the analysis is completed, the InputSummary file show the entered G* values in psi (unrealistically high).

If the G* is entered in Pa into the program, ASSHTO 2002 analysis shows that the pavement will fail immediately (during the 1st month) because of asphalt layer rutting for all mixes that I used (some of them, including SMA, are well known of excellent rutting resistance). If G* is entered into the program in psi or kPa, the pavement exhibits good resistance to rutting.

I have attached two shots from my analysis showing the input into the AASHTO 2002 program and a shot from the InputSummary file for the same asphalt cement.

I would very much appreciate if you could help me or suggest whom I should contact to clarify what units should be used for entering G* into AASHTO 2002.

Regards,
Ludomir Uzarowski

Ludomir Uzarowski, M.Sc., P.Eng.
Senior Pavement and Materials Engineer, Associate
Golder Associates Ltd.
100 Scotia Court
Whitby, Ontario
L1N 8Y6
Tel: 905-723-2727 Ext. 279
Fax: 905-723-2182
email: **Error! Hyperlink reference not valid.**
Web: **Error! Hyperlink reference not valid.**